Custom-designed Nano-enabled Antibacterial Combination Therapy to combat Persistent Bacterial Pathogens associated with Bovine Mastitis

Satwik Majumder

Department of Food Science and Agricultural Chemistry

Faculty of Agricultural and Environmental Sciences

McGill University, Canada

First Published on December 31st 2024

A thesis submitted to McGill University in partial fulfilment of the requirements of the degree of Doctor in Philosophy

This Thesis is dedicated to my family and teachers for their unwavering support and guidance throughout my personal and professional journey.

Table of Contents

Abstract

Bovine intramammary infection (IMI) or bovine mastitis (BM) is the inflammation of mammary gland tissues predominantly due to microbial infection. BM poses a significant threat to the dairy industry worldwide due to reduced milk production, treatment failures, etc., causing remarkable financial losses of over $2 billion and $310 million in the USA and Canada, respectively. The prevalence of disease and the rise of antibiotic resistance warrant alternate, cheaper, and sustainable control strategies. Such an effort demands a deeper understanding of the pathogen and host-related factors involved in BM. This thesis provides an overview of risk factors and pathogenesis associated with BM that challenge the success of current treatment strategies. It further highlights how those unique factors could be exploited for designing effective nano-enabled antibacterial combination therapy (NeACT) for BM treatment. The knowledge of the causative agents of mastitis and continuous monitoring of mastitis pathogens for AMR and virulence is pivotal for strategizing such treatment approaches.

In the first phase of this study, libraries of mastitis pathogens namely, *Escherichia coli* and *Staphylococcus aureus* originally isolated from Canadian dairy farms were thoroughly characterized for antimicrobial resistance (AMR), AMR mechanisms, and virulence through phenotypic and genotypic techniques. I found the prevalence of AMR, AMR mechanisms such as efflux pump, and beta-lactamase activity among *E. coli* isolates. Further, these strains demonstrated virulence characteristics such as biofilm formation and hemolysin production that might contribute to persistent BM infection. Generally, the whole genome sequence data corroborated phenotypic results. In the case of *S. aureus,* I investigated their pathogenic translation in human infection models in addition to AMR and virulence characteristics. Although few *S. aureus* isolates showed AMR, all isolates demonstrated crucial virulence factors, including

hemolysis, biofilm formation, intracellular infection in Caco-2 cells, and intestinal infection in *Caenorhabditis elegans*. While WGS data revealed no evidence for human immune invasion genes, their ability to invade human cells and cause intestinal infection in model organisms suggested their ability to adapt and possibly cause zoonosis. Interestingly, the antibiotics that were found to be effective against *S. aureus* when tested in isolation failed to remediate intracellular infection in Caco-2 cells and *C. elegans*. Overall, these studies proved the inadequacy of antimicrobials with a single mode of action to curtail intracellular pathogens with multiple AMR mechanisms and virulence characteristics.

Further, I hypothesized that antimicrobial-adjuvant combination with synergistic and complementary mode of action would yield superior outcome in BM treatment. However poor bioavailability, stability, burst release, and overdosing pose significant challenges in combination therapy. Nanotechnology could resolve these issues due to their exceptional ability as drug carriers. Therefore, the thesis involved screening antimicrobial-adjuvant combinations for antibacterial synergism and custom-developing a NeACT for BM treatment. Aligning with the United Nations' "one health" objective, I selected an antibiotic against which bacteria is often resistant, with an aim to reuse the antibiotic by improving its efficiency by harnessing the advantages of nanotechnology. I selected Ceftiofur (CF) as the primary antimicrobial Chlorpromazine (CPZ) and Tannic acid (TA) as the adjuvants considering their complementary antibacterial mechanism of action. Chitosan nanoparticles (CH Np) and cyclodextrin (CD Np) were selected as the carriers due to their desirable characteristics for drug delivery. NeACT constituted CF loaded CH nanoparticles conjugated with CPZ and TA loaded CD nanoparticles. NeACT showed excellent infection remediation of a multi-drug resistant mastitis MRSA pathogen Sa1158c, internalized in human intestinal epithelial (Caco-2) cells and CD-1 lactating mice model of mastitis infection. Such promising antibacterial effect was owed to the complementary mechanism of actions of the CF, CPZ, and TA and achieving effective dose at site-of-action since these molecules were

delivered using nanomaterial. NeACT showed anti-efflux pump, anti-beta-lactamase enzyme, and anti-biofilm effects. It showed desirable colloidal stability, slow drug-release profile, and no toxic responses to Caco-2 cells and CD-1 mammary tissues. With such promising observations, NeACT showed the potential to be an alternative to BM treatment, which could be highly beneficial in a sustained “One Health” approach.

Résumé

L'infection intramammaire bovine (IMI) ou mammite bovine (BM) est l'inflammation des tissus de la glande mammaire principalement due à une infection microbienne. La mammite bovine représente une menace importante pour l'industrie laitière dans le monde entier en raison de la réduction de la production laitière, des échecs thérapeutiques, etc. Elle entraîne des pertes financières considérables de plus de 2 milliards de dollars et 310 millions de dollars aux États-Unis et au Canada, respectivement. La prévalence de la maladie et l'augmentation de la résistance aux antibiotiques justifient des stratégies de contrôle alternatives, moins coûteuses et durables. Un tel effort exige une compréhension plus approfondie des facteurs liés à l'agent pathogène et à l'hôte impliqués dans BM. Cette thèse donne un aperçu des facteurs de risque et de la pathogenèse associés à la BM qui met en péril le succès des stratégies de traitement actuelles. Elle souligne également comment ces facteurs uniques pourraient être exploités pour concevoir une thérapie antibactérienne combinée nanométrique (NeACT) efficace pour le traitement de la BM. La connaissance des agents responsables de la mammite et la surveillance continue des agents pathogènes de la mammite pour la résistance aux antimicrobiens et la virulence sont essentielles pour élaborer de telles approches thérapeutiques.

Dans la première phase de cette étude, des bibliothèques d'agents pathogènes de la mammite, à savoir *Escherichia coli* et *Staphylococcus aureus*, isolés à l'origine dans des fermes laitières canadiennes, ont été caractérisées de manière approfondie en ce qui concerne la résistance aux antimicrobiens (RAM), les mécanismes de RAM et la virulence au moyen de techniques phénotypiques et génotypiques. Nous avons constaté la prévalence de la RAM, des mécanismes de RAM tels que la pompe à efflux et de l'activité bêta-lactamase parmi les isolats d'*E. coli*. En outre, ces souches présentaient des caractéristiques de virulence telles que la formation de biofilms

et la production d'hémolysine qui pourraient contribuer à une infection BM persistante. En général, les données relatives à la séquence du génome entier ont corroboré les résultats phénotypiques. Dans le cas de *S. aureus*, nous avons étudié leur traduction pathogène dans des modèles d'infection humaine, en plus de la RAM et des caractéristiques de virulence. Bien que peu d'isolats de *S. aureus* aient présenté une RAM, tous les isolats ont montré des facteurs de virulence cruciaux, notamment l'hémolyse, la formation de biofilms, l'infection intracellulaire dans les cellules Caco-2 et l'infection intestinale chez *Caenorhabditis elegans*. Bien que les données WGS n'aient révélé aucune preuve de l'existence de gènes d'invasion immunitaire chez l'homme, leur capacité à envahir les cellules humaines et à provoquer des infections intestinales chez des organismes modèles suggèrent qu'ils sont capables de s'adapter et de provoquer éventuellement des zoonoses. Il est intéressant de noter que les antibiotiques qui se sont avérés efficaces contre *S. aureus* lorsqu'ils ont été testés isolément n'ont pas réussi à remédier à l'infection intracellulaire dans les cellules Caco-2 et *C. elegans*. Dans l'ensemble, ces études ont démontré l'inadéquation des antimicrobiens à mode d'action unique pour lutter contre les pathogènes intracellulaires dotés de multiples mécanismes de RAM et de caractéristiques de virulence.

En outre, j'ai émis l'hypothèse qu'une combinaison antimicrobien-adjuvant avec un mode d'action synergique et complémentaire donnerait des résultats supérieurs dans le traitement de la BM. Cependant, la biodisponibilité médiocre, la stabilité, la libération en rafale et le surdosage posent des problèmes importants dans la thérapie combinée. Les nanotechnologies pourraient résoudre ces problèmes grâce à leur capacité exceptionnelle à transporter des médicaments. Par conséquent, la thèse a consisté à cribler des combinaisons antimicrobiennes-adjuvants pour la synergie antibactérienne et à développer sur mesure un NeACT pour le traitement de la maladie de Malte. Conformément à l'objectif "One Health" des Nations unies, nous avons choisi un antibiotique contre lequel les bactéries sont souvent résistantes, dans le but de réutiliser l'antibiotique en améliorant son efficacité en exploitant les avantages de la nanotechnologie. Nous

avons choisi le ceftiofur (CF) comme antimicrobien principal, la chlorpromazine (CPZ) et l'acide tannique (TA) comme adjuvants, compte tenu de leur mécanisme d'action antibactérien complémentaire. Les nanoparticules de chitosane (CH Np) et la cyclodextrine (CD Np) ont été choisies comme vecteurs en raison de leurs caractéristiques souhaitables pour l'administration de médicaments. NeACT est constitué de nanoparticules CH chargées de CF et conjuguées avec CPZ et de nanoparticules CD chargées de TA. NeACT a montré une excellente remédiation à l'infection d'un pathogène MRSA multirésistant à la mastite, Sa1158c, internalisé dans des cellules épithéliales intestinales humaines (Caco-2) et dans le modèle d'infection de la mastite chez la souris allaitante CD-1. Cet effet antibactérien prometteur est dû au mécanisme d'action complémentaire du CF, du CPZ et du TA et à l'obtention d'une dose efficace au site d'action puisque ces molécules ont été délivrées à l'aide d'un nanomatériau. NeACT a montré des effets anti-pompe à efflux, anti-enzyme bêta-lactamase et anti-biofilm. Il a montré une stabilité colloïdale souhaitable, un profil de libération lente du médicament et aucune réponse toxique pour les cellules Caco-2 et les tissus mammaires CD-1. Grâce à ces observations prometteuses, NeACT a montré qu'il pouvait constituer une alternative au traitement par la BM, ce qui pourrait être très bénéfique dans le cadre d'une approche "One Health" durable.

Acknowledgments

The work conducted in this thesis was only possible with effective collaboration and constant guidance and support from several researchers, colleagues, and funding agencies. Foremost, I sincerely thank my supervisor, Dr. Saji George, who vetted me for the master's thesis program in his group and further supported me in a doctoral degree. His encouragement and guidance since day one helped me achieve my academic and personal goals. I am obliged to my supervisory committee members, Dr. Jennifer Ronholm and Dr. Jaswinder Singh, for their counsel over the years, which was tremendously beneficial throughout this research.

Parenting is hard and I was always the 'naughty' kid of the family. As a son, I can't thank my parents as no acknowledgment is enough for the sacrifices, they have made for me. Coming from a lower-middle-class family, my parents have provided me with immense care, raised me with cultural values, and fulfilled my necessities more than they could afford. The thesis and my past, present, and future career are dedicated to my father Mr. Pradip Kumar Majumder, my mother Mrs. Dola Majumder, and my elder brother, Mr. Shakyasom Majumder. I am forever indebted to my partner, Ms. Romasa Ahmed, her mother, Mrs. Anisa Begum, and my Canadian mother, Professor Marianne Stenbaek, who celebrated when I succeeded, scolded me when I was wrong, fed me when I was hungry, loved me as their own, and helped me to pass through tough times; without them, I couldn't achieve any of the professional and personal milestones. I am truly grateful to Dr. Arup Kumar Mitra from St. Xavier's College Kolkata, who guided me towards the path of scientific research. Without his support and mentorship, I would not be where I am today.

I sincerely appreciate all the past, present, and honorary members from George's lab, Ronholm's lab, Lu's lab, Karboune's lab, and Wang's lab for their generous support and help. I am thankful to Dr. Wut Hmone Phue, Dr. Ke Xu, Dr. Aneela Hameed, Dr. Lele Shao, Dr. Regina

Basumatary, Dr. Amal Sahyoun, Dr. Soyoun Park, Trisha Sackey, Estee Ngew, Elisa Ferrante, Amarpreet Brar, Zirou Liu, Mahesh Bastakoti, Emily Legault, Sky Castaing, Veronica Jaramillo, Jinyu Zhou, Kaidi Wang, Rana Roshanineshat, Elham Chidar, and Pratibha Sharma for their encouragement and all the wonderful memories in and off McGill campus. I am grateful to my collaborators and co-authors from McGill University, the University of Sherbrooke, and the University of Glasgow, for their advice and support throughout my Ph.D. tenure.

I thank the Facility of Electron Microscopy Research (McGill University), Electron Microscopy and Histology Platform (Université de Sherbrooke), McGill Chemistry Characterization Facility (McGill University), McGill Institute for Advanced Materials (McGill University), Facility of the Department of Earth and Planetary Sciences (McGill University), Parasitology Core Facilities (McGill University), and Multi-scale Imaging Facility (McGill University) for providing me training of analytical instruments and microscopes without which no research would have been possible.

I am obliged to the funding sources including Fonds de recherche du Québec - Nature et technologies (FRQNT), Natural Science and Engineering Research Council (NSERC), CRC/George/X-coded/248,475, Centre de recherche en infectiologie porcine et avicole (CRIPA), McGill Graduate Excellence Funding, Institute of Nutritional and Functional Foods (INAF), Institutes of Food Technologists (IFT), Fondation Initia, CTAQ, INAF, and Fruit d'OR, which made my tenure as a Ph.D. candidate feasible.

Contribution of authors

The work reported in all the chapters was designed, and conducted by Satwik Majumder, Ph.D. candidate in consultation with his supervisor, Dr. Saji George. Satwik Majumder has performed the experiments, collected, and analyzed results, and drafted manuscripts and this thesis for scientific presentations and publications. Dr. Saji George is the thesis supervisor who guided and supervised the candidate in performing the research as well as in reviewing and editing manuscripts. Satwik Majumder contributed as the first author while Dr. Saji George acted as the corresponding author in all the projects.

Chapter 2 is a review article that was published in the journal, ACS Agricultural Science and Technology. Prof David Peter Eckersall, University of Glasgow, UK co-authored Chapter 2 and brought his immense experience in the field of bovine mastitis while editing the manuscript. Satwik Majumder conducted a comprehensive literature search and wrote the review article in discourse with Dr. Saji George. All the authors read and approved the final manuscript.

Chapter 3 is an original research article that was published in the journal, BMC Microbiology. It was co-authored by Dongyun Jung and Dr. Jennifer Ronholm. All authors are affiliated with McGill University, Canada. Dr Saji George and Dr. Jennifer Ronholm provided the necessary resources and access to the level 2 microbiology laboratory for conducting the project. The *Escherichia coli* isolates used in this study were originally obtained from the Mastitis Pathogen Culture Collection (MPCC) and stored in Dr. Jennifer Ronholm's inventory. The *E. coli* isolates were sequenced by Dongyun Jung. Dongyun Jung handled and interpreted the whole genome sequence data. Dr. Jennifer Ronholm and Dongyun Jung helped in editing and proofreading the manuscript. Satwik Majumder and Dr. Saji George designed the study. Satwik Majumder performed susceptibility testing using antibiotics and metals, investigated AMR

mechanisms, and virulence, analyzed data, interpreted results, and wrote the manuscript. Dr. Saji George conceived, funded, coordinated and supervised the whole project. The final manuscript was read and approved by all the authors.

Chapter 4 is an original research article that was published in the journal, BMC Microbiology. It was co-authored by Trisha Sackey, Dr. Charles Viau, Dr. Soyoun Park, Dr. Jianguo Xia, and Dr. Jennifer Ronholm. All the authors are affiliated with McGill University, Canada. Dr. Saji George conceived the project, provided the necessary resources and access to the microbiology (level 2) and cell biology laboratories for conducting the project. Dr. Jianguo Xia provided the necessary resources and access to his laboratory to conduct research using the *Caenorhabditis elegans* model of infection. The *Staphylococcus aureus* isolates used in this study were also obtained from the MPCC and stored in Dr. Jennifer Ronholm's inventory. The *S. aureus* isolates were sequenced by Dr. Soyoun Park. Trisha Sackey helped in culturing Caco-2 cells and assessing antibiotic efficiency against internalized *S. aureus*. Dr. Charles Viau helped in culturing *Caenorhabditis elegans* under *S. aureus* exposure. Dr. Jianguo Xia and Dr. Jennifer Ronholm helped in editing and proofreading the manuscript. Satwik Majumder conducted susceptibility testing using antibiotics, and examined AMR mechanisms, and virulence in Caco-2 cells and *C. elegans*. Satwik Majumder and Trisha Sackey handled and interpreted the whole genome sequence data. Satwik Majumder analyzed data, interpreted results, and wrote the manuscript. Dr. Saji George conceptualized, provided necessary funds, validated, supervised the project and contributed to preparing the manuscript. All authors read and approved the final manuscript before publication.

Chapter 5 is an original research article that will be communicated soon in a peer-reviewed journal. It is co-authored by Guillaume Millette, Trisha Sackey, and Dr. Francois Malouin. Guillaume Millette and Dr. Francois Malouin are affiliated with the University of Sherbrooke, Canada. Dr. Francois Malouin provided the necessary resources and access to his lab to conduct

in vivo analysis in the CD-1 mice model of mastitis infection. Trisha Sackey helped in culturing the human intestinal epithelial Caco-2 cells and checked the efficiency of the nanotherapeutic against *S. aureus* infection. Guillaume Millette assessed the efficiency of the nanotherapeutic *in vivo* and helped in histopathology. Satwik Majumder designed and developed the nanotherapeutic, conducted characterization, release kinetics analysis, and antibacterial testing against bacterial resistance *in vitro* and in Caco-2 cells. Satwik Majumder analyzed data, interpreted results, and wrote the manuscript. Dr. Saji George conceptualized, funded, validated and supervised the whole project.

Publications

Original research articles included in this thesis

1. **Majumder, S**.; P. D.; George, S., Bovine Mastitis: Examining Factors Contributing to Treatment Failure and Prospects of Nano-enabled Antibacterial Combination Therapy. ***ACS Agricultural Science & Technology*** **2023,** *3* (7), 562-582. https://doi.org/10.1021/acsagscitech.3c00066.

   Copyright approval: *Reprinted (adapted) with permission from {**Majumder, S**.; P. D.; George, S., Bovine Mastitis: Examining Factors Contributing to Treatment Failure and Prospects of Nano-enabled Antibacterial Combination Therapy. **ACS Agricultural Science & Technology 2023,** 3 (7), 562-582. https://doi.org/10.1021/acsagscitech.3c00066}. Copyright 2023 American Chemical Society.*

2. **Majumder, S**.; Jung, D.; J.; George, S., Prevalence and mechanisms of antibiotic resistance in Escherichia coli isolated from dairy cattle in Canada. ***BMC Microbiology*** **2021,** *21* (1), 222. https://doi.org/10.1186/s12866-021-02280-5

   Copyright approval: *This article is licensed under a Creative Commons Attribution 4.0 International License, which permits use, sharing, adaptation, distribution and reproduction in any medium or format. To view a copy of this licence, visit http://creativecommons.org/licenses/by/4.0/.*

3. **Majumder, S**.; T.; C.; Park, S.; J.; J.; George, S., Genomic and phenotypic profiling of *Staphylococcus aureus* isolates from bovine mastitis for antibiotic resistance and intestinal infectivity. ***BMC Microbiology*** **2023,** *23* (1), 43. https://doi.org/10.1186/s12866-023-02785-1

   Copyright approval: *This article is licensed under a Creative Commons Attribution 4.0 International License, which permits use, sharing, adaptation, distribution and reproduction in any medium or format. To view a copy of this licence, visit http://creativecommons.org/licenses/by/4.0/.*

4. **Majumder, S.**; Guillaume, M; Trisha, S; Malouin, F; George, S., Nanocomposite of chitosan-cyclodextrin loaded with antibiotic-adjuvant combinations remediates multi-drug resistant *Staphylococcus aureus* infection in CD-1 mice model of bovine mastitis. **(Under preparation)**

Original research articles not included in this thesis

5. **Majumder, S**.; C.; A.; J.; George, S., Silver nanoparticles grafted onto tannic acid-modified clay eliminated -resistant Salmonella in a model of intestinal infection. ***Applied Clay Science*** **2022**, 106569. https://doi.org/10.1016/j.clay.2022.106569
6. **Majumder, S**.; B.; Mitra, A. K.; Dey, S., Applications and implications of carbon nanotubes for the sequestration of organic and inorganic pollutants from wastewater. ***Environmental Science and Pollution Research*** **2023**. https://doi.org/10.1007/s11356-023-25431-9
7. **Majumder, S**.; George, S., Multi-Functional Properties of Nano-Clays in Food Safety and Security. In ***Materials Science and Engineering in Food Product Development***, **2023**; pp 261-277. https://doi.org/10.1002/9781119860594.ch13
8. **Majumder, S**.; Huang, S.; Zhou, J.; Wang, Y.; George, S., Tannic acid-loaded clay grafted with silver nanoparticles enhanced the mechanical and antimicrobial properties of soy protein isolate films for food-packaging applications. ***Food Packaging and Shelf Life*** **2023,** *39*, 101142. https://doi.org/10.1016/j.fpsl.2023.101142
9. **Majumder, S**.; George, S., Chapter Twenty-Three - Nanotechnology-enabled from Ayurvedic herbs for the treatment of disorders: an overview. In ***Ayurvedic Herbal Preparations in Neurological Disorders***, M.; P. S., Eds. Academic Press: 2023; pp 611-633. https://doi.org/10.1016/B978-0-443-19084-1.00001-6
10. **Majumder S**, M. S., A, A, A, Mitra AK, Antimicrobial Assessment of a Novel Humectant-Hand-Sanitizer against Microbes Transferred To Human Palms from Mobile Phones With/Without Flip Covers. ***Annals of Advanced Biomedical Sciences*** **2022,** *5* (1). https://doi.org/10.23880/aabsc-16000176
11. George, S.; Teo, L. L.; **Majumder, S**.; Chew, W. L.; G. H., Low levels of silver in food packaging materials may have no functional advantage, instead enhance microbial spoilage of

food through hormetic effect. ***Food Control*** **2020**, 107768. https://doi.org/10.1016/j.foodcont.2020.107768

12. Brar, A.; **Majumder, S**.; Navarro, M. Z.; Benoit-, M.-O.; J.; George, S., Nanoparticle-Enabled Combination Therapy Showed Superior Activity against Multi-Drug Resistant Bacterial Pathogens in Comparison to Free Drugs. ***Nanomaterials*** **2022,** *12* (13), 2179. https://doi.org/10.3390/nano12132179
13. Shao, L.; **Majumder, S**.; Z.; Xu, K.; R.; George, S., Light activation of gold nanorods but not gold enhance antibacterial effect through and mechanisms. ***Journal of Photochemistry and B: Biology*** **2022,** *231*, 112450. https://doi.org/10.1016/j.jphotobiol.2022.112450

Patent applications not included in this thesis

14. Patent application - **US 63/393,624**: Multi-functional nanocomposite for sustainable agricultural food and environmental applications; George, S., **Majumder, S**. https://mcgill.flintbox.com/technologies/54a14a5a-05cd-4438-a273-018f42e99749
15. Granted Patent Number - **390561**: Hand and Surface Sanitizer; **Majumder, S**., Mitra. AK. https://www.sxccal.edu/wp-content/uploads/2020/01/Humectant-Hand-SurfaceSanitizer.pdf

Conference presentations

Oral presentation

1. *"Nanotechnology for improving the sustainability index of bio-based food packaging"*, **Satwik Majumder**, Shuting Huang, Jinyu Zhou, Yixiang Wang, Saji George. **2023**. Gordon Research Seminar (GRS) - Environmental Nanotechnology: Nanotechnology for a More Sustainable World. Newry, ME, USA.
2. *"Nanotechnology for improving the sustainability index of bio-based food packaging"*, **Satwik Majumder**, Shuting Huang, Jinyu Zhou, Yixiang Wang, Saji George. **2023**. Gordon Research Conference (GRC) - Environmental Nanotechnology: Nanotechnology for a More Sustainable World. Newry, ME, USA.
3. *"Nanocomposite of Halloysite clay to combat multidrug-resistant Salmonella Typhimurium in Caco-2 and C. elegans models of intestinal infection"*. **Satwik Majumder**, Charles Viau, Amarpreet Brar, Jianguo Xia, Saji George. **2022**. Gordon Research Seminar (GRS) - Convergence of Nanotechnology with Food and Agriculture. Manchester, NH, USA.
4. *"Nanocomposite of halloysite nanotube with silver and tannic acid as a sustainable antibacterial material for food safety and security"***. Satwik Majumder**, Charles Viau, Amarpreet Brar, Jianguo Xia, Saji George. **2022**. Canadian Food Summit - Canadian Institute of Food Science and Technology (CIFST). University of Guelph, Ontario, Canada.
5. *"Prevalence and mechanisms of antibiotic resistance in Escherichia coli isolated from mastitic dairy cattle in Canada".* **Satwik Majumder**, Dongyun Jung, Jennifer Ronholm, Saji George. **2022**. Animal Science and Veterinary Medicine Conference. (Virtual)
6. *"Prevalence and mechanisms of antibiotic resistance in Escherichia coli isolated from mastitic dairy cattle in Canada".* **Satwik Majumder**, Dongyun Jung, Jennifer Ronholm, Saji George. **2021**. World Congress on Food Safety and Nutrition Science Conference. (Virtual)

7. *"Prevalence and mechanisms of antibiotic resistance in Escherichia coli isolated from mastitic dairy cattle in Canada".* **Satwik Majumder**, Dongyun Jung, Jennifer Ronholm, Saji George. 2021. Conference on research workers in Animal Diseases (CRAWD). (Virtual)

Poster presentation

1. *"Prevalence and mechanisms of antibiotic resistance in Escherichia coli isolated from mastitic dairy cattle in Canada".* **Satwik Majumder**, Dongyun Jung, Jennifer Ronholm, Saji George. **2023**. Antimicrobial Resistance Symposium. McGill University, Montreal, Canada.
2. *"Tannic acid-loaded halloysite clay grafted with silver nanoparticles as reinforcement for Soy Protein Isolate-based food packaging system"*. **Satwik Majumder,** Shuting Huang, Jinyu Zhou, Yixiang Wang, Saji George. **2023**. Institute of Nutrition and Functional Foods (INAF) Student Member Symposium, Quebec, Canada.
3. *"Nanotechnology for improving the sustainability index of bio-based food packaging"*. **Satwik Majumder**, Shuting Huang, Jinyu Zhou, Yixiang Wang, Saji George. **2023**. Gordon Research Conference (GRC) - Environmental Nanotechnology: Nanotechnology for a More Sustainable World. Newry, ME, USA.
4. *"Nanocomposite of Halloysite Clay, Nano-silver, and Tannic Acid as a Therapy to Combat Multidrug-resistant Salmonella Typhimurium in a Caenorhabditis elegans Model of Intestinal Infection".* **Satwik Majumder**, Charles Viau, Amarpreet Brar, Jianguo Xia, Saji George. **2023**. International Conference on Sustainable and Applied Nanotechnology for Agriculture and Health (*SANTAH*). IIT Madras, India.
5. *"Nanocomposite of Halloysite clay to combat multidrug-resistant Salmonella Typhimurium in Caco-2 and C. elegans models of intestinal infection".* **Satwik Majumder**, Charles Viau, Amarpreet Brar, Jianguo Xia, Saji George. **2023**. ASM/ESCMID Joint

Conference on Drug Development to Meet the Challenge of Antimicrobial Resistance. Boston, Mass, USA.

6. *"Nanocomposite of Halloysite clay to combat multidrug-resistant Salmonella Typhimurium in Caco-2 and C. elegans models of intestinal infection".* **Satwik Majumder**, Charles Viau, Amarpreet Brar, Jianguo Xia, Saji George. **2022**. Gordon Research Conferences (GRC) - Nanoscale Science and Engineering for Agriculture and Food Systems. Manchester, NH, USA.
7. *"Nano-silver grafted onto tannic acid-modified halloysite clay demonstrates a combinatorial effect to eliminate multidrug-resistant Salmonella Typhimurium in Caenorhabditis elegans model of intestinal infection".* **Satwik Majumder**, Charles Viau, Amarpreet Brar, Jianguo Xia, Saji George. **2021**. PORC Show 2021 – Centre de recherche en infectiologie porcine et avicole (CRIPA). (Virtual)

Awards and accomplishments

During my Ph.D., I received a series of awards and scholarships from research consortium, institutes, conferences, and competitions.

1. **Graduate Excellence Award** (2020-21, 2021-22, 2022-23) Recipient; McGill University, Canada.
2. **Excellence in Graduate and Undergraduate Teaching Assistantship** 2023 Award Recipient; McGill University, Canada.
3. **IFT Feeding Tomorrow Fund Scholarship** 2023 Recipient; Institute of Food Technologists, USA.
4. **CRIPA's Allowance for Research Outreach** 2023 Recipient; Centre de recherche en porcine et (CRIPA), University of Montreal, Canada.
5. **Together For The Next Generation scholarship** (2021-22, 2022-23) Recipient; Centre de recherche en porcine et (CRIPA), University of Montreal, Canada.
6. **INITIA TRANFO-INNO Scholarship** 2022 Recipient; Fondation Initia, CTAQ, INAF, Fruit d'OR, Canada
7. **Short-term financial support to graduate students** (2020-21) Recipient; Centre de recherche en porcine et (CRIPA), University of Montreal, Canada
8. **McGill-Glasgow Award** (2020-21, 2021-22) Recipient; McGill University, Canada.
9. **Complementary grants for new graduate students** 2020 Recipient; Institute of Nutrition and Functional Foods (INAF), University of Laval, Canada
10. **Travel awards** (2021, 2022, 2023) Recipient; INAF, CRIPA, and McGill University.

Designations

During my Ph.D., I received several opportunities to serve the McGill community.

1. Teaching assistant of the courses 'Food Chemistry-FDSC 251', 'Separation Techniques in Food Analysis-FDSC 315', 'Food Packaging-FDSC 400', 'Food Quality Assurance-FDSC 525', 'Food Microbiology-FDSC 442' and 'Principles of Food Analysis-FDSC 651'. (2020-2023)
2. Graduate Student Representative (2022-2023)
3. Association of Graduate Students Employed at McGill (AGSEM) Delegate (2020-2023)
4. Representative of the Student Safety Committee (2020-2023)
5. Tomlinson Undergraduate mentor (2020-2023)

During my Ph.D., I have been affiliated with the following scientific consortiums.

1. Member, Canadian Institute of Food Science and Technology: Burlington, ON, CA, 2021 to date
2. Member, National Mastitis Council: New Prague, Minnesota, US, 2022 to date
3. Member, American Society for Microbiology: Washington, DC, US, 2023 to date
4. Member, Centre de recherche en infectiologie porcine et avicole (CRIPA), University of Montreal: Montreal, Quebec, CA, 2020 to date
5. Member, Université Laval Institut sur la nutrition et les aliments fonctionnels (INAF): Quebec, QC, CA, 2020 to date
6. Member, Food Science Association, McGill University, Montreal, Quebec, CA, 2019 to date

List of Abbreviation

ABR	Antibiotic resistance
AMR	Antimicrobial resistance
ATR-FTIR	Attenuated total reflectance-Fourier transform infrared
BM	Bovine mastitis
CFU	Colony forming units
CLSI	Clinical and Laboratory Standard Institute
DLS	Dynamic Light Scattering
DMEM	Gibco Dulbecco's Modified Eagle Medium
DMSO	Dimethylsulfoxide
ERK1/2	Extracellular signal-regulated kinase 1/2
EPR	Enhanced permeability and retention
EPS	Extracellular polymeric substances
ESBL	Extended-spectrum β-lactamases
FBS	Fetal bovine serum
FITC	Fluorescein isothiocyanate
IC	Inhibitory concentration
IL-1ra	Interleukin-1 receptor antagonist
IL-10	Interleukin-10 (IL-10)
IL-1α	Interleukin-1 alpha
IL-6	Interleukin-6
IMI	Intramammary infection
LbL	Layer-by-layer
LPS	Lipopolysaccharides
MDR	Multi-drug resistance
MFS	Major facilitator superfamily
MHB	Mueller-Hinton broth

MIC	Minimum inhibitory concentration
MPCC	Mastitis Pathogen Culture Collection
MR	Mannose receptors
MRSA	Methicillin-resistant Staphylococcus aureus
MSCC	Milk somatic cell count
NeACT	Nano-enabled antibacterial combination therapy
NGM	Nematode growth medium
PBP	Penicillin-binding protein
PBS	Phosphate-buffered saline
PIA	Polysaccharide intercellular adhesin
PMN	Polymorphonuclear neutrophils
PPB	Potassium phosphate buffer
QC	Quality control
QS	Quorum sensing
RND	Resistance Nodulation Division
ROS	Reactive oxygen species
RT	Room temperature
SCV	Small colony variants
SEM	Scanning Electron Microscope
ST	Sequence types
TNF	Tumor Necrosis Factor
TSA	Tryptic Soy Agar
USDA	United States Department of Agriculture
WGS	Whole genome sequence

List of Figures

List of Tables

Preface and Contribution to Knowledge

The thesis is written in the manuscript format following the "Guidelines for Thesis Preparation" outlined by McGill University. Chapter 1 is a general introduction of the thesis detailing research motivation, background, knowledge gaps, and outline for research objectives and hypothesis. Chapter 2 is a comprehensive literature search and review of the topics dealt in this thesis. This chapter has been published in a peer-reviewed journal, ACS Agricultural Science and Technology as a review article. Chapter 3, 4, and 5 includes introductions, methods, results, and discussions for each objective of the thesis. Chapters 3 and 4 have been published in the peer-reviewed journal, BMC Microbiology as original research articles. Chapter 5 has been prepared and would be communicated to a peer-reviewed journal soon. Chapter 6 summarizes the thesis with a comprehensive discussion, conclusion, and future perspectives.

This thesis fills important knowledge gaps and contributes to the advancement of knowledge as follows:

Chapter 2: The literature review implied the necessity to address the dynamic evolution of AMR and virulence among bacterial pathogens from dairy cows. It suggested the importance of a thorough understanding of the interplay between environmental, host, and pathogen-related factors. As the current mastitis treatment strategies have struggled significantly to curtail bacteria with MDR mechanisms, the chapter emphasized on the potential application of combination therapy, involving antibiotic-adjuvant combinations with complementary antipathogen actions. Although nanotechnology has been advantageous in resolving the challenges associated with combination therapy and explored in various biomedical sectors, little has been investigated in bovine mastitis treatment. Thus, the chapter filled the knowledge gaps by addressing the unique

potential of nanotechnology-enabled combination therapy to target mastitis pathogens considering specific challenges.

Chapter 3: This study found that resident *E. coli* isolated from mastitis dairy cows carries multiple drug resistance and virulence characteristics, which has implications for public health. Further, I suggested that using antimicrobials with a single mode of action may not be sufficient in curbing antibiotic-resistant bacteria with multiple mechanisms of resistance and virulence factors. Instead, combinatorial therapy may be necessary to effectively manage antibiotic-resistant infections in dairy farms and prevent transmission to the food supply chain through milk and dairy products.

Chapter 4: This study demonstrated *S. aureus* from mastitis dairy cows exhibit critical pathogenesis in human intestinal infection models despite lacking human immune invasion genes, thus underscoring the need for ongoing monitoring of zoonotic pathogens. Notably, the antibiotics that showed efficacy against the isolates in the disc diffusion assay did not effectively remediate intracellular and intestinal infections. Therefore, the chapter highlights the need for models capable of testing the effectiveness of antibiotics against internalized bacteria and the urgency of developing therapeutics that can combat AMR and intracellular pathogens.

Chapter 5: This chapter demonstrated the remarkable efficiency of nanomaterials as carriers of antibiotic-adjuvant combinations in the remediation of MDR *S. aureus* from models of bovine mastitis infection owing to antibacterial synergistic action among the payloads and their sequential delivery from the nanocarriers at the site of infection. NeACT showed impressive colloidal stability in the alkaline mammary gland microenvironment, adequate retention in tissues, low immunogenicity, and no toxicity. Despite the widespread use of nanotechnology in different fields, its potential in the treatment of mastitis remains largely unexplored. This research has

contributed to the advancement of veterinary medicine by highlighting the potential of nano-enabled combination therapy as an effective treatment to curtail MDR mastitis pathogens and also other recalcitrant infections in animal agriculture.

CHAPTER 1. Introduction

1.1. Thesis motivation

Bovine mastitis is an inflammatory response of the mammary gland tissues in cows primarily caused by microbial infections (Majumder, Eckersall, & George, 2023). This disease is a major concern in the global dairy cattle industry, resulting in substantial financial losses in billions of dollars due to reduced milk production, milk loss, extra labor charges, treatment failures, *etc* (Majumder, Eckersall, & George, 2023). Despite applying hygienic milking practices, pre- and post-milking teat disinfectant, and antibiotic dry cow therapy, several studies have shown the presence of mastitis pathogens in bulk milk tanks (Gillespie & Oliver, 2005; Jayarao & Henning, 2001; Steele et al., 1997). These pathogens have a higher chance of acquiring AMR characteristics due to exposure to high antibiotic concentrations as part of preventive or prophylactic treatment regimens practiced in dairy farms. Pathogens spilled over to environmental matrices are a concern from a public health standpoint as some of them are highly pathogenic to humans, even though they originated in cows. Therefore, continuous monitoring of mastitis pathogens for AMR, virulence, and zoonoses is crucial.

Conventional disease management practices are becoming less effective in resolving BM due to the rise in AMR and the wide range of virulence factors among mastitis-associated pathogens (Majumder, Eckersall, & George, 2023). Although significant progress has been made in identifying new antimicrobial strategies since the 1930s, achieving an effective concentration of therapeutics at the site of infection has been a major stumbling point in the successful curing of bovine mastitis because of the challenges associated with specific tissue environments. Therefore,

there is scope of alternate cost-effective and sustainable therapeutic strategy for the clinical management of the disease that also aligns with the United Nations' "One Health" approach.

Recent advancements in nanotechnology have provided unprecedented benefits in diagnosing and treating multifactorial infectious diseases (Brar et al., 2022; Majumder, Viau, Brar, Xia, & George, 2022). However, effective nano-enabled strategies for mastitis treatment are still an untapped area of research and application. This thesis examined a library of mastitis pathogens for AMR, virulence, and zoonoses through phenotypic and genotypic profiling and developed Nano-enabled Antibacterial Combination Therapy (NeACT) for effective treatment of bovine mastitis.

1.2. Knowledge gaps

From the survey of literature on the nature of mastitis and treatment options, I have identified the following knowledge gaps:

- There is a need to address the dynamic evolution of antimicrobial resistance and virulence among bacterial pathogens isolated from dairy cows in Canada to custom-design treatment modalities.
- Multi-drug resistant mechanisms in mastitis bacteria have made commonly used antibiotics ineffective, thus there is a need to address the potential application of combination therapy involving antibiotic-adjuvant combinations with complementary antipathogen actions.
- While there have been advancements in nanotechnology applications in different sectors, little effort has been made into developing nanotherapeutic specific for the treatment of mastitis considering specific challenges.

1.3. Research Objective, Hypothesis, and Rationale

Objective 1: Comprehensive review of the risk factors, pathogenesis, and current treatment strategies associated with bovine mastitis

The aim of this project is to conduct a comprehensive review for an extensive understanding of the host, pathogen, and environmental risk factors, pathogenesis, and current treatment paradigm associated with bovine mastitis. Ultimately, the goal is to highlight how those unique challenges could be exploited for designing NeACT for effective mastitis treatment.

Rationale: A clear understanding of the risk factors, pathogenesis, and current treatment challenges associated with bovine mastitis is pivotal for the clinical management of the disease as well as for designing new therapeutic agents.

Objective 2: Phenotypic and genotypic characterization of bacterial isolates from mastitis-infected bovines for antimicrobial resistance and virulence mechanism

The aim of this project is to investigate a library of *Escherichia coli* and *Staphylococcus aureus* isolates originally isolated from mastitis cows for antimicrobial resistance (against antibiotics and metals), mechanisms (such as efflux activity and beta-lactamase enzyme activity), virulence characteristics (such as hemolysis manifestation, biofilm-forming ability, and intracellular survival), and zoonoses through phenotypic and genotypic profiling.

Hypothesis: Bacteria from mastitis dairy cows exhibit AMR and virulence characteristics enabling them to survive hostile environmental and host conditions.

Rationale: Bovine mastitis is the most common infectious disease in dairy cattle with major economic implications for the dairy industry worldwide. Continuous monitoring for the emergence

of AMR and virulence factors among bacterial isolates from dairy farms is vital for veterinary/public health, and strategizing treatment approaches.

Objective 3: Synthesis and *in vitro* characterization of Nano-enabled Antibacterial Combination Therapy (NeACT) to combat multi-drug resistant mastitis pathogens

The aim is to develop and conduct *in vitro* characterization (physicochemical and antimicrobial) of a NeACT.

Hypothesis: NeACT with synergistic effect due to common or complementary antibacterial mechanism of action is effective for eliminating MDR intracellular mastitis pathogens.

Rationale: The extensive use of antibiotics relevant to human health in animals has contributed significantly to the emergence and transmission of AMR. Combination therapy with more than one antimicrobial agent has shown possibilities to combat multiple mechanisms of resistance and virulence traits in bacteria. However, such therapies have still shown vulnerability towards AMR or faced challenges related to poor bioavailability, cytotoxicity, stability, release, and overdosing. The application of NeACT with complementary actions could resolve these issues and play a significant role in formulating cost-effective antibacterial therapeutics for animal agriculture.

Objective 4: *In vivo* assessment of NeACT for mastitis remediation efficiency

The aim is to investigate the consequences of mastitis infection, immune responses, toxicological responses, and infection remediation efficiency of NeACT in CD-1 mastitis mice model.

Hypothesis: The NeACT exhibits no toxicity and causes significant reduction in mastitis infection *in vivo* because the nano-enabled strategies facilitate enhanced stability, site-specific payload

delivery, payload bioavailability, low immunogenicity, adequate drug-retention time, and thus significantly reduce the effective concentration of the payloads.

Rationale: *In vivo* testing is a vital aspect as it uncovers the mechanisms that underlie disease progression and assesses the safety and effectiveness of emerging medical treatments, thus enabling researchers the opportunity to monitor various biological effects within complex genetically similar living organisms. Despite positive preclinical results, almost 30% of drug candidates fail animal clinical trials due to toxic effects whereas, around 60% do not provide the desired effect. Therefore, it is important to investigate the reliability of the NeACT in combating bovine mastitis through *in vivo* studies. Studies have reported that an intraductal mouse model can mimic bovine CNS mastitis and has the potential as a complementary *in vivo* tool (Breyne, De Vliegher, De Visscher, Piepers, & Meyer, 2015).

Preface to Chapter 2

The previous chapter detailed on the thesis motivation, knowledge gaps, research objectives, hypothesis, and experimental design. Chapter 2 is a comprehensive literature review that takes a closer look at the risk factors and pathogenesis related to bovine mastitis, that contributes significantly to treatment failures of conventional disease management strategies. I also explored the potential for utilizing these unique challenges in the development of effective NeACT for bovine mastitis treatment.

Chapter 2 – Literature review

Bovine mastitis: Examining factors contributing to treatment failure and prospects of nano-enabled antibacterial combination therapy

Abstract

Bovine mastitis, primarily caused by microbial infections of cow mammary glands leading to inflammation, is the costliest disease in the dairy industry. The severity and the responsiveness of mastitis to treatment depend on the dynamic interplay between the host, pathogen, and environmental factors. Evidently, the prospects of managing mastitis with conventional antibiotic treatment and disease management strategies are grim with the emergence of antimicrobial resistance (AMR) and the prevalence of virulence characteristics such as biofilm formation and intracellular survival among persistent pathogens. Thus, there is a need for safe and economically viable alternate therapies capable of targeting broad-spectrum pathogens displaying AMR and virulence characteristics. Recent progress in the application of nanotechnology in drug delivery and infection control provides unprecedented opportunities for resolving recalcitrant infections. While the advantages of nanotechnology have been exploited for therapeutic delivery in humans, the potential of nanotechnology is yet to be realized in animal agriculture, especially for treating bovine mastitis. This review provides an overview of risk factors and pathogenesis associated with bovine mastitis that challenge the success of current treatment strategies and highlights how those unique challenges could be exploited for designing effective nano-enabled antibacterial combination therapy for bovine mastitis treatment.

Keywords: intramammary infection (IMI), bovine mastitis, pathogenesis, risk factors, antimicrobial resistance (AMR), virulence, nano-enabled antibacterial combination therapy.

2.1. Bovine mastitis – impact on agriculture and public health

Bovine intramammary infection (IMI) or bovine mastitis is the inflammatory response of the mammary gland tissues of cows primarily to microbial infections (Shaheen, Tantary, & Nabi, 2016). According to the estimates, the yearly financial loss from bovine mastitis incurred in some of the prominent milk-producing countries such as the United States, Canada, India, and Australia amount to $2 billion, $794 million, $971 million, and $130 million, respectively (Audarya et al., 2021; "How much does mastitis cost dairy producers annually?," 2020; Ismail, 2017). Reduced milk production, milk loss, extra labor charges, treatment, and veterinary service costs all cumulatively account for financial losses, making mastitis the most threatening bacterial disease in the dairy cattle industry globally (Petrovski, Buneski, & Trajcev, 2006).

Mastitis can be classified into clinical and subclinical based on the symptoms. Clinical mastitis can be distinguished by discernible inflammatory abnormalities in the mammary gland tissue, accompanied by fever, loss of appetite, dehydration, and a swollen udder. Meanwhile, subclinical mastitis involves inflammation of the mammary gland without distinguishable changes in the milk or the udder but is associated with high somatic cell count and shedding of causative bacteria in milk and is difficult to detect. Subclinical mastitis affecting 20-50% of cows in a herd is ~40 times more frequent than clinical mastitis and may lead to permanent loss of milk synthesizing capability by the mammary tissue, thus, contributing to a more significant economic impact (Gonçalves et al., 2018).

Although there are strict industry standards for avoiding milk with unusual somatic cell count, accidental contamination could lead to the consumption of partially processed milk. Further, undercooked meat of culled mastitic dairy cows could also spread pathogens associated with mastitis. Several studies have shown the presence of pathogens in bulk milk tanks even after

applying hygienic milking practices, pre-and post-milking teat disinfectant, and antibiotic dry cow therapy (curing existing infection with antibiotics at the end of lactation or dry period) (Gillespie & Oliver, 2005; Jayarao & Henning, 2001; Steele et al., 1997). Pathogens spilled over to environmental matrices are a cause of concern from a public health standpoint as some of them are highly pathogenic to humans despite their origin in cows (O. Dego, 2020). Besides, these bacteria have a high chance of acquiring antimicrobial resistance (AMR) characteristics as they are exposed to high antibiotic concentrations as part of preventive or prophylactic treatment regimens practiced in dairy farms. For instance, the transmission of extended-spectrum beta-lactam drug-resistant *Escherichia coli and* Methicillin-resistant *Staphylococcus aureus* (MRSA) to humans through direct contact with infected/carrier animals or indirectly through the food chain has been reported (Wyres et al., 2019; Wyres & Holt, 2018). Thus, apart from losing productivity, mastitis is a significant public health concern since mastitis pathogens and their products can contaminate the food supply chain and cause foodborne diseases.

Conventional disease management practices are becoming less effective in resolving IMI due to the rise in AMR and the wide range of virulence factors among mastitis-associated pathogens. Effective treatments for mastitis infection have been sought since the 1930s, starting with intramammary Penicillin use (Ruegg, 2017). Considerable progress has been made in identifying new antimicrobial strategies since then, including the application of new antibiotics, combination therapy, phage therapy, and vaccination strategies (Waller & Sampson, 2018). However, achieving an effective concentration of therapeutics at the site of infection has been a major stumbling point in the successful curing of bovine mastitis because of the challenges associated with specific tissue environments. Recent advancements in nanotechnology have provided unprecedented benefits in diagnosing and treating multifactorial infectious diseases (Brar et al., 2022; Majumder & George, 2023; Majumder et al., 2022). However, effective nano-enabled strategies for mastitis treatment are still an untapped area of research and application.

This review examines the host and pathogen-related factors leading to mastitis, current disease management strategies, and their limitations, and ultimately proposes unique benefits of nano-enabled antibacterial combination therapy to combat bovine mastitis.

2.2. Risk factors associated with bovine mastitis

Treatment of bovine mastitis is challenging due to several factors involving the host, pathogen, and environment **(Figure 2.1)**. Major host factors implicated are the age of the animal (parity), lactation stage, breed, unique anatomy of the mammary gland, and immune surveillance. Pathogen-related risk factors include microbial load, virulence, frequency of exposure, tissue adherence and invasion (conferring pathogens with the ability to withstand milk flush), adaptability (conferring bacteria to jump to and fro from animals to human/other hosts), and the acquisition of AMR characteristics (A. J. Bradley, 2002). Besides, environmental factors such as the type of milking machine, hygiene measures, nutrition, climate, season, management practices, and housing conditions are also determining factors in the causation of IMI (Sordillo & Streicher, 2002). The frequency and severity of mastitis depend upon the dynamic interplay of these factors and, thus, vary from farm to farm. Subsequent paragraphs examine how these factors challenge antibiotic treatment regimes and are critical for designing effective nano-enabled antibacterial strategies for treating bovine mastitis.

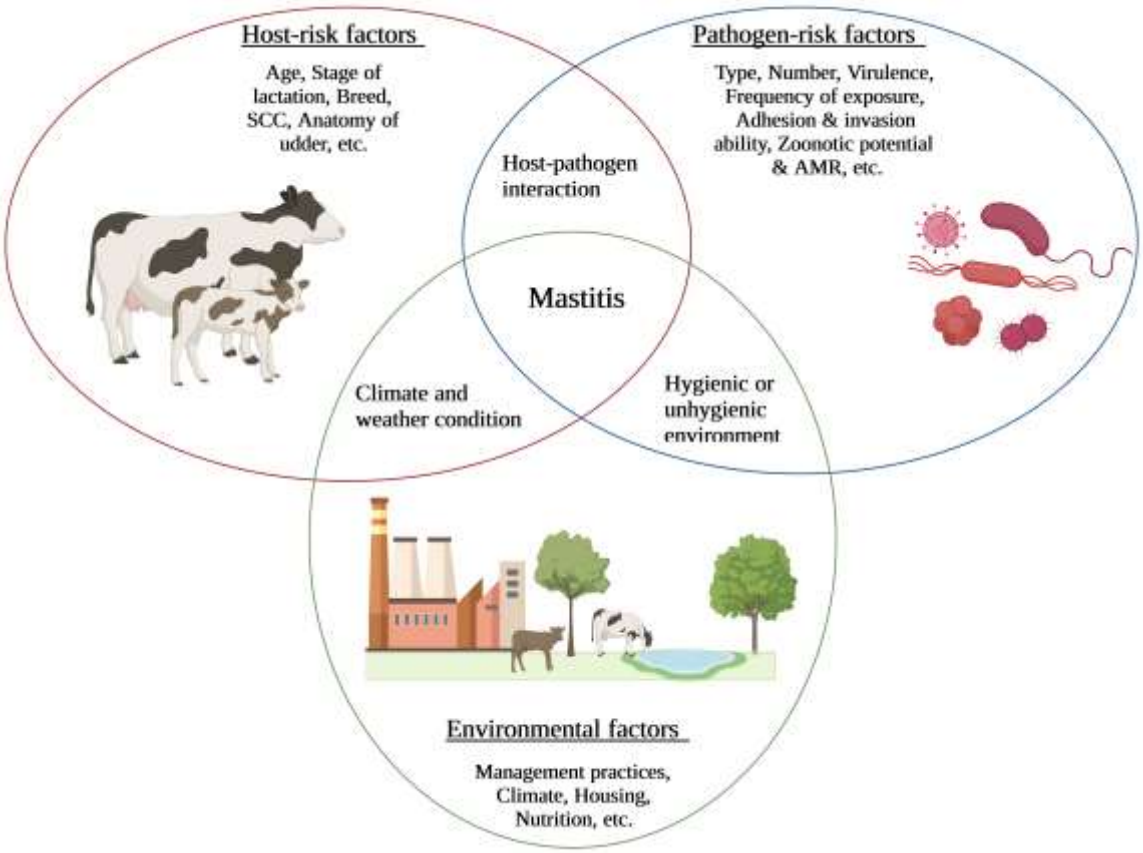

Figure 2.1. Risk factors associated with bovine mastitis. The severity and the responsiveness of mastitis to treatment depend on the dynamic interplay between the host (age, lactation stage, breed, immune competence, etc.), pathogen (microbial load, virulence, frequency of exposure, etc.), and environmental (hygiene measures, nutrition, climate, management practices, housing, etc.) factors.

2.2.1. Host-related factors associated with bovine mastitis

The anatomical and functional characteristics of the bovine mammary gland are related to udder health, and understanding its morphology is vital for designing treatment strategies for IMI **(Figure 2.2)**. The mammary gland is a highly vascularized structure that meets the high demand for transporting fluids and nutrients (Nichols, 2022). It starts developing in the fetal stage (Nichols, 2022). The connective tissue and fat invade the small primitive quarters resulting in the development of the milk ducts and the milk-secreting tissues under the influence of estrogen between puberty and parturition (Nichols, 2022). The formation of teats starts in the second month

of gestation and continues till the sixth month (Nichols, 2022). Prolactin hormone stimulates the lactocytes for milk production. Between 60-80% of the milk gets stored in the lobule (group of alveoli), milk ducts, and udder, while the teat cistern holds the rest ("Anatomy of the mammary gland," 2022). The vascular endothelium plays a vital role in the development of the mammary gland and initiates and sustains the production of milk (Andres & Djonov, 2010). The thin and single-layered mammary capillary endothelial cells form a semipermeable barrier and support the transfer of serum components to maintain the supply of O_2, removal of CO_2, and exchange of solutes and macromolecules for maintaining healthy cellular metabolism (Andres & Djonov, 2010). These cells facilitate the transfer of blood-derived components (e.g., amino acids and glucose) required for the robust synthesis and secretion of milk (Mattmiller, Corl, Gandy, Loor, & Sordillo, 2011). Moreover, endothelial cells regulate blood fluidity, vascular tone, and vascular permeability to assist vasculature and underlying milk-producing tissues **(Figure 2.2)** (Prosser, Davis, Farr, & Lacasse, 1996). During the initial stages of bacterial invasion, the vascular endothelium plays a significant role in the host defences in mammary tissues (Ryman, Packiriswamy, & Sordillo, 2015). Abnormal inflammatory responses lead to endothelial leakiness leading to excessive accumulation of leukocytes at the infection site, escalated leakage of plasma proteins, and disruption in the blood flow. This ultimately causes damage to the mammary tissues **(Figure 2.2)** (Ryman et al., 2015). Overall, these changes also affect the stability, absorption, and efficiency of mastitis therapeutics.

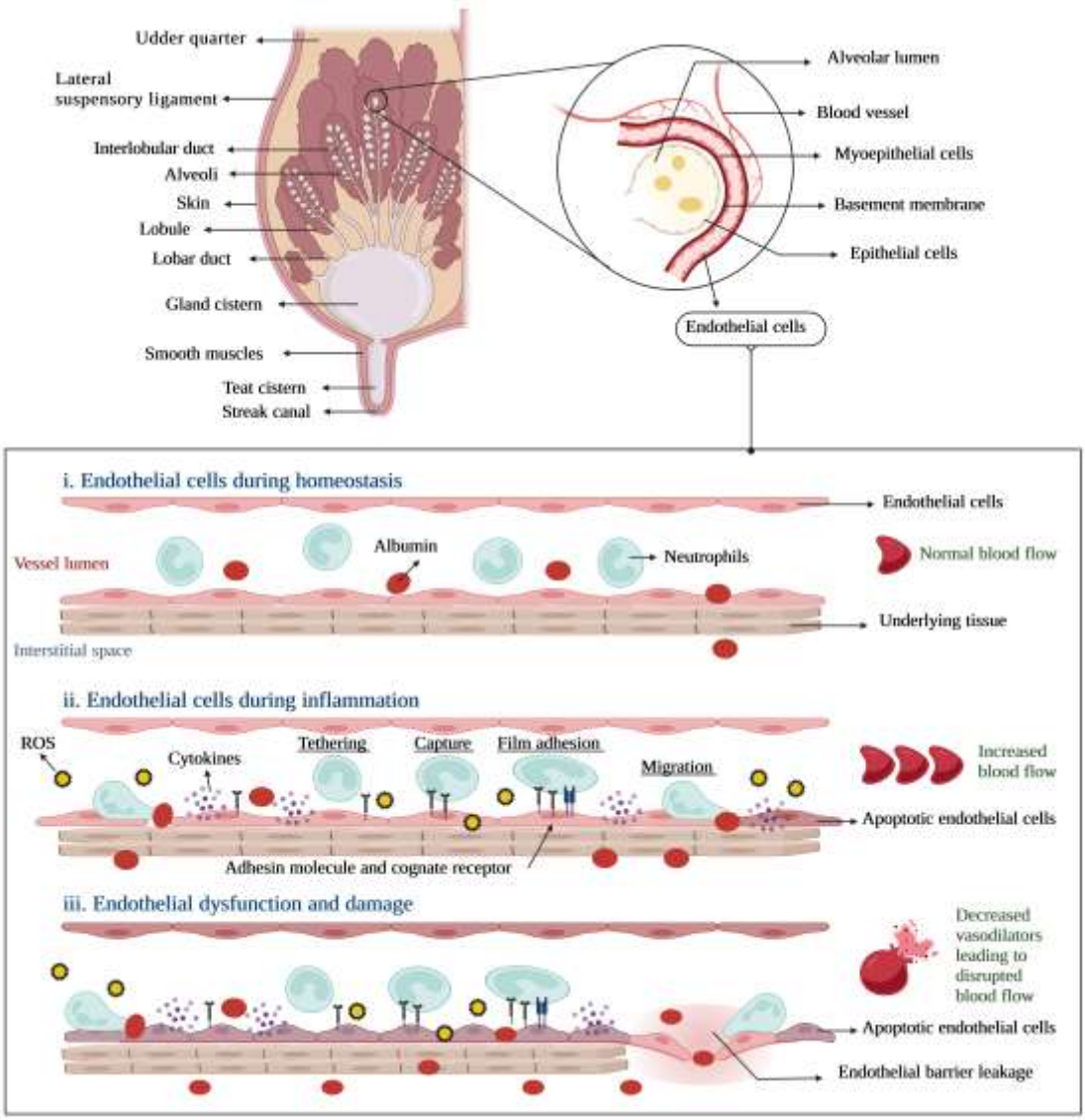

Figure 2.2. Schematic illustration of the anatomy of the udder and consequence of mastitis in the endothelial barrier (Modified from Ryman *et al.*). (Ryman et al., 2015) (i) Endothelial cells possess a favorable vascular permeability with adequate leukocyte migration during homeostasis. Meanwhile, at the onset of (ii) inflammation, the endothelial cells promote bacterial clearance by expressing adhesion molecules, ROS generation, cytokines, and vasoactive lipid mediators (Ryman et al., 2015). (iii) Restricted immune responses activate endothelial cells and accumulate neutrophils contributing to oxidative stress, free radicals, and lipid hydroperoxides, causing irreversible cell damage and apoptosis (Ryman et al., 2015).

In a healthy animal, smooth-muscled sphincter cells seal the teat canal to avoid milk flow and prevent the invasion of pathogens. The teat lining produces keratin that restricts bacterial invasion of the tissues owing to its bacteriostatic action. However, physical injury to the keratin or mucous membrane lining the teat makes the teat vulnerable to bacterial invasion, colonization,

and infection by one or more mastitis pathogen/s. As detailed by Akers *et al.*, (Akers & Nickerson, 2011) the establishment of the infections occur in the following steps: (i) bacteria infiltrate the teat duct of a mammary quarter (usually during the milking process and inter-milking period); (ii) they colonize, infect, and multiply in the teat and gland cisterns, and advance to the milk-producing tissues; (iii) they adhere to the mammary gland tissues and show persistence inside the gland, ideally during lactation; (iv) lastly, they enter small ducts and alveolar areas of the ventral portions of the gland *via* milk currents.

Cattle are more prone to IMIs during the transition period or at parturition and the first month of lactation ensuing immunosuppression, associated with increased oxidative stress and decreased antioxidant defence (N. Sharma, Singh, Singh, Pandey, & Verma, 2011). The udder continues to increase in the amount of secreting tissue, or the number of secreting cells, and size throughout the first five lactations, which also increases the capacity of milk production (Nichols, 2022). Synthesis of colostrum and milk during lactation demands a higher level of energy and nutrient supply. Consequently, the deficiency of trace elements, amino acids, and vitamins in the diet can lead the cattle to exhibit negative energy balance and immunosuppression at a cellular and humoral level, making them more prone to infectious diseases such as mastitis (Shaheen et al., 2016).

The innate immune system of the host responds to invading pathogens by mounting cellular defence (e.g., leukocytes), humoral defence (e.g., immune-modulating factors like pro- and anti-inflammatory cytokines, lactoferrin, transferrin, *etc.*), generation of ROS, and a vast range of antimicrobial peptides and proteins (Stelwagen, Carpenter, Haigh, Hodgkinson, & Wheeler, 2009; Uthaisangsook, Day, Bahna, Good, & Haraguchi, 2002). Macrophages are the predominant leukocyte that carries out vital functions such as detecting invading pathogens, restriction of infection establishment, and induction of inflammatory responses (Akers & Nickerson, 2011). Consequently, mastitis is characterized by the presence of unusually high milk

somatic cell count (MSCC). A healthy cow with uninfected glands typically contains <200,000 cells per mL of milk constituted by epithelial cells, macrophages, and neutrophils (Akers & Nickerson, 2011). This, however, could increase to >400,000/mL depending on the stage and severity of IMI (El-Tahawy & El-Far, 2010). Notably, the dissolved oxygen level in milk dips during IMI as oxygen is consumed by the increased somatic cell population in IMI milk (Wittek, Mader, Ribitsch, & Burgstaller, 2019).

Bacteria and their by-products trigger macrophages to release chemo-attractants that recruit polymorphonuclear neutrophils (PMNs) to the site of invasion to provide the second line of innate immune protection (Campos et al., 2022). The intracellular granules of PMNs contain several bactericidal peptides, such as defensins, and neutral and acidic proteases (such as elastase, cathepsin, and procathepsin) that can inhibit a variety of mastitis pathogens (Bank & Ansorge, 2001; Linde et al., 2008). Mastitis milk proteases hydrolyze casein, gelatin, collagen, hemoglobin, lactoferrin, and mammary gland membrane proteins (Mehrzad et al., 2005). The lack of specificity of the released oxidants and proteases causes major negative impacts as they often degrade milk casein and cause milk putrefaction. The lactoferrin (iron-binding protein) concentrations in bovine milk released at the sites of infection increase due to the influx of neutrophils during inflammation (R. M. Bennett & Kokocinski, 1978). In addition, a decrease in the citrate-bound iron in milk is observed during mastitis, which otherwise remains abundant during early lactation. Citrate forms a ferric citrate complex by competing with lactoferrin for iron (Carlson, Erickson, & Wilson, 2020; Garnsworthy, Masson, Lock, & Mottram, 2006). Bacteria extract iron from host-iron complexes (heme, lactoferrin, or transferrin) by producing siderophores with a higher affinity for iron (Carlson et al., 2020). Iron is an essential element for the survival of bacteria in mammalian tissue environments. Therefore, strategies that restrict bacterial assimilation of iron could have profound implications in determining the success of mastitis treatment. Studies have reported an increase in pH (up to 7.5), electrical conductivity, malondialdehyde, whey proteins contents

(including acute phase proteins such as haptoglobin and mammary amyloid A), and a decrease in lactose, fat, casein, potassium, calcium, magnesium, phosphorous, iron, zinc, urea, and nitrogen in mastitis milk (Eckersall et al., 2001; Kayano et al., 2018). Further, the release of hydroxyl radicals by immune cells could damage the epithelium leading to decreased milk secretion by the mammary gland during IMI. These factors unique to bovine mastitis often interfere with the half-life of drug molecules (Bourzac, 2012; Hubbell & Chilkoti, 2012) and thus warrant special attention when designing effective nano-therapeutics to treat IMI.

2.2.2. Environmental factors associated with bovine mastitis

The prevalence of mastitis pathogens may vary depending on the prevailing environmental conditions of different geographical locations and herd management practices (Oliver & Mitchell, 1984). Contaminated floors, feed and/or milking machines, wet bedding, poor ventilation, high stocking density, and a hot and humid climate contribute to harboring and exposure to mastitis pathogens (Shaheen et al., 2016; Zeinhom, Abdel Aziz, Mohammed, & Bernabucci, 2016). Usually, pre-milking sanitation involves washing udders and teats with water or disinfectants, however, poor water quality and the rise of disinfectant resistance in bacteria (Schwaiger et al., 2014) could contribute to pathogen exposure and induction of IMI. In milking machines, the effects of vacuum fluctuations and milking duration have been reported to cause physical discomfort and contribute to spreading mastitis among cows (Ruegg, 2017). Cow manure harbors a wide range of pathogenic and non-pathogenic microorganisms, making it a major source of pollution in the environment triggering infection among cows and zoonoses in case of a spill (Manyi-Loh et al., 2016). During the milking of the cow, the sphincter muscles relax, allowing the orifice to open. The teat canal remains open for an hour after milking, allowing bacterial entry. The post-milking germicidal teat dips, the presence of antibacterial epidermal tissue lining the teat

meatus (forming a keratin plug), and hygienic management are thus essential to avoid infection (M. Khan, Weary, & Von Keyserlingk, 2011).

2.2.3. Pathogen-related factors associated with bovine mastitis

Mastitis pathogens are differentiated into contagious and environmental pathogens based on their variability in natural habitat and mode of transmission to the bovine mammary glands (Calvinho & Oliver, 1998). Environmental pathogens are tough to control as they are abundant in the surrounding environment and are often transmitted to the cow mammary glands. These types of pathogens include coliform bacteria (*Escherichia coli, Klebsiella* sp.*, etc.),* environmental *Streptococcus sp.* (*Streptococcus uberis, Streptococcus zooepidemicus, Streptococcus agalactiae, etc.)*, environmental coagulase-negative *Staphylococcus* sp. (*S. chromogenes, S. epidermidis, etc.), Pseudomonas sp.*, *Proteus sp.*, *Listeria sp.*, Yeast, *etc.* (O. Dego, 2020). Meanwhile, contagious mastitis pathogens include coagulase-positive *Staphylococcus aureus, Streptococcus agalactiae, Corynebacterium bovis*, and *Mycoplasma bovis,* which harbor on the teat skin and transmit from infected to the non-infected udder during the milking process, usually from milker's hand or milking machine liners (O. Dego, 2020).

S. aureus, *E. coli*, *Klebsiella pneumoniae*, *Mycoplasma bovis*, and *Streptococcus agalactiae* are the most prevalent organisms associated with bovine mastitis (Shaheen et al., 2016; Sugiyama et al., 2022). While *E. coli* multiplies rapidly, *Streptococcus agalactiae* and *S. aureus* show adherence to the tissues lining the milk-collecting spaces (Burvenich, Van Merris, Mehrzad, Diez-Fraile, & Duchateau, 2003; Jensen et al., 2013). An increased level of neutrophil chemoattractants and the cytokines IL-1ß, IL-6, IL8, and TNF-α are associated with inflammation in the mammary gland (M. Z. Khan et al., 2020). Specifically, the expression levels of two NF-κB-dependent cytokines: IL8 and granulocyte/macrophage colony-stimulating factors are associated with the regulation of neutrophilic inflammation (M. Z. Khan et al., 2020). Studies

have shown higher IL8 and TNF-α expression levels in the mammary epithelial cells infected by Gram-negative bacteria such as *E. coli*, provoking a strong inflammation of the udder. This results in the activation of host immune defence *via* pathogen receptor-driven activation of IκB/NF-κB signaling leading to the eradication of the pathogens in most incidences (Burvenich et al., 2003; Jensen et al., 2013). In contrast, Gram-positive bacteria such as *S. aureus* induce a weaker inflammation and host immune response due to weak lipoteichoic acid induction or activating the wnt/β-catenin cascade, suppressing NF-κB signaling (M. Z. Khan et al., 2020). This ability of *S. aureus* contributes significantly to their invasion into host epithelial cells, persistence, and causing chronic infection (Günther et al., 2017b). Further, mastitis pathogens may possess AMR and virulence characteristics such as biofilm formation, serum resistance, hemolysin, and intracellular survivability that lead to persistent IMI, making the treatment and prevention of mastitis challenging (J.-H. Fairbrother et al., 2015; Majumder, Jung, Ronholm, & George, 2021; Veh et al., 2015).

2.2.3.a. Antimicrobial resistance and virulence traits in mastitis pathogens

Antimicrobials have been used extensively since the 1930s in livestock to avoid infectious diseases and improve animal productivity . Despite the benefits, the extensive use of antibiotics in food-producing animals constitutes public health concerns due to the potential emergence and spread of AMR among bacteria (O. K. Dego, 2020). In the US, Canada, the UK, *etc*. (with some exceptions like the Netherlands and Nordic countries), intramammary infusion and parenteral administration of antibiotics to dairy cows (blanket dry cow therapy) is a routine practice during the dry period regardless of their health status (Huey et al., 2021; Ruegg, 2017; *USDA APHIS. Antibiotic use on U.S. dairy operations, 2002 and 2007*). According to the United States Department of Agriculture (USDA), the common antibiotics in use to treat mastitis include cephalosporins (53.2%), lincosamide (19.4%), and non-cephalosporin β-lactam antibiotics

(19.1%) (*USDA APHIS. Antibiotic use on U.S. dairy operations, 2002 and 2007*). Non-selective blanket antimicrobials used as prophylactic control often impart selective pressure on mastitis pathogens and commensal bacteria that inhabit the animal host (Barbosa & Levy, 2000). This selective pressure can lead to AMR, leading to microbial persistence and spread among animals and occasionally to humans through farm environments and food products (Normanno et al., 2007). Moreover, mastitis isolates possessing intrinsic or acquired resistance mechanisms could limit drug uptake, inactivate/modify a drug, or induce efflux/beta-lactamase activities resulting in treatment failures **(Figure 2.3)** (Reygaert, 2018).

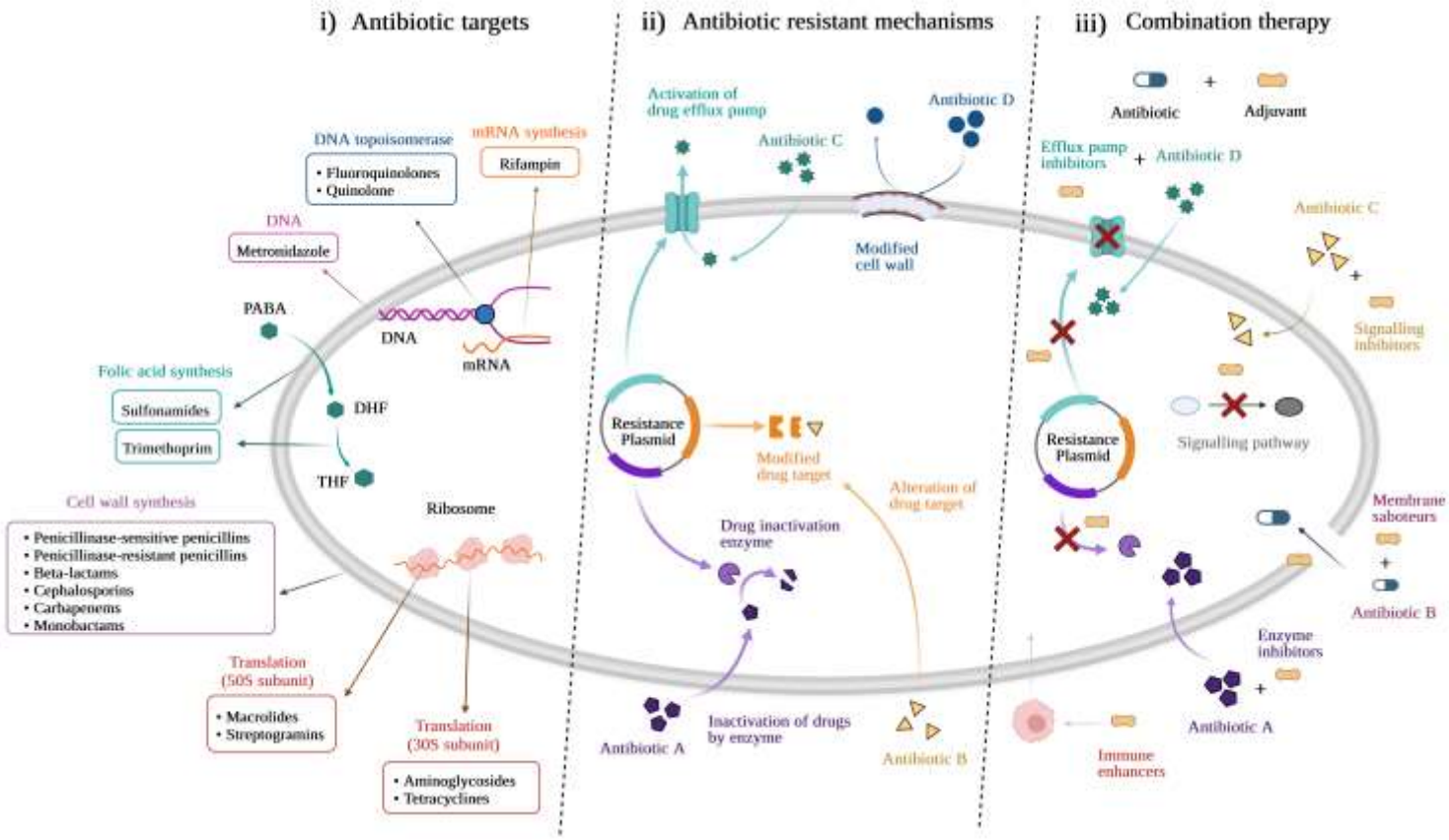

Figure 2.3. Antibiotic targets, resistance mechanisms in bacteria, and the potential of combination therapy against resistance. i) Antibiotics in mastitis treatment usually exploit five bacterial targets, including cell wall synthesis (beta-lactam, cephalosporins), protein synthesis (aminoglycosides, macrolides, tetracyclines), ribonucleic acid synthesis (rifampicin), desoxyribonucleic acid (quinolone, fluoroquinolone), and intermediary metabolism (sulfonamides, trimethoprim). ii) In response to antibiotics, mastitis pathogens show resistance mechanisms, including efflux pump activity, drug target modification, drug inactivation, and drug

uptake limitation. iii) Combination therapy, i.e., combining antibiotic/s and adjuvant molecules (efflux pump/signalling/enzyme inhibitors, metabolism saboteurs, immune enhancers, etc.) with synergistic properties, show potential against multi-drug resistant mastitis pathogens.

The ability to adhere and form biofilms protect pathogens against hostile environmental threats, the host's immune system, and antibiotic treatments **(Figure 2.4)** (Almeida, Matthews, Cifrian, Guidry, & Oliver, 1996). Biofilm formation bestowing selective advantages in mastitis pathogenesis is a notable characteristic of bacterial strains isolated from bovine mastitis (Fox, Zadoks, & Gaskins, 2005). Isolates of *S. aureus* from dairy cows possess a fibronectin-binding protein that helps tissue adhesion (Lammers, Nuijten, & Smith, 1999). Studies have pointed out various mechanisms of AMR in biofilm bacteria. This includes poor diffusion of antibiotics in the biofilm matrix, presence of persister cells, and slow growth rate of biofilm bacteria that limit the action of antibiotic (Anderl, Franklin, & Stewart, 2000; Lewis, 2007; Walters et al., 2003). The sharing of AMR genes is more frequent among bacterial communities in biofilm facilitated through the horizontal transfer of genes (Mah, 2012). Interestingly, subinhibitory concentrations of several antimicrobial agents, especially enrofloxacin, have been reported to induce biofilm formation (Bernardi et al., 2021; Costa, de Freitas Espeschit, Pieri, dos Anjos Benjamin, & Moreira, 2012). Costa *et al.* attributed this resistance mechanism to 'persister cells' in biofilm communities (Costa et al., 2012). Another interesting observation is the correlation between efflux pumps in bacteria, such as *Pseudomonas* sp., *E. coli, etc*., and their biofilm-forming ability (De Kievit et al., 2001; Kvist, Hancock, & Klemm, 2008; Majumder et al., 2021). Bay *et al.* reported that compared with the wild-type control, the *E. coli* strain that lacked an RND efflux system displayed a significant reduction in biofilm formation and showed susceptibility against antimicrobials (Bay, Stremick, Slipski, & Turner, 2017). This relation between biofilm-forming ability and efflux activity could be used for designing therapeutic strategies. The composition of milk and the intramammary environment during the infection also influence the formation of biofilms (Atulya, Mathew, Rao, & Rao, 2014). For instance, the concentration of dipotassium

hydrogen phosphate retard the biofilm formation of *S. aureus*, while a decrease in pH favors biofilm formation (Atulya et al., 2014).

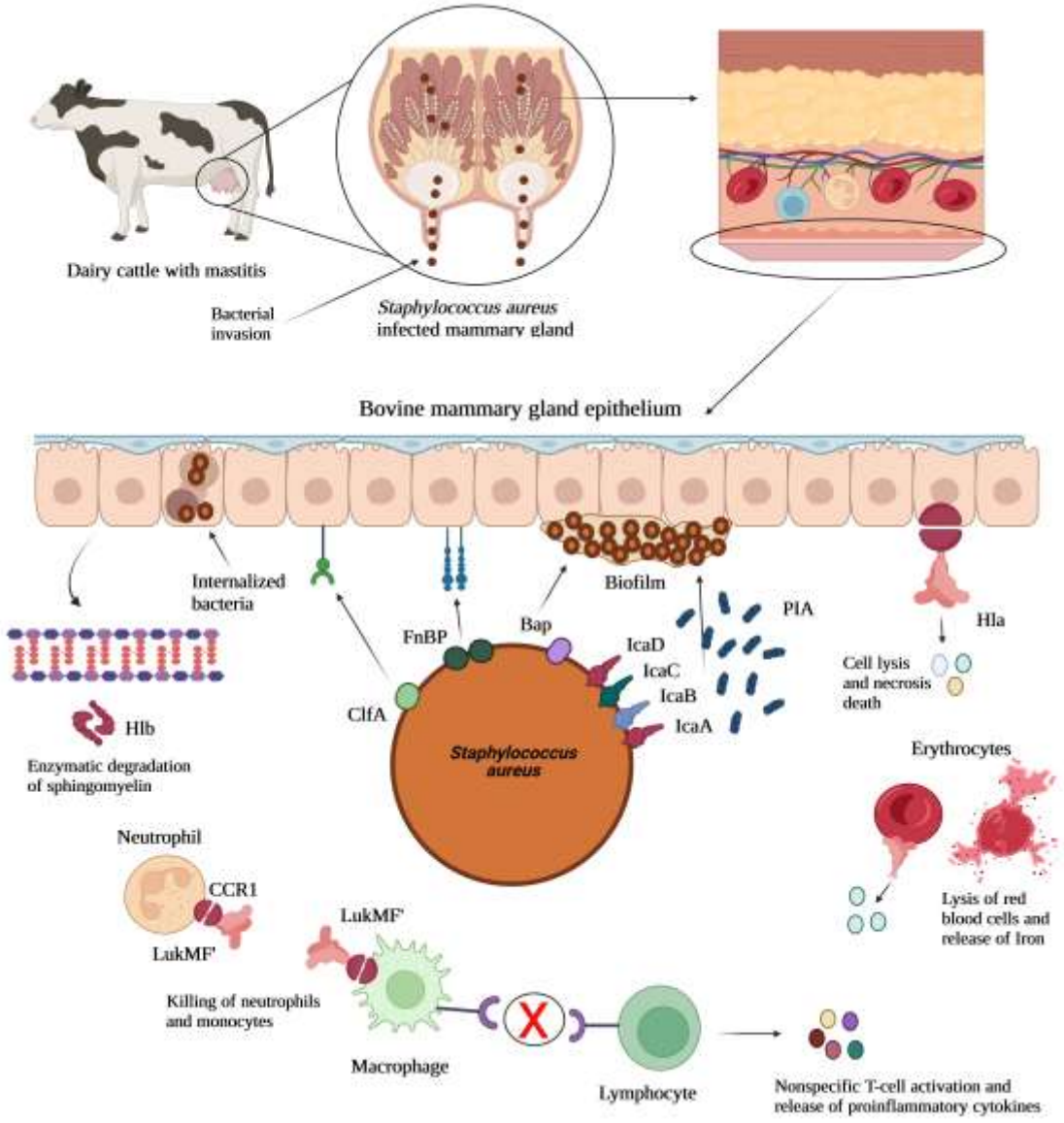

Figure 2.4. Virulence characteristics of *S. aureus* associated with bovine mastitis (Modified from Campos *et al.*) (Licensed under a Creative Commons Attribution 4.0 International License: http://creativecommons.org/licenses/by/4.0/) (Campos et al., 2022). The surface proteins of *S. aureus* interact with host proteins enabling their adhesion and invasion within mammary epithelial cells. Biofilm-associated protein (Bap) and intracellular adhesin (ica) locus play a significant role in the biofilm formation and internalization pathway, also mediated by FnBP (Campos et al., 2022). Hemolysins induce necrosis of the mammary gland tissues and disintegrate bovine erythrocytes (Campos et al., 2022). Leukotoxins bind to neutrophils. The staphylococcal superantigens activate the T-cells enabling pro-inflammatory cytokine release inducing inflammatory responses in the udder (Campos et al., 2022).

The extensive use of heavy metals such as copper, zinc, and silver in antiseptics, therapeutics, and animal feeds to improve reproductive functions could contribute to the emergence of metal resistance among farm isolates of bacteria (Becerra-Castro, Machado, Vaz-Moreira, & Manaia, 2015; S. George, Tay, Phue, Gardner, & Sukumaran, 2019; Pal, Bengtsson-Palme, Kristiansson, & Larsson, 2015). For instance, recently, our group reported the resistance of *E. coli* isolates to copper, zinc, and silver (Majumder et al., 2021). Notably, heavy metals are reported to induce the expression of efflux pumps and other stress responses in bacteria, including biofilm formation, production of extracellular polymeric substances (EPS), and development of resistance genes and signaling pathways (S. George et al., 2019; Prabhakaran, Ashraf, & Aqma, 2016). The promiscuous activity of efflux pumps on antibiotics and general stress coping mechanisms complicates the management of AMR characteristics. For instance, despite having strong antibacterial properties, a sub-lethal concentration of silver was reported to increase cell proliferation and biofilm formation in *E. coli* and *S. aureus* because of the hormetic effect (George, Teo, Majumder, Chew, & Khoo, 2020). Moreover, repeated exposure to sub-lethal silver has been reported to enhance efflux activity and biofilm-forming ability in bacteria (Yang & Alvarez, 2015).

2.2.3.b. Intracellular survival of mastitis pathogens

Mastitis pathogens, especially *S. aureus,* show intracellular survival and multiply within mammary epithelial cells of the lactating udder parenchyma **(Figure 2.4)** (Majumder, Sackey, et al., 2023; Renna et al., 2019; Zaatout, Ayachi, & Kecha, 2019). This ability of bacteria protects them from host immune responses and makes them inaccessible to antimicrobials (Barkema, Schukken, & Zadoks, 2006; Garzoni & Kelley, 2009). Internalization of *S. aureus* in the bovine mammary gland is facilitated through ligand-mediated endocytosis (Dziewanowska et al., 1999; Bhanu Sinha & Fraunholz, 2010). The cellular uptake of bacterial cells starts with docking

fibrinogen-binding proteins (FnBP) to their specific receptor molecules on the host cell surface. These bindings trigger cytoskeletal rearrangements enabling bacteria to internalize into an endosome by a zipper-type mechanism (Foster, Geoghegan, Ganesh, & Höök, 2014; Günther et al., 2017a; Medina-Estrada, López-Meza, & Ochoa-Zarzosa, 2016). *S. aureus* invasion in epithelial cells involves rearrangement of the actin cytoskeleton (triggered by β1-integrin aggregation) *via* Rho GTPase activation, while *S. aureus* internalization within cells involves the interaction between FnBp and fibronectin through the α5β1 integrin bridge (Günther et al., 2017a; Josse, Laurent, & Diot, 2017; Ridley, Douglas, & Whawell, 2012). Intracellular bacteria exhibit several mechanisms to survive intracellularly. For instance, some bacteria may downregulate cytotoxins to extend their stay intracellularly and induce apoptosis, or some may escape from the phagosome into the cytoplasm (Tuchscherr et al., 2015). The biofilm-forming ability has also been reported to be associated with bacterial invasiveness (Berlutti et al., 2005; Latasa et al., 2005). Previous studies have reported that the polysaccharide capsules could mask surface adhesins and further confirmed a correlation between invasiveness and the absence of capsule polysaccharides (McKenney et al., 1998; Pragman, Yarwood, Tripp, & Schlievert, 2004). Recently, our group reported the ability of a library of mastitis *S. aureus* isolates from Canadian dairy farms to get internalized in human intestinal Caco-2 epithelial cells and cause intestinal infection in the *Caenorhabditis elegans* model (Majumder, Sackey, et al., 2023). Moreover, we showed that the antibiotics, including beta-lactams, cephalosporins, aminoglycosides, etc., which were effective during direct exposure, failed to remediate the intracellular infection (Majumder, Sackey, et al., 2023).

2.2.3.c. Metal scavenging ability of mastitis pathogens

Essential metals such as iron, zinc, copper, *etc.*, play a significant role in cellular functioning critical for bacterial survivability. The metal scavenging ability in *S. aureus*

contributes to surviving the host immune response and as a facultative intracellular pathogen. Studies have found that the genes responsible for metal homeostasis are also crucial virulence traits during IMI (Carlson et al., 2020). Mammary pathogenic *E. coli* strains that encode a specific receptor (Fec A) were reported to utilize ferric citrate as an iron source for survival (Blum et al., 2018; Olson, Siebach, Griffitts, Wilson, & Erickson, 2018). Similarly*, S. aureus* has been reported to produce staphyloferrin A and staphyloferrin B, two high-affinity iron-scavenging siderophores that contribute to virulence in murine kidney and intravenous infections (Carlson et al., 2020). Moreover, *S. aureus* may extricate iron from hemoglobin in the cytoplasm by the iron-regulated surface determinant (Isd) system (Mazmanian et al., 2003).

2.2.3.d. Persistence of pathogens as small colony variants

Another survival mechanism that mastitis bacteria such as *S. aureus* uses inside the mammary gland is the formation of small colony variants (SCVs) or a slow-growing population (Atalla et al., 2008; Proctor et al., 1998). SCVs, with their doubling time of 180 mins against 20 mins of wild strains, are difficult to be detected using conventional techniques as they are usually mixed with their parent strains (Proctor et al., 1998). SCVs of *S. aureus* are reported to survive within phagocytic cells without provoking cell-mediated immune response because of their ability to down-regulate the production of α-toxin (Brouillette, Martinez, Boyll, Allen, & Malouin, 2004; Bhanu Sinha & Fraunholz, 2010). Studies have confirmed that *S. aureus* SCVs exhibit a higher biofilm-forming ability and resistance to antimicrobials *in vivo* than the wild-type control (Brouillette, Martinez, et al., 2004; R. Singh, Ray, Das, & Sharma, 2009). For instance, Atalla *et al.* reported the killing of normal phenotype *in vivo* by high dosage of antimicrobials, while no significant reduction in the SCV phenotype population was observed, therefore, making SCVs a potential challenge in bovine mastitis treatment (Atalla et al., 2008).

2.3. Current strategies for controlling mastitis

2.3.1. Hygienic control measures

In 1969, the National Mastitis Council, USA, developed a 5-point program to address the challenges associated with mastitis and control its incidence rates. It involved; pre- and post-milking sanitization of (i) teats and (ii) milking equipment with antiseptic solutions, (iii) regular inspection of animals for potential infection, and early treatment of infected animals, (iv) dry cow therapy with antibiotics with prolonged retention rate to reduce existing infection and to prevent new IMI, and (v) culling of chronically infected animals (Neave, Dodd, Kingwill, & Westgarth, 1969). The program was further updated with additional guidelines such as establishing udder health goals and proper milking procedures, maintaining a hygienic, dry, and comfortable environment, and managing clinical mastitis during lactation (Middleton et al., 2014). A decrease in bacteria spreading, transmission, and subsequent infection by applying these hygienic strategies was observed, however, it still could not entirely prevent infections from establishing (Middleton et al., 2014).

2.3.2. Use of vaccines and antimicrobials

Common mastitis pathogens such as *S. aureus, S. uberis,* and *E. coli* are often targeted for vaccine development (Ismail, 2017). Vaccines are generally bacterins constituting inactivated bacteria or subunits of bacteria such as surface proteins, toxins, or polysaccharides (Merrill et al., 2019). The majority of the vaccines targeting coliform mastitis are composed of a Gram-negative core antigen that exhibits non-specific immunity against endotoxin or lipopolysaccharides (Merrill et al., 2019). Bacterins are reported not to prevent reinfection or new IMI but to show a remarkable reduction in their clinical severity (Hogan et al., 1995). Although vaccines such as J5,

Eviracor®J5 *E. coli* vaccine, and UBAC® *S. uberis* have been reported to reduce bacterial counts in milk and cow fatality and improve milk production, they achieved only partial reduction in clinical severity of mastitis (Allore & Erb, 1998; R Collado, Montbrau, Sitjà, & Prenafeta, 2018; Hogan et al., 1995). Moreover, two commercially available vaccines to combat *S. aureus*-mediated mastitis, namely Lysigin® in the United States and Startvac® in Europe and Canada, have shown a reduction in incidence, severity, and duration of mastitis but did not confer protection against reinfection (A. J. Bradley, Breen, Payne, White, & Green, 2015; Freick et al., 2016; Middleton et al., 2006; Schukken et al., 2014). In most other scenarios, the tested vaccines did not improve the udder health nor prevented the cows from reinfection or new *S. aureus* IMI (A. J. Bradley et al., 2015; Freick et al., 2016; Landin, Mörk, Larsson, & Waller, 2015; Schukken et al., 2014). The differences observed in these studies were mainly because of methodological differences such as vaccination schedules, route of vaccine administration, time of lactation, and challenge model. Bacteriocin-based teat disinfectant formulas involving bactofencin A, nisin, and reuterin have also been tested but failed to show >1 $\log_{10}$ reduction of the total bacterial counts on teat skin (S. Bennett, Fliss, Ben Said, Malouin, & Lacasse, 2022). Ster *et al.* developed a vaccine with recombinant proteins constituting Emulsigen®-D, a CpG oligodeoxynucleotide, and indolicidin which, when tested, exhibited a sustained reduction in MSCC, although didn't show any difference in the *S. aureus* count (Ster et al., 2021). Recently, Côté-Gravel *et al.* developed a genetically stable SCV to disable its ability to adapt and revert to the invasive phenotype and inactivated *vraG* gene, which is important for *S. aureus* virulence during IMIs. This study highlighted the potential application of this double mutant as a live-attenuated component in vaccines to cell-mediated immune responses against *S. aureus*-mediated IMIs (Côté-Gravel et al., 2016).

Mastitis treatments often involve antibiotics from cephalosporins, beta-lactams, and lincosamide. As mentioned in the preceding section, the prospects of antibiotics treatment to cure

IMI is dubious because of the rising AMR. For instance, the cure rate of *S. aureus*-mediated mastitis in cows is only about 37% (Scott McDougall, Clausen, Hussein, & Compton, 2022). The prevalence of AMR is increasing as studies reported that over 50% of mastitis, isolates show resistance properties to either beta-lactam drugs or penicillin (Ali et al., 2016; Freu, Tomazi, Filho, Heinemann, & dos Santos, 2022; Majumder et al., 2021). A possible transfer of resistance genes from human MRSA strains to bovines has also been reported (Feßler et al., 2010). The efficiency of some noteworthy antimicrobial agents and vaccines examined over the years against mastitis pathogens is provided in **Table 2.1** (Barkema et al., 2006; A. Bradley & Green, 2009; Rosa Collado, Prenafeta, González-González, Pérez-Pons, & Sitjà, 2016; Cortinhas, Tomazi, Zoni, Moro, & Veiga dos Santos, 2016; Côté-Gravel, Brouillette, & Malouin, 2019; Dingwell, Leslie, Sabour, Lepp, & Pacan, 2006; Federman, Ma, & Biswas, 2016; Fu et al., 2014; Gogoi-Tiwari et al., 2015; Gogoi-Tiwari et al., 2016; He et al., 2015; Liang et al., 2014; S. McDougall, 2003; S. McDougall, Agnew, Cursons, Hou, & Compton, 2007; S McDougall, Clausen, Hintukainen, & Hunnam, 2019; Oye, 1999; Prenafeta, March, Foix, Casals, & Costa, 2010; Pyörälä & Pyörälä, 1998; Roberson, Warnick, & Moore, 2004; Sérieys, Raguet, Goby, Schmidt, & Friton, 2005; Shephard, Burman, & Marcun, 2004; Taponen, Jantunen, Pyörälä, & Pyörälä, 2003; Truchetti, Bouchard, Descôteaux, Scholl, & Roy, 2014; Viveros, Lopez-Ordaz, Gutiérrez, Miranda-Calderón, & Sumano, 2018; Wraight, 2003; Zhao et al., 2018; Ziv & Storper, 1985).

Source	Compounds	Purpose	Mechanism of action	Efficiency
Plant-derived	Curcumin, Thymol, Baicalein	Attenuate inflammation stimulated by LPS	Suppress activation of TLR2, TLR4, NF-κB, and MAPK signaling pathways.	• Curcumin of 50 mg/kg reduced the infiltration of inflammatory cells by ~2-folds and attenuated the activity of myeloperoxidase (MPO) and the expression of TNF-α, IL-6, and IL-1β in the mastitis mice model (Fu et al., 2014).

compounds				• Thymol inhibited the production of TNF-α and IL-6 in LPS-stimulated mouse mammary epithelial cells by ~2.5 folds (Liang et al., 2014). • Baicalein of 20 mg/kg showed a reduction of ~2-folds in the mammary gland damage induced by LPS. It suppressed the activity of MPO, TNF-α, and IL-1β in the mastitis mice model (He et al., 2015).
	Citral, Linalool	Inactivation of *S. aureus*	Inhibits *S. aureus* growth and biofilm formation. Reduces adhesion and invasion in MAC-T by altering the expression of the virulence genes.	• Citral and linalool of 0.02 % and 0.12 %, respectively, inhibited *S. aureus* growth and pre-formed biofilms *in vitro*. A 0.12 % linalool downregulated the expression of *S. aureus* biofilm-forming genes (Federman et al., 2016).
	Baicalin	Inactivation of *E. coli*	Damages *E. coli* cell wall and alter drug-resistance genes.	• Minimum inhibitory concentration for Baicalin against *E. coli* was 4 mg/mL *in vitro*. Loss of genes including *qnrD*, *oqxA*, *qnrS*, bla_{SHV} 28.57%, bla_{TEM}, *oqxB*, and bla_{CTX-M} in some *E. coli* isolates was observed on the administration of 2 mg/mL of Baicalin (Zhao et al., 2018).
Synthetic and semi-synthetic compounds	Beta-lactams and Cephalosporins	Elimination of mastitis pathogens	*Act on penicillin-binding proteins (PBPs) responsible for bacterial cell wall synthesis.*	• A 56.5% and 14.3% cure rate against penicillin-sensitive and penicillin-resistant isolates, respectively, were observed after 4 days of penicillin G treatment at the quarter level (Ziv & Storper, 1985). Methicillin eliminated 32.4% of penicillin G-resistant *S. aureus* from the quarters (Ziv & Storper, 1985). • Penicillin G was administered parentally for 3-5 days in the quarters, and the cure rate against *S. aureus*, coagulase-negative Staphylococci, *Streptococcus dysgalactiae*, and *E. coli* evaluated after 3 weeks of treatment

				was 33.9%, 60.6%, 46.8%, and 74%, respectively (Pyörälä & Pyörälä, 1998). • Cloxacillin demonstrated a cure rate of 47-53% against *S. aureus*-mediated mastitis cows (Dingwell et al., 2006; Shephard et al., 2004). • The bacteriological cure rate by amoxicillin administered for 1.5 days ranged between 45-67%, respectively (Roberson et al., 2004). • 2nd generation cephalosporins such as cefuroxime with cloxacillin demonstrated a cure of 52.4% and 12.5%, respectively, against *S. aureus* mastitis (Wraight, 2003). • 3rd generation cephalosporin, ceftiofur, when administered to mastitis cow for 2 to 8 days, has shown a bacteriological cure of 32% and 61%, respectively. Specifically, 64% and 82% on the 2nd and 8th days, respectively, were observed against Streptococci, while 0% and 47% efficiency were observed against *S. aureus* on the 2nd and 8th days, respectively (Truchetti et al., 2014). • The resistance rate towards beta-lactam and cephalosporins has been reported to be between 30-70% in the USA and more than 85% in Ireland and Brazil (Barkema et al., 2006).
	Macrolides	Elimination of mastitis pathogens	Act as an inhibitor of protein synthesis by binding to the 50S subunit of bacterial ribosomes.	• Spiramycin was administered parentally for 3-5 days in the quarters, and the cure rate against *S. aureus*, coagulase-negative Staphylococci, and *Streptococcus dysgalactiae* evaluated after 3 weeks of treatment was 20%, 41.7%, and

				30%, respectively (Pyörälä & Pyörälä, 1998). • Tilmicosin demonstrated a cure rate of 74% against *S. aureus*-mediated mastitis cows (Dingwell et al., 2006). • Based on phenotypic testing, the resistance rate for macrolides such as erythromycin, spiramycin, and tilmicosin range between 14-17% (Barkema et al., 2006). • At the quarter level, Tylosin treatment showed a bacteriological cure rate of 83.8% (S. McDougall et al., 2007).
	Quinolone	Elimination of mastitis pathogens	Inhibits DNA and RNA synthesis by altering the action of DNA gyrase.	• Enrofloxacin was administered parentally for 3-5 days in the quarters, and the cure rate against *S. aureus* and *E. coli* evaluated after 3 weeks of treatment was 6.3% and 50%, respectively (Pyörälä & Pyörälä, 1998). • Enrofloxacin administration for 3 days in Mexican mastitis cows showed a bacteriological cure rate between 83-95% respectively (Viveros et al., 2018).
	Antimicrobial combinations	Elimination of mastitis pathogens	Antimicrobial synergistic effect arises from common or complementary interactions.	• A combination of amoxicillin-clavulanic acid demonstrated a cure rate of 5-31% against *S. aureus*-mediated mastitis cows (S McDougall et al., 2019; Taponen et al., 2003). • Combinations of lincomycin-neomycin and ampicillin-cloxacillin showed a bacteriological cure rate of 41.2% and 15.4%, respectively (Oye, 1999). • Combinations of penicillin-dihydrostreptomycin were administered thrice at 12 h intervals, and the cure rate assessed from milk collected on the 21st day after

				treatment was 76.7% (S. McDougall, 2003). • Combinations of cloxacillin-ampicillin have shown a cure rate of 24%, 71%, 53%, and 75% against *S. aureus*, *S. uberis,* Coagulase-negative staphylococci, Enterobacteriaceae including *E. coli*, respectively (Sérieys et al., 2005). • Combinations of cefalexin-kanamycin have shown a cure rate of 93.3%, 64.3%, 36.8%, 75%, and 69% against *E. coli*, *S. uberis*, *S. aureus*, *Enterococcus* spp., and *S. dysgalactiae,* respectively after 25 days of treatment (A. Bradley & Green, 2009). • Combinations of tetracycline-neomycin-bacitracin-prednisolone, when administered for 4 days, have shown a cure rate of 67%, 87%, 62%, and 70% against *Klebsiella* spp, *S. uberis*, *Streptococcus agalactiae*, and *S. aureus*, respectively (Cortinhas et al., 2016).
S. aureus	Vaccine - Protein A encoded by the *spa* gene	Reduction in *S. aureus* biofilm formation	Boosts humoral immune response by producing antibodies to neutralize Fcγ/Fab binding characteristics of SpA.	• Protein A showed a significant reduction ($p<0.05$) in bacterial loads of the mammary glands of mice; however, it failed to protect immunized mice post-challenge with biofilm-producing encapsulated *S. aureus* (Gogoi-Tiwari et al., 2016).
	Vaccine - Bacterin with Slime associated antigenic complex (SAAC)	Protection from *S. aureus* mastitis	Triggers the production of antibodies to poly-*N*-acetyl β-1,6 glucosamine surface polysaccharide (PNAG).	• *S. aureus* bacterin with high SAAC content significantly enhanced antibody titers against SAAC and reduced *S. aureus* load in milk during the post-challenge period. However, no difference between the vaccinated and control groups was observed in the clinical signs of mastitis following the

				challenges indicating failure of the vaccine to prevent *S. aureus* IMI (Prenafeta et al., 2010).
	Biofilm vaccine	Immunogenicity and protective potential of biofilm vaccine for mastitis prevention	Triggers the production of IFN-γ.	• Mastitis mice immunized with the biofilm vaccine showed significant reductions in colonization by *S. aureus* in mammary glands. It further reduced the severity of clinical symptoms and tissue damage in mammary glands in comparison with the mice immunized with formalin-killed whole cells of planktonic *S. aureus* (Gogoi-Tiwari et al., 2015).
	Vaccine - Genetically engineered stable double mutant small colony variant (SCV)	Combat intracellular persistence and reduce chronicity or recurrence of infections	Triggers the production of IL-17 and IFN-γ.	• The live-attenuated SCV induced strong humoral and cell-mediated immune responses in immunized mice. The release of high concentrations of IL-17 and IFN-γ was observed when compared to other vaccination formulations (Côté-Gravel et al., 2019).
S. uberis	Vaccine – Cell wall proteins, including glyceraldehyde-3-phosphate dehydrogenase (GAPDH), fructose-biphosphate aldolase (FBA), and elongation factor Ts (EFTs)	Protection from *S. uberis* mastitis	Triggers the production of IgG antibodies.	• All three proteins induced IgG antibodies; however, a significant reduction of mortality was observed in mice vaccinated with FBA and EFTs (Rosa Collado et al., 2016).

Table 2.1. Efficiency of some noteworthy antimicrobial agents and vaccines examined over the years against mastitis pathogens.

From the preceding discussions on host-pathogen-environment factors dictating severity and treatment outcomes, an ideal curative for mastitis should possess the following characteristics: (i) stability in alkaline mastitic udder with low oxygen tension; (ii) evade host immune clearance; (iii) reach infection site in effective concentration; (iv) show adequate tissue retention; (v) able to target intracellular and persistent pathogens; (vi) effective against MDR strains of pathogens, (vii) be biocompatible, and (viii) should not lead to prolonged tissue retention or release undesired chemical residues in milk.

It is unlikely that a single drug molecule could possess all the qualities. Nanotechnology, which deals with manipulating matter at the nanoscale, has provided unprecedented advantages in many sectors. The small size and multifunctionality of nanomaterials have been utilized for the targeted delivery of drugs across biological barriers. The possibility of modifying the surface of nanomaterials presents opportunities for grafting molecules that specifically identify biological targets. Currently, the benefits of nanotechnology in medicine are harnessed primarily for the targeted destruction of cancer cells and in treating bacterial infections. We argue that nanotechnology could be utilized to co-deliver multiple drugs to eliminate recalcitrant infections involving multi-drug resistant pathogens from complex tissue environments such as the one present in bovine mastitis.

2.4. Nano-enabled Antibacterial Combination Therapy (NeACT) for mastitis treatment – a future perspective

Antibacterial combination therapy is defined as combining antibiotic/s and/or adjuvant molecules with synergistic properties to improve antibacterial treatment outcomes **(Figure 2.3)**. The benefit of combination therapy has already been exploited for the clinical management of medical conditions, such as cancer, cardiovascular, and infectious diseases (Worthington &

Melander, 2013). The mechanism of action of antibiotics-adjuvant combinations involves common or complementary interactions, including sequential inhibition of the same biochemical pathway, inhibition of bacterial antimicrobial-modifying enzymes, etc (Majumder et al., 2022). Phytochemicals such as tannic acid interferes with bacterial cellular metabolism, inhibit or delay virulence and adaptive resistance mechanisms. It has shown synergism with silver nanoparticles, cefotaxime, and rifampicin against a range of *Salmonella* spp. and *S. aureus* isolates (Dong et al., 2018; Kyaw, Arora, & Lim, 2012; Majumder et al., 2022). Essential oils such as cinnamon, peppermint, and oregano that act by disrupting the bacterial cell membrane have shown synergism in combination with antibiotics such as sulfamethoxazole, piperacillin, and chloramphenicol, respectively, against *E. coli*, *Salmonella* spp., and *S. aureus* isolates (Solarte et al., 2017; Yap, Lim, Hu, & Yiap, 2013). Efflux pump inhibitors, such as chlorpromazine, inhibit the Na/K and affect the proton pumps in the respiratory chain leading to reduced ATP generation, leading to the superior performance of tetracycline against MDR *Salmonella* spp. and *S. aureus* (Brar et al., 2022). Similarly, ß-lactamase enzyme inhibitors such as tazobactam combined with piperacillin and ampicillin have shown antibacterial synergism against MDR *Salmonella* spp., and *S. aureus* isolates (Brar et al., 2022; Bush & Bradford, 2016). While such strategies have been applied before in the biomedical and agricultural sectors, the challenges of poor bioavailability, cytotoxicity, stability, release, and overdosing have often restricted their widespread acceptance. These issues could be resolved by introducing nanotechnology-enabled approaches (Brar et al., 2022; S. George et al., 2019; Majumder et al., 2022). Nano-enabled Antibacterial Combination Therapy (NeACT) is defined as the therapeutic strategy aimed at harnessing the power of a nano-delivery platform to deliver more than one drug molecule with complementary function for effective mastitis treatment.

Nanomaterials, typically with one or more dimensions in size range between 1-100 nm, possess novel characteristics over their bulk counterparts in terms of biological activity **(Figure**

2.5.a) (Saji George, 2015; Majumder & George, 2023). The application of nanomaterials in intramammary drug delivery has distinct advantages (Algharib, Dawood, & Xie, 2020; W. Wang et al., 2015). For instance, nanomaterials can be used to encapsulate more than one drug molecule and increase the payload's pharmacological action (Gholipourmalekabadi et al., 2017; Pissuwan, Niidome, & Cortie, 2011). Specifically, in the context of IMI, the host-pathogen-environment factors could be made advantageous for the targeted and sustained delivery of drugs (W. Wang et al., 2015) **(Figure 2.5.b, 2.6)**. The following sections detail the general methodologies for preparing nanotherapeutics and the unique opportunities of nano-enabled strategies for mastitis treatment.

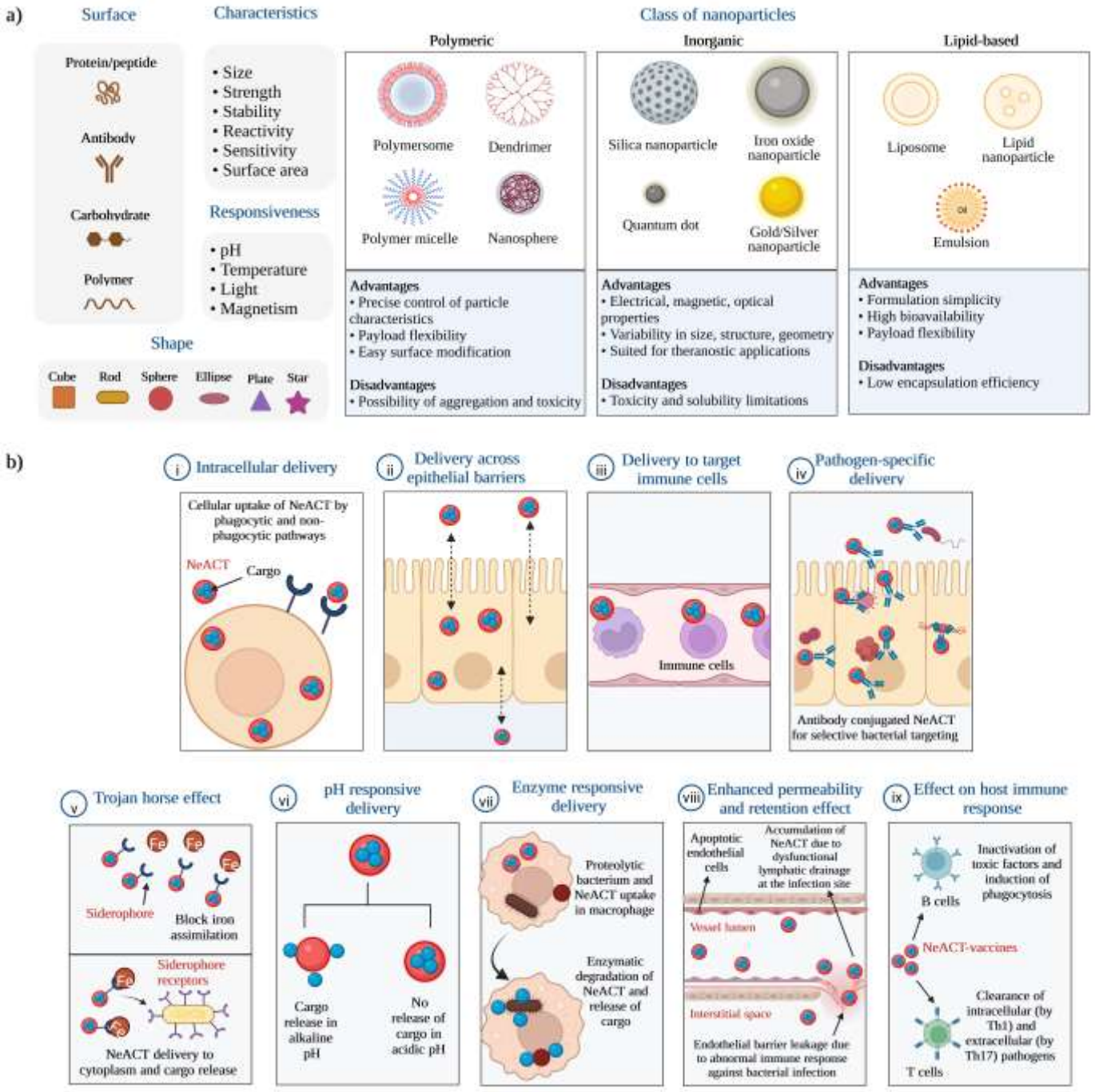

Figure 2.5. Classification of nanomaterials and potential attributes of Nano-enabled Antibacterial Combination Therapy (NeACT) in mastitis treatment. a) Different classes of nanomaterials, including polymeric, inorganic, and lipid-based, possess tunable shapes, surface chemistry, and physical properties that can be manipulated for superior cargo delivery to intramammary infection sites. b) For effective mastitis treatment, NeACT could be tuned for pathogen-specific delivery, intracellular delivery, delivery across epithelial barriers, pH/enzyme responsive delivery, targeted delivery to immune cells triggering host immune responses, trojan horse effect, and EPR effect.

2.4.1. Strategies for developing nano-enabled therapeutics

Nanotherapeutics have been developed through different strategies depending on the nature of the nanomaterials, the cargo, and the specific function for which they are designed. Major synthesis strategies include layer-by-layer deposition strategy, loading of cargo into preformed nanomaterial, or co-synthesize of nanomaterials with cargo.

Layer-by-layer (LbL) self-assembly to design multilayered nanocomposites is a versatile fabrication method driven by electrostatic interactions between oppositely charged multivalent compounds with complementary interactions. This strategy facilitates desirable incorporation and preservation of the biological activity of therapeutic agents, coating multiple substrates of variable physicochemical properties and exhibiting tuned, targeted, and/or responsive drug release behavior (Alkekhia, Hammond, & Shukla, 2020). Over the years, several techniques such as dipping, spraying, spin coating, electromagnetic, fluidic assembly, 3D printing, and micropatterning have been explored to employ LbL assembly (Alkekhia et al., 2020). Most frequently, synthetic polymers (such as polyethyleneimine, poly-l-lysine), naturally derived polymers (such as chitosan, alginate), macromolecules (such as proteins), micro-and nanomaterials, and inorganic materials (such as clay, graphene) are incorporated to implement this approach (Alkekhia et al., 2020). LbL systems constituting magnetic nanomaterials coated with gentamycin, tannic acid, and silver nanomaterials and capped with hyaluronic acid as a responsive shell exhibited dual-responsive release at low pH. The composite also enhanced the penetration of the particles into biofilm through magnetic field radiation overall, leading to a significant reduction in *S. aureus* and *E. coli* (X. Wang et al., 2018). Considering the potential, LbL self-assembly for nano-enabled therapeutic design for mastitis treatment holds significant promise.

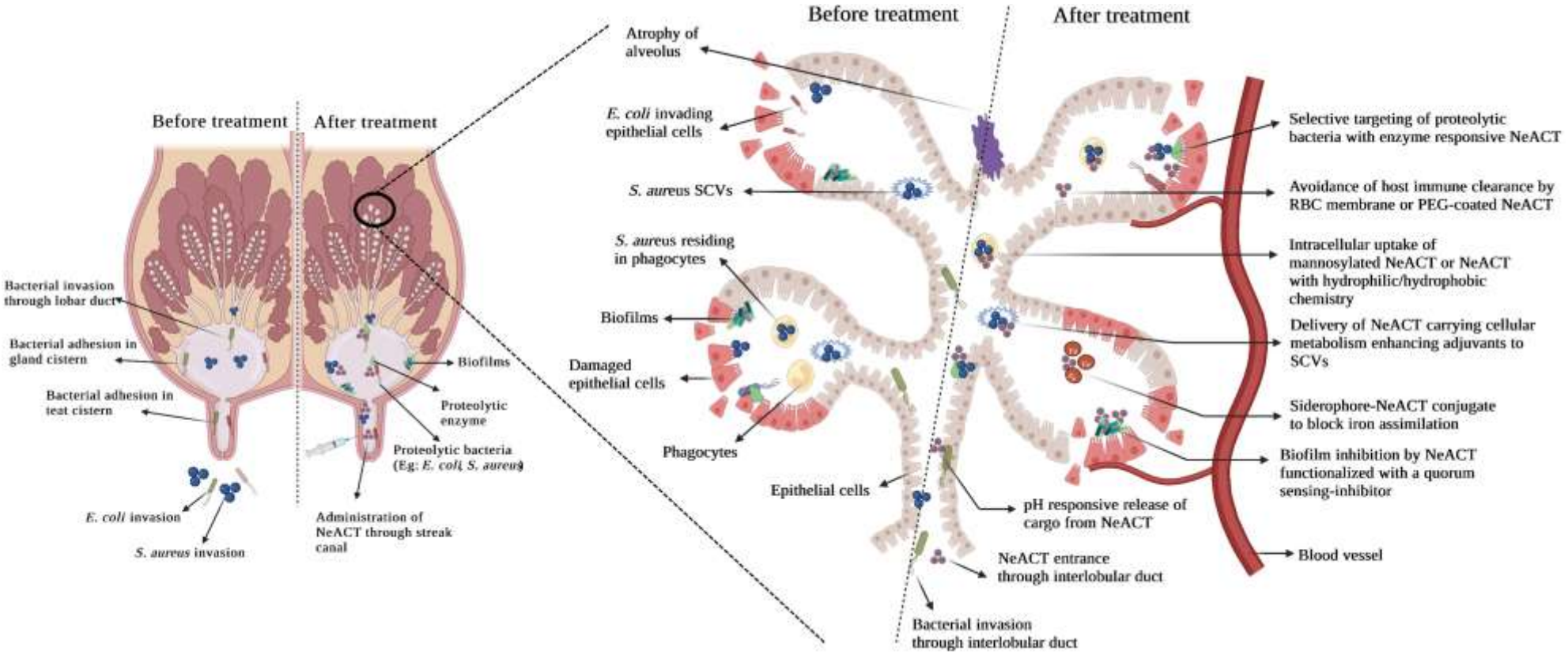

Figure 2.6. Schematic illustration of the application of Nano-enabled Antibacterial Combination Therapy (NeACT) for mastitis treatment. For effective mastitis treatment, i) RBC membrane or PEG-coated NeACT could be developed to avoid host immune clearance, ii) NeACT could be manipulated for cargo release in the alkaline mastitis udder through pH-responsive delivery, iii) NeACT could be tuned for selective targeting of proteolytic bacteria through enzyme-responsive delivery, iv) mannosylated NeACT or NeACT with hydrophilic/hydrophobic surface chemistry could be used for superior intracellular uptake, v) siderophore-NeACT conjugates could be used to block bacterial iron assimilation, vi) NeACT functionalized with quorum sensing inhibitors for biofilm inhibition, and vii) NeACT carrying cellular metabolism-enhancing adjuvants could be effective against SCV.

The strategy for drug design could also involve nanomaterials with ionic cores and specific hydrophobic/hydrophilicity chemistry of the shell with an ability to encapsulate more than one drug with variable polarity **(Figure 2.6)**. For instance, the hydrophobic core of cyclodextrin nanomaterials could be employed to encapsulate lipophilic molecules, while the water-miscible drug can be adsorbed on the hydrophilic external surface (Gadade & Pekamwar, 2020). Liposomes, self-assembled (phospho)lipid-based drug vesicles, on the other hand, contain an internal aqueous core and a lipid bilayer and thus can accommodate both hydrophilic and hydrophobic agents. Halloysite nanotubes, a tubular clay mineral with aluminosilicate chemistry, contain a positively charged lumen and a negatively charged external surface, thus enabling selective loading/adsorption of cargos with alternate surface charges (Majumder & George, 2023). Recently, our group reported the design of a nanocomposite of halloysite nanotube loaded with tannic acid and silver nanomaterials grafted on the surface. These particles showed excellent remediation of *Salmonella* infection in the *Caenorhabditis elegans* model resulting from the combinatorial effect of silver ions and tannic acid (Majumder et al., 2022). Fusion through electrostatic interaction of oppositely charged nanomaterials loaded with either an antimicrobial or adjuvant with opposite polarity could also be an alternate approach to facilitate combination therapy. The possibility of a 'dumbbell-shaped' chimeric nanocomposite constituting tetracycline-loaded chitosan and chlorpromazine-loaded silica nanomaterials as an example of NeACT against multi-drug resistant *Salmonella enterica* ser. Typhimurium was reported (Brar et al., 2022). The nanocomposite showed a slow-release behavior in acidic pH, inhibited efflux and beta-lactamase enzyme activity, and reduced intracellular *Salmonella* colonization from human intestinal epithelial Caco-2 cells (Brar et al., 2022). In both examples, the efficiency of primary antimicrobial was improved by combining adjuvants and delivery using nano-carriers that

improved bioavailability and release behavior. Similar strategies of therapeutic design could be effective in mastitis treatment as well.

2.4.2. Characteristics of nanomaterials relevant for targeted delivery of cargo

The shape, size, and surface chemistry of nanomaterials governs the intracellular uptake, *in vivo* biodistribution, stability, macrophage phagocytosis, toxicity, and pharmacokinetics of nanomaterials **(Figure 2.5.a,b)**. The rod or cube-shaped metallic nanomaterials were reported to be more effective for bacterial interactions mediated through crystal facets (Shao et al., 2022; L. Wang et al., 2014). Surface functionalization of nanomaterials with biomolecules could be utilized to tune their behavior in biological fluids. For instance, functionalization with PEG, RBC, poloxamer polymers, *etc*., encourages particle dispersion and reduces protein absorption in the blood, thus preventing phagocytosis **(Figure 2.5.b)** (Oh & Park, 2014). Nanomaterials developed with thiolated chitosan have shown superior mucoadhesiveness and prolonged control release of payload cargo (Bernkop-Schnürch, Hornof, & Guggi, 2004). The surface functional groups and charge of nanomaterials determine the type of endocytosis (uptake into cells) process. Positively charged nanomaterials are mainly internalized by cells *via* micropinocytosis, while negatively charged nanomaterials undergo clathrin-/caveolae-independent endocytosis (Oh & Park, 2014). The positively and negatively charged polymeric nanomaterials (such as chitosan hydrochloride and carboxymethyl chitosan) have been reported to exhibit a higher phagocytic uptake than the PEGylated and neutrally charged particles (Algharib et al., 2020). Furthermore, negatively charged nanomaterials interact more with opsonin proteins, which stimulates phagocytosis by macrophages, compared to positively charged nanomaterials (Oh & Park, 2014). Therefore, nanomaterials with charge-reversible shells could be designed where surface charges could alter from negative to positive depending on the pH prevailing in the microenvironment at the site of

action. While these strategies have been explored in anticancer drug therapy, they could also be utilized for cellular uptake in the inflamed intramammary microenvironment.

2.4.3. Nanocarriers harnessing the enhanced permeability and retention (EPR) effect for passive targeting of inflamed intramammary tissues

The EPR effect enables macromolecules to accumulate and retain at the sites of increased vascular permeability. This effect has been widely explored as an efficient strategy for anti-cancer drug design, (Azzopardi, Ferguson, & Thomas, 2012) although the clinical outcome of anticancer strategies relying on EPR is frustrating so far (Danhier, 2016). The EPR phenomenon has been reported not to be exclusive to solid neoplasms but also the site of bacterial infection (Azzopardi et al., 2012). The release and accumulation of bacterial protease and lipopolysaccharide or lipoteichoic acid from bacteria trigger immune cells that interact with vascular endothelium, leading to barrier dysfunction and increased permeability **(Figure 2.2)** (Taylor, Wahl-Jensen, Copeland, Jahrling, & Schmaljohn, 2013). Moreover, the dysfunctional lymphatic drainage during bacterial infection potentially promotes the accumulation of nanomaterials at the infection site (W. Gao, Thamphiwatana, Angsantikul, & Zhang, 2014). Non-functionalized and PEGlyated liposomes and super magnetic iron oxide nanomaterials are reported to accumulate in the soft tissues and lungs of *S. aureus*-infected rodent models (W. Gao et al., 2014; Kaim et al., 2002). Since targeted drug delivery to the intramammary infected tissues is a challenge in mastitis treatment, the EPR effect could be used to achieve partial targeting of nanocarriers at the site of inflammation, thus improving the bioavailability of the active compounds **(Figure 2.5.b)**.

2.4.4. Nanocarrier-siderophore conjugates for cargo delivery

Antibiotics often fail to cross the outer membrane of Gram-negative pathogens contributing to treatment failures, and therefore, a strategy that emphasizes using nutrient-import transporters to transport the antibiotics might be useful to bypass the impermeability of the cell wall (Schalk, 2018). The Trojan Horse strategy involving siderophore-mediated drug delivery could also be an approach to circumvent membrane-associated drug resistance **(Figure 2.5.b).** For instance, a nano-enabled drug that fails to cross the bacterial membrane barrier could be fused to a siderophore such as tannins. The cognate receptor would perceive the Fe(III)–siderophore complex and facilitate the transport through the membrane barrier with the drug attached (Miller et al., 2009; Möllmann, Heinisch, Bauernfeind, Köhler, & Ankel-Fuchs, 2009). The release of drug molecules in bacterial cytoplasm, along with the iron chelating activity of iron could culminate in the elimination of bacteria (Miller et al., 2009; Möllmann et al., 2009). This strategy has been successfully introduced for diseases such as tuberculosis and malaria and targets several gram-negative bacteria, but its application in veterinary medicine is yet to be investigated (Ji, Juárez-Hernández, & Miller, 2012; Ribeiro & Simões, 2019).

2.4.5. Stimuli-responsive nanomaterials for active targeting

Responsive modulation of nanomaterial-pathogen interaction would increase specificity, minimize bacterial exposure to diluted concentrations of antimicrobials, and thus reduce or slow down the development of resistance towards it. Nano-carriers that respond to the alkaline pH of mastitis tissue could be designed to achieve targeted delivery of drug molecules **(Figure 2.5.b)**. For instance, microporous silica nanomaterials prepared using the reverse microemulsion method showed stability in the acidic pH of the stomach (pH 1-4) and triggered cargo release in alkaline conditions (Giovaninni, Moore, Hall, Byrne, & Gubala, 2018). Another possibility is the development of nano-carriers that respond to specific enzymes abundant at infected tissue sites

(Figure 2.5.b). Nano-gel formulations containing polyphosphoester cross-linked cores showed stability but underwent enzyme degradation in response to the phosphatase or phospholipase-positive MRSA, thus facilitating a site and pathogen-specific cargo release (Xiong et al., 2012). These strategies could be utilized for designing nanomaterials to deliver antimicrobial-adjuvant combinations for mastitis.

2.4.6. Intracellular uptake of nanomaterials for targeting intracellular pathogens

The therapeutic effect of antimicrobials against intracellular pathogens such as *S. aureus* depends on their penetration into the cell membrane, intracellular accumulation, and drug retention time above the effective therapeutic levels. Nano-enabled platforms can improve the permeability and accumulation of the cargo within cells in sufficient concentration to eliminate intracellular pathogens **(Figure 2.5.b)**. Nanomaterials are transported into the host cells by phagocytosis and pinocytosis routes, which influence the extent of cellular uptake, intracellular distribution, and pharmacokinetics of the cargo **(Figure 2.5.b)** (Geiser, 2010). Phagocytosis and pinocytosis vary in the size of their endocytotic vesicles; while phagocytosis employs larger vesicles of ~250 nm, pinocytosis encompasses the uptake of smaller polar and charged biomolecules through vesicles of a few nanometers to few micron sizes (Foroozandeh & Aziz, 2018).

Clathrin-mediated endocytosis engulfs extracellular molecules (of <250 nm size) through the formation of clathrin-coated vesicles (Sahay, Alakhova, & Kabanov, 2010). Poly(lactic-co-glycolic acid)-based nanomaterials, chitosan nanomaterials, solid lipid nanomaterials, silica (SiO_2)-based nanomaterials, and gold nanomaterials have been reported to utilize the clathrin-mediated uptake pathway (L. Q. Jiang et al., 2017; W. Jiang, Kim, Rutka, & Chan, 2008; Rivolta

et al., 2011). On the other hand, caveolae-dependent endocytosis involves flask-shaped membrane invaginations called caveolae (50-80 nm in size) (Sahay et al., 2010). Caveolae get detached from the plasma membrane and fuse with cell compartments called caveosomes which shield the cargo from hydrolytic enzymes and lysosomal degradation (Foroozandeh & Aziz, 2018). Nanomaterials in between 50-80 nm size range are often designed to be internalized through this pathway, as the cargo does not end up in the lysosome, and also for selective targeting of viruses and bacteria that use this route of entry to avoid elimination (Sandvig, Pust, Skotland, & van Deurs, 2011). As detailed by Algharib *et al.*, the "*Proton sponge*" effect could salvage this issue where the nanocarrier delivers the cargo to the endosome and release it to the cytosol, thus preventing undesirable degradation of cargo in the lysosome (Algharib et al., 2020). Polycations (such as polyhistidine and poly amino esters) would mediate the disruption of the endosomal compartment by binding with the endosomal membrane and promoting osmotic swelling, leading to destabilization of the membrane (Algharib et al., 2020). The shape, size, and surface chemistry of extracellular molecules have a profound impact on endocytosis thus, nano-enabled delivery platforms could be tuned for phagocytosis or pinocytosis pathways to target intracellular pathogens as discussed below.

Modification of nanomaterials with specific ligands of macrophages can enhance the phagocytosis efficiency and thus may contribute to improving the intracellular concentration of antimicrobial agents (Zhou et al., 2018). Many pathogens are surface-coated with specific carbohydrates that are often recognized by the macrophage mannose receptors (MR) or other C-type lectins. They are manifested by tissue macrophages, dendritic cells, and lymphatic or endothelial cells, which are exploited by intracellular pathogens for survival (Azad, Rajaram, & Schlesinger, 2014). For instance, the cell surface glycopolymer, teichoic acid in *S. aureus*, contains *N*-acetylglucosamine residue, a functional ligand of mannose-binding lectin (K. H. Park et al., 2010). Therefore, mannosylated 'pathogen-like' polyanhydride nanomaterials and

liposomes could employ enhanced uptake of payload cargo into phagocytes in target tissues and thus could be a promising approach to combat intracellular mastitis pathogens **(Figure 2.5.b, 2.6)**. Polymeric nanomaterials with customized ionic cores and hydrophobic/hydrophilic shells can play a complementary role. Nano-delivery platforms with a hydrophobic surface layer could interact with the hydrophobic cell membrane surface, thus improving the chance of recognition by particular receptors for intracellular uptake **(Figure 2.6)** (Zhou et al., 2018). The uptake of rod-shaped chitosan nanomaterials by the macrophage and epithelial cells has been reported to be effective in targeting intracellular *S. aureus* (Maya et al., 2012). PLGA nanomaterials, chitosan folic acid nanomaterials, liposomes, solid lipid nanomaterials, β-tricalcium phosphate nanomaterials, *etc*., have been reported to enhance the intracellular efficiency of antimicrobials (Gupta, Nirwane, Belubbi, & Nagarsenker, 2017; Uskoković & Desai, 2014; Shuyu Xie et al., 2017) which, however, have not been tested against intracellular mastitis pathogens and thus merits further investigations in this direction.

2.4.7. Nanomaterials to breach microbial biofilms

The biofilm mode of bacterial growth protects them from biotic and abiotic stresses. (Balcázar, Subirats, & Borrego, 2015) Multilayers of bacterial cells attached to a solid surface and thick layers of EPS shield bacteria from antimicrobial agents (Balcázar et al., 2015). Nano-enabled drug delivery platforms capable of trespassing thick layer of EPS and biofilm matrix and releasing drug molecules in a sustained manner is expected to remediate infections involving bacterial biofilms. The size and shape of nanomaterials play a decisive role in antibiofilm performance. Spherical-shaped chitosan nanomaterials of 15-25 nm loaded with iron oxide showed superior penetration of *S. aureus* biofilm (Shi et al., 2016). Tunable smart nanomaterials exhibiting desirable drug release under endogenous or external stimuli (e.g., pH, bacterial toxins, redox

potential, enzymatic activation, temperature, *etc.*) (Q. Hong, Huo, Tang, Qu, & Yue, 2021) could be used to counter biofilms associated with mastitis. For instance, pH-triggered size-tunable silver nanomaterials have shown superior penetration in infection sites and prolonged retention in biofilms leading to its disruption (Cheng et al., 2022). Nanozymes with intrinsic enzymes-like properties in the surface-bound state or coated form could be another option to explore as they have shown better efficiency in eliminating pathogens in biofilms because of their ability to digest biofilm matrix (F. Gao, Shao, Yu, Xiong, & Yang, 2021; Meng, Li, Pan, & Gadd, 2020). Nano-delivery systems constructed by self-assembly of berberine and rhein phytochemicals have shown desirable biocompatibility and inhibition of *S. aureus* biofilms (Tian et al., 2020). Biofilms could also be disrupted by switching off the quorum-sensing systems that significantly contribute to biofilm formation (B. N. Singh et al., 2017). ß-cyclodextrin or N-acylated homoserine lactonase proteins interfere with signal/receptor interaction thus, could be used for surface modification of nanomaterials to disrupt the functioning quorum sensing (Kato, Morohoshi, Nozawa, Matsumoto, & Ikeda, 2006; Ortíz-Castro, Martínez-Trujillo, & López-Bucio, 2008).

2.4.8. Nanomaterials to target SCVs

As mentioned in the preceding section, lower metabolism levels and growth rate of SCV phenotypes differentiate them from the normal phenotype making the elimination of SCVs complicated through antibiotic treatment. Zhou *et al*. reported the combination of the iron-chelator deferiprone (Def) and the heme-analog gallium-protoporphyrin (GaPP) to show significant activity against planktonic and sessile SCVs and increase the survivability of *S. aureus* SCV-infected *C. elegans* (Richter et al., 2017). Nano-carriers enabled with adjuvants that can increase cellular metabolisms, such as protoporphyrin and Def in combination with antibiotics, could be an exciting approach to combat SCVs of *S. aureus* in mastitis **(Figure 2.6)**. Recently, silica-based

nanocarrier systems with tuned surface chemistries were reported to be effective against SCV phenotypes. For instance, mesoporous silica nanomaterials loaded with rifampicin showed enhanced adsorption and uptake into Caco-2 cells facilitating a significant reduction against SCV *S. aureus*, compared to the pristine rifampicin (Joyce et al., 2020). The compatibility and efficiency of these strategies for mastitis treatment still need to be explored.

2.4.9. Fate of nanomaterials in bovine mastitis udder

The fate of nanomaterials used for infection control, especially for mastitis, is an important consideration for gauging the suitability of the material used. Nanomaterials resistant to biodegradation will likely be retained in tissue for a prolonged period, eventually leading to undesirable tissue responses (S. Xie et al., 2014; Zhou et al., 2018). Usually, intravenously administered nanomaterials circulate in the blood and are cleared by renal and hepatobiliary elimination (Y. N. Zhang, Poon, Tavares, McGilvray, & Chan, 2016). From a bovine mastitis perspective, antimicrobials are generally administered in the mammary gland, and their elimination vastly depends on the pharmaceutical and host factors. For instance, an intensely swollen udder during mastitis may lead to poor drug distribution and elimination due to a compressed milk duct or blockage by inflammatory products (Gehring & Smith, 2006). Increased vascular permeability also affects systemic absorption, distribution, and elimination into/from the udder (Gehring & Smith, 2006). Studies have reported contrasting evidence on drug elimination. Some reports suggest a slow elimination of antibiotics in mastitis cows compared to healthy cows, while several other studies found insignificant differences (Gehring & Smith, 2006). The level of milk production influence drug elimination from mammary glands. Accordingly, slower elimination of intramammary drugs in cows with a lower volume of milk has been observed compared to cows producing a higher volume of milk (Han et al., 2017). There has not been much

investigation on the fate of nanomaterials entering the mammary glands. However, based on observations made on other tissue environments, it is logical to assume the dissolution (of metallic nanomaterials) and disintegration of polymeric nanomaterials used to encapsulate drug molecules. In either of these cases, the elimination of 'nanomaterials' from the tissue environment is expected within a reasonable duration of the treatment. However, prolonged retention could be expected with silica or carbon-based nanomaterials as they are less prone to the digestive enzymes or pH of the mammary glands and could be retained in tissues. In short, the choice of materials for drug delivery in mammary tissue should consider the possible tissue retention, degradation, and release of volatile residues that may adversely affect the milk quality.

2.5. Conclusion

Bovine mastitis is the inflammatory response of the mammary gland tissues to physiological or metabolic changes and microbial infections. Inherent challenges associated with eliminating bacteria from mammary tissues coupled with the emergence of AMR have dwindled the prospects of conventional treatments in the clinical management of bovine mastitis. Advances in nanotechnology, especially in drug design, development, and delivery, offer unprecedented opportunities for treating bovine mastitis. However, developing effective nanotherapeutics demands a thorough knowledge of the interplay of environmental, host, and pathogen-related factors significant in the initiation and prevalence of this disease. Tissue environment characterized by alkaline pH, presence of digestive enzymes, leaky endothelial cells, *etc.,* provide opportunities for custom designing of nanotherapeutics for targeted delivery of drug molecules. Combining antimicrobial agents (antibiotics, metals, bacteriocins, *etc.*) with effector molecules (that curtain AMR and virulence mechanisms) is proposed as a rational strategy to fight AMR pathogens forming biofilms and invading epithelial layer. The effectiveness of combination

therapy could be further enhanced through nanotechnology, where nano-delivery platforms designed to respond to specific tissue scenarios are used for the targeted delivery of multiple drugs. The success of any nano-enabled antibacterial combination therapy (NeACT) for mastitis treatment, however, depends on how it responds to the constraints of performance, safety to animals and humans, financial viability, and social acceptance.

Preface to Chapter 3

In the previous chapter, a comprehensive literature review was conducted on the risk factors and pathogenesis associated with bovine mastitis. I further elaborated on the current disease management strategies, and their limitations. The review examined related literatures on the mastitis pathogens to possess intrinsic or acquired resistance mechanisms that can lead to microbial persistence and spread among animals to humans through farm environments and food products. Continuous monitoring of prevalent mastitis pathogens for AMR mechanisms and virulence was deemed critical. Thus, Chapter 3 deals with phenotypic and genotypic characterization of the first library of pathogens namely *Escherichia coli* isolates obtained for Canadian dairy farms for AMR and virulence mechanisms. I examined the *E. coli* isolates for resistance against a set of antibiotic classes and heavy metals to verify susceptibility and conducted assays to determine resistance mechanisms and virulence characteristics. I also examined the whole genome sequences for each isolate corresponding to the observed resistance and virulence.

Chapter 3

Prevalence and mechanisms of antibiotic resistance in *Escherichia coli* isolated from mastitic dairy cattle in Canada

Abstract

Bovine mastitis is the most common infectious disease in dairy cattle with major economic implications for the dairy industry worldwide. Continuous monitoring for the emergence of antimicrobial resistance (AMR) among bacterial isolates from dairy farms is vital not only for animal husbandry but also for public health. In this study, the prevalence of AMR in 113 *Escherichia coli* isolates from cases of bovine clinical mastitis in Canada was investigated. Kirby-Bauer disk diffusion test with 18 antibiotics and microdilution method with 3 heavy metals (copper, zinc, and silver) was performed to determine the antibiotic and heavy-metal susceptibility. Resistant strains were assessed for efflux and ß-lactamase activities besides assessing biofilm formation and hemolysis. Whole-genome sequences for each of the isolates were examined to detect the presence of genes corresponding to the observed AMR and virulence factors. Phenotypic analysis revealed that 32 isolates were resistant to one or more antibiotics and 107 showed resistance against at least one heavy metal. Quinolones and silver were the most efficient against the tested isolates. Among the AMR isolates, AcrAB-TolC efflux activity and ß-lactamase enzyme activities were detected in 13 and 14 isolates, respectively. All isolates produced biofilm but with different capacities, and 33 isolates showed α-hemolysin activity. A positive correlation (Pearson r = + 0.89) between efflux pump activity and quantity of biofilm was observed. Genes associated with aggregation, adhesion, cyclic di-GMP, quorum sensing were detected in the AMR isolates corroborating phenotype observations. This investigation showed the prevalence of AMR in *E.*

coli isolates from bovine mastitis. The results also suggest the inadequacy of antimicrobials with a single mode of action to curtail AMR bacteria with multiple mechanisms of resistance and virulence factors. Therefore, it calls for combinatorial therapy for the effective management of AMR infections in dairy farms and combats its potential transmission to the food supply chain through the milk and dairy products.

Keywords: Antibiotics, Antimicrobial resistance (AMR), Virulence, Bovine mastitis, *E. coli*; Efflux pump, Heavy-metals, Whole-genome sequencing, ß-lactamase enzyme.

3.1. Introduction

Bovine mastitis is a common and very costly infectious disease that has a high prevalence in the global dairy industry. In the US and Canada, bovine mastitis results in a net annual loss of about $2 billion (USD) and $794 million (CAD), respectively (Aghamohammadi et al., 2018). Clinical management of mastitis is challenging because of the multiple etiological agents including *Staphylococcus aureus*, non-aureus staphylococci (NAS), *Escherichia coli*, *Klebsiella spp.*, and *Streptococcus spp.* (Hoque et al., 2020). *E. coli* is one of the most common environmental bovine mastitis pathogens, found in almost 80% of the cases of coliform mastitis which infects the mammary glands during the dry period (O. Dego, 2020). While intramammary infection (IMI) involving *E. coli* are usually short-lived, 5-20% are reported to persist due to their ability to adhere and survive intracellularly (A. Bradley & Green, 2001; J. H. Fairbrother et al., 2015).

Antibiotics have been used extensively in animal agriculture for infection control and as growth promoters (Saini, McClure, Léger, et al., 2012). Heavy metals are also widely used in farms as therapeutics, in feed, and to improve reproductive efficiency (Argudín, Hoefer, & Butaye,

2019). Indiscriminate use of antimicrobials in farms has been suspected as a major factor in the emergence of antimicrobial resistance (AMR) among pathogenic bacteria. Prevalence of AMR bacteria in IMI is not only a challenge for clinical management of mastitis but also a public health concern is given the possibilities of transfer of AMR bacteria or genetic determinants from animals to humans *via* the food chain (Argudín et al., 2019; Catry, Laevens, Devriese, Opsomer, & De Kruif, 2003; Piddock, 1996).

Identified mechanisms of resistance to clinically important drugs used in bovine mastitis treatment in Canada include extended-spectrum β-lactamases (ESBLs), plasmid-mediated AmpC β-lactamases, carbapenemases, and generalized efflux pump activity (B. B. Awosile et al., 2017; Bohnert, Karamian, & Nikaido, 2010). Due to a wide range of substrate specificity and high levels of constitutional expression under physiological conditions, the RND-based tripartite efflux pump-AcrAB-TolC is considered the most significant contributor to intrinsic multidrug resistance in *E. coli* (Bohnert et al., 2010). In addition to AMR, other virulence factors favor the survival of bacteria in host tissue. For instance, *E. coli* survives and colonizes bovine udder by hemolysis and biofilm formation (A. Bradley & Green, 2001).

Biofilms protect resident bacteria from antibiotic activity and host defenses leading to bacterial persistence in hostile host tissues and increasing the risk of disease transmission (O. Dego, 2020; Hoque et al., 2020). Secretory virulence factors, such as hemolysin, are also reported to be responsible for pore formation and cellular necrosis which involve in cell to cell interaction during bacterial biofilm formation, increase in inflammatory responses and decrease in macrophage function (A. Bradley & Green, 2001; O. Dego, 2020).

The Canadian Bovine Mastitis Research Network maintains a culture collection of bacterial isolates from mastitis infected dairy cows- Mastitis Pathogen Culture Collection (MPCC). These isolates were collected from 91 dairy farms across Canada over 2 years in 2007

and 2008 (Reyher et al., 2011). In this study, we assessed the prevalence of AMR and virulence characteristics of 113 *E. coli* isolates obtained from MPCC using phenotypic assays. Further, the presence of genes corresponding to the identified AMR and virulence characteristics were verified from the whole genome data reported recently (D. Jung et al., 2021; Jung, Park, Ruffini, Dufour, & Ronholm, 2021). Knowledge about the prevalence of AMR and virulence factors involved in the survival and persistence of *E. coli* causing IMI is pivotal for clinical management of disease as well as for designing new therapeutic agents.

3.2. Materials and methods

3.2.1. Isolation of the *E. coli* isolates from cases of bovine mastitis

E. coli isolates used in this study were a part of the mastitis pathogen culture collection (MPCC) across Alberta, Ontario, Quebec, and Atlantic provinces (Prince Edward Island, Nova Scotia, and New Brunswick) (Reyher et al., 2011) **(Supplementary table S1)**. The process of sampling milk of infected dairy cows for the isolation of *E. coli* is detailed in **Supplementary information 1**. Single colonies of bacterial isolates grown in Tryptic Soy Agar (TSA) plates containing 5% sheep blood agar (Hardy Diagnostics, Canada) were inoculated in Mueller-Hinton broth (MHB) (Millipore Sigma, Canada) and kept for incubation at 37°C under shaking (4xg) for 18 h for obtaining freshly grown bacterial cells for conducting assays.

3.2.2. Susceptibility testing of *E. coli* isolates against a panel of antibiotics

The *E. coli* isolates were subjected to Kirby-Bauer disk diffusion susceptibility tests following the protocol in the Clinical and laboratory standard institute (CLSI) guidelines (CLSI,

2017). Eighteen antibiotics (Oxoid, Thermo Fischer Scientific, Canada) relevant to human and animal health from the classes of ß-lactams, aminoglycosides, cephalosporins, quinolones, tetracycline, chloramphenicol, sulphonamide, and polymyxin were included in this study. The list of antibiotics tested, and their corresponding MIC values are given in **Supplementary table S2.a**. *E. coli* ATCC 25922, *S. aureus* ATCC 25923, and *P. aeruginosa* ATCC 27853 (Oxoid company, Canada) were used as the quality control (QC) strains.

3.2.3. Susceptibility testing of *E. coli* isolates against heavy metals

The sensitivities of the *E. coli* isolates to metals were assessed using the broth microdilution method as previously reported (Hoque et al., 2020). Three metal salts *viz* copper sulfate ($CuSO_4$), zinc sulfate ($ZnSO_4$), and silver nitrate ($AgNO_3$) were used in this assay. Ten-twofold serial dilutions of metal salts were prepared in 100 µL of autoclaved Mueller-Hinton broth (MHB) (Millipore Sigma, Canada) in a 96 well plate (Millipore Sigma, Canada) wherein the final concentrations were 5, 5, and 2 mg/mL for $CuSO_4$, $ZnSO_4$, and $AgNO_3$, respectively. Wells in these plates were added with 10 µL of freshly prepared bacterial culture in MHB adjusted to 0.5 MacFarland standard. *E. coli* ATCC 25922 was used as the quality control (QC) strain. These 96 well plates were incubated for 18 h at 37 °C in a shaking incubator.

The bacterial viability was monitored by resazurin assay (George et al., 2020). Briefly, 30 µL of resazurin solution (0.5% in PBS) was added to each of the wells and further incubated for 2 h at 37 °C under shaking. The fluorescent intensity (530 nm for excitation and 590 nm for emission) was measured using a plate reader (SpectraMax-i3X, Molecular Devices, USA).

Background corrected fluorescence intensity data were used to generate a dose-response curve. The inhibitory concentration (50%) or IC_{50} values of each metal salts against each *E. coli* isolate were calculated using GraphPad Prism 7 software where IC_{50} is the ability of the metal salts

to inhibit 50% of bacterial growth. The IC_{50} value of each metal salt against the QC strain was considered as the cut-off concentration. *E. coli* isolates with IC_{50} values less or equal or non-significant ($p>0.05$) to than that of the cut-off were considered as susceptible whereas, significant ($p\leq0.05$) non-susceptible isolates were categorized into weakly resistant isolates (WRI) ($QCIC_{50cut-off} < WRI \leq 1.5$ folds of $QCIC_{50cut-off}$), moderately resistant isolates (MRI) (1.5 folds of $QCIC_{50cut-off} < MRI \leq 2$ folds of $QCIC_{50cut-off}$) and strongly resistant isolates (SRI) (SRI > 2 folds of $QCIC_{50cut-off}$).

3.2.4. Assessing efflux pump activity in antibiotic-resistant *E. coli* isolates

Quantification of efflux pump activity in the AMR *E. coli* isolates was carried out by Nile red efflux assay as previously described (Iyer, Ferrari, Rijnbrand, & Erwin, 2015). Briefly, 1 mL of bacterial cells in MHB was centrifuged at 2,300 x g for 10 mins at room temperature (RT). The supernatant was discarded, and the cell pellet was re-suspended with 20 mM potassium phosphate buffer (pH 7) containing 1 mM $MgCl_2$ (PPB). Cells washed and suspended in PPB (1.0 MacFarland standard) in glass test tubes were added with carbonyl cyanide 3-chlorophenylhydrazone (CCCP) (50 µM) and incubated for another 15 mins at RT. Subsequently, Nile red (10 µM) (dissolved in 10% dimethyl formamide-90% ethanol (v/v)) was added to each of the tubes, incubated for 2 h at 37 °C under shaking, and then kept at RT for an hour. After incubation, the cell suspensions were centrifuged, washed twice, and resuspended in PPB. 140 µL of the suspension was transferred to the wells of the 96 well plate. The fluorescent intensity (544 nm for excitation and 650 nm for emission) was monitored for 120 s using the plate reader. Nile red efflux was triggered by rapid energization with 10 µL of glucose (25 mM) and fluorescence was monitored for another 300 s. PPB without cell suspension was used as blank and *E. coli* ATCC 25922 was used as a control.

Data from the experiments were plotted using GraphPad Prism 7. Time-dependent efflux of Nile red was fitted using a single exponential decay equation:

$$Y = (Y_{\circ} - \text{Plateau}) \times \exp(-K \times X) + \text{Plateau}$$

where $Y_{\circ}$ is the Y value when X (time) is zero, the plateau is the Y value at infinite times and K is the rate constant. Efflux was initiated at t=0 by energization with glucose and reached 50% complete at $t_{efflux50\%}$. The equation was used to calculate the $t_{efflux50\%}$ which indicates the time required for the *E. coli* cells to extrude half of the preloaded Nile red molecules.

3.2.5. Detection of ß-lactamase activity in antibiotic-resistant *E. coli* isolates

Bacterial isolates grown for 18 h in MHB were used for preparing 1.0 MacFarland standard in 1 mL of fresh MHB. Ampicillin (50 µg/mL) was added to each of the cell suspensions and incubated for 3 h at 37 °C under constant shaking. After incubation, the cell suspensions were centrifuged at 8,900 x g or 10 mins, suspended in sodium phosphate buffer (pH7.0), and washed. The suspensions were resuspended again in the buffer, sonicated for 3 mins in the presence of ice, and centrifuged at 17500 x g or 25 mins to obtain the cell-free extract, which was used as the source of ß-lactamase enzyme for Nitrocefin assay as detailed previously (Dai, Xiang, Li, Gao, & Yang, 2012; S. Sharma, Ramnani, & Virdi, 2004). Briefly, 10 µL of nitrocefin (Abcam, Canada), a chromogenic cephalosporin dissolved in 5% DMSO (stock concentration of 0.5 mg/mL), was mixed with 10 µL of the cell-free extract and the volume was adjusted to 100 µL using buffer solution in a 96-well plate. The absorbance was immediately detected in kinetic mode at 390 nm for 10 mins using a plate-reader. Nitrocefin was added to buffer solution without cell-free extract and *E. coli* ATCC 25922 was used as a media and negative control, respectively.

A nitrocefin standard curve (concentration ranging from 125 µg/mL to 0.49 µg/mL) was plotted against absorbance (390 nm). The ß-lactamase enzyme activity was calculated using the formula: ß-lactamase enzyme activity = (S_a/(Reaction time x S_v))s

where, S_a is the amount of Nitrocefin (in µM) hydrolyzed in the unknown sample well between T1 and T2 of the standard curve, Reaction time is the difference between absorbance detected in two-time intervals (T1 and T2 in minutes), S_v is the sample volume (in mL) added to the well. ß-lactamase activity is reported as U/mL.

3.2.6. Assessing virulence factors and evaluating the relationship between efflux activity and biofilm-formation in AMR isolates

Detection of hemolysis was carried out as previously reported (Buxton, 2005). A loopful of *E. coli* from agar plates was inoculated into 10 mL of sterile TSB media and incubated overnight. The isolates were then streaked in TSA plates containing 5% sheep blood. The pattern of hemolysis was detected by visual inspection for the translucency around the bacterial colony that occurs due to the lysis of red blood cells.

The biofilm-forming ability was assessed by crystal violet assay (George et al., 2020). Briefly, 100 µL of autoclaved MHB was transferred to each of the wells of a 96 well plate and 10 µL of the bacterial culture maintained at 0.5 MacFarland standard was added to each of the wells. The plates were incubated for 24 h at 37 °C without shaking. After 24 h of incubation, the media was removed from the wells and washed twice with pre-autoclaved saline to remove non-adherent cells. A 100 µL of 99% methanol was added to each well to fix the biofilms and kept undisturbed for 15 mins at room temperature. The wells were further washed with saline and air-dried and added with 200 µL of crystal violet (0.4%) and left undisturbed for 2 h. The wells were again

washed with saline, air-dried followed by the addition of 30% acetic acid. The absorbance was detected at 570 nm using a plate reader.

The classification of the biofilm-forming ability of *E. coli* isolates were obtained by using the following formula as previously mentioned by Hoque et al.: $OD_{cut\text{-}off} = OD_{avg}$ of control + 3 x standard deviation (SD) of ODs of control; $OD \leq OD_{cut\text{-}off}$ = Non-biofilm-former (NBF); $OD_{cut\text{-}off} < OD \leq 2 \times OD_{cut\text{-}off}$ = Weak biofilm-former (WBF); $2 \times OD_{cut\text{-}off} < OD \leq 4 \times OD_{cut\text{-}off}$ = Moderate biofilm-former (MBF); $OD > 4 \times OD_{cut\text{-}off}$ = Strong biofilm-former (SBF) (Hoque et al., 2020). A similar assay was performed with a concentration range of CCCP (from 100 µg/mL to 0.19 µg/mL) to assess the relation between biofilm-forming ability and efflux activity of the bacterial isolates. Media with bacteria but no efflux inhibitor were included as a negative control, and wells without bacteria and efflux inhibitor were included as media controls. *E. coli* ATCC 25922 was used as a control strain to check the difference in biofilm formation. Pearson correlation test was performed between efflux activity of each isolate at a saturation point (considering 180s after re-energization) and the biofilm-forming capacity of the corresponding isolates at 50 µM of CCCP. The Pearson's correlation and One-way ANOVA (p-value ≤0.05 was regarded as significant) tests were performed using GraphPad Prism 7 software. Irrespective of the *E. coli* isolates, the biofilm inhibitory concentrations below the MIC of CCCP (checked at OD_{600}) were considered as the concentrations of interest to demonstrate an antibiofilm effect rather than a generalized growth inhibition (Baugh, Phillips, Ekanayaka, Piddock, & Webber, 2013).

3.2.7. Identification of sequence type, antibiotic, and metal resistance genes

Whole-genome sequencing, genome assembly, and annotation were conducted as previously described (D. Jung et al., 2021; Jung et al., 2021) (**Supplementary information 2** and **Supplementary table S3)**. Sequence types (STs) of each isolate were identified using the tool MLST (https://github.com/tseemann/mlst) which incorporates data from the PubMLST database

(Jolley & Maiden, 2010). AMR genes were identified by Prokka and ABRicate v1.0 (https://github.com/tseemann/abricate) with CARD and ResFinder databases (Seemann, 2014). Metal resistance genes were identified by Prokka v.1.14.5 and ABRicate with MEGARES database (Lakin et al., 2017; Seemann, 2014). Minimum coverage and identity settings for all the screening was set to 90%.

3.3. Results

3.3.1. Antibiotic and metal resistance profiles of the *E. coli* isolates

Out of 113 isolates, 32 isolates (28.31 %) showed resistance to either single (13/32) or multiple (19/32) antibiotics **(Figure 3.1)**. Based on their responses against the antibiotic classes, 13 out of the 32 antibiotic-resistant isolates were labelled as multi-drug resistant isolates, 6 were marked as extensively drug-resistant, whereas the rest 13 isolates were designated to be single drug-resistant **(Table 3.1)**. The frequency of resistance among the tested *E. coli* isolates was highest towards streptomycin (17.7 %) followed by tetracycline (15.93 %) and ampicillin (11.5 %), whereas less than 10 % resistance was seen towards the remaining antibiotics **(Supplementary table S2.b.)**. Out of 113 isolates, 1.76 and 4.42 % of them showed resistance towards cefotaxime and cefazolin, respectively. 1.76 % of the isolates showed resistance against colistin. None of the isolates showed resistance to quinolones (ciprofloxacin and ofloxacin) and aminoglycosides (gentamycin and tobramycin). Out of the 32 resistant isolates, 28.12 and 50.00 % of them were collected from the cattle with mastitis severity score 2 (abnormal milk, swollen quarter) and 3 (abnormal, milk, swollen quarter, and sick cow), respectively.

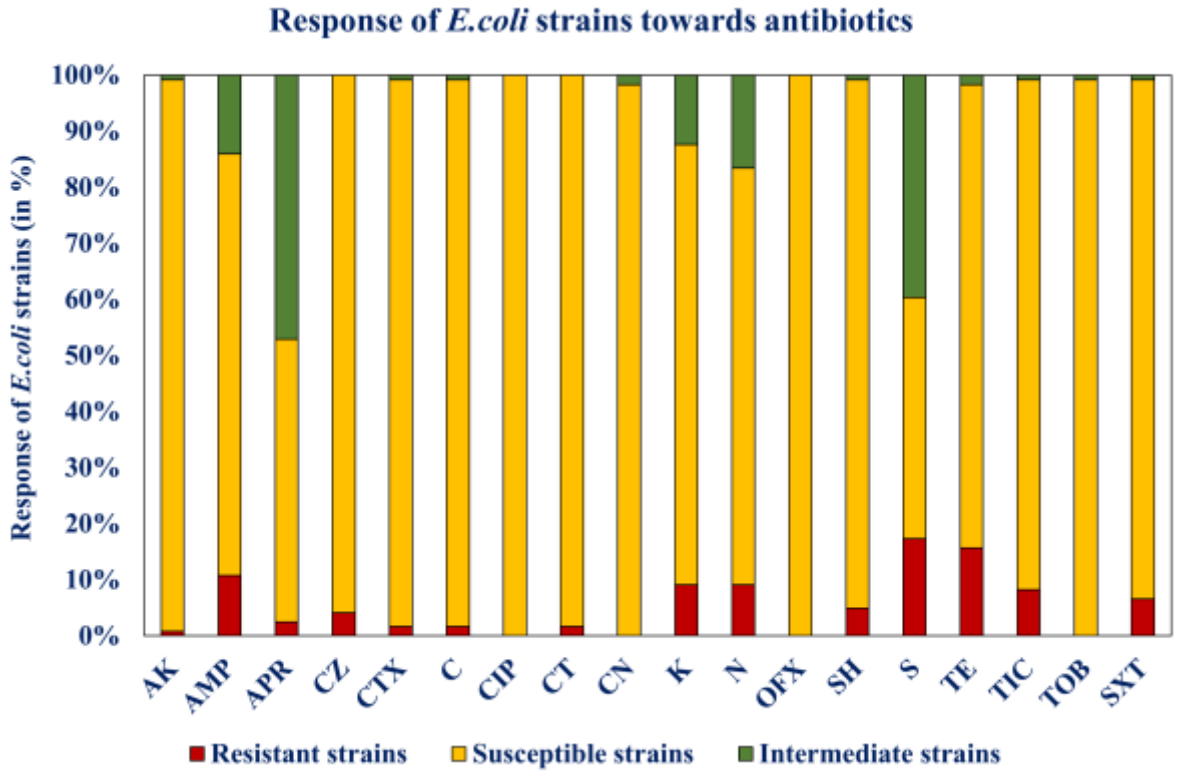

Figure 3.1. Response pattern (%) of 113 *E. coli* isolates towards 18 antibiotics. The *E. coli* isolates were subjected to Kirby-Bauer disk diffusion susceptibility tests. The scores based on CLSI guidelines for susceptibility or resistance to an antibiotic were generated for each isolate. Abbreviations used - AK: Amikacin; AMP: Ampicillin; APR: Apramycin; CZ: Cefazolin; CTX: Cefotaxime; C: Chloramphenicol; CIP: Ciprofloxacin; CT: Colistin; CN: Gentamycin; K: Kanamycin; N: Neomycin; OFX: Ofloxacin; SH: Spectinomycin; S: Streptomycin; TE: Tetracycline; TIC: Ticarcillin; TOB: Tobramycin; SXT: Trimethoprim/Sulfamethoxazole.

Resistant *E. coli* ID no.	Antibiotic resistance pattern														Efflux pump activity $t_{efflux50\%}$ (secs)	ß-lactamase activity (U/mL)	Gene profiling
	AK	AMP	APR	CZ	CTX	C	CT	K	N	SH	S	TE	TIC	SXT			
40202761															12.16	60.51	*bla_{TEM-1}, aph(3')-Ia, aph(3")-Ib, aph(6)-Id, tetB, emrK, emrY, marA, sul2, acrA, acrB, acrD, tolC, mdtf, dfrA1, mdfA, ampC, kdpE, baeR*
41100011																	*acrA, acrB, acrD, tolC, baeR, kdpE, emrA, emrB, mdtE, marA*
20202040																	*acrA, acrB, acrD, tolC, baeR, kdpE, emrA, emrB, mdtE, marA*
41300398																	*tet(C), acrA, acrB, tolC, emrK, emrY, mdf(A), marA*
41613979															12.77	64.18	*blaTEM-1, aph(3')-Ia, aph(3")-Ib, aph(6)-Id, acrA, acrB, acrD, tolC, mdtf, mdf(A), ampC, kdpE, baeR*
32708899															6.88	64.88	*blaTEM-1, aph(3')-Ia, aph(3")-Ib, aph(6)-Id, sul2, acrA, acrB, acrD, tolC, mdtf, dfrA5, mdf(A), ampC, kdpE, baeR*

21012914																*tet(A), acrA, acrB, tolC, emrK, emrY, mdf(A), marA*
10415566																*tet(A), acrA, acrB, tolC, emrK, emrY, mdf(A), marA*
40714004															6.05	63.42	*blaTEM-1, tet(B), aph(6)-Id, sul2, acrA, acrB, acrD, tolC, mdtf, dfrA5, mdf(A), ampC, kdpE, baeR, emrK, emrY, marA*
10715833															10.43	73.00	*blaCMY-59, aph(3")-Ib, aph(6)-Id, aadA2, sul2, sul1, floR, acrA, acrB, acrD, tolC, mdtf, dfrA12, tet(A) mdf(A), emrK, emrY, marA, ampC, ampH, marA, H-NS, kdpE, baeR*
41701140															9.18	62.49	*blaCARB-3, aph(3")-Ib, aph(6)-Id, aadA2, sul2, floR, acrA, acrB, acrD, tolC, mdtf, dfrA16, tet(A), emrK, emrY, marA, mdf(A), ampC, ampH, kdpE, baeR*
30215009																	*aph(3")-Ib, aph(6)-Id, acrA, acrB, acrD, tolC, kdpE, baeR*
22113962																39.40	*acrA, acrB, acrD, tolC, baeR, kdpE, mdf(A), emrK, emrY, ampC, ampH*

20314330																	*acrA, acrB, acrD, tolC, baeR, kdpE, emrA, emrB, mdtE, marA*
11211990															9.75	76.23	*blaCMY-59, aph(3')-Ia, aph(3")-Ib, aph(6)-Id, sul2, acrA, acrB, acrD, tolC, mdtf, tet(B), mdf(A), emrK, emrY, marA, ampC, ampH, H-NS, kdpE, baeR*
21317859																	*acrA, acrB, acrD, tolC, baeR, kdpE, emrA, emrB, mdtE, marA*
21309335																27.40	*acrA, acrB, acrD, tolC, baeR, kdpE, emrA, emrB, mdtE, marA*
31209373																	*aph(3")-Ib, aph(6)-Id, kdpE, baeR, tet(A), acrA, acrB, acrD, tolC, emrK, emrY, mdf(A), marA*
40611099																	*acrA, acrB, acrD, tolC, baeR, kdpE, emrA, emrB, mdtE, marA*
30300071															17.37		*aph(3")-Ib, aph(6)-Id, kdpE, baeR, tet(B), acrA, acrB, acrD, tolC, mdtf, emrK, emrY, mdf(A), marA*

11800057		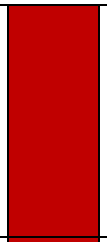		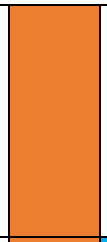							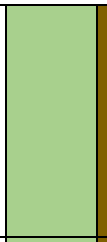			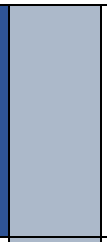	13.15	56.45	*blaTEM-1, tet(B), aph(3")-Ib, aph(6)-Id, sul2, acrA, acrB, acrD, tolC, mdtf, dfrA5, mdf(A), ampC, kdpE, baeR, emrK, emrY, marA*
41505922		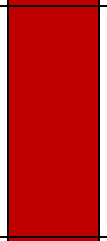		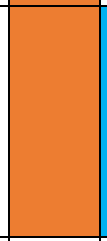	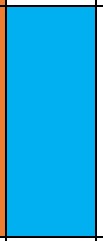			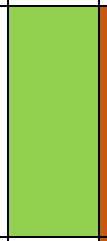	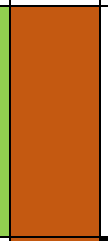		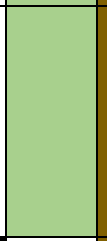	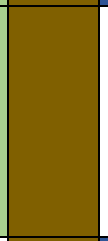		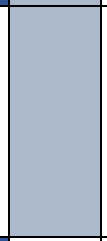	11.35	46.76	*tet(B), aph(3')-Ia, aph(3")-Ib, aph(6)-Id, sul2, acrA, acrB, acrD, tolC, mdtf, mdf(A), ampC, ampH, H-NS, kdpE, baeR, emrK, emrY, marA*
32608632		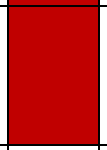										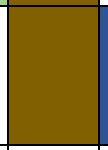				33.47	*acrA, acrB, acrD, tolC, baeR, kdpE, mdf(A), emrK, emrY, ampC, ampH, H-NS, marA*
22713162									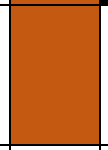								*acrA, acrB, acrD, tolC, baeR, kdpE, emrA, emrB, mdtE, marA*
20814168											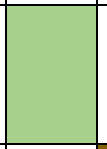						*acrA, acrB, acrD, tolC, baeR, kdpE, emrA, emrB, mdtE, marA*
10417409																	*tet(A), acrA, acrB, tolC, emrK, emrY, mdf(A), marA*
40816739											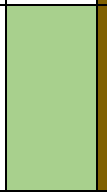	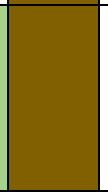		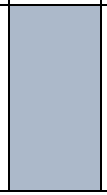	18.09		*aph(3")-Ib, aph(6)-Id, kdpE, baeR, tet(B), acrA, acrB, acrD, tolC, mdtf, emrK, emrY, mdf(A), marA, sul2*

10216675															46.43	*acrA, acrB, acrD, tolC, baeR, kdpE, mdf(A), emrK, emrY, ampC, ampH, H-NS, marA*
40317434																*acrA, acrB, acrD, tolC, baeR, kdpE, emrA, emrB, mdtE, marA*
21215100														15.03		*aph(3'')-Ib, aph(6)-Id, kdpE, baeR, tet(A), acrA, acrB, acrD, tolC, mdtf, emrK, emrY, mdf(A), marA*
21416415																*acrA, acrB, acrD, tolC, baeR, kdpE, emrA, emrB, mdtE, marA*
20508456														7.03	54.27	*blaTEM-1, aph(3')-Ia, aph(3'')-Ib aph(6)-Id, sul2, acrA, acrB, acrD, tolC, mdtf, dfrA5, ampC, ampH, H-NS, kdpE, baeR, marA*

Table 3.1. Antibiotic resistance patterns (denoted in distinguishable colors), efflux pump, ß-lactamase activity, and gene profile of the 32 antibiotic resistant *E. coli* isolates. Abbreviations used- AK: Amikacin; AMP: Ampicillin; APR: Apramycin; CZ: Cefazolin; CTX: Cefotaxime; C: Chloramphenicol; CT: Colistin; K: Kanamycin; N: Neomycin; SH: Spectinomycin; S: Streptomycin; TE: Tetracycline; TIC: Ticarcillin; SXT: Trimethoprim/Sulfamethoxazole.

Of the 113 isolates, 19 isolates were resistant to all the tested heavy metals, 67 isolates showed resistance towards two heavy metals, whereas 21 isolates showed single metal resistance. These bacterial isolates showed the highest resistance towards $ZnSO_4$ (85.87 %) followed by $CuSO_4$ (61.96 %) and $AgNO_3$ (38.93 %) **(Figure 3.2)**. In the case of $ZnSO_4$, 50.44 % of the isolates showed weak resistance, whereas 26.55 % of the isolates were moderately resistant. Similarly, 31.86 % of the isolates showed weak resistance towards $CuSO_4$, whereas 25.66 % were moderately resistant. The least resistance was seen towards $AgNO_3$ where 7.96 % of the isolates were weakly resistant, 18.58 % were moderately resistant and the rest showed strong resistance **(Supplementary table S5.b)**. Out of 32 antibiotic-resistant isolates, 29 isolates were observed to be resistant towards $AgNO_3$ where 40.62 % of them were moderately resistant, 34.37 % showed strong resistance and the rest were weakly resistant. It was followed by $ZnSO_4$ (87.50 %) where 50 % of the isolates showed weak resistance, 37.5 % showed moderate resistance and the rest were susceptible. Lastly, 53.13 % of antibiotic-resistant isolates were weakly resistant to $CuSO_4$, 37.50 % were susceptible and less than 7 % were either strong or moderately resistant **(Table 3.2)**.

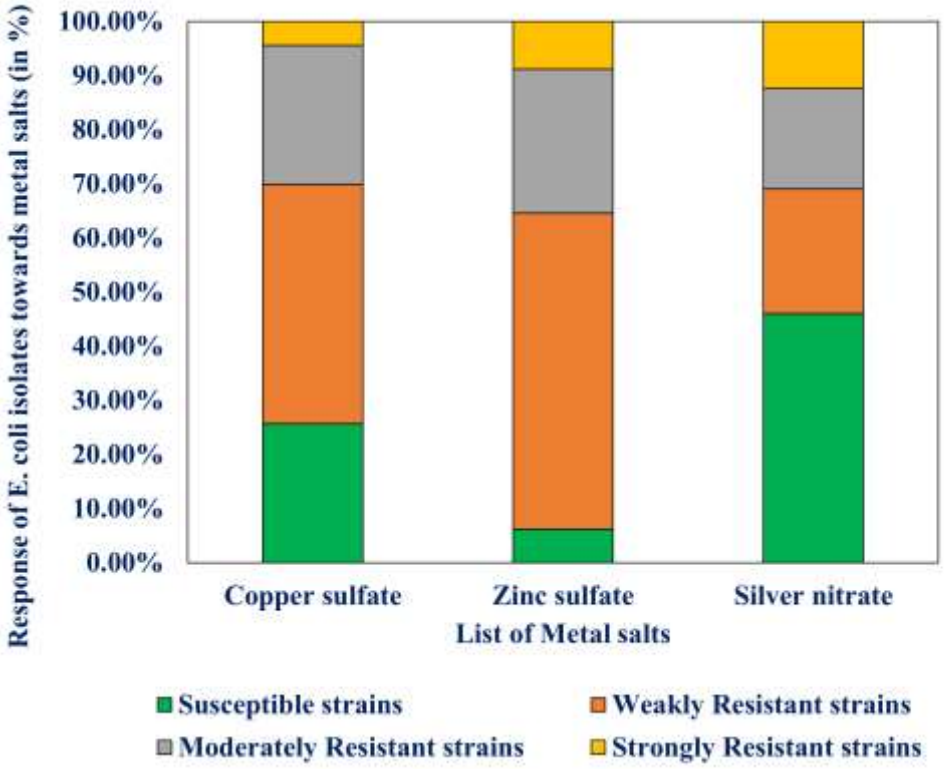

Figure 3.2. Response pattern (%) of 113 *E. coli* isolates towards the metal salts. Ten-twofold serial dilutions of the metal salts added in MH broth were prepared in 96 well plates and each well were added with bacterial cells. After overnight incubation, bacterial viability was assessed using Resazurin assay. *E. coli* ATCC 25922 was considered as the QC strain. The IC_{50} values of each metal salts against each *E. coli* isolate were calculated using GraphPad Prism 7 software. The IC_{50} value of each metal salt against the quality control strain was considered as the cut-off concentration. *E. coli* isolates with IC_{50} values less or equal or non-significant ($p>0.05$) to the cut-off were considered as susceptible whereas, statistically significant ($p\leq0.05$) non-susceptible isolates were categorized into weakly resistant isolate (WRI) ($QCIC_{50cut\text{-}off} < WRI \leq 1.5$ folds of $QCIC_{50cut\text{-}off}$), moderately resistant isolate (MRI) (1.5 folds of $QCIC_{50cut\text{-}off} < MRI \leq 2$ folds of $QCIC_{50cut\text{-}off}$) and strongly resistant isolate (SRI) (SRI > 2 folds of $QCIC_{50cut\text{-}off}$).

Resistant *E. coli* ID no.	Metal resistance pattern			Gene profiling
	$CuSO_4$	$ZnSO_4$	$AgNO_3$	
40202761				*cusA, cusB, cusC, cusF, cusS, cusR, copA, cueO, zntA, zntB, znuA, znuB, znuC, zitB, zraP*
41100011				*pcoC, pcoE, copB, copD, silE, silP, cusA, cusB, cusC, cusF, cusS, cusR, copA, cueO, zntA, zntB, znuA, znuB, znuC, zitB, zraP*
20202040				*cusA, cusB, cusC, cusF, cusS, cusR, copA, cueO, zntA, zntB, znuA, znuB, znuC, zitB, zraP*
41300398				*pcoC, pcoE, copB, copD, silE, silP, cusA, cusB, cusC, cusF, cusS, cusR, copA, cueO, zntA, zntB, znuA, znuB, znuC, zitB, zraP*
41613979				*cusA, cusB, cusC, cusF, cusS, cusR, copA, cueO, zntA, zntB, znuA, znuB, znuC, zitB, zraP*
32708899				*cusA, cusB, cusC, cusF, cusS, cusR, copA, cueO, zntA, zntB, znuA, znuB, znuC, zitB, zraP*
21012914				*cusA, cusB, cusC, cusF, cusS, cusR, copA, cueO, zntA, zntB, znuA, znuB, znuC, zitB, zraP*
10415566				*cusA, cusB, cusC, cusF, cusS, cusR, copA, cueO, zntA, zntB, znuA, znuB, znuC, zitB, zraP*
40714004				*pcoC, pcoE, copB, copD, silE, silP, cusA, cusB, cusC, cusF, cusS, cusR, copA, cueO, zntA, zntB, znuA, znuB, znuC, zitB, zraP*
10715833				*cusA, cusB, cusC, cusF, cusS, cusR, copA, cueO, zntA, zntB, znuA, znuB, znuC, zitB, zraP*

41701140				*cusA, cusB, cusC, cusF, cusS, cusR, copA, cueO, zntA, zntB, znuA, znuB, znuC, zitB, zraP*
30215009				*cusA, cusB, cusC, cusF, cusS, cusR, copA, cueO, zntA, zntB, znuA, znuB, znuC, zitB, zraP*
22113962				*cusA, cusB, cusC, cusF, cusS, cusR, copA, cueO, zntA, zntB, znuA, znuB, znuC, zitB, zraP*
20314330				*cusA, cusB, cusC, cusF, cusS, cusR, copA, cueO, zntA, zntB, znuA, znuB, znuC, zitB, zraP*
11211990				*cusA, cusB, cusC, cusF, cusS, cusR, copA, cueO, zntA, zntB, znuA, znuB, znuC, zitB, zraP*
21317859				*cusA, cusB, cusC, cusF, cusS, cusR, copA, cueO, zntA, zntB, znuA, znuB, znuC, zitB, zraP*
21309335				*cusA, cusB, cusC, cusF, cusS, cusR, copA, cueO, zntA, zntB, znuA, znuB, znuC, zitB, zraP*
31209373				*cusA, cusB, cusC, cusF, cusS, cusR, copA, cueO, zntA, zntB, znuA, znuB, znuC, zitB, zraP*
40611099				*cusA, cusB, cusC, cusF, cusS, cusR, copA, cueO, zntA, zntB, znuA, znuB, znuC, zitB, zraP*
30300071				*cusA, cusB, cusC, cusF, cusS, cusR, copA, cueO, zntA, zntB, znuA, znuB, znuC, zitB, zraP*
11800057				*cusA, cusB, cusC, cusF, cusS, cusR, copA, cueO, zntA, zntB, znuA, znuB, znuC, zitB, zraP*
41505922				*cusA, cusB, cusC, cusF, cusS, cusR, copA, cueO, zntA, zntB, znuA, znuB, znuC, zitB, zraP*
32608632				*cusA, cusB, cusC, cusF, cusS, cusR, copA, cueO, zntA, zntB, znuA, znuB, znuC, zitB, zraP*
22713162				*cusA, cusB, cusC, cusF, cusS, cusR, copA, cueO, zntA, zntB, znuA, znuB, znuC, zitB, zraP*
20814168				*cusA, cusB, cusC, cusF, cusS, cusR, copA, cueO, zntA, zntB, znuA, znuB, znuC, zitB, zraP*
10417409				*cusA, cusB, cusC, cusF, cusS, cusR, copA, cueO, zntA, zntB, znuA, znuB, znuC, zitB, zraP*
40816739				*cusA, cusB, cusC, cusF, cusS, cusR, copA, cueO, zntA, zntB, znuA, znuB, znuC, zitB, zraP*
10216675				*cusA, cusB, cusC, cusF, cusS, cusR, copA, cueO, zntA, zntB, znuA, znuB, znuC, zitB, zraP*
40317434				*cusA, cusB, cusC, cusF, cusS, cusR, copA, cueO, zntA, zntB, znuA, znuB, znuC, zitB, zraP*
21215100				*cusA, cusB, cusC, cusF, cusS, cusR, copA, cueO, zntA, zntB, znuA, znuB, znuC, zitB, zraP*

21416415				*cusA, cusB, cusC, cusF, cusS, cusR, copA, cueO, zntA, zntB, znuA, znuB, znuC, zitB, zraP*
20508456				*cusA, cusB, cusC, cusF, cusS, cusR, copA, cueO, zntA, zntB, znuA, znuB, znuC, zitB, zraP*

Table 3.2. Metal resistance pattern and gene profile of the 32 antibiotic resistant *E. coli* isolates. Abbreviations used- $CuSO_4$: Copper sulfate; $ZnSO_4$: Zinc sulfate; $AgNO_3$: Silver nitrate. Color codes: Weakly resistant isolates-Light Grey; Moderately resistant isolates-Dark Grey; Strongly resistant isolates-Black.

Antibiotic and metal resistance genes were identified from whole genomes of *E. coli* isolates **(Tables 3.1 and 3.2, Supplementary table S4 and S5.b)**. Clinically important AMR genes were identified from these isolates. For example, ESBL producing genes (bla_{TEM-B}; 6/113 bla_{CARB-3}; 1/113), plasmid-mediated AmpC ß-lactamase gene (bla_{CMY-59}; 2/113), aminoglycoside resistance genes (*aph(3')-Ia*; 5/113, *aph(3'')-Ib*; 14/113, *aph(6)-Id*; 15/113, *aadA2*; 2/113 *kdpE*; 28/113), tetracycline resistance genes (*tetA*; 7/113, *tetB* ; 7/113, *tetC* ; 1/113, *emrK* ; 18/113, *emrY*; 18/113, *mdfA*; 20/113,), chloramphenicol resistance genes (*floR*; 2/113), trimethoprim/sulfamethoxazole resistance genes (*sul1*; 1/113, *sul2*; 10/113, *dfrA1*; 1/113, *dfrA5*; 4/113, *dfrA12*; 1/113, *dfrA16*; 1/113) and multi-drug efflux pump genes (*acrA, acrB, acrD*; 28/113, *tolC, baeR, emrA*; 10/113, *emrB*; 10/113) were all identified from WGS data. We identified 42 different sequence types (ST) covering 113 isolates where ST 10 was significant in 25 isolates followed by ST 1125 (10 isolates), ST 58 (8 isolates), ST 731 (6 isolates), ST 88 and 1121 (5 isolates). Of the 42 different STs, isolates from 16 STs showed resistance towards at least one antibiotic. More specifically, 36 % of the isolates from ST 10, 30 % from ST 1125, 50 % from ST 58, and 60 % from ST 88 showed single/multi/extensive drug-resistance.

Genomic studies revealed the distribution of both acquired and intrinsic metal resistance genes among the isolates **(Table 3.2)**. Acquired copper and silver resistant genes such as *pcoC, pcoE, copB, copD*, and *silE, silP* respectively were detected in 6 out of 113 isolates. Cationic efflux

system protein genes such as *cusA, cusB, cusC, cusF, cusS*, *cusR* were detected in 98.23 % of the isolates. Intrinsic copper resistant genes such as *copA* and *cueO*, and zinc resistant genes such as *zntA, zntB, znuA, znuB, znuC, zitB, zraP* were identified in all the isolates.

3.3.2. Efflux pump and ß-lactamase enzyme activities among the AMR isolates

We calculated the time required for the *E. coli* cells to extrude half of the probe molecule (Nile Red) and denoted it as $t_{efflux50\%}$ **(Table 3.1 and Supplementary figure S1)**. Isolate 41602577 had the fastest extrusion (6.05 seconds) and whereas isolate 40816739 had the slowest extrusion (18.09 seconds) **(Figure 3.3a-c)**.

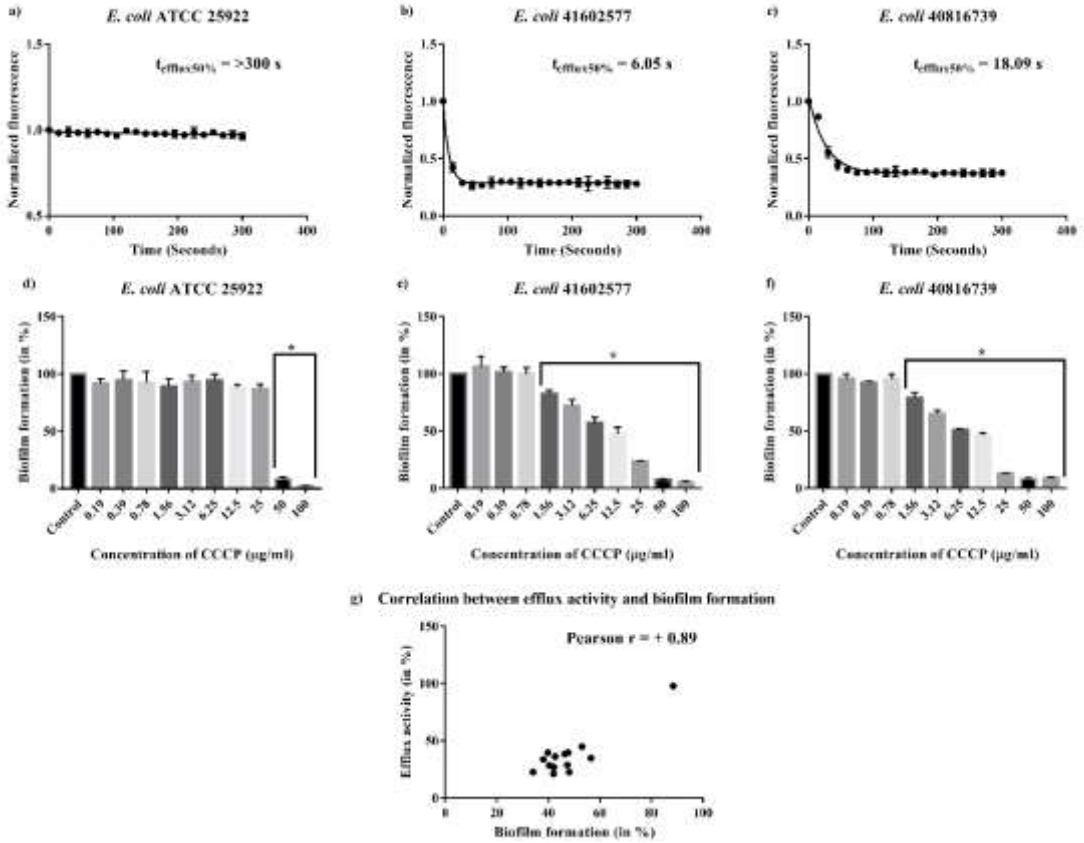

Figure 3.3. Efflux-pump activity, and the impact of efflux inhibitor on biofilm formation. Representative data on efflux activities of E. coli QC strain (a), isolate 41602577 (b), and isolate 40816739 (c). Nile red efflux assay was performed using 50 µM of CCCP and 10 µM of Nile red. The fluorescent intensity (544 nm/650 nm) of bacterial cells prior exposed to Nile red was monitored for 120 s before triggering the efflux pump by glucose addition. The fluorescence intensity was monitored for another 300 s. Likewise, a crystal violet assay was performed to assess the relation between biofilm-forming ability and the efflux activity of the bacterial isolates (d-f). '*' indicates a significant decrease in biofilm formation when compared with the control. One-way ANOVA was performed to check the statistical significance of the obtained data where a p-value ≤ 0.05 was considered significant. **g.** Depicting a significant positive correlation ($p<0.0001$, Pearson $r = +0.89$) between efflux activity and biofilm-forming ability of the isolates. GraphPad Prism 7 software was used to perform statistical analysis.

We detected 14 out of 32 AMR isolates exhibiting ß-lactamase enzyme activity **(Table 3.1 and Supplementary figure S2)**. Isolates 21317859 and 21309335 showed the highest (76.23 U/mL) and lowest (27.40 U/mL) enzyme activities, respectively **(Figure 3.4)**. Out of 14 isolates with ß-lactamase activity, 10 isolates were also identified with functional AcrAB-TolC efflux genes. Out of 14 isolates showing ß-lactamase activity, 42.85% of them carried *bla*$_{\text{TEM-1}}$, 14.28% of the isolates carried *bla*$_{\text{CMY-59}}$, and 7.14% isolates had *bla*$_{\text{CARB-3}}$. We observed a discrepancy between the phenotypic observations and WGS analysis as no particular gene was detected in 5 out of the 14 isolates exhibiting ß-lactamase activity.

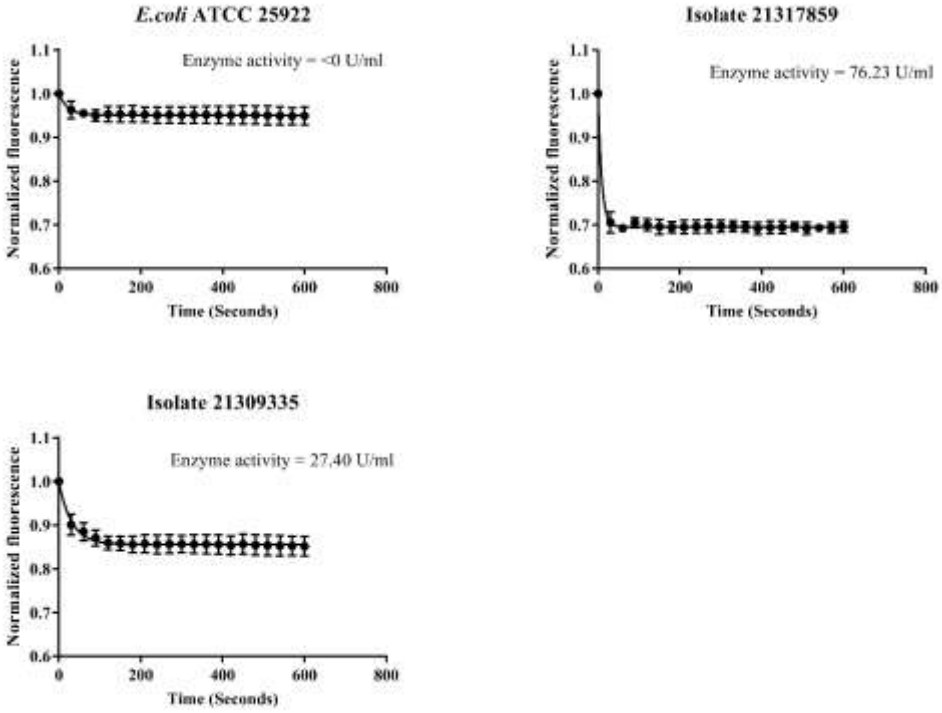

Figure 3.4. ß-lactamase enzyme activity. Bacterial cultures in MHB media were subjected to Ampicillin and incubated under constant shaking. The cell suspensions were further washed and centrifuged. The cell-free extract was obtained and used as the source of ß-lactamase enzyme for the Nitrocefin assay. The absorbance of the cell-free extract mixed with nitrocefin and buffer solution was immediately detected in kinetic mode at 390 nm for 10 mins using a plate-reader. The ß-lactamase enzyme activity was calculated using the formula: ß-lactamase enzyme activity = $(S_a/(\text{Reaction time} \times S_v))s$.

3.3.3. Production of hemolysis and correlation between efflux activity and biofilm formation

Out of 113 *E. coli* isolates, 33 isolates (29.20%) produced the exotoxin α-hemolysin out of which 10 isolates were either single or multiple-antibiotic resistant **(Table 3.3)**. *hlyE* was identified in all 113 isolates whereas, 32 isolates that produced α-hemolysin had *hlyA, hlyB, hlyC,* and *hlyD* **(Table 3.3 and Supplementary table S6.b.)**.

We detected biofilm-forming ability in all 113 *E. coli* isolates **(Supplementary table S6.b.)**. 19.46% of the isolates were observed to be strong biofilm formers whereas, 49.55% of them were moderate biofilm formers and 30.99% of the isolates were weak biofilm formers **(Figure 3.5)**. All antibiotic-resistant isolates (n=32) were either moderate (n=18) or strong (n=14)

biofilm formers **(Table 3.3)**. Genomic characterization revealed the presence of several genes that are responsible for adhesion, aggregation, c-di-GMP formation, stress response, and autoinducer-2 quorum sensing **(Table 3.3)**.

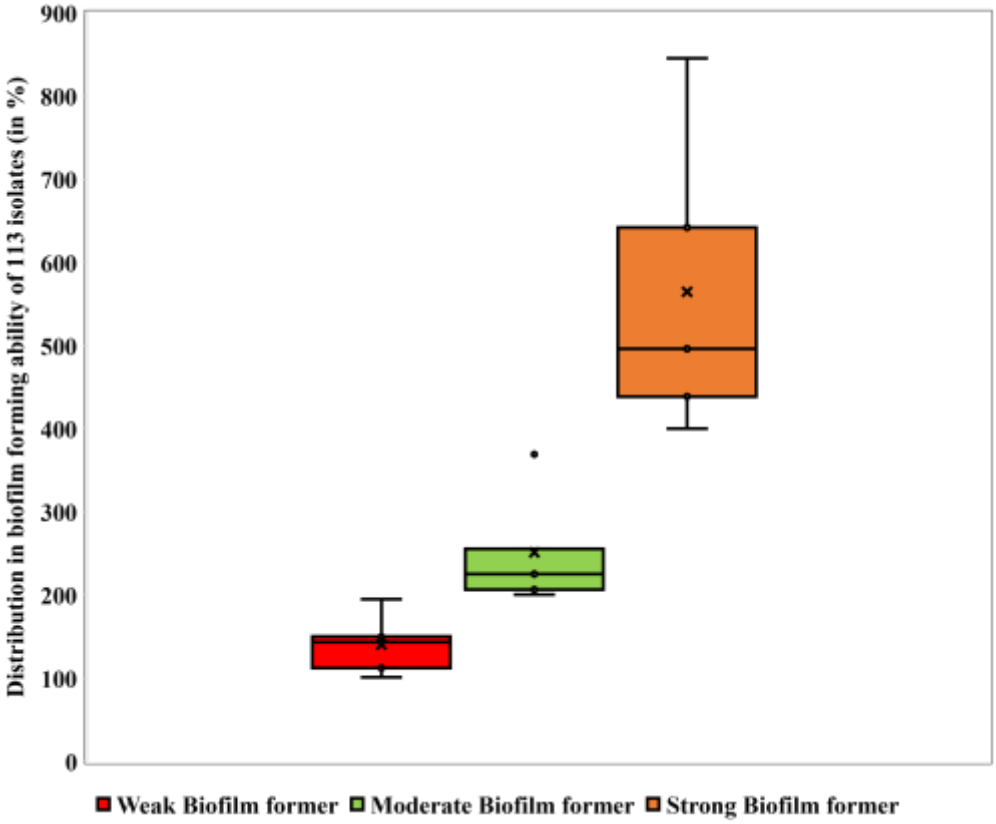

Figure 3.5. Distribution/diversity of biofilm-forming ability and skewness of 113 *E. coli* isolates. Bacterial cultures maintained at 0.5 MacFarland standard were subjected to the MH broth. The plates were incubated without shaking. The biofilm formation was assessed using crystal violet assay and the levels of biofilm formation were categorized based on the $OD_{cut\text{-}off}$ value which was considered as 100%. The biofilm-forming ability was further classified as: Biofilm breakpoint (%) ≤ 100% = Non-biofilm formers (NBF), 100% < Biofilm breakpoint (%) ≤ 200% = Weak Biofilm formers (WBF), 200% < Biofilm breakpoint (%) ≤ 400% = Moderate Biofilm formers (MBF), Biofilm breakpoint (%) > 400% = Strong Biofilm formers (SBF).

Resistant *E. coli* ID no.	Hemolysis production	Biofilm formation pattern	Gene profiling				
			Hemolysis associated genes	Adhesion and aggregation	c-di-GMP formation	Stress response	Autoinducer-2
40202761				*fdeC, fimA, fimH , csgA/B/C, csgD/E/F/G*	*pdeA/D/F/H/K/N, pdeG, pdeR, bdcA, bdcR, bcsA/E, bcsB/G/Z, bcsC, bcsQ, pgaA/C/D, pgaB*	*rpoS, hfq, tabA, hha, bshA, cspA/D, cspC/E/G, cspJ, marA, rob, soxS, ariR*	*tqsA, luxS*
41100011				*fdeC, fimA, fimH , csgA/B/C, csgD/E/F/G*	*pdeA/D/F/H/K/N, pdeG, pdeR, bdcA, bdcR, bcsE, bcsB/G/Z, bcsC,, pgaA/C/D, pgaB*	*rpoS, hfq, tabA, hha, bshA, cspA/D, cspB, cspC/E/G_I, cspJ, marA, rob, soxS, ariR*	*tqsA, luxS*
20202040			*hlyA, hlyB, hlyC, hlyD, hlyE*	*fdeC, fimA, fimH , csgA/B/C, csgD/E/F/G*	*pdeA/D/F/H/K/N, pdeG, pdeR, bdcA, bdcR, bcsA/E, bcsB/G/Z, bcsC, bcsQ, pgaA/C/D, pgaB*	*rpoS, hfq, tabA, hha, bshA, cspA/D, cspB, cspC/E/G_I, cspJ, marA, rob, soxS, ariR*	*tqsA, luxS*
41300398			*hlyA, hlyB, hlyC, hlyD, hlyE*	*fdeC, fimA, fimH , csgA/B/C, csgD/E/F/G*	*pdeA/D/F/H/K/N, pdeG, pdeR, bdcA, bdcR, bcsA/E, bcsB/G/Z, bcsC, bcsQ, pgaA/C/D, pgaB*	*rpoS, hfq, tabA, hha, bshA, cspA/D, cspB, cspC/E/G_I, cspJ, marA, rob, soxS*	*tqsA, luxS*
41613979				*fdeC, fimA, fimH , csgA/B/C, csgD/E/F/G*	*pdeA/D/F/H/K/N, pdeG, pdeR, bdcA, bdcR, bcsA/E, bcsB/G/Z, bcsC, bcsQ, pgaA/C/D, pgaB*	*rpoS, hfq, tabA, hha, bshA, cspA/D, cspB, cspC/E/G_I, cspJ, marA, rob, soxS, ariR*	*tqsA, luxS*
32708899				*fdeC, fimA, fimH , csgA/B/C, csgD/E/F/G*	*pdeA/D/F/H/K/N, pdeG, pdeR, bdcA, bdcR, bcsA, bcsB/G/Z, bcsC, pgaA/C/D, pgaB*	*rpoS, hfq, tabA, hha, bshA, cspA/D, cspC/E/G_I, cspJ, marA, rob, soxS, ariR*	*tqsA, luxS*

21012914			*hlyA, hlyB, hlyC, hlyD, hlyE*	*fdeC, fimH , csgA/B/C, csgD/E/F/G*	*pdeA/D/F/H/K/N, pdeG, pdeR, bdcA, bdcR, bcsA/E, bcsB/G/Z, bcsC, bcsQ, pgaA/C/D, pgaB*	*rpoS, hfq, tabA, hha, bshA, cspA/D, cspB, cspC/E/G_I, cspJ, marA, rob, soxS, ariR*	*tqsA, luxS*
10415566			*hlyA, hlyB, hlyC, hlyD, hlyE*	*fdeC, fimH , csgA/B/C, csgD/E/F/G*	*pdeA/D/F/H/K/N, pdeG, pdeR, bdcA, bdcR, bcsA/E, bcsB/G/Z, bcsC, bcsQ, pgaA/C/D, pgaB*	*rpoS, hfq, tabA, hha, bshA, cspA/D, cspB, cspC/E/G_I, cspJ, marA, rob, soxS, ariR*	*tqsA, luxS*
40714004				*fdeC, fimA, fimH , csgA/B/C, csgD/E/F/G*	*pdeA/D/F/H/K/N, pdeG, pdeR, bdcA, bdcR, bcsA/E, bcsB/G/Z, bcsC, bcsQ, pgaA*	*rpoS, hfq, tabA, hha, bshA, cspA/D, cspC/E/G_I, marA, rob, soxS*	*tqsA, luxS*
10715833				*fdeC, fimA, fimH , csgA/B/C, csgD/E/F/G*	*pdeA/D/F/H/K/N, pdeG, pdeR, bdcA, bdcR, bcsA/E, bcsB/G/Z, bcsC, bcsQ*	*rpoS, hfq, tabA, hha, bshA, cspA/D, cspB, cspC/E/G_I, cspJ, marA, rob, soxS, ariR*	*tqsA, luxS*
41701140				*fdeC, fimA, fimH , csgA/B/C, csgD/E/F/G*	*pdeA/D/F/H/K/N, pdeG, pdeR, bdcA, bdcR, bcsA/E, bcsB/G/Z, bcsC, bcsQ, pgaA/C/D, pgaB*	*rpoS, hfq, tabA, hha, bshA, cspA/D, cspB, cspC/E/G_I, cspJ, marA, rob, soxS, ariR*	*tqsA, luxS*
30215009			*hlyA, hlyB, hlyC, hlyD, hlyE*	*fdeC, fimA, fimH , csgA/B/C, csgD/E/F/G*	*pdeA/D/F/H/K/N, pdeG, pdeR, bdcA, bdcR, bcsA/E, bcsB/G/Z, bcsC, bcsQ, pgaA/C/D, pgaB*	*rpoS, hfq, tabA, hha, bshA, cspA/D, cspC/E/G_I, marA, rob, soxS, ariR*	*tqsA, luxS*
22113962				*fdeC, fimA, fimH , csgA/B/C, csgD/E/F/G*	*pdeA/D/F/H/K/N, pdeG, pdeR, bdcA, bdcR, bcsA/E, bcsB/G/Z, bcsC, bcsQ, pgaA/C/D, pgaB*	*rpoS, hfq, tabA, hha, bshA, cspA/D, cspB, cspC/E/G_I, cspJ, marA, rob, soxS, ariR*	*tqsA, luxS*

20314330				*fdeC, fimA, fimH , csgA/B/C, csgD/E/F/G*	*pdeA/D/F/H/K/N, pdeR, bdcA, bdcR, bcsA/E, bcsB/G/Z, bcsC, bcsQ, pgaA/C/D, pgaB*	*rpoS, hfq, tabA, hha, bshA, cspA/D, cspB, cspC/E/G_I, cspJ, marA, rob, soxS*	*tqsA, luxS*
11211990				*fdeC, fimA, fimH , csgA/B/C, csgD/E/F/G*	*pdeA/D/F/H/K/N, pdeG, pdeR, bdcA, bdcR, bcsA/E, bcsB/G/Z, bcsC, bcsQ, pgaA/C/D, pgaB*	*rpoS, hfq, tabA, hha, bshA, cspA/D, cspB, cspC/E/G_I, cspJ, marA, rob, soxS, ariR*	*tqsA, luxS*
21317859				*fdeC, fimA, fimH , csgA/B/C, csgD/E/F/G*	*pdeA/D/F/H/K/N, pdeG, pdeR, bdcA, bdcR, bcsA/E, bcsB/G/Z, bcsC, bcsQ, pgaA/C/D, pgaB*	*rpoS, hfq, tabA, hha, bshA, cspA/D, cspC/E/G_I, cspJ, marA, rob, soxS, ariR*	*tqsA, luxS*
21309335				*fdeC, fimA, fimH , csgA/B/C, csgD/E/F/G*	*pdeA/D/F/H/K/N, pdeG, pdeR, bdcA, bdcR, bcsA/E, bcsB/G/Z, bcsC, bcsQ, pgaA/C/D, pgaB*	*rpoS, hfq, tabA, hha, bshA, cspA/D, cspB, cspC/E/G_I, cspJ, marA, rob, soxS, ariR*	*tqsA, luxS*
31209373			*hlyA, hlyB, hlyC, hlyD, hlyE, hlyB_2*	*fdeC, fimA, fimH , csgA/B/C, csgD/E/F/G*	*pdeA/D/F/H/K/N, pdeR, bdcA, bdcR, bcsA/E, bcsB/G/Z, bcsC, bcsQ, pgaA/C/D, pgaB*	*rpoS, hfq, tabA, hha, bshA, cspA/D, cspB, cspC/E/G_I, cspJ, marA, rob, soxS, ariR*	*tqsA, luxS*
40611099				*fdeC, fimA, fimH , csgA/B/C, csgD/E/F/G*	*pdeA/D/F/H/K/N, pdeG, pdeR, bdcA, bdcR, bcsC, pgaA/C/D, pgaB*	*rpoS, hfq, tabA, hha, bshA, cspA/D, cspB, cspC/E/G_I, cspJ, marA, rob, soxS, ariR*	*tqsA, luxS*
30300071				*fdeC, fimA, fimH , csgA/B/C, csgD/E/F/G*	*pdeA/D/F/H/K/N, pdeG, pdeR, bdcA, bdcR, bcsA/E, bcsB/G/Z, bcsC, bcsQ, pgaA/C/D, pgaB*	*rpoS, hfq, tabA, hha, bshA, cspA/D, cspC/E/G_I, marA, rob, soxS*	*tqsA, luxS*

11800057			*hlyE, hlyB_2*	*fdeC, fimA, fimH , csgA/B/C, csgD/E/F/G*	*pdeA/D/F/H/K/N, pdeG, pdeR, bdcA, bdcR, bcsA/E, bcsB/G/Z, bcsC, bcsQ, pgaA/C/D, pgaB*	*rpoS, hfq, tabA, hha, bshA, cspA/D, cspC/E/G_I, marA, rob, soxS*	*tqsA, luxS*
41505922				*fdeC, fimA, fimH , csgA/B/C, csgD/E/F/G*	*pdeA/D/F/H/K/N, pdeG, pdeR, bdcA, bdcR, bcsA/E, bcsB/G/Z, bcsC, bcsQ, pgaA/C/D, pgaB*	*rpoS, hfq, tabA, hha, bshA, cspA/D, cspB, cspC/E/G_I, cspJ, marA, rob, soxS, ariR*	*tqsA, luxS*
32608632				*fdeC, fimH , csgA/B/C, csgD/E/F/G*	*pdeA/D/F/H/K/N, pdeG, pdeR, bdcA, bdcR, bcsB/G/Z, bcsC, pgaC/D*	*rpoS, hfq, tabA, hha, bshA, cspA/D, cspB, cspC/E/G_I, cspJ, marA, rob, soxS, ariR*	*tqsA, luxS*
22713162				*fdeC, fimA, fimH , csgA/B/C, csgD/E/F/G*	*pdeA/D/F/H/K/N, pdeG, pdeR, bdcA, bdcR, bcsA/E, bcsB/G/Z, bcsC, bcsQ, pgaA/C/D, pgaB*	*rpoS, hfq, tabA, hha, bshA, cspA/D, cspB, cspC/E/G_I, cspJ, marA, rob, soxS, ariR*	*tqsA, luxS*
20814168				*fdeC, fimA, fimH , csgA/B/C, csgD/E/F/G*	*pdeA/D/F/H/K/N, pdeG, pdeR, bdcA, bdcR, bcsA/E, bcsB/G/Z, bcsC, bcsQ, pgaA/C/D, pgaB*	*rpoS, hfq, tabA, hha, bshA, cspA/D, cspB, cspC/E/G_I, cspJ, marA, rob, soxS, ariR*	*tqsA, luxS*
10417409			*hlyA, hlyB, hlyC, hlyD, hlyE*	*fdeC, fimH , csgA/B/C, csgD/E/F/G*	*pdeA/D/F/H/K/N, pdeG, pdeR, bdcA, bdcR, bcsA/E, bcsB/G/Z, bcsC, bcsQ, pgaA/C/D, pgaB*	*rpoS, hfq, tabA, hha, bshA, cspA/D, cspB, cspC/E/G_I, cspJ, marA, rob, soxS, ariR*	*tqsA, luxS*
40816739				*fdeC, fimA, fimH , csgA/B/C, csgD/E/F/G*	*pdeA/D/F/H/K/N, pdeG, pdeR, bdcA, bdcR, bcsA/E, bcsB/G/Z, bcsC, bcsQ, pgaA/C/D, pgaB*	*rpoS, hfq, tabA, hha, bshA, cspA/D, cspC/E/G_I, marA, rob, soxS, ariR*	*tqsA, luxS*

10216675				*fdeC, fimA, fimH , csgA/B/C, csgD/E/F/G*	*pdeA/D/F/H/K/N, pdeG, pdeR, bdcA, bdcR, bcsA/E, bcsB/G/Z, bcsC, bcsQ, pgaA/C/D, pgaB*	*rpoS, hfq, tabA, hha, bshA, cspA/D, cspB, cspC/E/G_I, cspJ, marA, rob, soxS, ariR*	*tqsA, luxS*
40317434			*hlyA, hlyB, hlyC, hlyD, hlyE*	*fdeC, fimA, fimH , csgA/B/C, csgD/E/F/G*	*pdeA/D/F/H/K/N, pdeG, pdeR, bdcA, bdcR, bcsA/E, bcsB/G/Z, bcsC, bcsQ, pgaA/C/D, pgaB*	*rpoS, hfq, tabA, hha, bshA, cspA/D, cspB, cspC/E/G_I, cspJ, marA, rob, soxS, ariR*	*tqsA, luxS*
21215100			*hlyA, hlyB, hlyC, hlyD, hlyE*	*fdeC, fimA, fimH , csgA/B/C, csgD/E/F/G*	*pdeA/D/F/H/K/N, pdeG, pdeR, bdcA, bdcR, bcsA/E, bcsB/G/Z, bcsC, bcsQ, pgaA/C/D, pgaB*	*rpoS, hfq, tabA, hha, bshA, cspA/D, cspB, cspC/E/G_I, cspJ, marA, rob, soxS, ariR*	*tqsA, luxS*
21416415				*fdeC, fimA, fimH , csgA/B/C, csgD/E/F/G*	*pdeA/D/F/H/K/N, pdeG, pdeR, bdcA, bdcR, bcsA/E, bcsB/G/Z, bcsC, bcsQ, pgaA/C/D, pgaB*	*rpoS, hfq, tabA, hha, bshA, cspA/D, cspB, cspC/E/G_I, cspJ, marA, rob, soxS, ariR*	*tqsA, luxS*
20508456				*fdeC, fimA, fimH , csgA/B/C, csgD/E/F/G*	*pdeA/D/F/H/K/N, pdeG, pdeR, bdcA, bdcR, bcsA/E, bcsB/G/Z, bcsC, bcsQ, pgaA/C/D, pgaB*	*rpoS, hfq, tabA, hha, bshA, cspA/D, cspC/E/G_I, marA, rob, soxS*	*tqsA, luxS*

Table 3.3. Patterns associated to the virulence factors and gene profile of the 32 antibiotic resistant *E. coli* isolates. Color codes: Weak biofilm-formers-Light Grey; Moderate biofilm formers-Dark Grey; Strong biofilm formers-Black, Hemolysis production-Blue Grey.

We also investigated a possible relationship between efflux pump activity and the biofilm-forming ability of *E. coli*. The biofilm formation of all the 13 isolates with functional efflux pump was significantly lowered ($p<0.05$) when they were subjected to the efflux-pump inhibitor, CCCP, while the biofilm-forming ability of the QC strain (without efflux pump activity) wasn't affected by CCCP **(Supplementary figure S3 and S4)**. **Figure 3.3d-f** shows the impact of CCCP on the biofilm-forming ability of isolate 41602577 (with the fastest extrusion), isolate 40816739 (with the slowest extrusion), and QC strain (with non-functional AcrAB-TolC). The efflux activity showed a significant positive correlation ($p<0.0001$, Pearson $r = +0.89$) with the biofilm-forming ability of the 13 isolates **(Figure 3.3g)**.

3.4. Discussion

In this study, we evaluated the prevalence of AMR in *E. coli* isolates from the cases of clinical bovine mastitis in Canada. Several strains showed resistance towards one or more antibiotics and metals. Further investigation identified efflux pump activity and ß-lactamases along with corresponding genes (ß-lactamase producing genes: *bla*$_{\text{TEM-1}}$, *bla*$_{\text{CARB-3}}$, *bla*$_{\text{CMY-59}}$, efflux pump inducing genes: *acrA, acrB, acrD, tolC, baeR, emrA, emrB*). Apart from AMR properties, we also found virulence factors such as biofilm formation and hemolysis in several isolates that support bacterial survival in host tissues. Notably, there was a positive correlation between efflux pump activity and biofilm formation.

Of the 113 isolates included in this study, 28.31% were shown to be resistant to at least one antibiotic. The rate of resistance seen in our study was comparable with previous studies that had examined a larger library of *E. coli* isolates from bovine mastitis (Saini, McClure, Léger, et al., 2012). All isolates showed susceptibility towards ciprofloxacin and ofloxacin, which was in

agreement with earlier observations (Makovec & Ruegg, 2003; Saini, McClure, Léger, et al., 2012). The effectiveness of these antibiotics was possibly due to their less frequent application in Canadian dairy farms. In Canada, the use of these antibiotics has been restricted for farm applications to minimize the chance of resistance emergence against these last-resort drugs for human applications (*Uses of antimicrobials in food animals in Canada: impact on resistance and human health*, 2002).

Although antimicrobial susceptibility testing for Canadian *E. coli* isolates from cases of bovine mastitis has been performed in the past, this study went on to identify the genes that confer AMR including the ones that are transmissible through horizontal gene transfer (J. H. Fairbrother et al., 2015). Out of the fourteen isolates with β-lactamase enzyme activity, two isolates carried $bla_{\text{CMY-59}}$, three isolates carried $bla_{\text{TEM-1B}}$, one carried $bla_{\text{CARB-3}}$. This was one of a few cases that identified *cmy* and *tem* genes in the isolates from Holstein dairy cattle among other two studies which identified these genes in *E. coli* isolates from colostrum and feces of the cattle in New Brunswick (B. Awosile et al., 2018; B. B. Awosile et al., 2017). Other important emerging resistance genes found in our study included tetracycline resistance genes (*tetA, tetB, tetC*) and aminoglycoside resistance gene (*aadA2*) which were not identified from any isolates from CM by the previous studies although the phenotypic resistance to corresponding drugs was identified (J. H. Fairbrother et al., 2015).

The isolates 10800294 and 21914232 showed resistance to cefazolin and cefotaxime without ESBL or plasmid-mediated AmpC β-lactamase genes. The expression of their β-lactamase enzyme activities was less than that of other isolates that had $bla_{\text{CMY-59}}$, $bla_{\text{TEM-1B}}$, and $bla_{\text{CARB-3}}$. Their resistance might be due to extrusion by efflux pump and biofilm-forming ability: Isolate 10800294 was a strong biofilm former and had an active AcrAB-TolC whereas, isolate 21914232 was a moderate biofilm former ($t_{\text{efflux50\%}}$=11.35 secs) (Amanatidou et al., 2019; Nishino, Yamada, Hirakawa, Hirata, & Yamaguchi, 2003). Interestingly, two other isolates,

40611099 and 31801812 showed resistance to colistin while none of them harbored MCR genes and plasmid-mediated colistin determinants genes. This also might be due to complex mechanisms by efflux pump in the case of isolate 31801812 which had a strong efflux pump activity ($t_{efflux50\%}$=7.03 secs) (Olaitan, Morand, & Rolain, 2014). Therefore, despite the ESBL, plasmid-mediated AmpC β-lactamase, and MCR as emerging resistance, the assessment of the efflux pump mediated-resistance to clinically important drugs such as β-lactams and colistin is required for a better understanding of AMR emergence and its potential increase in dairy farms. Isolates 40611099 and 21914232 had no AcrAB-TolC efflux activity and it might employ several other previously reported strategies against polymixins including a variety of lipopolysaccharides (LPS) modifications, such as modifications of lipid A with phosphoethanolamine and 4-amino-4-deoxy-L-arabinose, and overexpression of the outer membrane of protein OprH (Olaitan et al., 2014). Ampicillins and cephalosporins resistant isolates without any acquired β-lactamase genes could be because of the mutations in the promoter regions of the chromosomal *E. coli* AmpC gene (Davis et al., 2011). Efflux or ß-lactamase enzyme activities were not identified in 15 of the 32 AMR isolates. The existence of alternate resistant mechanisms such as limiting hydrophilic drug uptake or drug-target modifications *via* the acquisition of the plasmids carrying 16S rRNA methyltransferases and other enzymes could be the possible reasons (Reygaert, 2018).

We observed 33 isolates with hemolysin activity. Of the hemolytic isolates, 10 were also resistant to one or more antibiotics. The hemolysin phenotype corresponded with the presence of genetic determines *HlyA/E/C/B/D*, which were also identified in our genomic analysis. α-hemolysis is an important secretory virulence factor that is reported to be produced by 20-50% of strains from bovine IMI (O. Dego, 2020).

The *E. coli* isolates produced biofilms, that included weak (n=35), moderate (n=56), and strong (n=22) biofilm formers. Different sets of genes that confer biofilm formation were

identified which encode adhesion, aggregation, c-di-GMP formation, stress inducer, and autoinducer-2. The potential contributions of *csgB/A* and *csgD/E/F/G* as a host cell adhesion and invasion mediator, and inducers of the host inflammatory responses; *pde, bdc, bcs* and *pga* gene involvement in chemotaxis, surface colonization, and persistence have already been established (Barnhart & Chapman, 2006; Reinders et al., 2016). The transcription factors; *marA, soxS,* and *rob* found in our study is reported to play a crucial role in mediating MDR by up-regulating the expression of the AcrAB-TolC efflux pump (Duval & Lister, 2013).

Efflux systems have been established to be a contributing factor in the intrinsic antibiotic resistance by *E. coli* (Li et al., 2020). The decreased biofilm formation in the 13 AMR isolates by inhibiting their efflux activity showed a possible role of efflux pump in *E. coli* biofilm formation. Generally, four possible roles of efflux pumps in biofilm formation are postulated: indirect regulation of genes involved in biofilm formation, efflux of extra-polymeric substances/quorum sensing (QS) and quorum quenching molecules to facilitate biofilm matrix formation and regulate QS respectively, efflux of threatening antibiotics and metabolic intermediates, promote aggregation or prevent adhesion to surfaces and other cells (Alav, Sutton, & Rahman, 2018). The QseBC regulator found in our study has previously been reported to upregulate the transcription of the efflux-pump-associated genes in *E. coli* isolated from mastitis cases (Li et al., 2020).

Of the 113 isolates, 107 of them were resistant to at least one metal tested. The antibacterial efficiency of copper and zinc against *E. coli* isolates identified in our study contradicts significantly by more than 80 and 60-folds respectively, from a study reported by Hoque et al. with *E. coli* isolates from mastitis cases of Bangladesh (Hoque et al., 2020). However, less is known about the use of these heavy metals in Canadian dairy cow feed and their content in raw milk (Zwierzchowski & Ametaj, 2019). Therefore, it is difficult to identify the significance of the metal-resistant *E. coli* from bovine mastitis which requires more

investigations on the use of heavy metals to correlate with its resistance. The identified copper and silver resistant genes such as *pcoC, pcoE, copB, copD* and *silE, silP* respectively and cationic efflux system proteins such as CusA, CusB, CusC, CusF, CusS, CusR in our study are previously reported to be involved in the detoxification of copper and silver in *E. coli* as a part of the CusCFBA copper/silver efflux system (Franke, Grass, Rensing, & Nies, 2003). Genes such as *zntA, zntB, znuA, znuB, znuC, zitB, zraP* identified in the *E. coli* chromosome are also reported to be one of the key factors for zinc resistance (Rensing, Mitra, & Rosen, 1997).

3.5. Conclusion

Unlike other pathogens, intramammary infections caused by *E. coli* rarely require antibiotic interventions but are reported to cause persistent infection (A. Bradley & Green, 2001). Given the possibility of *E. coli* shedding in milk and AMR transmittance to other pathogenic bacteria, the finding that resident *E. coli* harbors multiple drug resistance and virulence characteristics has implications for public health. Further, unveiling prevalent mechanisms of AMR in pathogenic bacteria from animal farms is vital for designing novel drugs and treatment strategies. Results from our study suggest the inadequacy of antimicrobials with a single mode of action to curtail AMR bacteria with multiple mechanisms of resistance and virulence factors and therefore, calls for combinatorial therapy for effective management of AMR infections in dairy farms and combat its potential transmission to the food supply chain through the milk and dairy products. As biofilm formation and efflux activity play a major role in the persistence of bacteria in bovine udders and resistance towards several antimicrobials, the relation between efflux property and biofilm-forming ability shown in our study would possibly open up a new horizon in the development of combinatorial-therapeutic strategies.

3.6. Supplementary information

Supplementary tables are provided in: https://static-content.springer.com/esm/art%3A10.1186%2Fs12866-021-02280-5/MediaObjects/12866_2021_2280_MOESM2_ESM.xlsx

Caption: Table S1. Details of the isolates used in the study. **Table S2.a.** Antibiotic ranges based on CLSI guidelines. **Table S2.b.** Antibiotic susceptibility test result. **Table S3.** Information of genome of mammary pathogenic *E. coli*. **Table S4.** List of antibiotic resistant genes. **Table S5.a.** Categorization of responses by *E. coli* isolates based on the IC50 values of metal salts against the QC stains. **Table S5.b.** Whole genome sequencing data (metal resistant genes). **Table S6.a.** Classification of the levels of biofilm formation by the *E. coli* isolates. **Table S6.b.** Virulence traits of *E. coli* and corresponding genes.

Supplementary figures are provided in: https://static-content.springer.com/esm/art%3A10.1186%2Fs12866-021-02280-5/MediaObjects/12866_2021_2280_MOESM1_ESM.docx

Caption: Figure S1. Representation of the efflux efficiency implying a functional AcrAB-TolC efflux gene in all 13 *E. coli* isolates after re-energizing cells by adding 25mM of glucose.

Caption: Figure S2. Depiction of the nitrocefin hydrolysis with respect to time implying the ß-lactamase enzymatic activity induced by 14 *E. coli* isolates.

Caption: Figure S3. Representation of the MIC (50 µg/ml) of CCCP against 13 *E. coli* isolates and QC strain at OD_{600}. Ten-twofold serial dilutions of the CCCP (from 100 µg/mL to 0.19 µg/mL) were prepared in 100 µL of MH broth in 96 well plates. Ten microliters of pure bacterial cultures

maintained at 0.5 McFarland standard were subjected to the wells. The plates were incubated and read at OD_{600} using a plate reader. The study was done to ensure the engagement of CCCP as an anti-biofilm agent rather than interfering in bacterial viability. Asterisks indicate a significant decrease in bacterial viability when compared with the control. One-way ANOVA was performed to check the statistical significance of the obtained data where p-value <0.05 was considered as significant.

Caption: Figure S4. Representation of the impact of efflux inhibitor, CCCP on the ability of 13 *E. coli* isolates to form biofilms. One-way ANOVA was performed to check the statistical significance of the obtained data where p-value <0.05 was considered as significant. GraphPad Prism 7 software was used to carry out statistical analysis and for graphical representation.

Preface to Chapter 4

In the previous chapter, I characterized a library of 113 *E. coli* isolates for AMR and virulence characteristics. *E. coli* showed resistance against heavy metals and multiple antibiotics that are considered essential for animal agriculture and public health. They exhibited active efflux pump and beta-lactamase enzyme activity and possessed virulence characteristics such as biofilm forming and hemolysin production ability. Genes associated with AMR and virulence were detected, corroborating phenotype observations. Overall, Chapter 3 reported the inadequacy of antimicrobials with a single mode of action to curtail AMR bacteria with multiple resistance mechanisms and virulence factors. Another contagious bacterium that are highly prevalent in bovine mastitis is *Staphylococcus aureus* as it has been reported to cause 40-70% of persistent and chronic intramammary infection, globally. *S. aureus* possess threat to both veterinary and public health due to the emergence of AMR and possible zoonotic spillovers. Therefore, Chapter 4 assesses AMR and virulence status in a library of *S. aureus* and their pathogenic translation in human infection models. Here, *S. aureus* isolates were tested for ABR and virulence through phenotypic and genotypic profiling. I further investigated the infectivity of the isolates in intestinal infection models of Caco-2 cells and *Caenorhabditis elegans* and assessed the efficiency of antibiotics in remediating such infections. Whole genome data was used to check for human adaptive genes and the possibility of zoonoses. An extensive understanding of these factors is pivotal for clinical management of disease as well as for designing new therapeutic agents.

Chapter 4

Genomic and phenotypic profiling of *Staphylococcus aureus* isolates from bovine mastitis for antibiotic resistance and intestinal infectivity

Abstract

Staphylococcus aureus is one of the prevalent etiological agents of contagious bovine mastitis, causing a significant economic burden on the global dairy industry. Given the emergence of antibiotic resistance (ABR) and possible zoonotic spillovers, *S aureus* from mastitic cattle pose threat to both veterinary and public health. Therefore, assessment of their ABR status and pathogenic translation in human infection models is crucial. In this study, 43 *S. aureus* isolates associated with bovine mastitis obtained from four different Canadian provinces (Alberta, Ontario, Quebec, and Atlantic provinces) were tested for ABR and virulence through phenotypic and genotypic profiling. All 43 isolates exhibited crucial virulence characteristics such as hemolysis, and biofilm formation, and six isolates from ST151, ST352, and ST8 categories showed ABR. Genes associated with ABR (*tetK, tetM, aac6', norA, norB, lmrS*, *blaR, blaZ*, *etc*.), toxin production (*hla, hlab*, *lukD*, *etc*.), adherence (*fmbA, fnbB, clfA, clfB*, *icaABCD*, *etc*.), and host immune invasion (*spa, sbi, cap, adsA*, *etc*.) were identified by analyzing whole-genome sequences. Although none of the isolates possessed human adaptation genes, both groups of ABR and antibiotic-susceptible isolates demonstrated intracellular invasion, colonization, infection, and death of human intestinal epithelial cells (Caco-2), and *Caenorhabditis elegans*. Notably, the susceptibilities of *S. aureus* towards antibiotics such as streptomycin, kanamycin, and ampicillin were altered when the bacteria were internalized in Caco-2 cells and *C. elegans*. Meanwhile, tetracycline,

chloramphenicol, and ceftiofur were comparatively more effective with ≤2.5 $\log_{10}$ reductions of intracellular *S. aureus*. This study demonstrated the potential of *S. aureus* isolated from mastitis cows to possess virulence characteristics enabling invasion of intestinal cells thus calling for developing therapeutics capable of targeting drug-resistant intracellular pathogens for effective disease management.

Keywords: *Staphylococcus aureus*, bovine mastitis, antibiotics, antibiotic resistance (ABR), virulence characteristics, intracellular pathogens, zoonotic spillover, intestinal infection, Caco-2 cells, *Caenorhabditis elegans*.

4.1. Introduction

Staphylococcus aureus is a versatile pathogen that is reported to cause a plethora of infections ranging from superficial skin infections to life-threatening diseases in livestock (S. Park et al., 2022). It is considered to be the most prevalent etiological agent of contagious bovine mastitis worldwide causing a significant economic burden on the dairy industry (S. Park & Ronholm, 2021). The prevalence of bacterial infections is not only a challenge for the clinical management of mastitis but could also be a public health concern as mastitis may contribute to zoonotic spillover (the transfer of bacteria or genetic determinants to humans) majorly through direct contact with the infected dairy cattle (Boss et al., 2016). In humans, *S. aureus* has been associated with a wide range of infectious diseases such as endocarditis, hemolytic pneumonia, toxin-mediated conditions such as scalded skin syndrome, staphylococcal food poisoning or gastroenteritis, toxic shock syndromes, etc. (S. Y. Tong, Davis, Eichenberger, Holland, & Fowler, 2015).

In contrast to environmental pathogens, infections caused by contagious mastitis pathogens such as *S. aureus* are difficult to treat in agricultural settings due to an array of virulence traits including the production of biofilms, toxins, and enzymes, evasion of phagocytic/non-phagocytic host cells, and immune defence mechanisms (Dego, Van Dijk, & Nederbragt, 2002). *S. aureus* can switch its phenotypes between wild types and small colony variants, and survive intracellularly contributing to persistent colonization in the intramammary environment and leading to recurrent bovine mastitis (O. Dego, 2020). The persistence of such infection within the mammary gland demands the frequent use of antibiotics, the excessive application of which over the years has led to antibiotic resistance (ABR) and treatment failures (Majumder et al., 2021). Antibiotics including aminoglycosides, ß-lactams, cephalosporins, tetracyclines, *etc*. have been used for controlling *S. aureus* infection, however, these antibiotics have shown inconsistent efficiency (Larsen et al., 2022).

Although there is plenty of information on the infectivity of *S. aureus* from cattle in mastitis infection models, there are prominent knowledge gaps on the pathogenic translation of mastitic *S. aureus* in human infection models. Human intestinal epithelial Caco-2 cells are considered to be an efficient model to investigate bacterial intracellular invasion, while *Caenorhabditis elegans* are broadly accepted as an *in vivo* model with higher throughput to assess bacterial intestinal pathogenicity and antimicrobial efficacy (Kwak et al., 2012). The acceptability of *C. elegans* is based on the key similarities with the mammalian intestine such as the presence of polarized epithelial cells with microvilli, and the first line of defence against invading pathogens (H. Jiang & Wang, 2018).

In this study, we examined 43 *S. aureus* isolates collected from Canadian dairy cattle with active mastitis for ABR and virulence characteristics through genotypic and phenotypic profiling. These isolates were chosen as a subpopulation of the entire collection available at the Mastitis Pathogen Culture Collection (MPCC). We investigated the infectivity of the

isolates in intestinal infection models of Caco-2 cells and *C. elegans* and assessed the efficiency of antibiotics in remediating such infections. Additionally, the whole genome analysis data available for the selected isolates were used to compare the genotype and phenotype for ABR and virulence characteristics.

4.2. Materials and methods

4.2.1. Isolation of the *S. aureus* from cases of clinical mastitis

A library of 43 *S. aureus* isolates analyzed in this study are a part of the mastitis pathogen culture collection (MPCC) and collected from different Canadian provinces (Alberta, Ontario, Quebec, and Atlantic provinces) (Dufour, Labrie, & Jacques, 2019; Reyher et al., 2011). The metadata including the numbers and locations of the herd, sampling dates, mastitis severity score, isolate IDs, and notations are summarized in **Table S1**. The isolates were grown in Tryptic Soy Agar (TSA) plates with 5% sheep blood (Hardy Diagnostics, Canada), but were cultured in Mueller-Hinton broth (MHB) (Millipore Sigma, Canada) for conducting assays.

4.2.2. Susceptibility testing of the isolates against antibiotics

The *S. aureus* isolates were subjected to the Kirby-Bauer disc diffusion susceptibility tests following the clinical and laboratory standard institute (CLSI) guidelines (CLSI, 2017). Briefly, 24 antibiotics (Oxoid, Thermo Fischer Scientific, Canada) relevant to human and veterinary health from the classes of ß-lactams, aminoglycosides, cephalosporins, quinolones, macrolides, lincosamide, tetracycline, chloramphenicol, and sulphonamide were included in the study. The list of antibiotics and their corresponding antibiotic concentration breakpoints

suggested by CLSI are provided in **Table S2** (CLSI, 2017). *Escherichia coli* ATCC 25922, *Staphylococcus aureus* ATCC 25923, and *Pseudomonas aeruginosa* ATCC 27853 (Oxoid company, Canada) were used as quality control (QC) strains.

4.2.3. Detection of antibiotic resistance mechanisms in the isolates

Activities of the efflux pump and ß-lactamase enzyme in the isolates were determined as phenotypic characteristics of ABR. The efflux pump activities in the isolates were assessed following a pre-established protocol (Brar et al., 2022). Briefly, bacterial cells cultured overnight in MHB were washed twice in phosphate-buffered saline (PBS) (1X) and adjusted to 1.0 McFarland standard (approximately 3×10^8 c.f.u/mL) using DensiCHEK plus (BioMerieux, USA)). Ethidium bromide (EtBr) (3 µg/mL) was added to the bacterial suspensions followed by 30 µg/mL of an efflux pump inhibitor, chlorpromazine (CPZ). The bacterial suspensions were incubated under shaking at 25 ˚C for an hour to allow maximum intracellular accumulation of EtBr. The suspensions were washed, resuspended in PBS, and transferred (140 µL) to 96-well plates. The cells were reenergized to trigger the efflux of EtBr by adding 10 µL of glucose (0.4% v/v), and the fluorescence was monitored for 60 min at 37 ˚C using a plate reader (SpectraMax-i3X, Molecular Devices, USA) at 530/590 nm (excitation/emission). *S. aureus* ATCC 25923 with no efflux pump activity was used as a reference strain. GraphPad Prism 7 software was used to determine the time-dependent efflux of EtBr using a single exponential decay equation as detailed previously (Majumder et al., 2021). The time taken for the bacterial cells to extrude 50% of EtBr was denoted as $t_{efflux50\,\%}$.

The Nitrocefin assay was performed to determine the ß-lactamase enzyme activity (Brar et al., 2022). For this, isolates grown overnight in MHB were adjusted to McFarland 1.0. Ampicillin (5 µg/mL and 25 µg/mL for ampicillin susceptible and resistant isolates,

respectively) was added to the cell suspensions and incubated for 3 h at 37°C. Subsequently, suspensions were centrifuged at 8,900 × g for 10 min and the cells were washed in sodium phosphate buffer (pH – 7.0). Cells resuspended in buffer were sonicated on ice for 3 mins and the cell-free extract was collected by centrifugation (17,500 × g for 25 min). Ten microlitres of Nitrocefin (Abcam, Canada) (stock concentration: 0.5 mg/mL) were added to 10 µL of the cell-free extract in a 96-well plate. The final volume was adjusted to 100 µL using the buffer. The absorbance was recorded in kinetic mode for 15 min at 490 nm using a plate reader. *S. aureus* ATCC 25923 with no ß-lactamase enzyme activity was used as a reference strain. The β-lactamase enzyme activity was calculated using the formula:

$$\beta\text{-lactamase enzyme activity} = \frac{S_a}{Reaction\ time\ X\ S_v}$$

where S_a is the amount of nitrocefin (in µM) hydrolyzed between t_1 and t_2 of the standard curve; reaction time is the time difference between t_1 and t_2, and S_v is the sample volume (in mL) added to the well. The β-lactamase activity was reported as U/mL.

4.2.4. Determination of virulence characteristics in the isolates

The isolates were tested for hemolysin activity by growing colonies on Tryptic Soy Agar (TSA) plates containing 5% sheep blood. These plates were incubated for 24 h at 37 ˚C. The pattern of hemolysis was detected by visual inspection for the translucency around the bacterial colony as detailed previously (Buxton, 2005).

Biofilm-forming abilities of isolates were assessed by the crystal violet assay (George et al., 2020). Briefly, 10 µL of bacterial culture maintained at 0.5 McFarland standard (approximately 1.5×10^8 cfu/mL) was added to 100 µL of MHB media in a 96-well plate. The plates were incubated for 24 h at 37 °C without shaking. After incubation, the media was

discarded, and the wells were washed with saline to remove non-adherent cells. These plates were kept undisturbed to fix the biofilms at room temperature for 15 min after adding 100 µL of methanol (99% v/v) to each well. The wells were air-dried, followed by the addition of 200 µL of crystal violet (0.4% v/v) and incubation for 2 h. Wells in these plates were washed with saline and 100 µL of acetic acid (30% v/v) was added. The biofilm biomass was quantified by detecting absorbance at 570 nm. The isolates were classified into non-biofilm-formers, weak biofilm-formers, moderate biofilm-formers, and strong biofilm-formers by using the following formulae: $OD_{cut-off}$ = OD_{avg} of control + 3 × standard deviation (SD) of ODs of control; $OD \leq OD_{cut-off}$ = Non-biofilm-former (NBF); $OD_{cut-off} < OD \leq 2 \times OD_{cut-off}$ = Weak biofilm-former (WBF); $2 \times OD_{cut-off} < OD \leq 4 \times OD_{cut-off}$ = Moderate biofilm-former (MBF); $OD > 4 \times OD_{cut-off}$ = Strong biofilm-former (SBF) [7]. *S. aureus* ATCC 25923 was used as a reference strain.

4.2.5. Evaluation of intracellular survival of *S. aureus* isolates in human intestinal epithelial cells

Cellular internalization of the isolates and the response of internalized bacteria to antibiotics were determined as previously described (Brar et al., 2022). Caco-2 cells (ATCC, Virginia, USA) was used as the *in vitro* model of the human intestinal epithelium. The cells were cultured in a 96-well plate (2×10^4 cells/well) until confluent. Five antibiotic-susceptible and five resistant isolates were randomly selected and cultured overnight. The bacterial isolates (1.5×10^8 cells/mL) were added to each well to infect the Caco-2 cells and the plate was incubated for an hour. The cells were washed using PBS (4 ˚C) and subjected to gentamicin (10 µg/mL) for 30 min. The extracellular gentamicin was removed by washing the cells with PBS followed by incubation with Gibco Dulbecco's Modified Eagle Medium (DMEM)

(ThermoFisher, Canada) for 4 h to establish the intracellular infection model. Six antibiotics relevant to animal and human infection including Ampicillin (10 µg/mL), Kanamycin (30 µg/mL), Streptomycin (10 µg/mL), Chloramphenicol (30 µg/mL), Tetracycline (30 µg/mL), and Ceftiofur (30 µg/mL) (the standard concentration breakpoints of antibiotics suggested by CLSI) were selected to check their efficiency against intracellular isolates. The plates were incubated for 24 h after the addition of antibiotics in a cell culture incubator at 37 °C, with 5% CO_2. Subsequently, the cells were washed using PBS and lysed using 0.5% (v/v) of Triton-X. Colony-forming units (cfu) of viable intracellular bacteria were enumerated using the drop culture method as detailed earlier (Shao et al., 2022). *S. aureus* ATCC 25923 was used as a reference strain and cells infected with bacteria but without any treatment were considered as the negative control.

4.2.6. Evaluation of *S. aureus* pathogenicity in *Caenorhabditis elegans* model of intestinal infection

The *C. elegans* CF512 worms were age-synchronized with an alkaline bleach solution to the first larval stage (L1) and further attained the fourth larval (L4) stage with lawns of *E. coli* OP50 on solid nematode growth medium (NGM) for 48 h at 21 °C (Majumder et al., 2022). These worms were washed with M9 buffer and transferred to NGM plates with lawns of 1.5×10^8 cells of *S. aureus* isolates to establish infection. The plates were incubated for 48 h at 25 ˚C. The infected worms were then washed, resuspended in S-basal media, and exposed to antibiotics in a 96-well plate. After 24 h, the infected worms were washed again and transferred (n=15-30) to fresh solid NGM plates with *E. coli* OP50 lawns. The plates were examined every 24 h for 20 days for worm survivability using a dissection microscope (Wild Heerbrugg,

Switzerland). Untreated infected and non-infected worms were considered as controls. Live worms in the plates were scored with a transfer pick.

4.2.7. Fluorescence microscopic analysis of *S. aureus* in Caco-2 cells and *Caenorhabditis elegans*

Cells of *S. aureus* 30 (Sa30) were transformed with plasmids pSGFPS1 (coding GFP) and pSRFPS1 (coding RFP) to visualize bacterial survival in Caco-2 cells and the *C. elegans* models, respectively. GFP-labeled Sa30 was used to establish infection in Caco-2 cells and avoid interference in the assessment of cell viability, while RFP-labeled Sa30 was used to infect C. *elegans* and avoid interference from green autofluorescent worms. For this, plasmids of pSGFPS1 (BEI resources, NR-51163) and pSRFPS1 (BEI resources, NR-51164) from *S. aureus* RN4220 were purified using the Monarch® Plasmid Miniprep Kit (NEB) after pre-treating with 20 µg of lysostaphin (Sigma-Aldrich) for 30 min at 37 °C (S. Park et al., 2021). The electrocompetent cells of *S. aureus* 30 (Sa30), originally isolated from mastitic cattle, were prepared as reported earlier (S. Park et al., 2021). Briefly, 0.1 µg of the purified plasmid DNA and 70 µL of the *S. aureus* competent cells were combined and pulsed at 2.3 kV, 100 Ω, and 25 µF in 0.1 cm cuvette using the Gene Pulser Electroporation System (Bio-Rad Laboratories). The pulsed cells were transferred to 1 mL of brain heart infusion broth and incubated for 1 h at 37 ˚C under constant shaking (5 × g). The cell suspensions were cultured on Luria-Bertani agar (containing 10 µg/mL of trimethoprim) and then incubated overnight at 37 ˚C.

Transformations of bacterial cells were confirmed by acquiring epi-fluorescence images of the bacterial cells using a high-content screening microscope, Cell Discoverer 7 (Carl Zeiss, Germany). The cell death in Caco-2 ensuing bacterial (Sa30) infection was assessed using fluorescence probes. Briefly, the cells were added with 30 µL of fluorescence probes in

saline containing Hoechst 33342 (1 μM) (ThermoFisher, Canada) and Propidium iodide (PI) (5 μM) (ThermoFisher, Canada) to image for the number of live and dead cells (Shao et al., 2022; Xu, Basu, & George, 2021). These plates were kept at 37 °C for 30 min in the dark and epi-fluorescence images of the Caco-2 cells were captured using channels of blue (Hoechst (461 nm), staining cell nucleus), green (GFP from Sa30), and red (PI (615 nm) staining nucleus of dead Caco-2 cells). Similarly, images of infected and non-infected *C. elegans* were also acquired by Cell Discoverer 7. Green (505 nm), and red (583 nm) filter combinations were used to image green autofluorescence from *C. elegans* and red fluorescence from RFP labeled Sa30.

4.2.8. Identification of antibiotic resistance, and virulence genes through whole-genome analysis

The extraction and quantification of DNA of each isolate, DNA library preparation, whole-genome sequencing, assembly, and annotation of sequenced reads were conducted as reported previously **(Table S1)** (Dufour et al., 2019; Soyoun Park, Jung, Dufour, & Ronholm, 2020; S. Park et al., 2022). Initially, the isolates were identified using matrix-assisted laser desorption ionization-time of flight (MALDI) mass spectrometry. A single well-isolated colony from the TSA plates was cultured overnight at 37°C with agitation. An aliquot of the liquid culture was used for DNA extraction with the DNAzol reagent (Invitrogen) and lysostaphin (Sigma-Aldrich) following the manufacturer's instructions. Briefly, the Nextera Flex DNA library preparation kit (Illumina, San Diego, CA) and Nextera DNA CD indexes (96 indexes, 96 samples) were used to prepare sequencing libraries as paired-end libraries. The libraries were then sequenced using a MiSeq benchtop sequencer (Illumina) (301 cycles in each direction). The raw DNA sequences of the isolates were assembled using ProkaryoteAssembly version 0.1.6 (https://github.com/bfssi-forest-dussault/ProkaryoteAssembly), and the quality

of the genome assemblies was assessed using Qualimap (v. 2.2.2) (Majumder et al., 2021). Default parameters were applied except for the trimming step for which command trimq=20 was used to trim low-quality sequences (Q score of <20). The sequence types (STs) of each isolate were identified using the tool MLST (v. 2.23.0) (https://github.com/tseemann/mlst) which incorporates data from the PubMLST database. The antibiotic-resistant genes were identified using ABRicate (https://github.com/tseemann/abricate) through the MEGARes database whereas, the genes associated with virulence were assessed using VFanalyzer (http://www.mgc.ac.cn/VFs/main.htm) (S. Park et al., 2022). Whole genome sequencing data were deposited in BioProject numbers PRJNA609123 (https://www.ncbi.nlm.nih.gov/bioproject/PRJNA609123) and PRJNA622791 (https://www.ncbi.nlm.nih.gov/bioproject/?term=PRJNA622791). The accession numbers for each genome are reported in **Table S1**.

4.3. Results

4.3.1. Prevalence of antibiotic resistance in *S. aureus* isolates

Out of the 43 isolates, 6 isolates showed either single antibiotic resistance (5/6) or multi-antibiotic resistance (1/6) **(Figure 4.1a and Table S3a)**. The isolates Sa3 and Sa9 showed resistance to tetracycline, whereas isolates Sa3489, Sa3493, and Sa3603 were resistant to lincomycin. Isolate Sa1158c showed resistance to multiple classes of antibiotics including Ampicillin, Gentamycin, Kanamycin, Penicillin, Tetracycline, Ticarcillin, and Ceftiofur. Intermediate responses to lincomycin and spectinomycin were observed from 39.5% and 46.5% of the isolates, respectively **(Figure 4.1b)**. Eight different sequence types (ST) covering the 43 isolates were identified where 34 of the isolates either belonged to ST151 or ST352

(Table S1). The two tetracycline-resistant and three lincomycin-resistant isolates were from ST151 and ST352 respectively, whereas the multi-drug-resistant isolate belonged to ST8. Clinically important ABR genes were identified from the whole genome data. For instance, tetracycline-resistant genes (*tet(K)*; 1/43, *tet(M)*; 3/43 and *tet(38)*; 43/43), lincomycin-resistant genes (*lnu(A)*; 3/43), aminoglycoside-resistant genes (*aac(6')*; 1/43, *aph(3')*; 43/43, *aac3*; 43/43), ß-lactam and cephalosporin-resistant genes (*blaI, blaR, blaZ*; 1/43, *mecA*; 1/43), and multi-drug resistant regulators (*arlR, arlS, mgrA*; 43/43) were evident.

a)

Isolate Notation	Sequence Types	Antibiotic
Sa3	ST151	TET
Sa9	ST151	TET
Sa1158c	ST8	AMP, CF, CN, K, P, TET, TIC
Sa3489	ST352	MY
Sa3493	ST352	MY
Sa3603	ST352	MY

b)

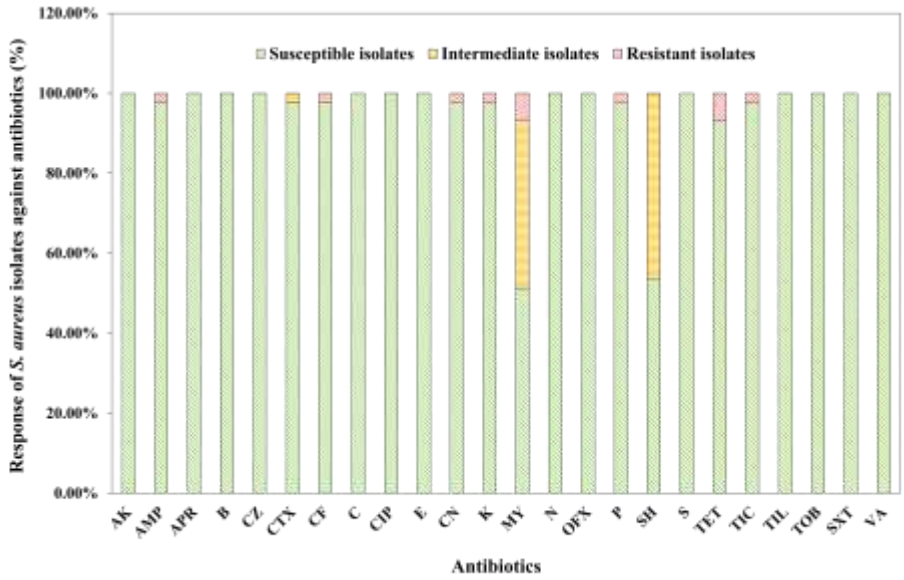

Figure 4.1. Response of 43 *S. aureus* isolates against antibiotics. a) List of antibiotic-resistant isolates. **b)** Bacterial responses toward 24 antibiotics. The *S. aureus* isolates were subjected to Kirby-Bauer disc diffusion susceptibility tests. The scores based on CLSI guidelines for susceptibility or resistance to an antibiotic were generated for each isolate. Abbreviations used - AK: Amikacin; AMP: Ampicillin; APR: Apramycin; B: Bacitracin; CZ: Cefazolin; CTX: Cefotaxime; CF: Ceftiofur; C: Chloramphenicol; CIP: Ciprofloxacin; E: Erythromycin; CN: Gentamycin; K: Kanamycin; MY: Lincomycin; N: Neomycin; OFX: Ofloxacin; P: Penicillin; SH: Spectinomycin; S: Streptomycin; TET: Tetracycline; TIC: Ticarcillin; TIL: Tilmicosin; TOB: Tobramycin; SXT: Trimethoprim/Sulfamethoxazole; VA: Vancomycin. The experiment was performed in triplicates and repeated thrice to assess reproducibility.

EtBr efflux assay and Nitrocefin assay were performed to assess efflux pump activity and ß-lactamase enzyme activity, respectively in all the isolates **(Table S3b)**. The tetracycline-resistant Sa3 and Sa9, lincomycin-resistant Sa3489, and the multi-drug-resistant Sa1158c showed active efflux pump activity. For instance, isolates Sa3, Sa9, Sa3489, and Sa1158c extruded 50% of the EtBr in 295.2 sec, 1067 sec, 3443 sec, and 271.9 sec, respectively **(Figure 4.2a, see the tabular data)**. The ß-lactamase enzyme activity was observed only in the multi-drug resistant isolate (50.36 U/mL) **(Figure 4.2b, see the tabular data)**. Genome analysis indicated the presence of genes associated with MFS efflux pumps (*norA*; 43/43, *norB*; 43/43, *lmrS*; 43/43, *tet(38)*; 43/43, *tet(K); 1/43, tet(M)*; 3/43), MATE efflux pumps (*mepR*, *mepA*, *mepB*; 43/43), and ß-lactamase enzyme activity (*blaI, blaR, blaZ*; 1/43). The list of genes associated with antibiotic resistance is provided in **Tables 4.1** and **S4**.

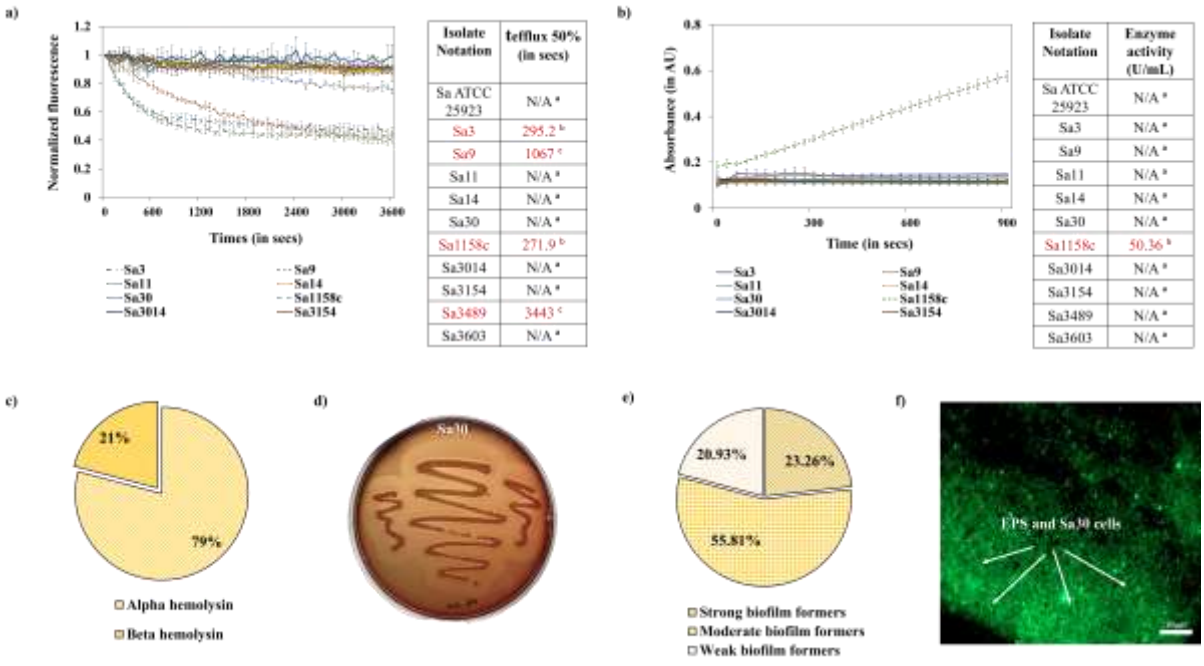

Isolate Notation	tefflux 50% (in secs)
Sa ATCC 25923	N/A [a]
Sa3	295.2 [b]
Sa9	1067 [c]
Sa11	N/A [a]
Sa14	N/A [a]
Sa30	N/A [a]
Sa1158c	271.9 [b]
Sa3014	N/A [a]
Sa3154	N/A [a]
Sa3489	3443 [c]
Sa3603	N/A [a]

Isolate Notation	Enzyme activity (U/mL)
Sa ATCC 25923	N/A [a]
Sa3	N/A [a]
Sa9	N/A [a]
Sa11	N/A [a]
Sa14	N/A [a]
Sa30	N/A [a]
Sa1158c	50.36 [b]
Sa3014	N/A [a]
Sa3154	N/A [a]
Sa3489	N/A [a]
Sa3603	N/A [a]

Figure 4.2. Antibiotic-resistance mechanisms and virulence factors in *S. aureus* isolates. a) Assessment of efflux pump activity in five antibiotic-resistant and five susceptible isolates. EtBr efflux assay was performed using 3 µg/mL of EtBr and 30 µg/mL of CPZ. The fluorescent intensity (530 nm/590 nm) was monitored for 60 mins after reenergizing the bacterial cells to trigger EtBr efflux with glucose (0.4% v/v). **b)** Assessment of ß-lactamase enzyme activity in the isolates. The isolates were subjected to a Nitrocefin assay where the absorbance of the cell-

free extract mixed with Nitrocefin was detected at 490 nm for 15 mins. **c)** Distribution of hemolysin manifestation by the 43 isolates. **d)** Alpha hemolysin manifestation by Sa30. Each isolate was cultured in TSA plates with 5% sheep blood for 24 h. The hemolysis was detected visually by the translucency around the bacterial colony. **e)** Distribution of biofilm-forming ability by the 43 isolates. The biofilm formation was assessed using a crystal violet assay. All isolates were classified into weak, moderate, and strong biofilm-formers based on their biofilm-forming ability. **f)** Fluorescence microscopic image of extracellular polymeric substances (EPS) and Sa30 cells. A green (505 nm) filter was used to acquire the GFP-labeled Sa30 biofilms using a high-content screening microscope, Cell Discoverer 7. Alphabets (in tabular data) indicate a significant difference ($p < 0.05$). 'N/A' stands for not applicable. More data on the resistance mechanisms and virulence factors are provided in **Tables S3** and **S5**. The experiment was performed in quadruplicates and repeated thrice to assess reproducibility.

Isolate ID	Isolate notation	Sequence Types	Antibiotic-resistant genes	Virulence genes			
				Clumping factor	Fibronectin binding proteins	Intercellular adhesin	Staphylococcal protein A
30704176	Sa3	ST151	aac3, aph(3'), arlR, arlS, dhaP, lmrS, mepA, mepB, mepR, mgrA, norA, norB, rlmH, tet38, tetK	clfB	xx	icaA, icaB, icaC, icaD, icaR	xx
41704653	Sa9	ST151	aac3, aph(3'), arlR, arlS, dhaP, lmrS, mepA, mepB, mepR, mgrA, norA, norB, rlmH, tet38	clfA, clfB	xx	icaA, icaB, icaC, icaD, icaR	xx
32200324	Sa11	ST352	aac3, aph(3'), arlR, arlS, dhaP, lmrS, mepA, mepB, mepR, mgrA, norA, norB, rlmH, tet38	clfA, clfB	fnbA, fnbB	icaA, icaB, icaC, icaD, icaR	spa
22200587	Sa14	ST3028	aac3, aph(3'), arlR, arlS, dhaP, lmrS, mepA, mepB, mepR, mgrA, norA, norB, rlmH, tet38	clfA	fnbA, fnbB	icaA, icaB, icaC, icaD, icaR	spa
21000024	Sa30	ST352	aac3, aph(3'), arlR, arlS, dhaP, lmrS, mepA, mepB, mepR, mgrA,	clfA, clfB	fnbA, fnbB	icaA, icaB, icaC, icaD, icaR	spa

			norA, norB, rlmH, tet38				
10812464	Sa1158c	ST8	aac3, aac(6'), arlR, arlS, blaI, blaR, blaZ, dhaP, fosB, lmrS, mecA, mepA, mepB, mgrA, norA, norB, rlmH, tet38, tetM, aph(3')	clfA, clfB	fnbA, fnbB	icaA, icaB, icaC, icaD, icaR	spa
11200086	Sa3154	ST351	aac3, aph(3'), arlR, arlS, dhaP, lmrS, mepA, mepB, mepR, mgrA, norA, norB, rlmH, tet38	clfA, clfB	xx	icaA, icaB, icaC, icaD, icaR	xx
40915913	Sa3603	ST352	aac3, aph(3'), arlR, arlS, dhaP, lmrS, lnuA, mepA, mepB, mepR, mgrA, norA, norB, rlmH, tet38	clfA, clfB	fnbA, fnbB	icaA, icaB, icaC, icaD, icaR	spa
40913704	Sa3489	ST352	aac3, aph(3'), arlR, arlS, dhaP, lmrS, lnuA, mepA, mepB, mepR, mgrA, norA, norB, rlmH, tet38	clfB	fnbA, fnbB	icaA, icaB, icaC, icaD, icaR	spa
40913568	Sa3493	ST352	aac3, aph(3'), arlR, arlS, dhaP, lmrS, lnuA, mepA, mepB, mepR, mgrA, norA, norB, rlmH, tet38	clfA, clfB	fnbA, fnbB	icaA, icaB, icaC, icaD, icaR	spa
31312165	Sa3014	ST352	aac3, aph(3'), arlR, arlS, dhaP, lmrS, mepA, mepB, mepR, mgrA, norA, norB, rlmH, tet38	clfA, clfB	fnbA, fnbB	icaA, icaB, icaC, icaD, icaR	spa

Table 4.1. List of the genes associated with antibiotic resistance and adherence in the six antibiotic-resistant isolates (Sa3, Sa9, Sa1158c, Sa3489, Sa3493, and Sa3603), and five antibiotic-susceptible isolates (Sa11, Sa14, Sa30, Sa3014, and Sa3154).

4.3.2. Virulence profile of *S. aureus* isolates

The 43 isolates were cultured on blood agar plates and checked for hemolysis. All the isolates either produced alpha-hemolysin (34/43) (encoded by *hla*) or beta-hemolysin (9/43) (encoded by *hlb*) **(Figure 4.2c,d)**. Beta-hemolysis was observed only in the members of ST151 and ST8. Crystal violet assay confirmed biofilm-forming ability in all isolates. Specifically, 23.26% of the isolates showed strong biofilm formation, 55.81% of them were moderate biofilm formers, whereas the rest formed weak biofilms **(Figure 4.2e,f and Table S5)**. None of the isolates except Sa16, Sa23, and Sa27 from ST352 and ST151 were strong biofilm formers, whereas, isolates from ST8 and ST2270 formed strong biofilms. Common virulence genes included: two-component leukotoxins, including gamma-hemolysin (Hlg, encoded by *hlgA, hlgB, and hlgC*), and leukotoxin D (LukD, encoded by *lukD*). None of the isolates had pyrogenic toxin superantigen (PTSAg) genes except for Sa3154 which contained enterotoxin C, enterotoxin L, and toxic shock syndrome toxin-associated *sec, sell,* and *tsst-1* genes, respectively. Adhesins that are involved in biofilm formation were also identified in all isolates. For instance, fibronectin-binding proteins, fnbA, and fnbB were observed in 60.46% of the isolates. Clumping factor A (clfA), a cell-wall anchored protein was identified in 58.13% of the isolates, whereas, clfB, a fibrinogen-binding adhesin was found in 95.56% of the isolates. Accessory gene regulator (agr) and staphylococcal accessory regulator (sarA) system associated with quorum sensing (Le & Otto, 2015) was identified among the isolates as well. Genes associated with intercellular adhesion such as *icaA*, *icaB*, *icaC*, *icaD*, and *icaR* were evident in all 43 isolates. The presence of the staphylococcal protein A (spa) gene, the product of which plays an important role in colonization and immune invasion (X. Hong et al., 2016) was found in 17 isolates including 4 ABR isolates. Ssp serine protease (encoded by *sspA*) that contributes to *in vivo* growth and survivability (Rice, Peralta, Bast, de Azavedo, & McGavin, 2001) was identified in all the isolates. The second immunoglobulin-binding protein (Sbi) which is a multifunctional immune invasion factor (Smith, Visai, Kerrigan, Speziale, & Foster,

2011) was observed in 34 isolates. Moreover, all the isolates had bovine immune invasion factors such as serotype 8 capsular polysaccharide (Cap), and adenosine synthase A (AdsA). The list of genes associated with adherence, toxin/enzyme production, and immune invasion is provided in **Tables 4.1, 4.2,** and **S6.**

Isolate ID	Isolate notation	Virulence genes											
		Toxins							Enzyme		Immune invasion		
		Alpha hemolysin	Beta hemolysin	Gamma hemolysin	Delta hemolysin	Enterotoxin-like L	Leukotoxin D	Toxic shock syndrome toxin	Cysteine protease	Serine protease	Capsule	AdsA	Sbi
30704176	Sa3	hly/hla	hlb	hlgA, hlgB, hlgC	hld	xx	lukD	xx	sspB, sspC	sspA	cap8A, cap8B, cap8C, cap8D, cap8E, cap8F, cap8G, cap8H, cap8I, cap8J, cap8K, cap8L, cap8M, cap8N, cap8O, cap8P	adsA	sbi
41704653	Sa9	hly/hla	hlb	hlgA, hlgB, hlgC	hld	xx	lukD	xx	sspB, sspC	sspA	cap8A, cap8B, cap8C, cap8D, cap8E, cap8F, cap8G, cap8H, cap8I, cap8J, cap8K, cap8L, cap8M, cap8N, cap8O, cap8P	adsA	xx
32200324	Sa11	hly/hla	hlb	hlgA, hlgB, hlgC	hld	xx	lukD	xx	sspB, sspC	sspA	cap8A, cap8B, cap8C, cap8D, cap8E, cap8F, cap8G, cap8L, cap8M, cap8N, cap8O, cap8P	adsA	sbi
22200587	Sa14	hly/hla	hlb	hlgA, hlgB, hlgC	hld	xx	lukD	xx	sspB, sspC	sspA	cap8A, cap8B, cap8C, cap8D, cap8E, cap8F, cap8G, cap8L,	adsA	sbi

											cap8M, cap8N, cap8O, cap8P		
21000024	Sa30	hly/hla	hlb	hlgA, hlgB, hlgC	hld	xx	lukD	xx	sspB, sspC	sspA	cap8A, cap8B, cap8C, cap8D, cap8E, cap8F, cap8G, cap8L, cap8M, cap8N, cap8O, cap8P	adsA	sbi
10812464	Sa1158c	hly/hla	hlb	hlgA, hlgB, hlgC	hld	xx	lukD	xx	sspB, sspC	sspA	cap8A, cap8B, cap8C, cap8D, cap8E, cap8F, cap8G, cap8L, cap8M, cap8N, cap8O, cap8P	adsA	sbi
11200086	Sa3154	hly/hla	hlb	hlgA, hlgB, hlgC	hld	sell	lukD	tsst-1	sspB, sspC	sspA	cap8A, cap8B, cap8C, cap8D, cap8E, cap8F, cap8G, cap8H, cap8I, cap8J, cap8K, cap8L, cap8M, cap8N, cap8O, cap8P	adsA	sbi
40915913	Sa3603	hly/hla	hlb	hlgA, hlgB, hlgC	hld	xx	lukD	xx	sspB, sspC	sspA	cap8A, cap8B, cap8C, cap8D, cap8E, cap8F, cap8G, cap8L, cap8M, cap8N, cap8O, cap8P	adsA	sbi
40913704	Sa3489	hly/hla	hlb	hlgA, hlgB, hlgC	hld	xx	lukD	xx	sspB, sspC	sspA	cap8A, cap8B, cap8C, cap8D, cap8E, cap8F, cap8G, cap8L,	adsA	sbi

											cap8M, cap8N, cap8O, cap8P		
40913568	Sa3493	hly/hla	hlb	hlgA, hlgB, hlgC	hld	xx	lukD	xx	sspB, sspC	sspA	cap8A, cap8B, cap8C, cap8D, cap8E, cap8F, cap8G, cap8L, cap8M, cap8N, cap8O, cap8P	adsA	sbi
31312165	Sa3014	hly/hla	hlb	hlgA, hlgB, hlgC	hld	xx	lukD	xx	sspB, sspC	sspA	cap8A, cap8B, cap8C, cap8D, cap8E, cap8F, cap8G, cap8L, cap8M, cap8N, cap8O, cap8P	adsA	sbi

Table 4.2. List of the genes associated with toxin and enzyme production, and immune invasion.

4.3.3. Internalization of the *S. aureus* isolates in human intestinal epithelial cells

Five antibiotic-resistant isolates (Sa3, Sa9, Sa1158c, Sa3489, and Sa3603), and five antibiotic-susceptible isolates (Sa11, Sa14, Sa30, Sa3014, and Sa3154) were tested for internalization in Caco-2 cells. All the isolates showed significantly ($p < 0.05$) higher internalization in Caco-2 cells in comparison to the reference strain, Sa ATCC 25923 **(Figure 4.3a)**. For instance, >8 $\log_{10}$ cfu/well of Sa14, Sa1158c, Sa3014, and Sa3603, and >6 $\log_{10}$ cfu/well of Sa3, Sa9, Sa11, Sa30, Sa3154, and Sa3489 were recovered from the Caco-2 cells, which was ~5.22 $\log_{10}$ higher ($p < 0.05$) than the reference strain. High-content microscopy confirmed the internalization of Sa30 and the death of Caco-2 cells **(Figure 4.3b(i-viii))**. Cysteine proteases, staphopain B (SspB), and staphopain C (SspC) which are often associated with biofilm formation and intracellular colonization of *S. aureus* (Dubin, 2002; Stelzner et al., 2021) were identified in all isolates (**Tables 4.1** and **S6**).

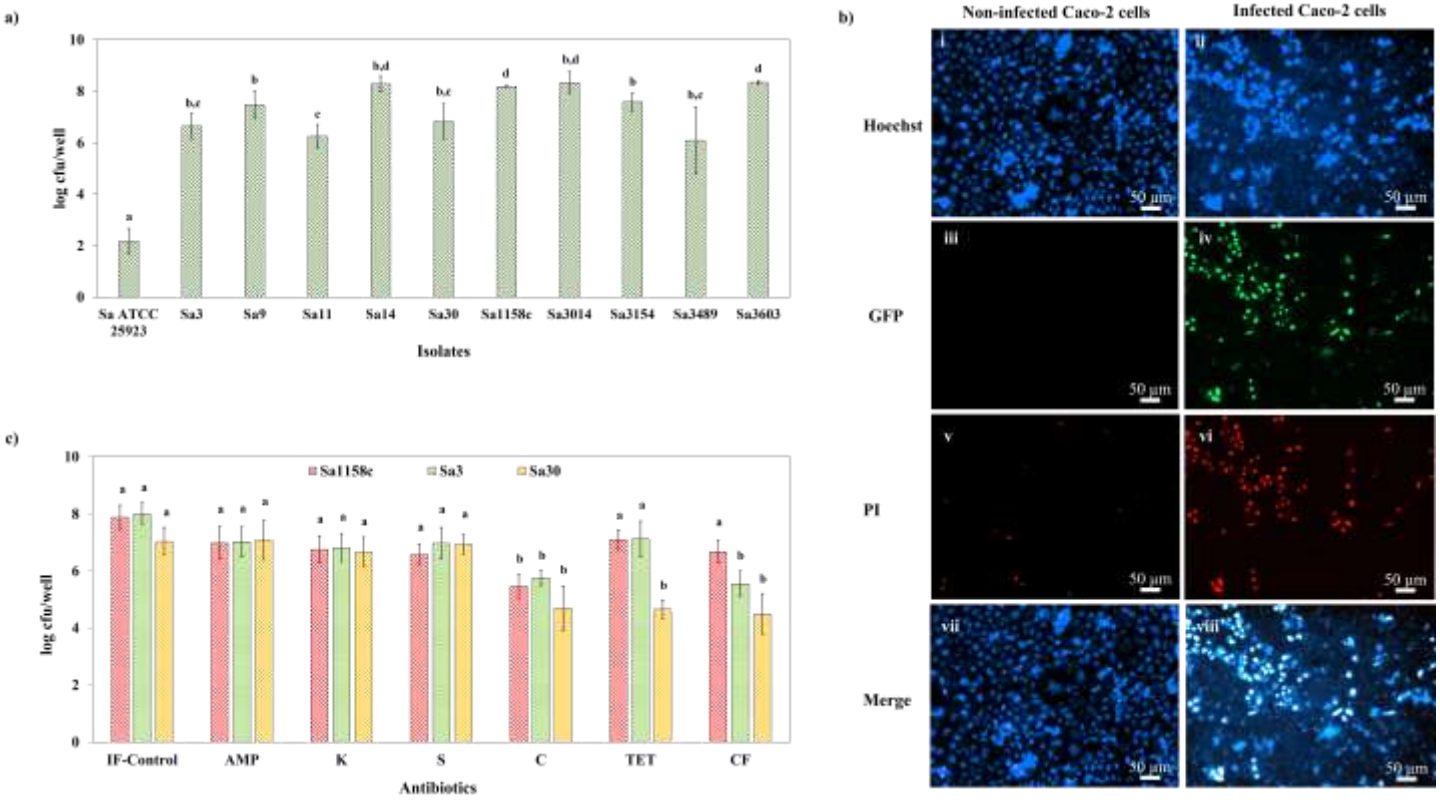

Figure 4.3. Internalization of *S. aureus* isolates and response to antibiotic treatment in Caco-2 cells. a) Intracellular survivability of *S. aureus* isolates in Caco-2 cells. Approximately 2×10^4 Caco-2 cells/well of a 96-well plate were exposed to the isolates maintained at 0.5 Macfarland standard ($1.5 \text{ X } 10^8$ cells/ mL). The cells were washed with PBS and subjected to gentamicin (10 µg/mL) to remove extracellular bacteria. The cells were washed further after 4 h of incubation and lysed using 0.5% (v/v) of Triton-X. Colony-forming units were determined using the drop culture method. **b)** Epifluorescence microscopic images of non-infected control and Sa30-infected Caco-2 cells. After 4 h incubation of the Caco-2 cells exposed to bacteria, 30 µL of Hoechst-PI cocktail was added and incubated for 30 mins in dark. These wells were imaged using an epifluorescence microscope with blue, green, and red filters. i-ii) Hoechst 33342 staining of non-infected and Sa30-infected Caco-2 cells. iii-iv) GFP-labeled Sa30 internalization in Caco-2 cells. Non-infected cells were considered as a control. v-vi) PI staining of non-infected and infected cells. vii-viii) Overlap of Hoechst and PI stained non-infected and Sa30-infected Caco-2 cells. The images confirmed Sa30 internalization and infection of the Caco-2 cells leading to cell death. **c)** Antibiotic efficiency against intracellular Sa1158c, Sa30, and Sa3. The infected Caco-2 cells were exposed to ampicillin (AMP) (10 µg/mL), kanamycin (K) (30 µg/mL), streptomycin (S) (10 µg/mL), chloramphenicol (C) (30 µg/mL), tetracycline (TET) (30 µg/mL), and ceftiofur (CF) (30 µg/mL). The plates were incubated for 24 h, followed by washing, lysing of the cells, and drop-culture method to enumerate the cfu/well. Average values plotted in the graph with different alphabets indicate a significant difference ($p < 0.05$). 'IF-control' stands for infected Caco-2 cells without antibiotic treatment. The experiment was performed in quadruplicates and repeated thrice to assess reproducibility.

The Caco-2 cells with internalized *S. aureus* were exposed to antibiotics to check for their colonization-remediation efficiency. The aminoglycosides and ß-lactam antibiotics failed to show effectiveness against any of the intracellular *S. aureus* whereas, chloramphenicol, tetracycline, and ceftiofur were comparatively more effective ($p < 0.05$) against all the antibiotic-susceptible and lincosamide resistant isolates. However, none of these antibiotics could reduce the intracellular bacterial load by more than 2.5 $\log_{10}$. For instance, chloramphenicol, tetracycline, and ceftiofur showed a 2.3-2.5 $\log_{10}$ reduction ($p < 0.05$) of Sa30 colonization **(Figure 4.3c)**. Moreover, no antibiotic demonstrated a significant reduction in the aminoglycoside/ß-lactam/tetracycline/cephalosporin-resistant Sa1158c colonization except chloramphenicol which showed a 2.42 $\log_{10}$ reduction ($p < 0.05$) **(Figure 4.3c)**. Similarly, tetracycline failed to show any

efficiency against the tetracycline resistant Sa3 and Sa9, while chloramphenicol and ceftiofur significantly reduced their colonization by ~2.35 $\log_{10}$ **(Figures 4.3c and S1a)**.

4.3.4. Pathogenicity of the *S. aureus* isolates in *Caenorhabditis elegans* model of intestinal infection

Infection of *C. elegans* with the selected isolates had a significant effect on the lifespan of worms when compared with non-infected or infected with reference strain (Sa ATCC 25923). For instance, 100% death in the infected worms was observed by the 15th day post-infection, whereas ~77.5%, and ~60% of the non-infected and Sa ATCC 25923 infected worms respectively, were alive on the 15th day **(Figure 4.4a)**. High-content microscopy confirmed Sa30 accumulation in the pharynx, intestinal lumen, rectum, and anus of the worms within 24 h post-infection **(Figure 4.5a).** After 48 h of infection, Sa30 accumulation was observed throughout the digestive tract of *C.* elegans leading to intestinal epithelium destruction, and complete degradation of internal organs **(Figures 4.5b-d and S2a-i).** The multiplication of Sa30 in *C. elegans* was evident with increased fluorescence when the microscopic images of 24 h and 48 h post-infection periods were compared.

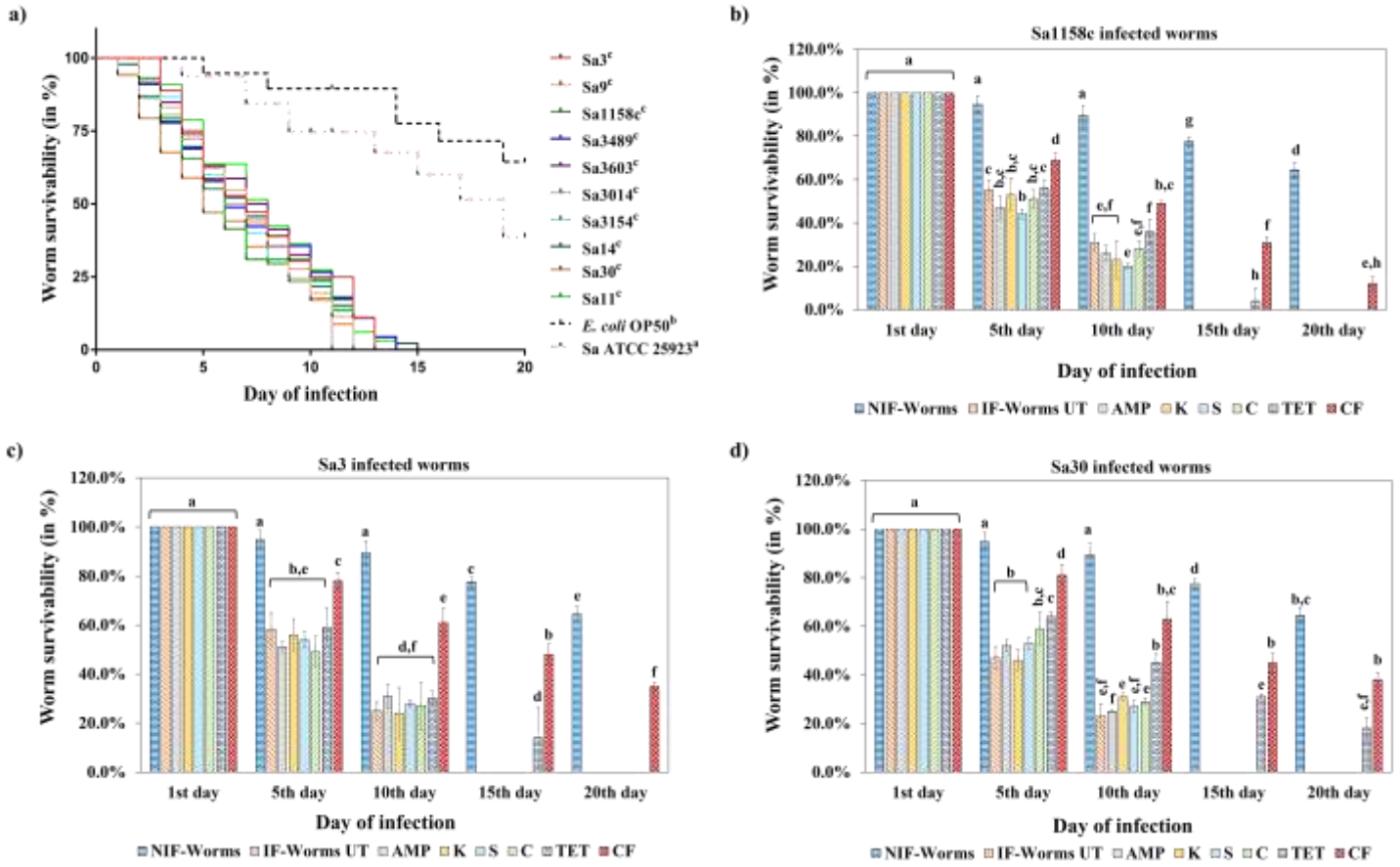

Figure 4.4. Life-span of *S. aureus* infected *C. elegans* and assessment of antibiotic efficiency. **a)** Life-span assay of *S. aureus* infected and non-infected *C. elegans*. The worms were grown to the L4 stage and exposed to 1.5×10^8 cells of *S. aureus* isolates for 48 h. The worms were washed, transferred to NGM plates with *E. coli* OP50 lawns, and monitored for survivability for 20 days. The mantel-Cox test was used to find the statistical significance ($p < 0.05$). **b-d)** Antibiotic efficiency against **b)** Sa1158c, **c)** Sa3, and **d)** Sa30 infection in *C. elegans*. The infected worms were subjected to ampicillin (AMP) (10 µg/mL), kanamycin (K) (30 µg/mL), streptomycin (S) (10 µg/mL), chloramphenicol (C) (30 µg/mL), tetracycline (TET) (30 µg/mL), and ceftiofur (CF) (30 µg/mL) for 24 h. The worms were washed and transferred to NGM plates with *E. coli* OP50 lawns. The survivability of the worms was monitored for 20 days. Average values plotted in the graph with different alphabets indicate a significant difference ($p < 0.05$). 'NIF-Worms' and 'IF-Worm UT' stands for non-infected worms and infected untreated worms, respectively. The experiment was performed in quadruplicates and repeated thrice to assess reproducibility.

The 24 h treatments with ampicillin, streptomycin, kanamycin, and chloramphenicol failed to improve ($p > 0.05$) the lifespan of *C. elegans* infected by any of the 10 selected isolates **(Figures 4.4b-d and S1b-h)**. For instance, 20-31% of the worms infected with Sa3 and Sa1158c were alive ($p > 0.05$) irrespective of treatment by these antibiotics on the 10^{th} day **(Figure 4.4b,c)**. Tetracycline failed to improve ($p > 0.05$) the survivability of Sa3 and Sa1158c infected worms on the 10^{th} day either, while ceftiofur treatment was comparatively effective ($p < 0.05$) against both these isolates. Only 25-29% of the Sa30 infected worms were alive after ampicillin, streptomycin, kanamycin, and chloramphenicol treatment on the 10^{th} day which was insignificant ($p > 0.05$) when compared to untreated control **(Figure 4.4d)**. The low antibiotic efficiency was verified through higher fluorescence showing Sa30 accumulation in the pharynx, intestinal lumen, and anus of the worms **(Figure 4.5e-h)**. In comparison, 45% of the Sa30 infected worms were alive after tetracycline treatment, which was supported by low fluorescence in the pharynx, rectum, and anus regions suggesting reduced Sa30 accumulation **(Figure 4.5i)**. A significant ($p < 0.05$) improvement in the survivability of Ceftiofur-treated Sa30 (63% until the 10^{th} day) infected worms was observed which was confirmed by a negligible accumulation of the isolate in the pharynx, and rectum regions **(Figure 4.5j)**.

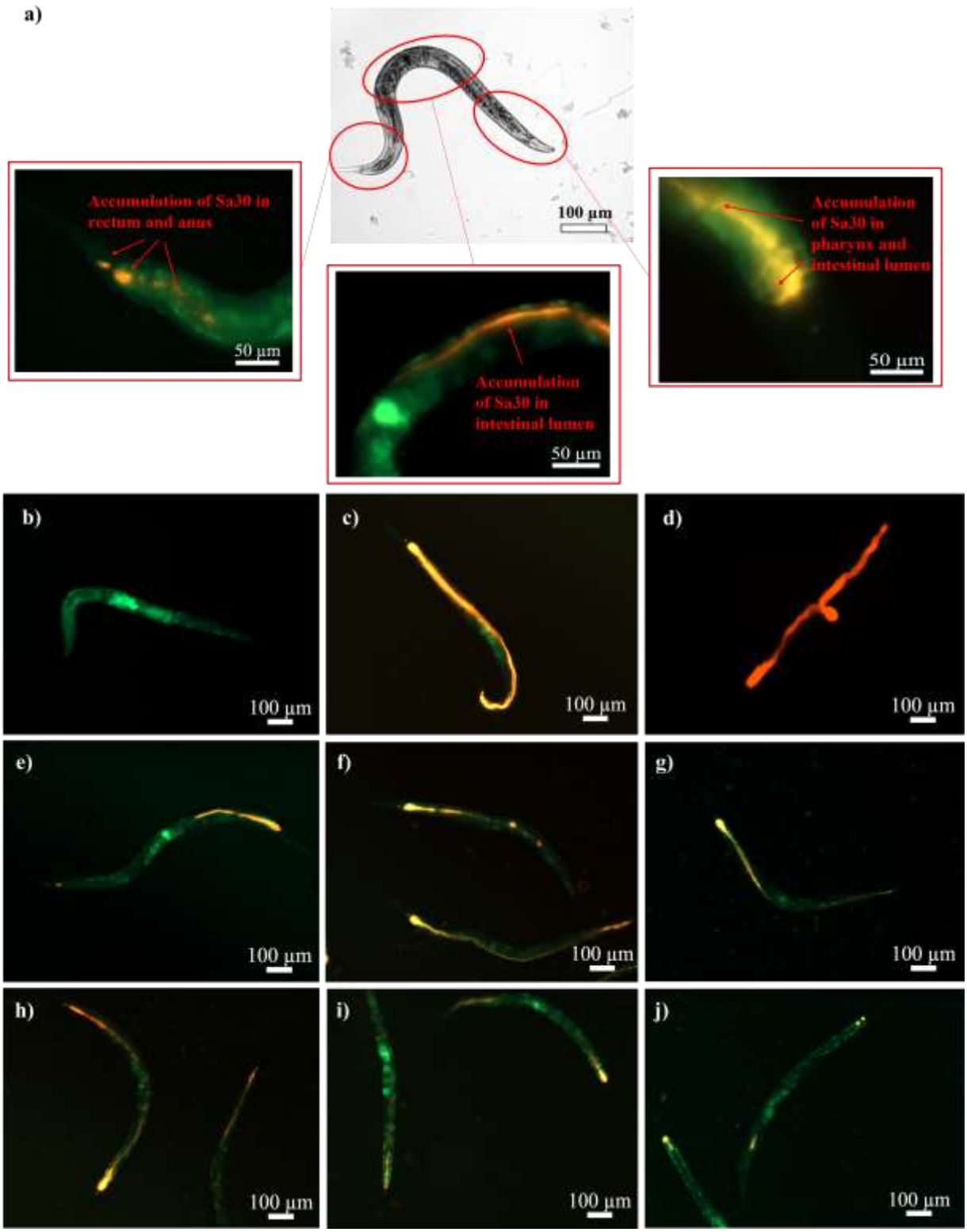

Figure 4.5. Microscopic images of non-infected, and antibiotic-treated/untreated Sa30-infected *C. elegans*. Epifluorescence images of **a)** Sa30 infected (24 h post-infection), **b)** non-infected, **c)** Sa30 infected (48 h post-infection), and **d)** dead infected worms. Sa30 accumulation

was observed in the pharynx, intestinal lumen, rectum, and anus of the worms 24 h post-infection. The increased fluorescence 48 h post-infection throughout the digestive tract of the worms suggested Sa30 multiplication leading to intestinal epithelium destruction. The antibiotics **e)** ampicillin, **f)** kanamycin, **g)** streptomycin, **h)** chloramphenicol, **i)** tetracycline, and **j)** ceftiofur were exposed to Sa30 infected worms for 24 h. The worms were washed and resuspended in S-basal media in a 96-well plate. Green (505 nm) and red (583 nm) filter combinations were used to acquire the green autofluorescence of *C. elegans* and RFP-labeled Sa30. The epifluorescence images were captured using the Cell Discoverer 7.

4.4. Discussion

A subpopulation of *S. aureus* isolates (n=43) from MPCC was investigated for ABR and virulence characteristics favoring intracellular survival and evasion of antibiotics. All isolates possessed critical virulence characteristics such as biofilm formation, and hemolysis manifestation while ABR phenotype was evident only among six isolates. Genes associated with ABR, toxin production, adherence, and host immune invasion were identified by analyzing the whole-genome sequences. Although none of the isolates carried human adaptation genes, they demonstrated intracellular invasion, infection, and death of human epithelial Caco-2 cells, and intestinal infection model, *Caenorhabditis elegans.* Our studies also showed the inefficiency of widely used antibiotics relevant to veterinary and public health to remediate intracellular and intestinal *S. aureus* infection.

Out of the 43 isolates, 5 isolates (Sa3, Sa9, Sa3489, Sa3493, and Sa3603) showed resistance to either tetracycline or lincomycin, whereas one isolate (Sa1158c) was resistant to multiple antibiotics. Approximately 39.5% and 47.5% of the isolates showed intermediate responses toward lincomycin and spectinomycin, respectively. These two antibiotics have been introduced in Canada to swine, poultry, and dairy cattle individually or in combinations to a large extent (Saini, McClure, Léger, et al., 2012). Bennett *et al.* have reported *S. aureus* showing resistance to lincosamides and aminoglycosides frequently and rapidly due to their similar

mechanism of action (J. E. Bennett, Dolin, & Blaser, 2020). Sa3 and Sa1158c carried *tetK* and *tetM* genes, respectively while all 43 isolates were identified with the major facilitator superfamily (MFS) of transporters such as *tet(38)*, *NorA*, and *NorB* efflux genes. These chromosomally encoded MFS efflux genes are associated with EtBr extrusion and their expressions are controlled in part by the transcriptional regulators *mgrA* and the *arlRS* (Kaatz, McAleese, & Seo, 2005; Narui, Noguchi, Wakasugi, & Sasatsu, 2002; Neyfakh, Borsch, & Kaatz, 1993; Truong-Bolduc, Dunman, Strahilevitz, Projan, & Hooper, 2005) which were also identified in all isolates. Interestingly, tetracycline resistance (from disc diffusion assay) and EtBr efflux activity were evident only in Sa3, Sa9, and Sa1158c. The role of functional efflux pumps regulated by the MFS transporters in conferring tetracycline resistance in the three isolates (Sa3, Sa9, and Sa1158c) is evidenced by the congruence of the EtBr assay result and the antibiotic disc diffusion tests (S. Kumar & Varela, 2012). While the exact reason for the failure of ABR genes to translate to functional proteins and phenotype was beyond the scope of this investigation, we speculate possibilities of gene mutations, failure in sensing antibiotic stress, defective gene products, *etc* as potential causes of the discrepancy between the genetic makeup of the isolates and their phenotypic characteristics (Ding, Onodera, Lee, & Hooper, 2008; Poole, 2000). The ß-lactam and cephalosporin resistance in Sa1158c could be associated with expressive ß-lactamase enzyme activity (50.36 U/mL) and the association of *blaI, blaR,* and *blaZ* genes. Moreover, the *mecA* gene identified in Sa1158c encodes the low-affinity penicillin-binding protein (PBP2a) and also plays a significant role in resistance towards ß-lactam antibiotics, especially methicillin, thus is considered to be a standard for MRSA confirmation (X. Hong et al., 2016). The *aac(6')*, *aac(3')*, and *aph(3')* genes in Sa1158c encode the aminoglycoside-modifying enzymes that mediate gentamycin and kanamycin inactivation, whereas, the prevalence of *lnuA* gene in Sa3489, Sa3493, and Sa3603 encode lincosamide

nucleotidyl transferases leading to lincomycin resistance (Efthymia & Constantinos, 2018; Khosravi, Jenabi, & Montazeri, 2017).

Every isolate exhibited crucial virulence characteristics essential for an intramammary and intestinal infection. For instance, all the isolates manifested either alpha or beta-hemolysin and formed biofilms. Hemolysins encoded by *hly/hla*, and *hlb* genes identified in the isolates often contribute to cell signaling pathways that mediate proliferation, cytokine secretion, inflammatory responses, and cell-cell interactions (L. Zhang et al., 2018). The role of the Clf-Sdr family consisting of fibrinogen-binding proteins, clfA, and clfB, and fibronectin-binding proteins (FnBPs), fnbA, and fnbB in biofilm formation and their contribution to *S. aureus* infection has been extensively discussed (Paharik & Horswill, 2016). Moreover, the *ica*ADBC locus identified in all the isolates mediates the synthesis of polysaccharide intercellular adhesin (PIA) which is poly *N*-acetyl glucosamine (PNAG), one of the extracellular polymeric substances of staphylococcal biofilms (Arciola, Campoccia, Ravaioli, & Montanaro, 2015). Here, all the members of ST151 manifested beta-hemolysis, and over 76% of the isolates formed strong or moderate biofilms. ST151 subclone of the bovine ET3 clone has also been reported to display greater virulence in mouse models of mastitis by Guinane *et al.* (Guinane et al., 2008). ST8 has been reported to be a human clone that has transferred to dairy cows causing mastitis and has been speculated for possible spillover and transmission under suitable selection pressure (S. Park et al., 2022).

All the tested isolates showed intracellular colonization (of $>6\ log_{10}\ cfu/well$), and infection of the Caco-2 cells causing cell death. The intracellular invasion and infection were possibly mediated by the cysteine proteases SspB, and SspC which were evident in all the isolates (Stelzner et al., 2021). The fibronectin bridging between *S. aureus* FnBPs and the Caco-2 fibronectin receptor integrin $\alpha_5\beta_1$ is also known to contribute to epithelial cell invasion (B. Sinha et al., 2000).

Moreover, Kwak *et al*. have reported the contribution of staphylococcal hemolysin in the disruption of the barrier integrity of Caco-2 cells (Kwak et al., 2012). As reported in this study, the internalized bacteria were able to cause cell death. Accordingly, cytotoxic *S. aureus* strains upon internalization by epithelial cells have the ability to escape from the phagosome, multiply in the cytosol, employ staphylococcal cysteine proteases and induce host cell death (Stelzner et al., 2021).

The microscopic images showed Sa30 accumulation in the pharynx, intestine, rectum, and anus of *C. elegans*. The consequence of the infection was evident as a significant reduction in worm survivability. Our observations are consistent with those made by Irazoqui *et al.* where *S. aureus* was reported to cause enterocyte effacement, lysis of the intestinal epithelial cells, followed by invasion in the rest of the body, and complete degradation of the internal tissues of *C. elegans* (Irazoqui et al., 2010). The pathogenicity of the isolates in *C. elegans* was probably executed by the production of alpha-hemolysin (encoded by *hla*), and V8 protease (encoded by *sspA*) (Sifri, Begun, Ausubel, & Calderwood, 2003). Moreover, overexpression of the *icaADBC* locus synthesizing PIA is also reported to be one of the contributing virulence mechanisms employed by *Staphylococci* during intestinal infection of nematodes (Begun et al., 2007). Sa ATCC 25923 infected worms showed better survivability in comparison to the worms infected by the bovine isolates. This is probably because the reference strain lacks expressive virulent genes and a strong intracellular internalization property which are reported to be essential for *C. elegans* infection.

Different classes of antibiotics including aminoglycosides, cephalosporin, ß-lactam, tetracycline, and chloramphenicol were tested for intracellular and intestinal infection remediation in Caco-2 cells, and *C. elegans*, respectively. The antibiotics were selected based on their frequent use against *S. aureus*-mediated mastitis and human infections. Kanamycin, streptomycin, and ampicillin failed to reduce bacterial colonization in the Caco-2 cells. The result was expected as

the conventional antibiotics especially ß-lactams, aminoglycosides, and cephalosporin (cellular/extracellular (C/E) ratio: <1) are known to have poor penetration, slow accumulation, or inferior retention in mammalian cells due to their high polarity and hydrophilic characteristics (Bongers, Hellebrekers, Leenen, Koenderman, & Hietbrink, 2019). Chloramphenicol showed superior efficiency which is probably because of higher accumulation (C/E ratio: 2-4) due to its hydrophobic nature (McLeod, Manyan, & Yunis, 1977). Tetracycline (C/E ratio: 1.8-7.1) is reported to moderately penetrate and accumulate inside neutrophils through active organic cation transport with a relatively low affinity (Cockeran et al., 2012). Despite being a cephalosporin, ceftiofur showed better efficiency against *S. aureus* infection in Caco-2 cells in comparison to other antibiotics. This could probably be due to a direct antibacterial effect of ceftiofur owing to a higher intracellular concentration above the minimum bactericidal concentration (Bongers et al., 2019). Although few antibiotics were comparatively effective, none of them reduced bacterial colonization by more than 2.5 $\log_{10}$. Our observations of lower antibiotic efficiency against intracellular *S. aureus* corroborate with several existing literature (Bongers et al., 2019; Jacobs & Wilson, 1983; Naess, Andreeva, & Sørnes, 2011). The other classes of antibiotics that are known for higher C/E ratios such as quinolones, carbapenems, *etc*. are mostly restricted for veterinary use as they are considered to be the last-resort drugs for human applications (*Uses of antimicrobials in food animals in Canada: impact on resistance and human health*, 2002).

Microscopic images indicated a reduction in Sa30 accumulation in *C. elegans* after aminoglycoside, ampicillin, and chloramphenicol treatment, which however was not enough to inhibit Sa30 multiplication leading to infection and cell death as suggested by the life-span assay. Tetracycline and ceftiofur were comparatively effective in remediating *S. aureus*-mediated intestinal infection in the nematodes. This is probably because, in addition to the antimicrobial activity, tetracycline has been reported to up-regulate *C. elegans* genes that function in xenobiotic

detoxification, redox regulation, and cytoprotection (Head & Aballay, 2014). Cephalosporins on the other hand have been reported to employ anti-quorum sensing activity, reduce bacterial motility, and biofilm formation (L. Kumar, Brenner, Brice, Klein-Seetharaman, & Sarkar, 2021). Despite its better performance in Caco-2 cells, chloramphenicol wasn't effective in infection remediation in worms which is probably because of the impermeability of the worm cuticle to hydrophobic compounds thus leading to inefficient drug uptake (O'Reilly, Luke, Perlmutter, Silverman, & Pak, 2014). The aminoglycosides and ß-lactam antibiotics failed as well possibly because of their poor penetration against the *S. aureus* internalized in the intestinal epithelial cells of *C. elegans*. Generally, antibiotics that were found effective against bacteria from the Kirby Bauer disc diffusion assay failed to show convincing efficiency in both the infection models. This discrepancy in the effectiveness of antibiotics when directly exposed to bacterial cells and those present as intracellular pathogens originating from differential pharmacokinetics of antibiotics highlight the importance of testing antibiotics in organism models.

Proteins associated with bovine immune invasions such as Sbi, Cap, and AdsA were identified in the isolates. Previous studies have reported Sbi to participate in the inflammatory response induced during staphylococcus infections whereas, Cap and AdsA inhibit neutrophil activity against *S. aureus* thus preventing chemotaxis and phagocytosis and promoting cell adhesion, during pathogen spillover to humans (Echániz-Aviles, Velazquez-Meza, Rodríguez-Arvizu, Carnalla-Barajas, & Noguerón, 2022; Gonzalez, Ledo, Giai, Garófalo, & Gómez, 2015; Thammavongsa, Kern, Missiakas, & Schneewind, 2009). Sa3154 from ST351 was the only isolate to carry PTSAgs which are known to regulate immune responses by abnormal activation of immune cells or exhibit destruction of the host cell membranes (Schmidt, Kock, & Ehlers, 2017). The prevalence of PTSAg genes varies considerably between studies probably due to variations in the herd selection criteria or geographical locations (Schmidt et al., 2017). In this study, the low

prevalence of PTSAg gene-positive *S. aureus*, the lack of virulence markers (*lukE*, *lukM*), and human immune evasion cluster-associated genes (*lytN, fmhC, dprA, chp, sak,* and *scn*) suggest a minimal risk of zoonotic infection. However, *S. aureus* is an opportunistic pathogen and thus, under certain environmental pressure, mobile genetic elements may disseminate within or across different lineages (S. Park et al., 2022). For instance, antibiotic pressure-inducing SOS response has been reported to promote horizontal gene transfer of pathogenicity islands in *Staphylococci* (Beaber, Hochhut, & Waldor, 2004; Úbeda et al., 2005).

4.5. Conclusion

S. aureus is highly prevalent in bovine mastitis cases worldwide, and thus investigations associated with ABR, ABR mechanisms, and virulence characteristics are crucial. In this study, we used phenotypic and genotypic profiling to inspect 43 *S. aureus* isolates associated with bovine mastitis. Antibiotic resistance was identified among six isolates based on a disc diffusion assay and all the isolates demonstrated crucial virulence characteristics including hemolysis induction, biofilm formation, intracellular infection in Caco-2 cells, and intestinal infection in *C. elegans*. Although these isolates lacked human immune invasion genes, their ability to invade human cells and cause intestinal infection in model organisms highlights the need for continuous monitoring for zoonosis. Notably, the antibiotics that showed efficiency against the isolates in the disc diffusion assay failed to a large extent in remediating their intracellular and intestinal infection. This observation suggested the need to include models capable of testing the effectiveness of antibiotics against internalized bacteria as well as the urgent need to develop therapeutics that can combat ABR and intracellular pathogens. Nano-enabled antibacterial combination therapies

designed to deliver multiple drugs hold promise in countering such recalcitrant infections caused by ABR bacteria (Coates, Hu, Holt, & Yeh, 2020; S. George et al., 2019).

4.6. Supplementary information

Supplementary tables are provided in: https://static-content.springer.com/esm/art%3A10.1186%2Fs12866-023-02785-1/MediaObjects/12866_2023_2785_MOESM3_ESM.xlsx

Caption: Metadata of the 43 *S. aureus* isolates. **Table S2.** List of antibiotics and antibiotic concentration breakpoints. **Table S3.** List of a) responses of *S. aureus* isolates towards antibiotics, and b) prevalence of antibiotic resistant mechanisms. **Table S4.** List of genes associated to antibiotic resistant mechanisms in *S. aureus* isolates. **Table S5.** List of *S. aureus* isolates with hemolysin production and biofilm formation ability. **Table S6.** List of genes associated to virulence characteristics in the *S. aureus* isolates.

Figure S1 is provided in: https://static-content.springer.com/esm/art%3A10.1186%2Fs12866-023-02785-1/MediaObjects/12866_2023_2785_MOESM1_ESM.pdf

Caption: a) Intracellular responses of Sa9, Sa11, Sa14, Sa3014, Sa3154, Sa3489, and Sa3603 to antibiotic treatment. The aminoglycosides and ampicillin failed to show efficiency against the Caco-2 internalized isolates, whereas chloramphenicol and ceftiofur were comparatively more effective ($p < 0.05$). Tetracycline was more efficient ($p < 0.05$) against all the isolates except the tetracycline-resistant Sa9. b-h) Assessment of antibiotic efficiency against b) Sa9, c) Sa11, d) Sa14, e) Sa3014, f) Sa3154, g) Sa3489, and h) Sa3603 infection in *C. elegans*. The infected worms

were exposed to ampicillin (AMP) (10 µg/mL), kanamycin (K) (30 µg/mL), streptomycin (S) (10 µg/mL), chloramphenicol (C) (30 µg/mL), tetracycline (TET) (30 µg/mL), and ceftiofur (CF) (30 µg/mL). The aminoglycosides, ampicillin, and chloramphenicol failed to show infection remediation in the worms, whereas, ceftiofur was comparatively more effective ($p < 0.05$). Tetracycline was effective ($p < 0.05$) as well except against Sa9 infected worms. Average values plotted in the graph with different alphabets indicate a significant difference ($p < 0.05$). 'IF-control' stands for infected Caco-2 cells without antibiotic treatment. 'NIF-Worms' and 'IF-Worm UT' stands for non-infected worms and infected untreated worms, respectively.

Figure S2 is provided in: https://static-content.springer.com/esm/art%3A10.1186%2Fs12866-023-02785-1/MediaObjects/12866_2023_2785_MOESM2_ESM.pdf

Caption: Microscopic images of non-infected, and antibiotic-treated/untreated Sa30 infected *C. elegans* under transmission light. Images of a) non-infected, c) Sa30 infected (48 h post-infection), and d) dead infected worms. Destruction of intestinal epithelium and degradation of internal organs was observed due to Sa30 infection. The antibiotics e) ampicillin, f) kanamycin, g) streptomycin, h) chloramphenicol, i) tetracycline, and j) ceftiofur were exposed to Sa30 infected worms for 24 h. The images were acquired using the Cell Discoverer 7.

Preface to Chapter 5

In the previous chapters, libraries of *E. coli* and *S. aureus* isolates were assessed for AMR and virulence characteristics. These investigations showed prevalence of bacteria possessing multiple mechanisms of resistance and virulence factors, suggesting that using antimicrobials with a single mode of action may not be sufficient in curbing the disease involving such pathogens. More importantly, *S. aureus* showed the ability to invade human cells and cause intestinal infection in model organisms. Several generally prescribed antibiotics failed to a large extent in remediating intracellular infection because of altered pharmacokinetics. Therefore Chapter 5 deals with designing and developing a NeACT to counter mastitis pathogens. NeACT constituted antibiotic/adjuvant combinations with a complementary antibacterial mechanism of action, encapsulated in nanocarriers constituted by biopolymers. I characterized the NeACT for colloidal stability and biocompatibility and assessed the release behavior of the cargos. NeACT was tested against AMR mechanisms (efflux pump and beta-lactamase activity), and virulence (biofilms, intracellular pathogens) *in vitro*, in human intestinal epithelial Caco-2 cells, and *in vivo* in CD-1 lactating mice model of mastitis infection. Histopathological studies were conducted on infected and NeACT-treated mammary tissues to assess infection consequences, immune responses, toxic responses, and NeACT efficiency.

Chapter 5

Chitosan conjugated cyclodextrin nanocomposite loaded with antibiotic-adjuvant combinations remediates multi-drug resistant *Staphylococcus aureus* infection in CD-1 mice model of bovine mastitis

Abstract

Bovine mastitis (BM), or bovine intramammary infection, is one of the costliest diseases in animal agriculture. The failure of conventional BM management strategies demands alternate therapeutic approaches. A combination therapy that deals with combining antibiotics and adjuvant molecules with synergistic properties shows the potential to improve treatment outcomes. However, the challenges of poor drug bioavailability, cytotoxicity, stability, and overdosing have restricted their acceptance. Nanotechnology-enabled antibacterial combination therapy (NeACT) that utilizes nanomaterials to co-deliver more than one drug molecule with synergistic and complementary antibacterial mechanisms holds promise for effective BM treatment. In this study, we developed a NeACT constituting ceftiofur (CF) loaded chitosan nanoparticles conjugated with chlorpromazine (CPZ) and tannic acid (TA) loaded cyclodextrin nanoparticles. CF, CPZ, and TA showed a synergistic antibacterial action (FICI=0.49) against mastitis MRSA pathogen Sa1158c. NeACT of size range ~250-400 nm, demonstrated impressive colloidal stability, biocompatibility, and slow-release behavior of the payloads. It showed low immunogenicity, no toxicity, and excellent antibacterial efficiency against Sa1158c. NeACT of ≥3.90 µg/mL demonstrated a ≥3.2 $\log_{10}$ reduction of internalized Sa1158c in human intestinal epithelial Caco-2 cells, while NeACT of 39 µg/gland showed a ≥4.46 $\log_{10}$ remediation of Sa1158c from CD-1 lactating mice model of BM infection. NeACT inhibited efflux pump, beta-lactamase enzyme activity, and biofilm-forming

ability of Sa1158c. By implementing NeACT, we successfully reduced the effective concentration of CF, CPZ, and TA, overcame Sa1158c resistance, and increased their potential for reapplication. This study supports the United Nations' "one health" goal and underscores the potential of NeACT as a viable treatment option for BM.

Keywords: bovine mastitis, methicillin-resistant *Staphylococcus aureus* (MRSA), nano-enabled antibacterial combination therapy (NeACT), chitosan nanoparticles, cyclodextrin nanoparticles, ceftiofur, chlorpromazine, tannic acid, One Health, animal agriculture.

5.1. Introduction

Bovine mastitis (BM) is the inflammation of the mammary gland tissues primarily resulting from microbial infections (Majumder, Eckersall, & George, 2023). Owing to reduced milk production, milk loss, treatment failures, *etc.*, the yearly financial loss in some prominent milk-producing countries such as the United States, Canada, and India amount to $2 billion, $794 million, and $971 million, respectively, making BM the most threatening bacterial disease in the dairy cattle industry (Aghamohammadi et al., 2018; Majumder et al., 2021). Out of several contagious pathogens, *Staphylococcus aureus* is one of the most prevalent organisms associated with BM, accounting for almost 40-70% of the cases globally (Shaheen et al., 2016). *S. aureus* colonizes tissues lining the milk-collecting spaces and induces weak inflammation and host immune responses (Majumder, Eckersall, & George, 2023). This ability in *S. aureus* is predominant in their persistence and chronic infection (Majumder, Eckersall, & George, 2023).

The treatment of BM often involves intramammary infusion and parental administration of antibiotics to dairy cows during the dry period, regardless of their health status, especially in the USA, Canada, UK, and India (Majumder, Eckersall, & George, 2023). According to the United

States Department of Agriculture (USDA), cephalosporins (53.2%), lincosamide (19.4%), and non-cephalosporin β-lactam antibiotics (19.1%) are the most common antibiotics in use to treat BM (*USDA APHIS. Antibiotic use on U.S. dairy operations, 2002 and 2007*). Non-selective blanket antimicrobials used as prophylactic control often impart selective pressure on mastitis pathogens such as *S. aureus*, leading to antimicrobial resistance (AMR) (Normanno et al., 2007). Such pathogens may possess intrinsic or acquired resistance mechanisms that could limit drug uptake, inactivate/modify a drug, or induce efflux/beta-lactamase activities and show virulence such as biofilm formation, hemolysin production, intracellular survivability, etc., contributing to treatment failures (J.-H. Fairbrother et al., 2015; Majumder et al., 2021; Majumder, Sackey, et al., 2023; Veh et al., 2015). Indeed, the cure rate of *S. aureus*-mediated mastitis in cows is only about 37% (Scott McDougall et al., 2022). Moreover, the prevalence of AMR is significantly rising as the resistance rate towards crucial antibiotics such as beta-lactams and cephalosporins is between 30-70% in the USA and more than 85% in Ireland and Brazil (Barkema et al., 2006). Even the commercially available vaccines for *S. aureus* BM, namely Lysigin® in the USA and Startvac® in Europe and Canada, haven't shown protection against reinfection (Majumder, Eckersall, & George, 2023). Overall, these challenges warrant cost-effective, sustainable alternate strategies that are efficient in BM treatment.

Antibacterial combination therapy is defined as *'combining antibiotic/s and/or adjuvant molecules with synergistic properties to improve antibacterial treatment outcomes'* (Majumder, Eckersall, & George, 2023). The mechanism of such a combination involves common or complementary interactions, including sequential inhibition of the same biochemical pathway, inhibition of bacterial antimicrobial-modifying enzymes, *etc.* (Majumder et al., 2022). The selection of antibiotics is crucial and aligning with the United Nations' "one health" objective, our goal is to select an antibiotic against which bacteria is often resistant and reuse it by improving its efficiency

with combination therapy. Ceftiofur (CF) is a cephalosporin antibiotic that inhibits bacterial cell wall synthesis and is extensively used in subclinical BM (Kang et al., 2018). Studies have reported the cure rate of MDR *S. aureus* infection by CF could be around 47% but could get as low as 0% (Roy, DesCôteaux, DuTremblay, Beaudry, & Elsener, 2009; Truchetti et al., 2014). Moreover, CF gets readily metabolized and eliminated from the mammary gland, thus having a poor retention time (Kang et al., 2018). The selection of adjuvants should ideally be based on their complementary mechanisms of action that can uplift the antibacterial efficiency of CF against MDR *S. aureus*. We selected Chlorpromazine (CPZ) and a polyphenol, Tannic acid (TA), to be the adjuvants as they *complement* CF by inhibiting bacterial efflux pumps, interfering in bacterial metabolism, disrupting biofilms and membrane integrity, *etc.* (Kong et al., 2016; Nistorescu et al., 2020; Villanueva et al., 2023). TA has been reported to inhibit or delay virulence and adaptive resistance mechanisms in bacteria (Majumder et al., 2022). It helps tissue regeneration and suppresses pro-inflammatory responses (Mndlovu, du Toit, Kumar, & Choonara, 2023). Overall, CF, CPZ, and TA are ideal candidates for combination therapy.

Although combination therapy has been employed in biomedical and agricultural sectors, poor drug bioavailability, retention rate, cytotoxicity, stability, and overdosing have restricted their widespread acceptance (Majumder, Eckersall, & George, 2023). We believe that nanotechnology-enabled approaches could resolve these issues. The nano size and multifunctionality of nanomaterials have provided unprecedented advantages over the years for targeted delivery of drugs across biological barriers (Brar et al., 2022; S. George et al., 2019; Majumder et al., 2022). In a complex BM tissue environment, nanomaterials could co-deliver more than one drug molecule with synergistic effect and complementary antibacterial mechanism and improve the payload's pharmacological action (Majumder, Eckersall, & George, 2023). We term this strategy as Nano-enabled Antibacterial Combination Therapy (NeACT) and define it as '*the therapeutic strategy*

aimed at harnessing the power of a nano-delivery platform to deliver more than one drug molecule with complementary function for effective antibacterial treatment' (Majumder, Eckersall, & George, 2023). Chitosan (CH) is a polysaccharide widely used in nanomedicine because of its desirable characteristics for drug delivery, such as cationic charge, biocompatibility, low toxicity, low immunogenicity, ability to adhere to mucosal surfaces and improved permeability of macromolecules through the epithelial tight junction (Yadav et al., 2022). These attributes help chitosan to exhibit prolonged residence time at drug absorption sites, enabling higher drug penetration and targeting intracellular pathogens, thus being suitable as a single drug carrier in complex BM environments (Yadav et al., 2022). Cyclodextrin are biocompatible cyclic oligosaccharides containing a relatively hydrophobic central cavity and hydrophilic outer surface (Tiwari, Tiwari, & Rai, 2010). This unique structure could be harnessed to encapsulate or adsorb multiple payloads. The hydroxypropyl derivatives of β-cyclodextrin (CD) have been reported to improve solubility enhance drug stability, drug molecule permeability, and bioavailability (Tiwari et al., 2010). Therefore, we used CH nanoparticles as a carrier for CF and CD nanoparticles as a carrier for CPZ and TA.

In this study, we designed a unique nanocomposite constituting CF-loaded CH nanoparticles conjugated with CPZ and TA-loaded CD nanoparticles. We termed the nanocomposite as NeACT. NeACT demonstrated impressive colloidal stability, biocompatibility, and slow-release behavior of the payloads. We successfully reduced the effective antibacterial concentration of CF, CPZ, and TA through NeACT owing to their synergistic action against multi-drug-resistant *Staphylococcus aureus*. NeACT showed low immunogenicity, no toxicity, and excellent remediation of MDR *S. aureus* infection in epithelial cells and CD-1 lactating mastitis mice model. Overall, the desirable therapeutic characteristics of NeACT propose its application for treating BM.

5.2. Materials and methods

5.2.1. Reagents and chemicals

The (2-Hydroxypropyl)-ß-cyclodextrin (CD), Chitosan (85% deacetylated) (CH), Tannic acid (TA), Chlorpromazine (CPZ), Ceftiofur (CF), Sodium tripolyphosphate (TPP), Mueller–Hinton Broth (MHB), Dimethyl sulfoxide (DMSO), Tryptic soy broth (TSB), Tryptic soy agar (TSA), Resazurin sodium salt, Acetic acid, Ethanol, Paraformaldehyde (PFA), Sodium hydroxide (NaOH), Crystal violet, Triton X-100, Paraffin wax, Hematoxylin solution, Eosin Y, Trichrome Stain (*Masson*) kit, Nylon filter membranes (of 0.22 µm and 0.45 µm), Insulin, Hydrocortisone, Poly-L-lysine, Fluorescein isothiocyanate (FITC), Glutaraldehyde solution, and Ethidium bromide (EtBr) were purchased from Sigma-Aldrich, Canada. The 32-gauge blunt needles were purchased from TSK Laboratory International, Canada. Gibco Dulbecco's Modified Eagle Medium (DMEM), Hoechst 33342, Propidium iodide (PI), Probe-On Plus slides, and Sterile petri dishes were purchased from ThermoFisher, Canada. Fetal bovine serum (FBS) was purchased from Wisent, Canada. Nitrocefin dye was purchased from Abcam, UK. Gentamicin sulfate was purchased from Bio Basic, Canada. Human colorectal adenocarcinoma (Caco-2) cells were purchased from ATCC, USA. The quality control (QC) strain *Staphylococcus aureus* ATCC 25923 was purchased from Oxoid Company, Canada. The methicillin-resistant *S. aureus* strains Sa1158c (Isolate ID: 10812464, Accession no. NCBI: SRR11471981) and Sa30 (Isolate ID: 21000024, Accession no. NCBI: JAANBF000000000) were collected from the Canadian mastitis pathogen culture collection (MPCC) (Majumder, Sackey, et al., 2023). CD-1 lactating mice were purchased from Charles River Laboratories, Canada.

5.2.2. Assessment of CF, CPZ, and TA for antibacterial synergism

A three-dimensional checkerboard assay, as previously described by Stein *et al*., was conducted to assess the antibacterial efficiency of the combination (CF, TA, and CPZ) (Stein et al., 2015). CF, CPZ, and TA concentrations were selected based on the pre-determined MICs against Sa1158c. Ten-twofold, six-twofold, and seven-twofold serial dilutions of CF, CPZ, and TA, respectively, were performed in a 96-well plate. Sa1158c culture maintained at 0.5 McFarland standard (1.5×10^8 cells/mL) in MHB broth was added further. The plates were incubated at 37 °C for 18 h, and a resazurin assay was performed to check bacterial viability. Briefly, a 30 µL of resazurin solution (0.5% of 100X resazurin in PBS buffer (pH-7.4)) was added to each well, and the plates were incubated for 2 h under mild shaking. The fluorescent intensity (530/590 nm) was measured using a plate reader (SpectraMax-i3X, Molecular Devices, USA).

The fractional inhibitory concentration index (FICI) was determined using the following formula:

$$FICI_{CF/TA/CPZ} = (MIC_{CF(combination)}/MIC_{CF(alone)}) + (MIC_{CPZ(combination)}/MIC_{CPZ(alone)}) + (MIC_{TA(combination)}/MIC_{TA(alone)}$$

FICI < 0.8, 0.8 < FICI < 4, and FICI ≥ 4 were considered synergism, additive or indifference, and antagonism effects, respectively.

5.2.3. Synthesis of CPZ and TA-loaded CD nanoparticles (CPZ-CD-TA)

A 6:6:6 mM ratio of CD, TA, and CPZ was used for CPZ-CD-TA preparation. Briefly, 138.6 mg of CD was dispersed to 3 mL of ethanol and sonicated for 10 mins. The suspension was added dropwise to a solution of CPZ (28.62 mg) in 10 mL of DI water under constant stirring. CPZ-CD was sonicated for 15 mins, and a 2 mL ethanol solution containing 153.09 mg of TA was added dropwise. CPZ-CD-TA was kept under constant stirring for 5 hours at 40 ˚C and then under vacuum for 30 mins. Subsequently, the solution was filtered using a 0.45 µm nylon filter membrane to

remove the unreacted agents and residual impurities. CPZ-CD-TA was refrigerated at -20 ˚C and lyophilized using a vacuum freeze dryer. The dried sample was stored in a desiccator for future use.

5.2.4. Synthesis of CPZ-CD-TA conjugated CF-loaded CH nanoparticles (CH Np-CF(CPZ-CD-TA) or NeACT)

CH of 2 mg/mL was added to DI water, dissolved by adding acetic acid (final concentration of 1%) and stirring the solution for 48 h. Subsequently, the pH was raised to 4.7-4.8 using 1 N NaOH. CF (1.5 mg/mL) was dissolved in DI water and added to the solution dropwise. The solution was stirred for 15 mins and sonicated for another 15 mins. TPP, at a concentration of 1/3rd of CH, was added dropwise to the solution under constant stirring to form CH Nps entrapping CF. The formed CH Np-CF was stirred for 30 mins, sonicated for 15 mins, and stirred for another 1 h. The sample was centrifuged (7500 × *g* for 10 mins) (Sorvall Instruments, Thermo Fisher Scientific, USA), washed, and resuspended in PBS. Dried CPZ-CD-TA was added to the PBS buffer and dispersed with sonication and vigorous stirring. CH Np-CF was added dropwise to the solution at a 3:1 ratio (CPZ-CD-TA: CH Np-CF) and stirred for 4 h to allow fusion between the two entities through electrostatic interaction. The CH Np-CF(CPZ-CD-TA), referred to as NeACT, was washed thrice, resuspended in PBS, and stored at 4 ˚C for further analysis.

5.2.5. Fluorescein isothiocyanate (FITC) labeling of NeACT

As-synthesized NeACT (10 mg/mL) was added with FITC (1 mg/mL, dissolved in DMSO) at room temperature and incubated under vigorous stirring in the dark for 12 h. The FITC-labeled NeACT (FITC-NeACT) was centrifuged (7,500 × *g* for 10 mins) and washed thoroughly with sterile DI water until no color or residue was observed in the supernatant. Fluorescence images of particles

were taken using an automated epi-fluorescence microscope (Cell Discoverer 7, Carl Zeiss, Germany) to confirm the labelling of NeACT with FITC.

5.2.6. Physicochemical characterization of the particles

An attenuated total reflectance-Fourier transform infrared (ATR-FT-IR) (ALPHA-P, Bruker, Billerica, MA, USA) was used to assess the surface functional groups of the particles (Majumder et al., 2022). Five microliters of the particle suspension were dropped on the ATR probe and allowed to dry. A wavelength range of 400–4000 cm^{-1}, with a resolution of 4 cm^{-1}, and 32 scans were used to obtain the FT-IR spectrum. The qualitative analysis was performed using the OMNIC 8.2.0.387 software.

A Scanning Electron Microscope (SEM) (FEG Quanta 450 Field Emission Scanning Electron Microscope, USA) was used to analyse the surface morphology of the particles (Brar et al., 2022). The particles (50 µg/mL) were dropped onto aluminum mounts, dried at room temperature, and coated with platinum before acquiring SEM images. ImageJ software was used to check the size of the particles.

The hydrodynamic size and surface charge of the particles (50 µg/mL) were measured by Dynamic Light Scattering (DLS) (NanoBrook Omni instrument, Brookhaven, USA) at 25 °C (Majumder et al., 2022). The particles were loaded into a pre-rinsed folded capillary cell. A 100 V was applied to measure the zeta potential.

5.2.7. Loading capacity of particles and release profile of CF, CPZ, and TA

The loading capacity of the particles and release profile of the drug molecules (CPZ, TA, and CF) were determined using a Varian ProStar HPLC system (Varian, USA) equipped with a

Gemini-NX 5u C18 110A column (100 × 4.60 mm, 5 µm particle size, Phenomenex, USA). For this, NeACT particles (1 mg/mL) were centrifuged (31,000 × g for 20 mins) (Sigma 3-30 KHS, Germany), as centrifugation at high RPM could disrupt polymeric matrix to release the contents (Soliman et al., 2022). The supernatants were filtered using a 0.22 µm nylon filter membrane. A 20 µL of the supernatant was injected into the chromatographic system. The mobile phase consisted of methanol-acetonitrile-acetic acid (5%) in a volume ratio of 6:7:87 at a 1.2 mL/min flow rate. The detection wavelengths for CPZ, TA, and CF were 306 nm, 280 nm, and 292 nm, respectively. The loading of CPZ, TA, and CF in NeACT was subsequently determined from a standard curve (concentration range: 1 mg/mL–0.05 mg/mL). The release profile of CPZ, TA, and CF from the suspended NeACT was assessed in PBS buffer added with 10% FBS (pH 7.4) to mimic bovine mammary microenvironment. NeACT (1 mg/mL) was gently centrifuged (3,000 × g for 1 min), and the supernatant was collected every 24 h for seven days. As described earlier, HPLC was used to assess the percentage of payload release as a function of time.

5.2.8. *In vitro* antibacterial efficiency of particles

The *in vitro* antibacterial efficiency of the particles was determined using the broth microdilution method, as detailed earlier (George et al., 2020). Briefly, the particles (250 µg/mL) were subjected to ten-twofold serial dilution in 100 µL of MHB media in a sterile 96-well plate. Bacterial culture of 10 µL taken from cell suspension with OD adjusted to 0.5 McFarland standard (1.5×10^8 cells/mL) was added to the wells. The plate was incubated at 37 °C for 18 h. The colony-forming units (CFU) were enumerated using a drop plate culturing method, as detailed earlier by George *et al*. (S. George et al., 2019). For this, 10 µL from the treated wells were subjected to seven-fold serial dilutions in 100 µL of PBS (1X, pH 7.4) in a new 96-well plate. Subsequently, 10 µL of the cell suspension (from 10^1, 10^3, 10^5, and 10^7 dilutions) was dropped onto one end of the

rectangular TSA plates and allowed to flow down vertically. The plates were further incubated at 37 °C for 18 h, and the CFU in respective lanes were counted using a plate counter.

The effect of particles on bacterial membrane integrity was assessed using the PI dye (Majumder et al., 2022). As detailed earlier, the particles (125 µg/mL) were subjected to ten-twofold serial dilution in 100 µL of MHB media in a 96-well plate. Ten µL of the culture maintained at 0.5 McFarland standard was added to the wells and incubated for 6 h at 37 °C. PI (3.34 µg/mL) suspended in PBS was added to the wells and incubated for 30 mins. The fluorescence intensity was measured at an excitation/emission wavelength of 555/645 nm using a plate reader.

SEM was used to assess changes in the morphological feature of bacteria after exposed to NeACT (Radziwill-Bienkowska et al., 2018). Briefly, bacterial culture maintained at 0.5 McFarland standard was subjected to a sub-lethal concentration (1.95 µg/mL or half of MIC value against Sa1158c) of NeACT and incubated for 6 h at 37 °C with gentle shaking. The bacterial cells were harvested by centrifugation (4,000 × g, 3 mins) and washed twice with PBS (1X, pH 7.4). The washed cells were fixed by subjecting them to 2.5% glutaraldehyde at 4 °C for 2 h. Fixed cells were dropped onto poly-l-lysine coated coverslips and subjected to serial dehydration by exposing them to incremental concentrations of ethanol (20-100%). Further, these cells were subjected to critical point drying (Leica EM CPD300, Germany) and were used for SEM examination after sputter coating with Platinum. ImageJ software was used to assess the size of bacterial cells.

5.2.9. Efficiency of NeACT against the resistance mechanisms of *S. aureus*

The anti-efflux property of NeACT was measured using a pre-established EtBr assay (Brar et al., 2022). Briefly, bacterial cultures maintained at 1.0 McFarland standard (3×10^8 cells/mL) were treated with sub-lethal concentrations ($1/3^{rd}$ of MIC value against Sa1158c) of the NeACT (1.30 µg/mL) and control groups (CH Np-CF (20.83 µg/mL) and CPZ-CD-TA (83.33 µg/mL)). The

suspension was vortexed and incubated at 37 °C for 30 mins. A sub-lethal concentration of EtBr (0.65 µg/mL or 1/3rd of MIC value against Sa1158c) was added further to the suspension and incubated for another 30 min. The bacterial cells were washed, re-suspended in PBS (1X, pH 7.4), and transferred (140 µL) to a 96-well plate. The EtBr efflux was triggered by glucose (10 µL; final concentration 0.1% w/v) and determined by monitoring fluorescence (530/590 nm) for 60 min using a plate reader. Sa1158c, without particle exposure, was considered a positive control, while Sa25923, with no efflux pump activity, was used as a negative control. GraphPad Prism 7 software was used to determine the time-dependent efflux of EtBr using a single exponential decay equation as detailed previously (Majumder et al., 2021). The time taken for the bacterial cells to extrude 50% of EtBr was denoted as $t_{efflux50\%}$.

The beta-lactamase enzyme inhibition property of the NeACT was assessed using the Nitrocefin assay, as detailed previously (Brar et al., 2022). Briefly, 100 µL of the bacterial isolates maintained at 1.0 McFarland standard was exposed to sub-lethal concentrations (1/3rd of MIC against Sa1158c) of the samples (NeACT (1.30 µg/mL), CH Np-CF (20.83 µg/mL), and CPZ-CD-TA (83.33 µg/mL)) and were incubated for 18 h at 37 °C. Subsequently, the cells were further adjusted to McFarland 1.0 and centrifuged at 5,000 × g for 10 mins. The cells were washed with sodium phosphate buffer (pH 7.0), resuspended in the same buffer, and sonicated for 3 mins on ice. The suspension was centrifuged (16,000 × g for 30 mins), and the cell-free extract containing beta-lactamase enzyme was collected. Nitrocefin was used as the substrate to measure beta-lactamase enzyme activity. For this, 15 µL of the nitrocefin solution (0.5 mg/mL in 5% DMSO) was mixed with 30 µL of the cell-free extract, and the volume was adjusted to 100 µL using sodium phosphate buffer solution in a 96-well plate. The absorbance was measured in kinetic mode at 490 nm for 15 mins using a plate reader. Sa1158c without particle exposure was treated with CF (10.41 µg/mL or 1/3rd of MIC value against Sa1158c) to trigger beta-lactamase enzyme activity and considered as

the positive control. Sa25923, with no beta-lactamase enzyme activity, was used as a negative control. The enzyme activity was calculated, as mentioned earlier (Majumder, Sackey, et al., 2023).

The antibiofilm property of NeACT was analyzed using a pre-established crystal violet assay (Majumder et al., 2022). Briefly, 200 µL of TSB media suspended with incremental concentrations (0.24-125 µg/mL) of NeACT and control particles in a 96-well plate were added with 20 µL of the Sa1158c culture adjusted to 0.5 McFarland standard. After 48 h of incubation, the media was removed from the wells, and the wells were washed with sterile PBS. Subsequently, 100 µL of 99% methanol was added, and the plates were kept undisturbed for 15 min. Methanol was removed from the wells, and 200 µL of CV solution (0.4%) was added. The plates were incubated for 2 h, washed, and 100 µL of acetic acid (33%) was added. The biomasses of the biofilms were quantified by measuring the absorbance values at 570 nm using a plate reader.

The viability of Sa1158c cells present in biofilm was assessed after treating with incremental concentration (0.24-125 µg/mL) of the particles (Cruz, Shah, & Tammela, 2018). Briefly, 10 µL of Sa1158c isolate maintained at 0.5 McFarland standard was added to 100 µL of TSB media in a 96-well plate. The plate was incubated for 24 h to allow biofilm formation, followed by the addition of NeACT and control particles. The plate was incubated for another 24 h at 37 °C. The 100 µL of TSB media was discarded without damaging the biofilm. Subsequently, 100 µL of PBS was added to the wells containing biofilms, and the biofilm cells were suspended by vigorous pipetting. The CFU was enumerated using the drop plate culturing method, as detailed in section 5.2.8.

To visualize the penetration of NeACT into the biofilm matrix, fluorescent labelled Sa30 isolate obtained by introducing plasmid pSRFPS1 (coding red fluorescence protein (RFP)) (Majumder, Sackey, et al., 2023) was used. Ten µL of RFP labelled Sa30 isolate (maintained at 0.5 McFarland standard) was incubated for 24 h (at 37 ˚C) in a 96-well plate containing 100 µL of TSB media to allow biofilm formation. FITC-NeACT (20.83 µg/mL or 1/3rd of MIC value against Sa30)

was exposed to the biofilms and incubated further for 24 h. Subsequently, 100 µL of the TSB media was discarded, and 100 µL of PBS was added to the wells. Fluorescence images of the biofilms (Red fluorescence imaged using a 583 nm filter) and FITC-NeACT (Green fluorescence imaged using a 519 nm filter) were captured at 20X magnification using an epifluorescence high content microscope (Cell Discoverer 7). 3D images were constructed by stacking images captured from different depths.

5.2.10. Efficiency of NeACT against internalized *S. aureus* in Caco-2 cells

The cytotoxicity of NeACT was tested in Caco-2 cells, as detailed earlier (Majumder, Huang, Zhou, Wang, & George, 2023). Briefly, the Caco-2 cells were cultured in a 96-well plate (2×10^4 cells/well) until confluent and exposed to increasing concentrations of the particles (3.90-250 µg/mL) suspended in DMEM media. After 24 h of incubation, resazurin of 50 µg/mL (prepared with DMEM) was added and incubated for 4 h. The fluorescence was measured at 530/590 nm using a plate reader. Cells without treatment and cells treated with silver nitrate ($AgNO_3$) were considered as negative and positive controls, respectively.

The efficiency of NeACT to target internalized *S. aureus* in Caco-2 cells was determined by a pre-established protocol with modifications (Brar et al., 2022; Majumder, Sackey, et al., 2023). Confluent Caco-2 cells (2×10^4 cells/well) were exposed to Sa1158c culture maintained at 1.5×10^8 cells/mL in a 96-well plate and incubated for an hour. The cells were washed using PBS (4 ˚C) and subjected to gentamicin (10 µg/mL) for 30 mins. The extracellular gentamicin was removed by washing, followed by incubation with DMEM for 4 h to establish the intracellular infection model. The particles at incremental concentrations (3.90-15.62 µg/mL) were added, and the plates were incubated for 24 h in a cell culture humidified incubator at 37 °C, with 5% CO_2. Subsequently, the cells were washed using PBS and lysed using 0.5% (v/v) of Triton X-100. CFU of viable

intracellular bacteria were enumerated using the drop culture method as detailed earlier in section 5.2.8. Sa25923 was used as a reference strain, and cells infected with bacteria without treatment were considered as controls.

5.2.11. Efficiency of NeACT on CD-1 mice model of mastitis infection

The institutional ethics committee on animal experimentation of the Faculté des Sciences of the Université de Sherbrooke (QC, Canada) approved the *in vivo* experiments, and the guidelines of the Canadian Council on Animal Care were respected during all procedures.

CD-1 lactating mice were separated from their pups (12-14 days following birth) and anesthetized using isoflurane (Brouillette, Grondin, Lefebvre, Talbot, & Malouin, 2004; Diarra et al., 2013). The fourth pair of glands found from head to tail (L4 and R4 glands) was first disinfected with 70% ethanol for inoculation. A 100 µL of PBS containing 100-125 CFUs of Sa1158c was slowly injected into the lactiferous duct with a 32-gauge blunt needle attached to a 1 mL syringe. Four hours post-inoculation, mice were anesthetized again, and incremental concentrations of NeACT (20 (78 µg/gland), 10 (39 µg/gland), and 5 (19.5 µg/gland) times of *in vitro* MIC value against Sa1158c) were injected directly into the mammary glands previously infected (6 mammary glands: n=6). Similarly, CH Np, CD, CH Np-CF, and CPZ-CD-TA (working concentration: 78 µg/gland or 20 times of *in vitro* NeACT MIC value against Sa1158c) were used as control particles and were injected into the infected mammary glands (6 mammary glands per control group). Hundred µL of PBS used as the media control were injected in eight infected mammary glands (n=8). Each infected gland was considered the experimental unit. After 14 h of bacterial inoculation, mice were anesthetized and humanely euthanized, mammary glands were harvested, and one set was homogenized for measuring bacterial count. CFU counts were obtained after plating a serial

dilution of mammary gland homogenates on TSA petri dishes that were incubated at 37 ˚C for 24 h. The detection limit was approximately 200 CFU per gram of mammary glands.

5.2.12. Tissue preparation and histological studies

Mammary glands from the NeACT-treated and untreated mice were fixed in 4% PFA overnight at 4°C, dehydrated in 70% ethanol to avoid adipose distortion, and embedded in paraffin (Brouillette, Grondin, Talbot, & Malouin, 2005). Subsequently, the paraffin blocks were incubated at -20 ˚C for 1 h. Tissue sections of 5 µm were cut using a microtome (Shandon Finesse ME+ paraffin sectioning microtome, GMI, USA), applied to Probe-On Plus slides, and kept at room temperature. Hematoxylin and Eosin Y (H&E) staining and Masson's trichrome staining were performed to investigate immune responses, morphological and cellular alterations in infected and NeACT-treated mammary glands, while Gram staining was performed to stain and detect Sa1158c in infected mammary tissues. H&E and Masson's trichrome staining was conducted on an automated platform (Shandon varistain 24-4 slide stainer, GMI, USA). Tissue preparation, embedding, and coloration (H&E, Masson's trichrome, and Gram staining) were performed by the Electron Microscopy and histology platform at the Université de Sherbrooke (Brouillette, Grondin, et al., 2004). Images were captured on a Nanozoomer Digital Slides Scanner (Hamamatsu, Japan).

5.2.13. Statistical analysis

t-test and one-way ANOVA were performed as required to check the statistical significance, wherein a p-value ≤ 0.05 was considered significant. 'GraphPad Prism 7' software was used to perform the statistical analysis.

5.3. Results

5.3.1. Checkerboard assay

The checkerboard assay assessed the combinatorial effect of the CF, CPZ, and TA against Sa1158c. A FICI of <0.8 was considered a synergistic relationship among the combinations. The MIC of CF, CPZ, and TA against Sa1158c were 31.25, 500, and 500 µg/mL, respectively, which were reduced significantly by 8-folds, 4-folds, and 8-folds, respectively, when combined. The FICI for combinations of CF, CPZ, and TA was 0.49, indicating a synergistic interaction.

5.3.2. Physicochemical characterization of the particles

The FTIR spectra of CPZ-CD-TA, CH Np-CF, and NeACT are provided in **Figure 5.1a**. The absorbance at 1151 cm^{-1} in CH Np-CF is characteristic of asymmetric vibration of the b-(1-4) glycosidic bond of chitosan. The low-intensity peaks at 2935 and 2887 cm^{-1} are attributed to stretching vibrations of methylene groups in the polymeric chain. The peaks at 1072 cm^{-1} and 1531 cm^{-1} represent C-O-C- stretching vibrations and $–NH_2$ bending vibration peaks, respectively. The peak at 1030 cm^{-1} shows characteristic of P=O stretching vibration from phosphate groups while the peak at 1628 cm^{-1} is attributed to the electrostatic cross-linking between the phosphate group of TPP and the ammonium group of chitosan, suggesting the formation of CH Np (Behl, Iqbal, O'Reilly, McLoughlin, & Fitzhenry, 2016; Lustriane, Dwivany, Suendo, & Reza, 2018). CF in CH Np-CF was evident from the additional signals in 1763, 1635, 1384, and 1287 cm^{-1} corresponding to C=O stretching, $-NH_2$ bending, C-N stretching, and C-O stretching, respectively. CD Np in CPZ-

CD-TA was evident from the characteristic bands of saccharides: 2932 cm^{-1} (C-H stretching vibration), 1651 cm^{-1} (O-H bending vibration), and 1154 cm^{-1} (C-O vibration) (Yuan, Liu, & Liu, 2015). The signal at 857 cm^{-1} corresponded to the α-type glycosidic bond, characteristics of CD Np formed by glucopyranose units through the α-1,4-glycosidic bond (Yuan et al., 2015). The peak at 2973 cm^{-1} corresponds to the anti-symmetric vibration of a methyl group, indicating the existence of the hydroxypropyl group in CD Np (Yuan et al., 2015). CPZ in CPZ-CD-TA was evident from the signals 1606 and 1651 cm^{-1} (phenyl rings), 1510 cm^{-1} (C-H deformation), and 752 cm^{-1} (aromatic C-H bending) (Hussain, Kushwaha, Rahman, & Akhtar, 2017). TA showed an adsorption band at approximately 3000–3500 cm^{-1} belonging to the stretching vibration of O-H groups. The absorption band at 1187 cm^{-1} belongs to the bending vibration of O-H groups. The skeleton vibration band of benzene rings appeared at 1443–1704 cm^{-1} (Majumder et al., 2022). In NeACT, CH Np-CF was evident from the peaks at 2938 and 2892 cm^{-1} (stretching vibrations of methylene groups), 1065 cm^{-1} (C-O-C stretching vibrations), 1526 cm^{-1} (-NH_2 bending vibration peak), 1026 cm^{-1} (P=O stretching vibration), 1759 cm^{-1} (C=O stretching), 1382 cm^{-1} (C-N stretching), and 1690 cm^{-1} (thioester group). The signals at 859 cm^{-1} (α-type glycosidic bond), 2938 cm^{-1} (C-H stretching vibration), 1187 cm^{-1} (O-H bending), 1442-1705 cm^{-1} (benzene rings), 1607 cm^{-1} (phenyl rings), 756 cm^{-1} (aromatic C-H bending) corresponded to the functional groups of CPZ-CD-TA in NeACT. The shifts in FTIR spectra in the case of NeACT indicate hydrogen bonding formation due to the interactions between the payloads and the nanocarriers.

SEM analysis revealed the morphology of the particles **(Figures 5.1b-g)**. CD Np had a typical nano-sized spherical morphology (Bashal et al., 2022), while CPZ-CD-TA showed aggregation of particles forming a chain-like arrangement. The size of CPZ-CD-TA ranged between ~120-260 nm. DLS studies indicated the hydrodynamic size of CD Np and CPZ-CD-TA to be ~135 nm and a zeta potential of -11.37±1.37 mV and -9.51±1.56 mV, respectively **(Table 5.1)**. The

weaker zeta potential might have led to the aggregation of these nanoparticles due to the Van Der Waals attractive forces (Majumder et al., 2022). CH Np was uniformly distributed and had a typical spherical structure with a size range between ~114-159 nm. Similarly, CH Np-CF also showed a spherical morphology and was of variable sizes (~92-229 nm). CPZ-CD-TA conjugated with CH Np-CF through electrostatic interactions to develop NeACT and ranged between ~250-400 nm. The hydrodynamic sizes of CH Np, CH Np-CF, and NeACT were 269.56±3.43, 309.52±5.11, and 539.58±12.36 nm, respectively. The zeta potential for CH Np and CH Np-CF ranged between +28-30 mV, which, however, reduced to +21.69±2.43 mV in the case of NeACT, indicating the electrostatic interaction between CH Np-CF and CPZ-CD-TA. However, a zeta potential close to +30 mV suggests sufficient repulsive forces and superior physical colloidal stability (Majumder et al., 2022).

Samples	Hydrodynamic size (nm)	Zeta potential (mV)
CD Np	137.41±5.91	-11.37±1.37
CH Np	269.56±3.43	+29.89±0.62
CH Np-CF	309.52±5.11	+30.68±1.21
CPZ-CD-TA	132.77±4.84	-9.51±1.56
NeACT	539.58±12.36	+21.69±2.43

Table 5.1. The hydrodynamic size and zeta potential of the particles.

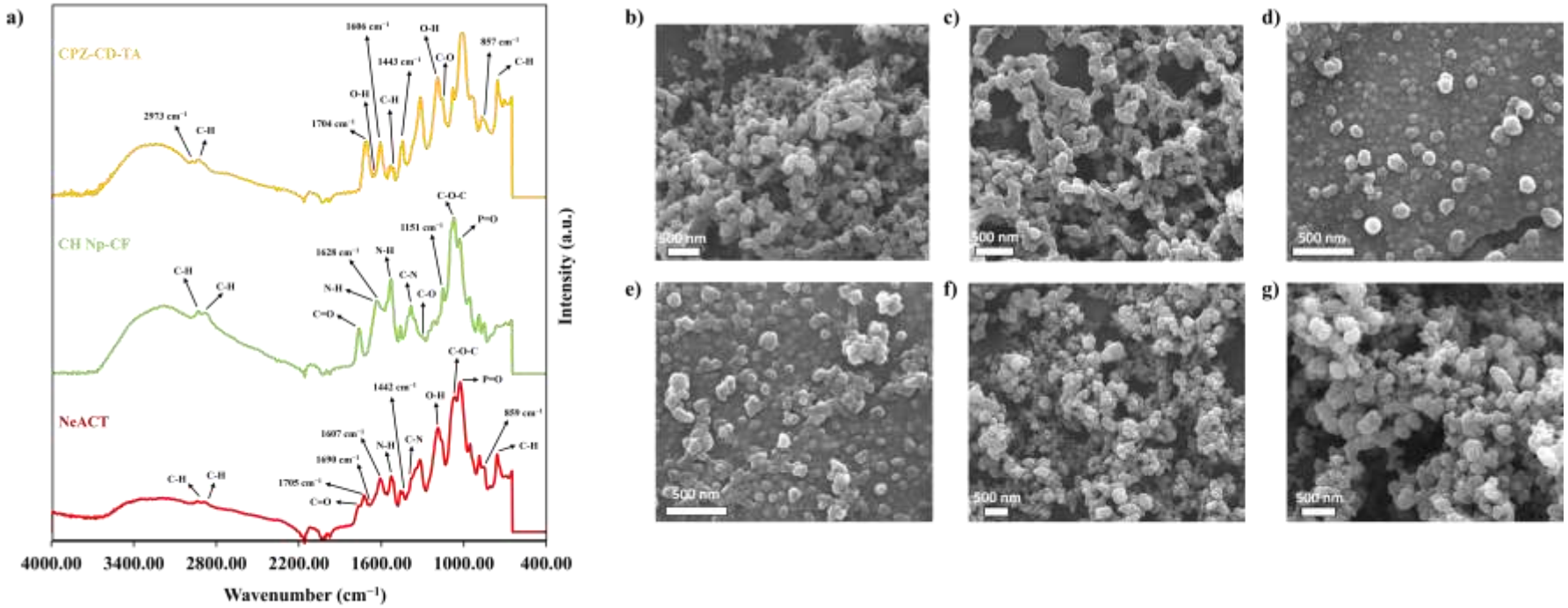

Figure 5.1. Physicochemical characterization of the particles. (a) FT-IR analysis of the particles analyzed at a wavelength range of 600–4000 cm^{-1} with a resolution of 4 cm^{-1}. Scanning electron microscopy (SEM) images of **(b)** CD-NP, **(c)** CPZD-CD-TA, **(d)** CH Np, **(e)** CH CF-Np, **(f-g)** NeACT. The particles were dropped onto aluminium mounts, dried, and coated with platinum. The images were acquired using an SEM.

5.3.3. Loading capacity of NeACT and release profile of CF, CPZ, and TA

The loading capacity of NeACT for the payloads was determined using HPLC. The loading of CF, CPZ, and TA in NeACT was 32.14±1.10%, 18.78±4.63%, and 16.85±1.31%, respectively **(Figure 5.2a)**. The loading of CF in CH CF-Np was 44.66±1.97%, while the loading capacity of CD Np for CPZ and TA were 26.88±2.04% and 25.78±2.41%, respectively. The release profile of NeACT was checked every 24 h for 7 days in PBS buffer supplemented with 10% FBS (pH 7.4). The release of 50% CF, CPZ, and TA from NeACT was observed between the 2nd and 3rd day, while a 100% release was seen by the 7th day **(Figure 5.2b)**.

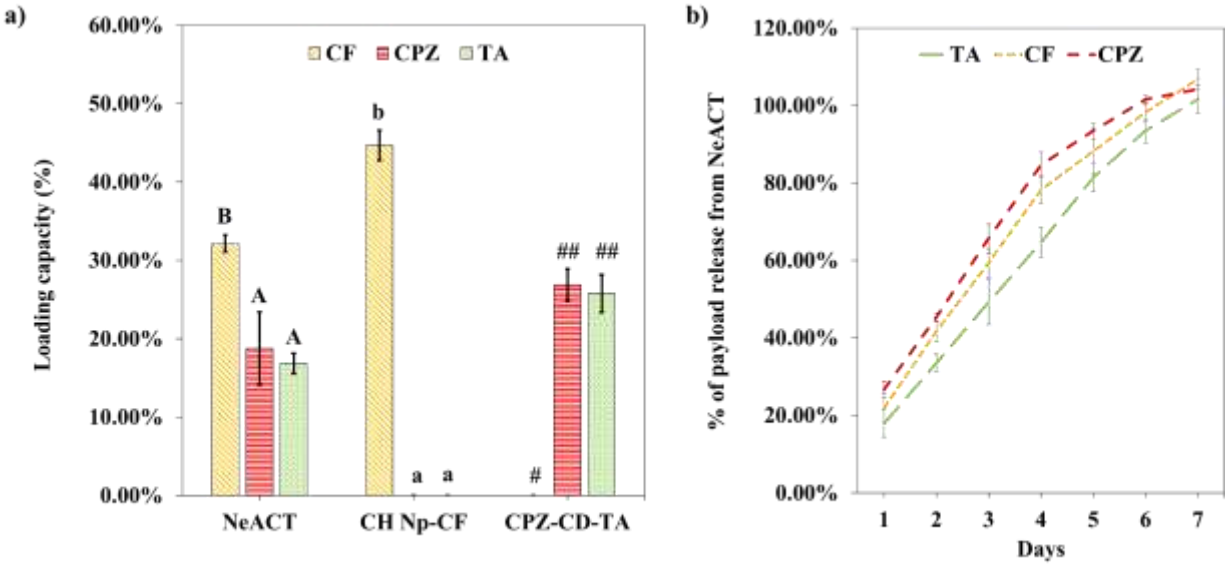

Figure 5.2. Loading capacity of particles and release profile of the payloads. (a) The loading capacity of the particles for CF, CPZ, and TA. The particles of 1 mg/mL were centrifuged and filtered. An HPLC system was used to assess the loading of CPZ, TA, and CF in the particles. **(b)** The release profile of CF, CPZ, and TA from NeACT. The release of CF, CPZ, and TA was checked every 24 h for seven days. NeACT of 1 mg/mL was centrifuged gently, and the supernatant was collected. HPLC was used to assess the percentage of payload release. Average values plotted in the graph with different alphabets and symbols indicate a significant difference *($p < 0.05$)*.

5.3.4. *In vitro* antibacterial efficiency and mechanism of action of NeACT

NeACT showed excellent antibacterial properties against the tested bacteria, Sa1158c and Sa25923. For instance, at the MIC of 0.48 and 3.91 µg/mL, NeACT showed a ~7.05 $\log_{10}$ Sa25923 reduction *($p<0.05$)* and ~7.51 $\log_{10}$ Sa1158c reduction *($p<0.05$)*, respectively **(Figure 5.3a and 5.3b)**. On the contrary, CF, CPZ, TA, CPZ-CD-TA, and CH Np-CF at the same concentration showed no significant difference *($p>0.05$)* from the control group (bacteria without treatment). The MIC for CPZ-CD-TA and CH CF-Np was 250 and 62.5 µg/mL. The MIC for pristine CF, CPZ, and TA were 31.25, >250, and >250 µg/mL, respectively, against Sa1158c. Interestingly, the loading of CF, CPZ, and TA in NeACT at its MIC against Sa1158c were 1.25, 0.73, and 0.65 µg/mL, respectively, suggesting a significant decrease in the effective concentration of CF (by 25-fold), CPZ (by >342-fold), and TA (by >384-fold) than their pristine form. This superior performance of NeACT was owed to the synergistic effect of the combination.

The effect of NeACT on bacterial membrane integrity was measured as PI uptake **(Figure 5.3c)**. NeACT showed significant damage to the Sa1158c membrane. For instance, at 3.91 µg/mL, a ~8.85-fold increase *($p<0.05$)* in PI fluorescence was observed, suggesting a compromised Sa1158c membrane. The rate of damage increased with increasing concentrations of NeACT. Compared to the control group (bacteria with no treatment), CPZ-CD-TA at 62.5 µg/mL and CH Np-CF at 31.25 µg/mL showed ~2.74 and ~8.03-fold increase in PI fluorescence, respectively. **Figures 5.3d** and **5.3e** represent Sa1158c cells before and after exposure to 1.95 µg/mL of NeACT. Ruptured membrane and corrugated morphology with wrinkles and cracks were evident in NeACT-treated Sa1158c cells due to the loss of membrane integrity (Sana, Datta, Biswas, & Sengupta, 2018).

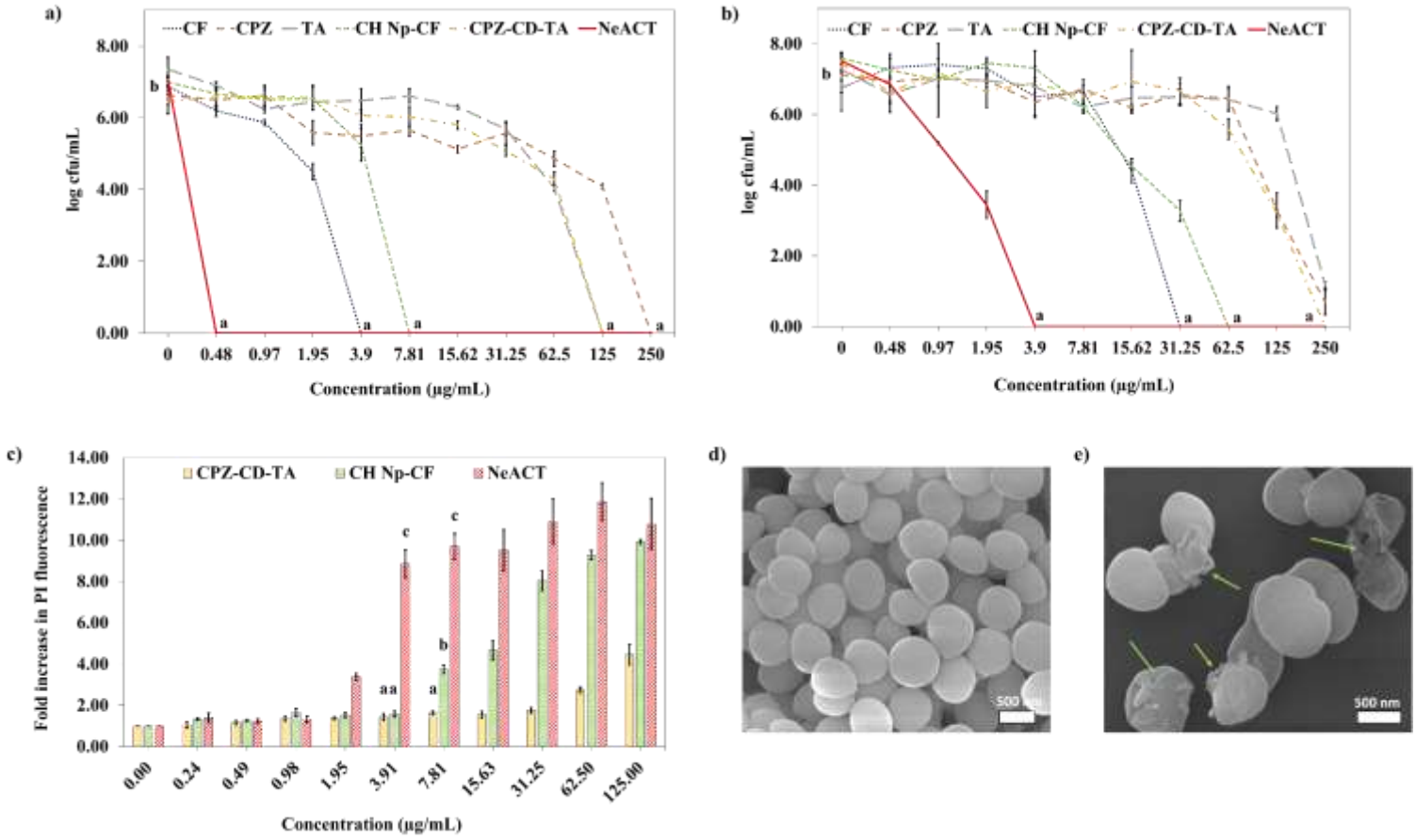

Figure 5.3. Antibacterial efficiency and mechanism of action of particles against *S. aureus*. (a-b) Antibacterial efficacy of NeACT and control groups against **(a)** Sa25923 and **(b)** Sa1158c. In a 96-well plate, the incremental concentration of the samples was subjected to MHB media containing bacteria maintained at 0.5 McFarland standard. The plate was incubated for 18 h, and the CFU was enumerated using the drop plate culturing method. **(c)** Sa1158c membrane integrity upon particle exposure. After 6 h of incubation, PI dye was added to the wells. The fluorescence intensity was measured at an excitation/emission wavelength of 555/645 nm using a plate reader. Average values plotted in the graph with different alphabets indicate a significant difference *($p < 0.05$)*. **(d-e)** SEM image of **(d)** untreated Sa1158c cells and **(e)** NeACT-treated Sa1158c cells. Bacterial cells were exposed to sub-lethal concentrations of NeACT for 6 h. The cells were harvested, washed, and fixed with 2.5% glutaraldehyde. Critical point drying was performed, and the cells were coated with platinum and examined under SEM. Green arrows indicate compromised membrane integrity.

Sa1158c cells extruded 50% of the EtBr molecules ($t_{efflux50\%}$) in only 94.10 secs, while the exposure (1/3rd of MIC value against Sa1158c) of CPZ-CD-TA (at 83.33 µg/mL), CH Np-CF (at 20.83 µg/mL), and NeACT (at 1.30 µg/mL) reduced the extrusion rate significantly (*$p<0.05$*) by

>38.25-fold, ~6.63, and ~15.53-fold, respectively, suggesting the efflux inhibition property of the particles **(Figures 5.4a and 5.4b)**. It was evident that CPZ-CD-TA has contributed to the efflux inhibition property in NeACT.

a)

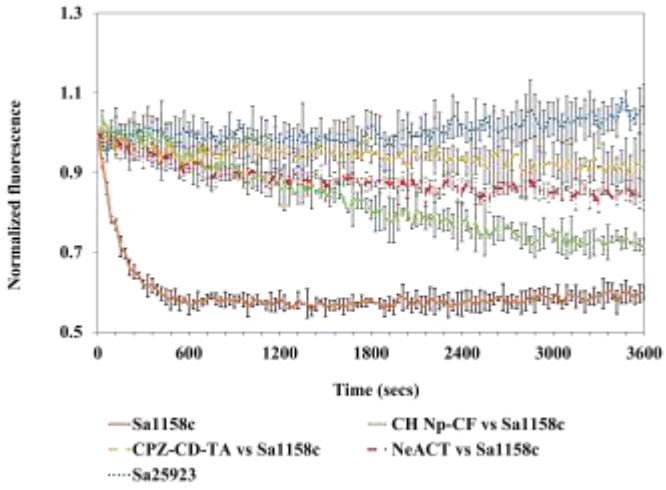

b)

Samples	$t_{efflux50\%}$ (secs)
Sa25923	>3600 [d]
Sa1158c	94.10±5.20 [a]
CPZ-CD-TA exposed Sa1158c	>3600 [d]
CH Np-CF exposed Sa1158c	624.16±17.84 [b]
NeACT exposed Sa1158c	1462±19.64 [c]

c)

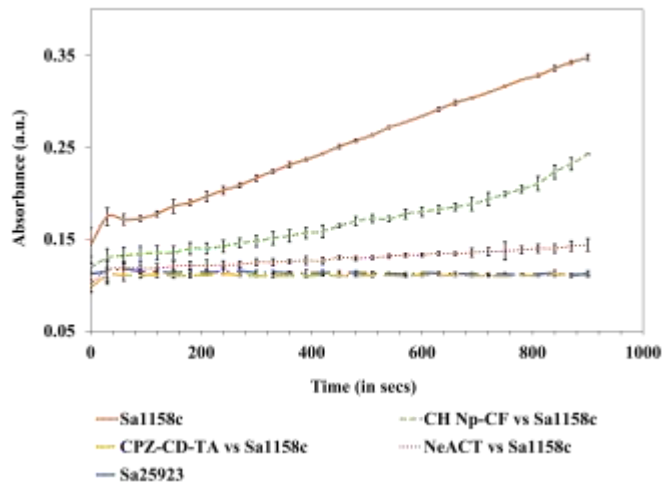

d)

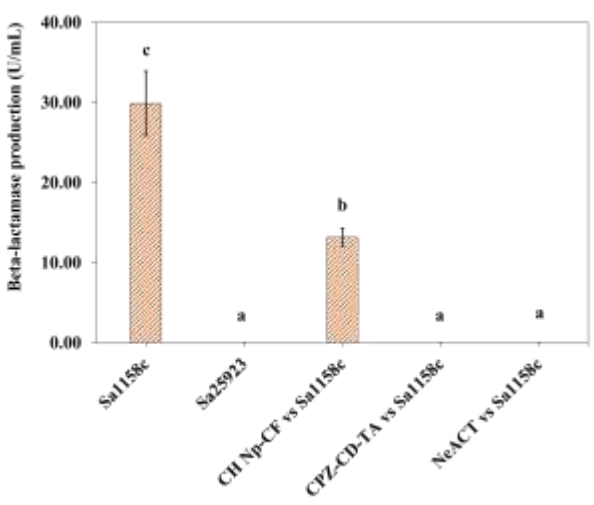

Figure 5.4. Antibacterial mechanism of action of the particles against Sa1158c. (a-b) Efflux pump inhibition property of the particles. Sa1158c culture was subjected to a sub-lethal concentration of the particles followed by a sub-lethal dosage of EtBr. The cells were harvested, washed, and transferred to a 96-well plate. Glucose was added, and EtBr efflux was monitored at an excitation/emission wavelength of 530/590 nm using a plate reader. A single exponential decay equation was used to determine the time-dependent efflux of EtBr. The time taken by the cells to extrude 50% of the EtBr was denoted as $t_{efflux50\%}$. **(c-d)** Beta-lactamase enzyme inhibition property of the particles. Sa1158c culture was exposed to sub-lethal concentrations of the particles were incubated for 18 h. The cells were maintained at 1.0 McFarland standard, harvested, and washed.

The suspension underwent high centrifugation, and the cell-free extract containing beta-lactamase enzyme was collected. Nitrocefin was added to the cell-free extract, and the color change was monitored in kinetic mode at 490 nm for 15 mins using a plate reader. Average values plotted in the table and graph with different alphabets indicate a significant difference *($p < 0.05$)*.

Sa1158c has shown resistance to CF, as previously mentioned (Majumder, Sackey, et al., 2023). At a sub-lethal dosage of CF (10.41 µg/mL) and CH Np-CF (20.83 µg/mL), the beta-lactamase enzyme production was 30±4.00 U/mL and 13.20±1.13 U/mL, respectively, suggesting that the primary mode of resistance shown by Sa1158c was through hydrolyzation of CF. Notably, a sub-lethal dosage of CPZ-CD-TA and NeACT showed a beta-lactamase inhibitory effect. For instance, no detectable enzyme production was observed when Sa1158c was exposed to CPZ-CD-TA (of 83.33 µg/mL) and NeACT (of 1.30 µg/mL) **(Figures 5.4c and 5.4d)**. It was evident that CPZ-CD-TA in NeACT has contributed to inhibiting beta-lactamase enzyme.

The ability of the nanoparticles to restrict biofilm formation was verified. CPZ-CD-TA, CH Np-CF, and NeACT inhibited 50% biofilm formation at 9.73, 69.14, and 0.45 µg/mL, respectively **(Figure 5.5a)**. While CPZ-CD-TA wasn't much effective in reducing (~3.18 $\log_{10}$ reduction) Sa1158c biofilms below 125 µg/mL, NeACT (at 3.91 µg/mL), and CH Np-CF (at 62.5 µg/mL) showed ~3.38 $\log_{10}$ and ~3.70 $\log_{10}$ reduction, respectively **(Figure 5.5b)**. To investigate the penetration and accumulation of FITC-labelled NeACT (coding green), a sub-lethal dosage (20.83 µg/mL or 1/3rd of FITC-NeACT MIC value against Sa30) was subjected to the biofilms of RFP-tagged Sa30 (coding red). Compared to untreated control, a significant reduction in biofilm biomass was evident **(Figure 5.5c-f)**. Moreover, Z-stack images suggested the accumulation and penetration of NeACT in Sa30 biofilms **(Figure 5.5e-f)**.

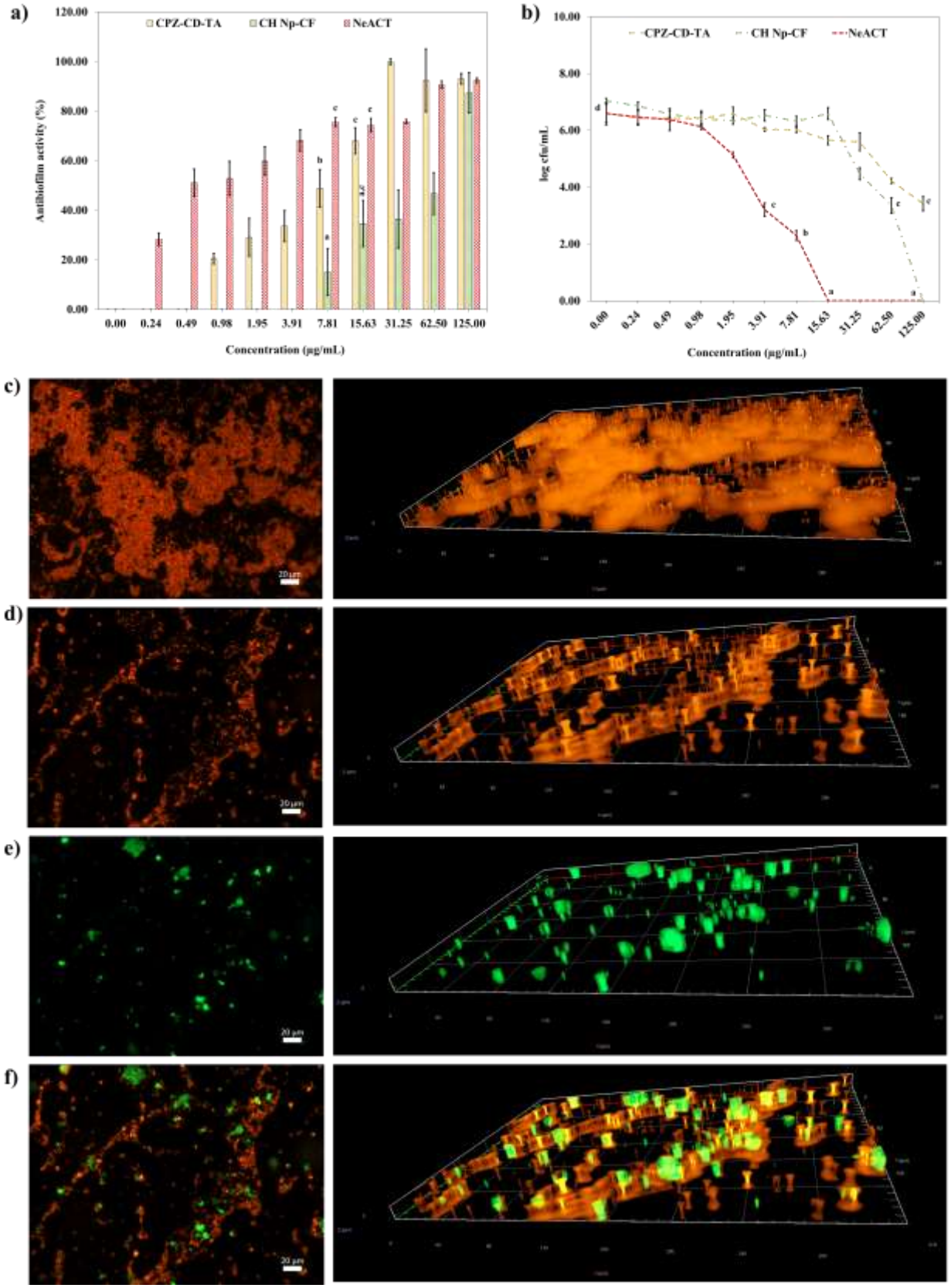
a)
CPZ-CD-TA
CH Np-CF
NeACT
Antibiofilm activity (%)
120.00
100.00
80.00
60.00
40.00
20.00
0.00
0.00 0.24 0.49 0.98 1.95 3.91 7.81 15.63 31.25 62.50 125.00
Concentration (µg/mL)
b)
CPZ-CD-TA
CH Np-CF
NeACT
log cfu/mL
10.00
8.00
6.00
4.00
2.00
0.00
0.00 0.24 0.49 0.98 1.95 3.91 7.81 15.63 31.25 62.50 125.00
Concentration (µg/mL)
c)
d)
e)
f)
20 µm

Figure 5.5. Mechanism of action of the particles against *S. aureus* biofilms. (a) Antibiofilm activity of the particles. Incremental concentrations of the particles were suspended in TSB media containing Sa1158c culture. After 48 h of incubation, the media was removed, 99% methanol was added, wells were washed gently, and resuspended with CV solution. The plates were incubated for 2 h, washed, and acetic acid (33%) was added. The biofilm biomass was quantified by measuring the absorbance at 570 nm. **(b)** Inhibition of matured biofilms by the particles. Matured biofilms formed after 24 h of incubation were exposed to incremental concentration of the particle in a 96-well plate. The plate was incubated for 24 h. The biofilms were collected, and the CFU was enumerated using the drop plate culturing method. Average values plotted in the graph with different alphabets indicate a significant difference *($p < 0.05$)*. **(c-f)** Epifluorescence and Z-stack images of **(c)** untreated RFP-tagged Sa30 biofilms, **(d)** treated RFP-tagged Sa30 biofilms, **(e)** FITC-NeACT signal in Sa30 biofilms, and **(f)** overlapped signals of FITC-NeACT penetrating RFP tagged Sa30 biofilms. A sub-lethal dosage of FITC-NeACT was exposed to matured biofilms of RFP-tagged SA30. Cell Discoverer 7 was used to capture epi-fluorescence images of the biofilms (coding red at 583 nm) and FITC NeACT (coding green at 519 nm). Z-stack images of different layers were constructed.

5.3.5. Efficiency of NeACT against internalized *S. aureus* in Caco-2 cells

The efficiency of NeACT against internalized pathogens was examined in the Caco-2 cells model of intracellular infection, where the Caco-2 cell line was used as model epithelial cells. No cytotoxicity was detected for the tested particles (NeACT, CH CF-Np, CPZ-CD-TA, CH Np, and CD Np) in Caco-2 cells, as 100% viability was observed at 250 µg/mL of the particles **(Figure 5.6a)** (the highest dose tested). NeACT showed a significant reduction in intracellular Sa1158c **(Figure 5.6b)**. For instance, at the MIC value of 3.9 µg/mL, NeACT showed a 3.27 $\log_{10}$ reduction *($p<0.05$)* of internalized Sa1158c from the Caco-2 cells. Similarly, at 7.81 and 15.62 µg/mL, NeACT reduced intracellular Sa1158c colonization by 4.49 $\log_{10}$ and 7.01 $\log_{10}$, respectively.

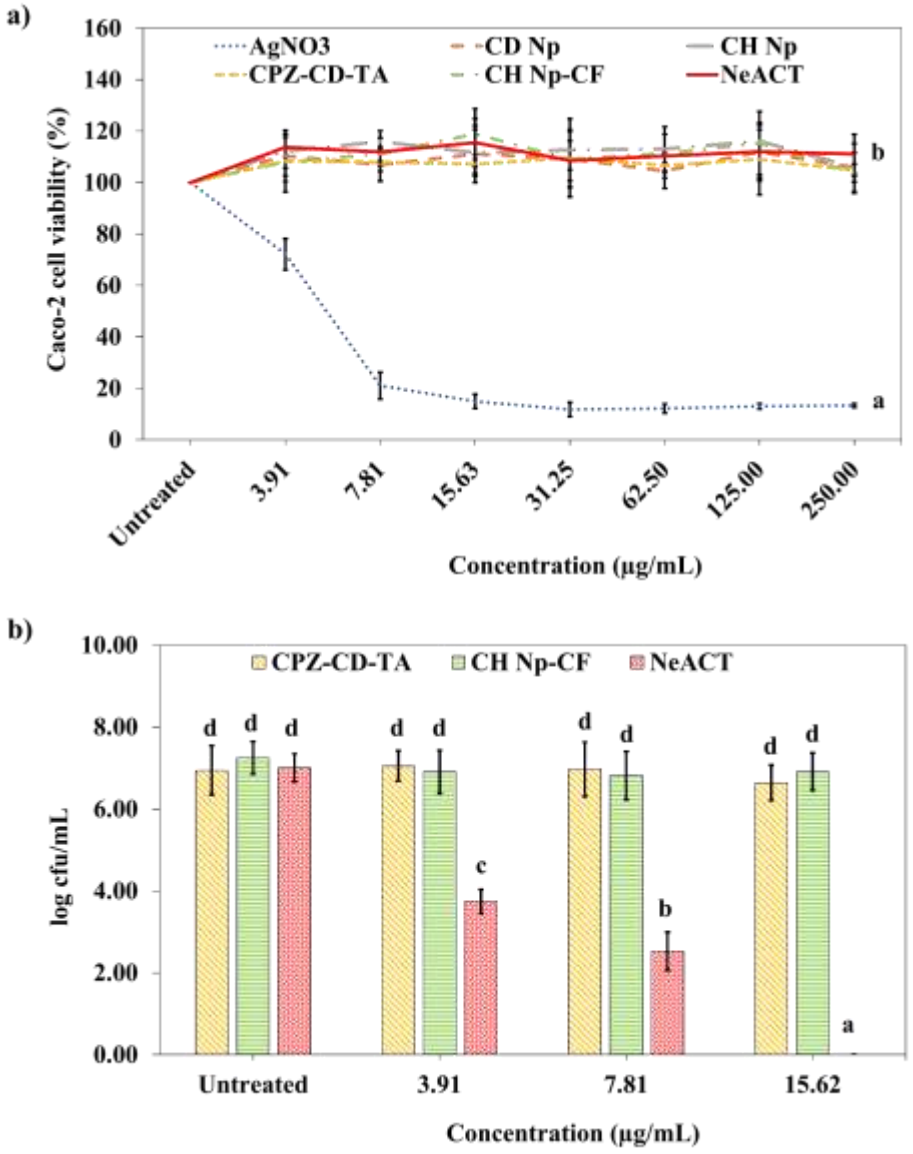

Figure 5.6. Cytoxicological assessment and intracellular infection remediation study in human intestinal epithelial Caco-2 cells. (a) Cytotoxicity of the particles in Caco-2 cells. Confluent cells (2×10^4 cells/well) were exposed to an incremental concentration of the particles in DMEM media in a 96-well plate. After 24 h of incubation, resazurin was added to the wells, and the plate was incubated for 4 h further. Fluorescence intensity was measured at 530/590 (excitation/emission). **(b)** Intracellular Sa1158c remediation efficiency of the particles. Confluent Caco-2 cells were exposed to Sa1158c culture and incubated in a 96-well plate for an hour. The cells were washed, subjected to gentamicin, and incubated for 30 mins. The extracellular gentamicin was washed, and the plate was incubated with DMEM for 4 h. Incremental concentrations of the particles were added to the wells and incubated for 24 h. Further, the cells were washed and lysed using Triton X. Drop culture method was used for CFU enumeration of viable intracellular Sa1158c. Average values plotted in the graph with different alphabets indicate a significant difference *($p < 0.05$)*.

5.3.6. *In vivo* efficiency of NeACT on CD-1 mice model of mastitis infection

CD-1 lactating mice were used as a mastitis infection model to evaluate the consequences of infection and NeACT efficiency. A 7.4 $\log_{10}$ Sa1158c CFU/g of tissue was detected from mammary glands without treatment **(Figure 5.7a)**. As expected, CPZ-CD-TA had no effect on Sa1158c inhibition, while CH Np-CF (at 78 µg/gland) showed a significant ~3.44 $\log_{10}$ Sa1158 reduction. NeACT showed a superior *($p<0.05$)* remediation of Sa1158c from the mammary gland compared to all control groups. For instance, a low dose of 78 µg/gland and 39 µg/gland of NeACT showed ~5.13 $\log_{10}$ (>99.999%) and ~4.46 $\log_{10}$ (>99.99%) Sa1158c reduction, respectively, from mice mammary gland. **Figures 5.7b and 5.7c** are representative images of infected mammary glands without and with NeACT treatment, respectively. In the untreated mammary gland, Gram staining revealed the presence of Sa1158c (0.5-1.0 µm size, cocci-shaped) in grape clusters, pairs, or short chain morphology within a polymorphonuclear leukocyte (PMN) cell, an observation that was in par with previous report (Brouillette, Grondin, et al., 2004). On the contrary, almost no bacteria were detected from the gland after NeACT treatment.

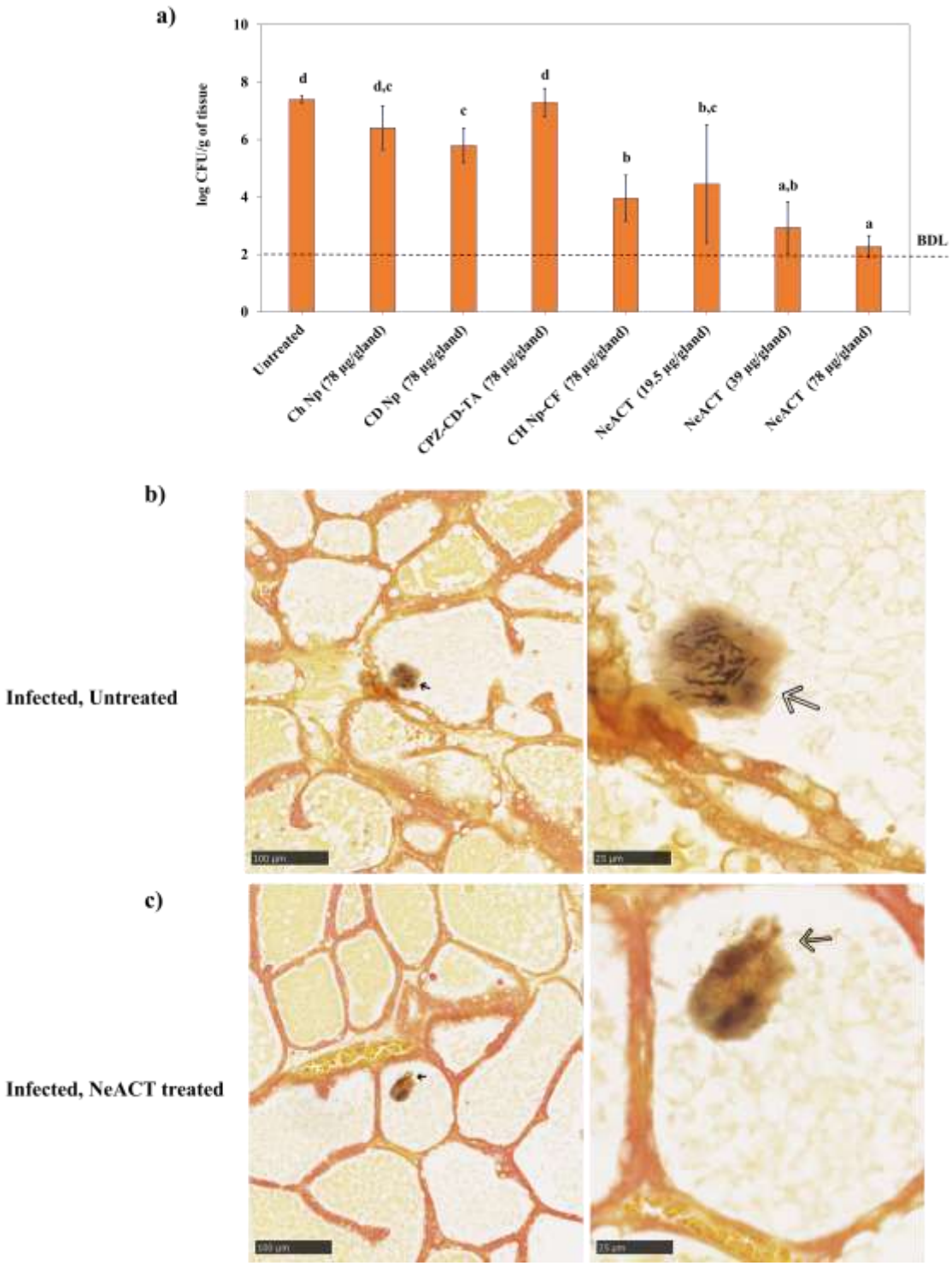

Figure 5.7. ***In vivo*** **antibacterial efficiency of the particles in CD-1 lactating mice model of bovine mastitis infection. (a)** Sa1158c infection remediation efficiency of the particles from CD-1 lactating mice mammary glands. Sa1158c of 100-125 CFUs were injected into the lactiferous duct of CD-1 lactating mice. Certain concentrations of the particles were directly injected into the mammary glands previously infected. After 14 h of incubation, mice were humanely euthanized,

and mammary glands were harvested and homogenized. CFU counts were obtained from mammary gland homogenates on TSA plates. The detection limit was approximately 200 CFU/g of mammary glands. Average values plotted in the graph with different alphabets indicate a significant difference *($p < 0.05$)*. Representative images of Gram-stained **(b)** untreated but infected mammary glands and **(c)** treated and infected mammary glands. Arrows indicated the presence of Sa1158c. Mammary glands were fixed in 4% PFA, dehydrated, and embedded in paraffin. Gram staining was performed by the Electron Microscopy and histology platform at the Université de Sherbrooke.

H&E and Masson's trichrome staining were performed on mammary tissues to examine PMN infiltration, morphological and cellular alternations. No inflammation and negligible PMN infiltration (as the large dark purple spheres with a multi-lobular nucleus, indicated with black arrows in **Figure 5.8a-d**) or lesions in the supportive connective tissue were observed in the untreated noninfected tissues and NeACT-treated noninfected tissues. Adipocytes (indicated with red arrows in **Figure 5.8a-h)** were evident in all the tissues as signet-shaped cells, with a nucleus at the periphery with visible fat droplets and a thin layer of cytoplasm. The pink staining within alveoli represented milk components (Sharp, Lefevre, Brennan, & Nicholas, 2007). Compared to NeACT-treated infected tissues, collapsed alveoli and necrotic areas were detected in untreated infected tissue. Moreover, PMN infiltration (indicated with black arrows in **Figure 5.8e-h**) was significantly evident in the connective tissue and intraluminal space of the untreated infected tissues.

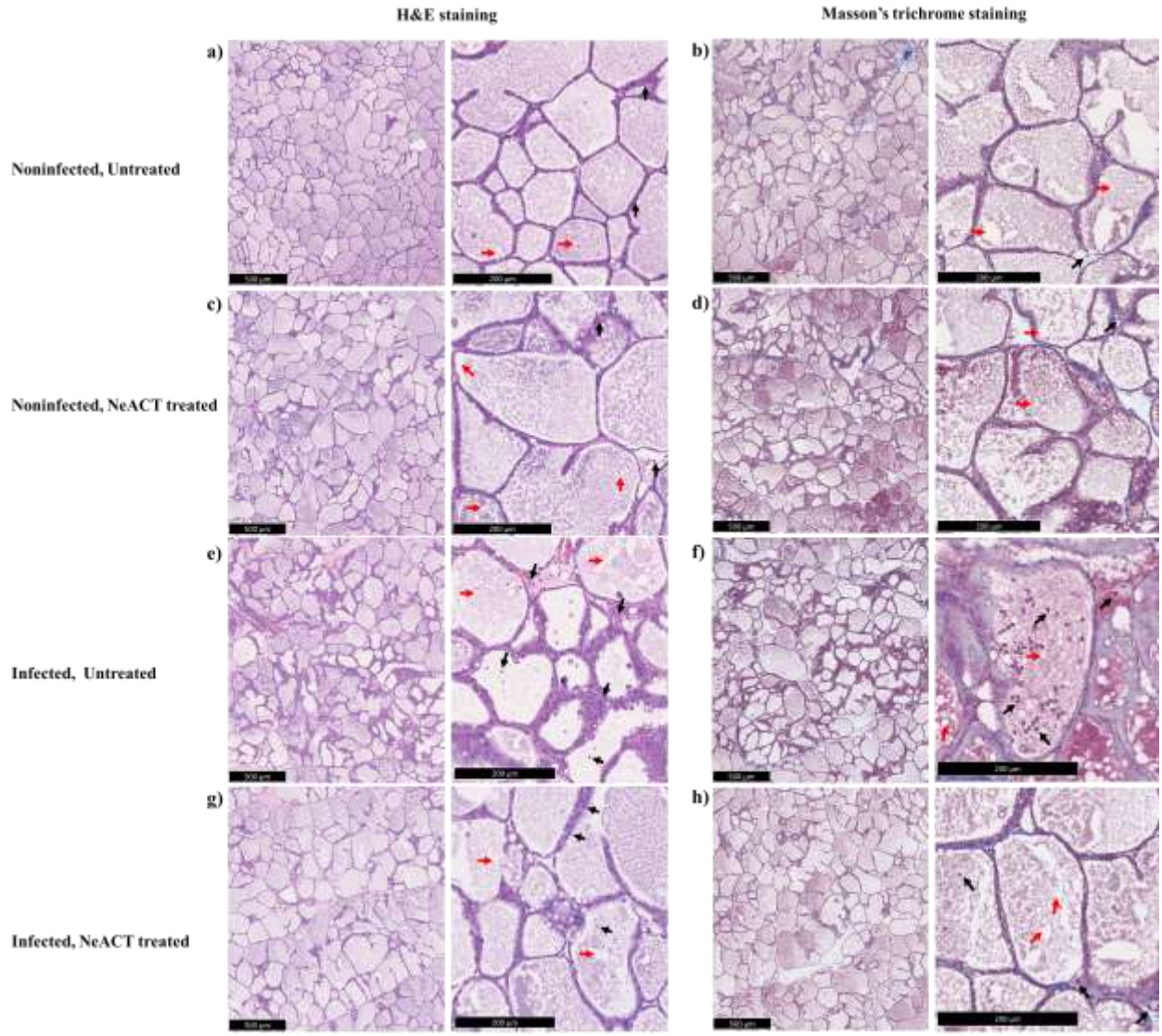

Figure 5.8. Histopathological analysis of CD-1 mice mammary tissue. (a) H&E staining and **(b)** Masson's trichome staining of noninfected and untreated mammary tissue. **(c)** H&E staining and **(d)** Masson's trichome staining of noninfected but NeACT-treated mammary tissue. **(e)** H&E staining and **(f)** Masson's trichome staining of infected but untreated mammary tissue. **(g)** H&E staining and **(h)** Masson's trichome staining of infected and NeACT-treated mammary tissue. The mammary glands were fixed in 4% PFA, dehydrated, and embedded in paraffin. Tissue preparation, embedding, and coloration were performed by the Electron Microscopy and histology platform at the Université de Sherbrooke. The black and red arrows denote the PMN infiltration and adipocytes, respectively.

5.4. Discussion

In this research, we designed and tested a novel NeACT comprised of ceftiofur (CF)-loaded chitosan nanoparticles (CH Np) conjugated with chlorpromazine (CPZ) and tannic acid (TA)-loaded cyclodextrin nanoparticles (CD Np). NeACT demonstrated exceptional colloidal stability, biocompatibility, and slow-release properties of the payloads. Due to the synergistic action against mastitis MRSA pathogen Sa1158c, we observed a significant reduction in the effective concentration of CF in NeACT. NeACT inhibited efflux pump, beta-lactamase enzyme, and biofilm-forming abilities of Sa1158c. Testing in epithelial cell model and CD-1 lactating mastitis mice model showed no signs of toxicity while it effectively eliminated Sa1158c infection. Overall, NeACT possesses promising therapeutic potential for the treatment of BM.

Previously, our group reported the MDR bovine mastitis pathogen, Sa1158c, to show resistance against CF (Majumder, Sackey, et al., 2023). Aligning with the United Nations' "one health" objective, one of the crucial aims of this current work was to reuse CF by improving its efficiency by applying nano-enabled combination therapy. As anticipated, we observed a synergistic action among CF, CPZ, and TA. This is ascribed to the complementary mode of action of the selected antibiotic-adjuvant combination. Accordingly, CF inhibits bacterial cell wall synthesis, while the adjuvant CPZ and TA complement CF by inhibiting efflux pump activity and destabilizing membrane potential, respectively (Brar et al., 2022; Majumder et al., 2022; Truchetti et al., 2014). CF has been approved by the US Food and Drug Administration (USFDA) and Health Canada, while CPZ has been approved by Health Canada for veterinary applications (*Summary report on antimicrobials sold or distributed for use in food-producing animals*, 2022; *Veterinary new drug*

list, 2000). TA has been approved by the FDA as a safe food additive (Jing, Xiaolan, Yu, Feng, & Haifeng, 2022).

We examined the release profile of CF, CPZ, and TA from NeACT every 24 h for seven days. A 50% release of all the payloads was observed within 2-3 days. The release of CPZ and TA from CD Np is probably through dissociation due to dilution (Stella, Rao, Zannou, & Zia, 1999), while the release of CF from CH Np is probably through diffusion or shrinkage, causing release due to attractive electrostatic interaction between anions and chitosan matrix at a higher pH (Herdiana, Wathoni, Shamsuddin, & Muchtaridi, 2022; Katas, Hussain, & Ling, 2012). Compared to previous studies that reported a much faster release of drugs (within 6 to 12 h) from polymeric nanoparticles (Herdiana et al., 2022), our observations suggested a slow release behavior of payloads from the nanocarriers. One of the most significant drawbacks of CF is its elimination before 12 h after intramammary infusion as they get rapidly metabolized (Kang et al., 2018). The slow release of payloads from NeACT could contribute significantly to improving the retention time of CF in the mastitis microenvironment.

NeACT showed excellent antibacterial efficiency *in vitro* against Sa1158c at a dosage of only 3.9 µg/mL. Recently, we have reported Sa1158c to display efflux pump activity, beta-lactamase enzyme production, and strong biofilm-forming ability (Majumder, Sackey, et al., 2023). Genomic studies revealed genes associated with major facilitator superfamily (MFS) efflux pumps (*norA*, *norB*, *tetM*, etc.), cephalosporin resistance (*blal*, *blaR*, *blaZ*, *mecA*, etc.), and fibronectin-binding proteins (*fnbA*, *fnbB,* etc.) (Majumder, Sackey, et al., 2023). Therefore, the efficiency of NeACT was tested against these resistance mechanisms. The increase in PI fluorescence suggested that NeACT disrupted the Sa1158c cell membrane. Interestingly, a significant increase in width was noticed among the Sa1158c cells under NeACT stress. Cell wall-targeting antibiotics such as CF

that bind to penicillin-binding proteins (PBPs) and inhibit peptidoglycan synthesis affect septal cell wall synthesis, forming wider cells with a lower surface-to-volume ratio (Ojkic, Serbanescu, & Banerjee, 2022). A sub-lethal dose of NeACT significantly inhibited Sa1158c efflux and beta-lactamase enzyme activity. The penetration of antimicrobials into the dense protective layer of biofilms is crucial for their eradication. NeACT was highly effective in restricting biofilm growth and inhibiting matured biofilms by accumulating and penetrating the biofilm layer.

The superior efficiency of NeACT against such resistance mechanisms of Sa1158c is ascribed to the complementary mode of action of the antibiotic-adjuvant combinations. CF is considered bactericidal as it binds to PBPs and interferes with cell wall enzymes, leading to cell lysis and death (Zeng & Lin, 2013). Although CPZ and TA are not known to inhibit bacterial growth at low dosages, they contribute significantly to anti-efflux, anti-beta-lactamase, and antibiofilm properties, as observed in this study. TA is a strong electron donor that interferes in the hydrolysis of ATP, causing an increase in bacterial membrane permeability, thus enabling passage for NeACT through cell wall. The free phenolic hydroxyl groups in TA affect bacterial enzymatic activity *via* covalent or non-covalent linking (Villanueva et al., 2023). Moreover, TA has been reported to disrupt peptidoglycan formation, iron chelation, and fatty acid synthesis (Villanueva et al., 2023). CPZ complements the effect of TA and CF by crippling the function of specific drug-resistance transporters and multi-drug MFS efflux pumps and exhibiting conformational changes in efflux protein structures (S. George et al., 2019; Seukep, Kuete, Nahar, Sarker, & Guo, 2020). CPZ has also been reported to interact with several membrane-active proteins, including FtsA and Fabl, and exhibit strong anti-biofilm action (Nistorescu et al., 2020). Moreover, CPZ has been reported to disrupt the sensor-inducer protein of the *S. aureus* cell membrane and suppress *bla* and *mec* gene expression, which play a predominant role in producing resistance factors such as PBP2a and β-lactamase (Kong et al., 2016).

One of the prominent virulence characteristics that enable *S. aureus* to persist in mammary tissue is their ability to invade and reside as an intracellular pathogen (Majumder, Sackey, et al., 2023). Therefore, we checked the efficiency of NeACT in combating intracellular Sa1158c in Caco-2 cells. NeACT showed no cytotoxicity and excellent remediation of intracellular Sa1158c. Earlier, our groups reported that pristine CF and CPZ were marginally effective against intracellular pathogens (Brar et al., 2022; Majumder, Sackey, et al., 2023). Therefore, the superior outcome observed in NeACT can be attributed to the combined impact of the drug molecules and the favorable interaction and absorption of NeACT by the Caco-2 cells. To ensure efficient cell interaction and intracellular transmission of a nanoparticulate system, a positive zeta potential, such as that observed in NeACT, is crucial (Nasti et al., 2009). Previous studies have shown that the endocytic uptake of CH Np is significantly influenced by clathrin-mediated translocation (Noha M Zaki, Nasti, & Tirelli, 2011). CD Np undergoes macropinocytosis as the primary uptake mechanism in Caco-2 cells (Rusznyák et al., 2021). It's likely that NeACT utilizes a sequential release mechanism for its payloads. According to Zaki *et al.*, delivering a high initial dose of antimicrobials inside cells followed by a sustained antibiotic release could be an effective approach for treating intracellular infections. This method reduces relapses and ensures efficient treatment (N. M. Zaki & Hafez, 2012).

Although promising preclinical studies may offer hope, animal clinical trials reveal that nearly 30% of drug candidates fail due to toxic effects, while 60% do not deliver the desired results. This underscores the significance of exploring the efficacy of NeACT in treating BM through *in vivo* research. Recent studies demonstrate that intraductal CD-1 lactating mice can accurately replicate bovine CNS mastitis, thereby serving as a valuable adjunct for *in vivo* research. (Breyne et al., 2015). CD-1 lactating mice were used to investigate the effects of mastitis infection, evaluate the efficacy of NeACT treatment, and assess potential toxic and immune responses. NeACT

demonstrated excellent remediation of Sa1158c infection by ~5.13 $\log_{10}$ and ~4.46 $\log_{10}$ in the mammary gland at a dosage of only 78 and 39 μg/gland, respectively. NeACT exhibited a slow-release behavior of the payloads, leading to improved drug retention in the mammary gland of mice and ultimately resulting in superior antibacterial efficacy. Histopathological examination suggested that the exposure to NeACT neither induces pro-inflammation and immune and toxic responses nor impacts cell and tissue morphology. An excessive amount of cell infiltration along with classical immune cell activation was observed in infected mouse mammary glands that led to tissue damage. Meanwhile, a minimal inflammatory cell infiltration, as observed in NeACT-treated and infected mammary glands, is a crucial element in the healing process. Several studies have demonstrated the potential anti-inflammatory and wound-healing properties of TA (Chen et al., 2019; Z. Tong, He, Fan, & Guo, 2022). The exact mechanism through which TA exerts these effects is not yet fully understood. However, scientific reports suggest that TA may stimulate healing by modulating growth factors and activating the extracellular signal-regulated kinase 1/2 (ERK1/2) pathway (Chen et al., 2019). Previous research has demonstrated that CH exerts anti-inflammatory effects by modulating macrophage polarization from the pro-inflammatory M1 to the anti-inflammatory M2 state (Jhundoo et al., 2020). In addition, it promotes an immune response that leads to the secretion of anti-inflammatory mediators, such as interleukin-1 receptor antagonist (IL-1ra) and interleukin-10 (IL-10) (Jhundoo et al., 2020). Previously, the CD was found to effectively decrease the concentration of various pro-inflammatory cytokines, including interleukin-1 alpha (IL-1α), tumor necrosis factor (TNF), and interleukin-6 (IL-6) (Lucia Appleton et al., 2021).

5.5. Conclusion

BM caused by microbial infections is one of the costliest diseases in the dairy industry worldwide. The failure of conventional treatment and management strategies demands alternative approaches. NeACT that harnesses the potential of nano-delivery platforms for antibiotic/adjuvant combination of synergistic functions holds promise in effective BM treatment. In this study, a NeACT was developed constituting CF-loaded CH Np conjugated with CPZ and TA-loaded CD Np. NeACT demonstrated exceptional stability, biocompatibility, slow-release behavior of payloads for efficient delivery, and successfully remediated intracellular and mastitis infections of multi-drug resistant *S. aureus*. By implementing NeACT, the effective concentration of CF, CPZ, and TA was reduced significantly. Overall, NeACT offers a cost-effective, eco-friendly, and therapeutically superior solution to traditional approaches for treating BM. In the future, clinical studies need to be conducted to assess the efficacy, safety, and tolerability of NeACT in treating mastitis in cattle. The fate of NeACT after achieving its therapeutic goals in the bovine mammary gland needs to be extensively studied. This includes evaluating the NeACT degradation, metabolism, and impact on the host and the environment. To accurately gauge the long-term sustainability and viability of NeACT, conducting a thorough life cycle assessment (LCA) is imperative. This assessment would take into account all stages of the NeACT life cycle, from the sourcing of raw materials to production, distribution, and disposal, providing a comprehensive overview of the environmental impact of NeACT.

Chapter 6

General Discussion, Conclusion, and Future Perspectives

6.1. General Discussion

Bovine Mastitis (BM) is a pathogenic disease manifested as inflammation of the mammary gland tissues primarily by microbial infection. This condition can lead to reduced milk production, treatment failures, and financial losses of over $2 billion and $794 million in the USA and Canada, respectively. Given the prevalence of this disease and the increase in AMR, it is crucial to explore alternative control strategies that are both cost-effective and sustainable. A deeper understanding of the factors involved in BM, from both the pathogen and host perspectives, is necessary to achieve this. Chapter 2 meticulously scrutinized host-pathogen-environment factors associated with BM. Furthermore, it delved into how these distinct factors can be leveraged to design a potent NeACT for BM treatment. It is crucial to identify and consistently monitor the mastitis-causing agents for AMR and virulence to design custom-tailored treatment approaches.

The interactions between pathogens, hosts, and the environment are complex and multifactorial. The interplay of these factors significantly influences the development and progression of infectious diseases (Engering, Hogerwerf, & Slingenbergh, 2013). The host-related factors include the age of the animal, its lactation stage, breed, mammary gland anatomy, and immunological status. The host's immunological status and genetics play a critical role in the clearance or exacerbation of the infection. Pathogens interact with their hosts in various ways, such as invading host cells, producing toxins, and evading the host immune system. Pathogen-related

factors include microbial load, virulence, frequency of exposure, ability to invade tissues and adaptability, and the acquisition of AMR characteristics. Environmental factors, such as temperature, humidity, nutrient availability, population density, geographical distributions, and microbiota, can influence the survival of pathogens, their transmission, and the severity of the infection. Further, the type of milking machine used, hygiene measures, climate, season, management practices, and housing conditions also contribute to the onset and severity of BM. The frequency and severity of BM can vary significantly from one farm to another, depending on the complex interplay of these factors. Therefore, understanding of the intricate interplay between the host, pathogen, and environment is crucial for developing effective strategies for the prevention and treatment of BM.

BM can be classified into subclinical and clinical based on the symptoms. Subclinical BM is characterized by the presence of bacteria in the milk and high milk somatic cell count, without any visible signs of inflammation in the udder (Thorberg, Danielsson-Tham, Emanuelson, & Persson Waller, 2009). Clinical BM, on the other hand, is an inflammatory response of the mammary gland to bacterial infection and is accompanied by visible changes in the milk and udder, such as swelling, redness, heat, and pain (Majumder, Eckersall, & George, 2023). The subclinical BM is 15-40 times more prevalent than the clinical form. Subclinical BM causes 70-80% of the total financial losses as it is difficult to detect, shows persistence, affects milk production and quality, and harbors a reservoir of microorganisms that can transmit to other animals within the herd (Cobirka, Tancin, & Slama, 2020). The somatic cells serve as reliable indicators of both resistance and susceptibility of cows to subclinical BM. The contagious pathogens such as *S. aureus*, *Streptococcus agalactiae, etc.* generally exhibit the highest SCC increase, while environmental pathogens such as *E. coli*, *Klebsiella pneumoniae*, *etc.* cause less SCC elevation (Cobirka et al., 2020; Shaheen et al., 2016; Sugiyama et al., 2022). Contagious pathogens have the ability to use the

infected udder as a reservoir and spread from one cow to another during milking. These pathogens can then develop into chronic subclinical infections, which may also manifest as clinical cases (Sağlam et al., 2017). Such pathogens can possess multiple AMR and virulence traits that make treatment and BM management challenging. Thus, continuous investigation of such factors is a prerequisite before designing alternate treatment strategies.

In the first phase of this research (Chapters 3 and 4), I have thoroughly characterized libraries of *Escherichia coli* and *Staphylococcus aureus* isolates originating from Canadian dairy farms for AMR, AMR mechanisms, and virulence characteristics through phenotypic and genotypic profiling. The *E. coli* and *S. aureus* isolates used in this research were a part of the MPCC across Alberta, Ontario, Quebec, and the Atlantic provinces. Out of the 113 *E. coli* and 43 *S. aureus* isolates exposed against over 20 antibiotics of different classes, 28.31% and 13.95% were found to be resistant to at least one antibiotic (Majumder et al., 2021; Majumder, Sackey, et al., 2023). The observed rate of resistance in this research corroborated with the reports from previous studies (Saini, McClure, Léger, et al., 2012). Previously, Canadian *E. coli* and *S. aureus* isolates obtained from BM cases have undergone antimicrobial susceptibility testing (Saini, McClure, Léger, et al., 2012). However, this study had a more specific aim of identifying the genetic determinants that are responsible for AMR, which includes those that can be transmitted through horizontal gene transfer (J. H. Fairbrother et al., 2015). Several *E. coli* isolates demonstrated β-lactamase enzyme activity and carried $bla_{\text{CMY-59}}$, $bla_{\text{TEM-1B}}$, and $bla_{\text{CARB-3}}$ genes. The *cmy* and *tem* genes from *E. coli* isolates were observed from the colostrum and feces of a few Holsteins dairy cattle in New Brunswick, Canada (B. Awosile et al., 2018; B. B. Awosile et al., 2017). These results suggest that the presence of *cmy* and *tem* genes in dairy cattle isolates may be more widespread than previously thought. Further research is necessary to explore the prevalence of these genes in cattle populations and their potential impact on Canadian veterinary and public health. Our research has uncovered several significant

emerging resistance genes, including genes for tetracycline resistance (*tetA, tetB, tetC*) and aminoglycoside resistance (*aadA2*). Few *E. coli* isolates showed resistance to cephalosporins and colistin without harboring ESBL or plasmid-mediated AmpC β-lactamase genes, MCR genes, and plasmid-mediated colistin determinants genes. This was probably owed to complex mechanisms of efflux pump activity by such isolates. Therefore, the evaluation of efflux pump-mediated resistance to clinically important drugs, such as β-lactams and colistin, is essential to gain a better understanding of the emergence of AMR and its potential increase in dairy farms. Notably, some strains of *E. coli* showed resistance to β-lactam and cephalosporin antibiotics, even though they did not have β-lactamase enzyme or efflux activity. This resistance may be due to mutations in the promoter regions of the chromosomal *E. coli* AmpC gene. It could also be due to other mechanisms, such as limiting the uptake of hydrophilic drugs or modifying the drug targets (Reygaert, 2018). Specifically, the *S. aureus* isolates, Sa1158c, showed an inducible ß-lactamase enzyme activity and carried *blaI, blaR,* and *blaZ* genes. In addition, the *mecA* gene, found in Sa1158c, is responsible for encoding the low-affinity penicillin-binding protein (PBP2a). It also plays a crucial role in conferring resistance towards ß-lactam antibiotics, particularly methicillin, and is regarded as the gold standard for MRSA confirmation (X. Hong et al., 2016). Although only a few *S. aureus* isolates showed AMR, genes encoding aminoglycoside-modifying enzymes (*aac(6')*, *aac(3')*, and *aph(3')*) and lincosamide nucleotidyl transferases (*lnuA*) were evident in them. Several *S. aureus* isolates carried *tetK* and *tetM,* and all the test isolates were identified with the major facilitator superfamily (MFS) of transporters such as *tet(38)*, *NorA*, and *NorB* efflux genes. However, only 3 isolates out of 43 showed an active efflux pump. Although the focus of this investigation was not to pinpoint the exact reason for the failure of AMR genes to produce functional proteins and phenotype, our hypothesis suggests that gene mutations, the inability to detect antibiotic stress, and defective gene products may be potential factors that contribute to the inconsistency between the genetic makeup

of the isolates and their phenotypic characteristics (Ding et al., 2008; Poole, 2000). This warrants further exploration and investigation in future studies.

Hemolysis is a significant secretory virulence factor that has been reported to be produced by 20-50% of strains from BM (O. Dego, 2020). While, all *S. aureus* isolates exhibited either alpha or beta-hemolysin, 29.20% of *E. coli* isolates showed alpha-hemolysis production (Majumder et al., 2021; Majumder, Sackey, et al., 2023). The genomic analysis confirmed that the hemolysin phenotype was associated with the presence of genetic determinants HlyA/E/C/B/D. The hemolysins encoded by the *hly/hla* and *hlb* genes, which were present in the isolates, often contribute to cell signalling pathways that mediate various cellular processes, including cytokine secretion and inflammatory responses (L. Zhang et al., 2018). Interestingly, all *E. coli* and *S. aureus* isolates demonstrated biofilm-forming activity (Majumder et al., 2021; Majumder, Sackey, et al., 2023). They carried different sets of genes that confer biofilm formation, including those that encode adhesion, aggregation, c-di-GMP formation, stress inducer, and autoinducer-2. Our study identified the transcription factors *marA, soxS*, and *rob* in the *E. coli* isolates, which are known to play a critical role in mediating multi-drug resistance by up-regulating the expression of the AcrAB-TolC efflux pump (Duval & Lister, 2013). The *S. aureus* isolates carried *ica*ADBC locus, which is responsible for the production of polysaccharide intercellular adhesin (PIA), fibrinogen-binding proteins, clfA, and clfB, and fibronectin-binding proteins, fnbA, and fnbB which contribute significantly to biofilm formation. Interestingly, I found a positive correlation between biofilm formation and efflux pump activity in the *E. coli* isolates (Majumder et al., 2021). Therefore, efflux pump inhibitors could present a promising avenue for targeting biofilms, thereby providing an immense opportunity for the development of alternate therapies.

After the invasion, *E. coli* undergoes rapid multiplication, while *S. aureus* tends to adhere to the tissues that line the milk-collecting spaces in the bovine udder (Majumder, Eckersall, & George, 2023). Gram-negative bacteria like *E. coli* in mammary epithelial cells instigate inflammation by inducing higher levels of IL8 and TNF-α expression. This results in a host immune response that eventually eliminates pathogens (Burvenich et al., 2003; Jensen et al., 2013). In contrast, Gram-positive bacteria like *S. aureus* induce a weaker inflammation and host immune response, attributed to their ability to suppress NF-κB signalling (Majumder, Eckersall, & George, 2023). This ability of *S. aureus* to facilitate their host epithelial cell invasion, persistence, and chronic infections is significant and contributes remarkably to the failure of BM treatment, as observed in Chapter 4. Reports have also suggested the zoonotic potential of mastitis *S. aureus* (Maity & Ambatipudi, 2021; S. Park et al., 2022). Sa1158c belongs to ST8, a human clone, which has been known to cause BM in dairy cows and may be capable of spillover and transmission under certain selection pressures, according to speculation (S. Park et al., 2022). Therefore, along with analyzing the prevalence of AMR and virulence characteristics in *S. aureus*, I delved into their pathogenic translation within human infection models: human intestinal epithelial Caco-2 cells and *Caenorhabditis elegans*.

All tested *S. aureus* isolates displayed the ability to colonize and infect Caco-2 cells intracellularly, leading to cell death (Majumder, Sackey, et al., 2023). This intracellular invasion and infection were likely facilitated by cysteine proteases, fibronectin bridging, and staphylococcal hemolysin, as these genes were detected from genotype profiling of the isolates (Kwak et al., 2012; B. Sinha et al., 2000; Stelzner et al., 2021). Microscopic images indicated the colonization of *S. aureus* in the pharynx, intestine, rectum, and anus of *C. elegans* (Majumder, Sackey, et al., 2023). This infection led to a significant decrease in worm survivability. Our research findings were consistent with earlier reports of *S. aureus* causing enterocyte effacement, lysis of intestinal epithelial cells, and body-wide invasion, resulting in the internal tissue degradation of *C. elegans*

(Irazoqui et al., 2010). The pathogenicity of the isolates in *C. elegans* was likely due to the production of alpha-hemolysin (hla), V8 protease (sspA), and overexpression of icaADBC locus (Sifri et al., 2003).

The efficacy of various antibiotics, namely aminoglycosides, cephalosporin, ß-lactam, tetracycline, and chloramphenicol, was evaluated for treating intracellular and intestinal infections in Caco-2 cells and *C. elegans*. These antibiotics were selected based on their frequent use in managing *S. aureus*-mediated BM and human infections. The high polarity and hydrophilic characteristics of kanamycin, streptomycin, and ampicillin rendered them ineffective in reducing bacterial colonization in the Caco-2 cells, as anticipated (Majumder, Sackey, et al., 2023). Although some antibiotics were relatively successful, none decreased bacterial colonization by more than 2.5 $\log_{10}$. Our observations indicate lower antibiotic efficacy against intracellular *S. aureus*, which is in agreement with existing literature (Bongers et al., 2019; Jacobs & Wilson, 1983; Naess et al., 2011). Based on microscopic images, the accumulation of *S. aureus* in *C. elegans* was reduced after treatment with aminoglycoside, ampicillin, and chloramphenicol. However, this was insufficient to prevent *S. aureus* from multiplying and causing infection and cell death, as indicated by the life-span assay. Tetracycline and ceftiofur were more effective in treating *S. aureus*-mediated intestinal infection in nematodes. Aminoglycosides and ß-lactam antibiotics were ineffective, likely due to their poor ability to penetrate the *S. aureus* cells inside the intestinal epithelial cells of *C. elegans*. Interestingly, antibiotics that showed effectiveness against bacteria in the Kirby Bauer disc diffusion assay were not efficient in either of the infection models. This difference in antibiotic effectiveness highlighted the importance of testing mastitis pathogens in organism models, as differential pharmacokinetics can affect their efficacy against intracellular bacteria.

I identified Sbi, Cap, and AdsA proteins in all the *S. aureus* isolates which are associated with bovine immune invasions (Echániz-Aviles et al., 2022; Gonzalez et al., 2015; Thammavongsa et al., 2009). The low prevalence of PTSAg gene-positive *S. aureus*, along with the absence of virulence markers (*lukE, lukM*) and human immune evasion cluster-associated genes (*lytN, fmhC, dprA, chp, sak,* and *scn*), suggests a low risk of zoonotic infection. However, it is worth noting that *S. aureus* is an opportunistic pathogen that may disseminate mobile genetic elements across various lineages under specific environmental pressures (S. Park et al., 2022). Research has demonstrated that the SOS response, induced by antibiotic pressure, can promote the horizontal transfer of pathogenicity islands in *Staphylococci* (Beaber et al., 2004; Úbeda et al., 2005).

Treatment strategies for BM often involve giving antibiotics through intramammary infusion or parental administration, regardless of the cow's health status. This is a common practice in high milk-producing countries such as the USA, Canada, the UK, and India (Majumder, Eckersall, & George, 2023). As observed from our research, these pathogens have intrinsic or acquired resistance mechanisms, which could limit drug uptake, modify or inactivate a drug, or induce efflux/beta-lactamase activities, leading to treatment failure (Majumder, Eckersall, & George, 2023; Majumder et al., 2021; Majumder, Sackey, et al., 2023). Even commercially available vaccines for *S. aureus* BM have not shown protection against reinfection (Majumder, Eckersall, & George, 2023). Therefore, there is a need for cost-effective, sustainable alternate strategies that are efficient in treating BM. NeACT designed to deliver multiple drugs with antibacterial synergistic effects, offer promise in addressing these challenging infections caused by antibiotic-resistant bacteria.

In the final phase of the thesis (Chapter 5), I developed an alternate strategy for treating BM, applying nanotechnology-enabled combination therapy. Combination therapy involves combining antibiotic and/or adjuvant molecules with synergistic antibacterial properties owing to their common

or complementary interactions. This strategy has been implemented in both biomedical and agricultural settings. However, its effectiveness has been limited due to issues such as poor drug bioavailability, cytotoxicity, stability, and the risk of overdosing (Majumder, Eckersall, & George, 2023). Nevertheless, I posited that nanotechnology-enabled approaches could address these challenges. Nanomaterials, due to their nano size and multifunctionality, offer unparalleled benefits for targeted drug delivery across biological barriers (Brar et al., 2022; S. George et al., 2019; Majumder et al., 2022). In complex tissue environments, nanomaterials could be utilized to co-deliver multiple drug molecules with synergistic effects and complementary antibacterial mechanisms, thereby enhancing the overall pharmacological action of the payload (Majumder, Eckersall, & George, 2023).

To synthesize NeACT, I designed a unique nanocomposite constituting CF loaded CH Np conjugated with CPZ and TA loaded CD Np. The careful selection of antibiotics was critical in achieving the United Nations' "one health" objective. The aim was to enhance the effectiveness of antibiotics against bacteria that are often resistant by combining them with other adjuvants. CF, a cephalosporin antibiotic that hinders bacterial cell wall synthesis, has been extensively used in subclinical BM (Kang et al., 2018). Studies have reported that the cure rate of multi-drug resistant *S. aureus* infections by CF could also be as low as 0% as it readily gets metabolized and eliminated from the mammary gland, resulting in poor retention time (Kang et al., 2018). Hence, I used CF as the primary antimicrobial, while CPZ and TA were selected based on their complementary action, such as by inhibiting efflux pump activity, destabilizing membrane potential, etc. (Brar et al., 2022; Majumder et al., 2022; Truchetti et al., 2014). Based on desirable drug delivery characteristics such as biocompatibility, low toxicity, low immunogenicity, ability to adhere to mucosal surfaces, and enhanced drug stability, CH Np and CD Np were used as the payload carriers. These unique attributes enable CH Np and CD Np to remain at drug absorption sites for extended periods,

enhancing drug penetration and enabling it to target intracellular pathogens. These properties make them excellent drug carriers in complex BM environments (Yadav et al., 2022).

As anticipated, the checkerboard assay implied synergism of the combination of CF, CPZ, and TA against MRSA Sa1158c, which I used as the test organism. This was most likely due to the complementary mode of action of the selected antibiotic-adjuvant combination. The FTIR spectra indicated the successful formation of CH Np and the association of CD Np, CF, CPZ, and TA in NeACT. The shifts observed in FTIR spectra of NeACT suggested that the payloads and nanocarriers interacted with each other, leading to the formation of hydrogen bonds. DLS analysis suggested a hydrodynamic size of NeACT to be around 539 nm. On the other hand, CPZ-CD-TA showed a much smaller hydrodynamic size of ~135 nm. The zeta potential of CPZ-CD-TA and CH Np-CF were -9.51 mV and +30.68 mV, respectively. Meanwhile, the zeta potential of NeACT was +21.69 mV, suggesting a conjugation of the CH Np-CF and CPZ-CD-TA through electrostatic interaction. Further, SEM analysis indicated aggregation of bigger CH Np-CF surrounded by smaller CPZ-CD-TA, forming NeACT with spherical morphology. The zeta potential of NeACT was close to +30 mV, suggesting sufficient repulsive forces and, thus, a desirable physical colloidal stability (Majumder et al., 2022). Positively charged nanomaterials such as NeACT provide immense advantages in combating complex infectious conditions. For instance, cationic nanocomposites could employ accumulation in bacterial cell walls with negatively charged peptidoglycan phosphopeptide molecules through electrostatic adsorption, interfere with metabolic processes or cause perforation, and exhibit membrane leakage (Lam et al., 2016). Cationic nanomaterials have been reported to interact with glycocalyx, the main component of *S. aureus* biofilms, and penetrate such thick biofilms (Kulshrestha, Qayyum, & Khan, 2017). Unlike negatively charged nanomaterials, positively charged polymeric particles show less interaction with opsonin proteins, thus limiting the chances of phagocytosis by macrophages (Oh & Park, 2014).

Further, cationic nanomaterials facilitate cellular interactions that influence endocytosis and endosomal escape, which is crucial to targeting intracellular pathogens (Aibani, Rai, Patel, Cuddihy, & Wasan, 2021; Nasti et al., 2009). I observed a 50% release of CF, CPZ, and TA from NeACT within the 2^{nd}-3^{rd} days while a 100% release by the 7^{th} day. According to our findings, the release of drugs from the nanocarriers is slower than previous studies have reported. For instance, Herdiana *et al*. reported the release of drugs from polymeric nanocarriers within a span of only 6 to 12 hours (Herdiana et al., 2022). NeACT showed excellent antibacterial efficiency against Sa1158c *in vitro*. NeACT destabilized *S. aureus* membrane integrity, inhibited efflux pump activity, ß-lactamase enzyme activity, and biofilm-forming ability of *S. aureus*. Microscopic images indicated the ability of NeACT to accumulate and penetrate *S. aureus* biofilms. One of our primary goals was to improve the efficiency of CF with combination therapy. With the application of NeACT, I significantly decreased the effective concentration of CF (by 25-fold), CPZ (>342-fold), and TA (>384-fold) than their pristine form against MDR *S. aureus*. As suggested earlier, the superior efficiency of NeACT against Sa1158c's resistance mechanisms could be attributed to the complementary mode of action of the antibiotic-adjuvant combinations. CF is bactericidal as it binds to PBPs and inhibits cell wall synthesis (Zeng & Lin, 2013). As found in our study, CPZ and TA complement CF by anti-efflux, anti-beta-lactamase, and antibiofilm properties.

Internalization of *S. aureus* in the endosomal compartment of mammary epithelial cells of the lactating udder parenchyma is facilitated through ligand-mediated endocytosis (Majumder, Eckersall, & George, 2023). *S. aureus* has evolved various mechanisms to survive within host cells. One of the strategies employed by these bacteria is to downregulate cytotoxins, which helps them to prolong their intracellular survival. Additionally, some can escape from the phagosome and enter the cytoplasm (Tuchscherr et al., 2015). These abilities to survive intracellularly not only shield *S. aureus* from host defenses but also make them resistant to numerous antimicrobial therapies.

Unfortunately, over two-thirds of prescribed antibiotics are ineffective against such pathogens (Butler & Cooper, 2011). While some antibiotics from fluoroquinolones, cephalosporins, and macrolides can diffuse into cells, they exhibit poor retention (Abed & Couvreur, 2014; Majumder, Sackey, et al., 2023). On the other hand, highly hydrophilic antibiotics like β-lactams and aminoglycosides have limited cellular penetration (Majumder, Sackey, et al., 2023). Consequently, treating infections caused by intracellular bacteria remains challenging. With the advent of nanotechnology-enabled platforms, it is possible to enhance the cargo permeability and accumulation within cells, leading to effective pathogen elimination. The transport of nanomaterials into host cells occurs through two primary routes - phagocytosis and pinocytosis – which provide desirable cellular uptake, intracellular distribution, and pharmacodynamics of the payloads (Majumder, Eckersall, & George, 2023). Earlier (in Chapter 4), I reported the internalization of Sa1158c in human intestinal Caco-2 cells, leading to infection and cell death, and showed the inadequacy of commonly used antibiotics, including CF, in combatting such infection (Majumder, Sackey, et al., 2023). Similarly, TA and CPZ have shown insignificant effects against intracellular pathogens due to limited penetration into cells (Brar et al., 2022; Farha et al., 2020). Therefore, CH and CD Np were designed to employ cellular uptake through endocytosis and intracellular delivery of the payloads. Evidently, NeACT successfully targeted and eliminated internalized *S. aureus* with no toxic responses to the Caco-2 cells. As suggested earlier, the positive zeta potential in nanocarriers as reported for NeACT, could influence cell interaction and endocytosis, leading to intracellular uptake (Nasti et al., 2009). Carbohydrate-based polymers have been previously reported to be an ideal carrier for cargo delivery in endosomes (Azevedo, Macedo, & Sarmento, 2018). As such, a timely endosomal escape of the nanomaterials to avoid the lytic environment of lysosomes and employ cargo delivery into the cytoplasm is crucial. CH Np has been found to exhibit superior endosomal escape ability due to the proton sponge effect (Aibani et al., 2021). This effect

occurs when the amine groups on chitosan become increasingly protonated in the acidic environment of the endosomes. As a result, an influx of water and chloride ions occurs to balance the resulting charges, leading to the swelling and rupture of lysosomes and ultimately releasing lysosomal contents into the cytoplasm (Aibani et al., 2021).

CD-1 lactating mice mimicking bovine CNS mastitis were used as an *in vivo* model (Breyne et al., 2015; Brouillette & Malouin, 2005). Similar to cows, mice possess two pairs of mammary glands situated in the inguinal region that are anatomically and functionally distinct from each other (Notebaert & Meyer, 2006). Each mammary gland in mice features a single teat opening and a primary duct, providing an ideal environment for pathogen growth in milk. The similarity of bacterial counts, immune components, and histological changes observed in mice to those in cows offer desirable advantages. Moreover, conducting research on cows requires significant resources in terms of both expense and time. As such, the mouse model is a valuable tool for investigating BM. From microscopic analysis, *S. aureus* in grape clusters, pairs, or short-chain morphology were detected within a polymorphonuclear leukocyte (PMN) cell on the infected CD-1 mammary gland. Previously, it was observed that *S. aureus* infiltrated PMN cells and persisted for almost 12 hours, during which the pathogen underwent cell division in both neutrophils and mammary epithelial cells (Brouillette, Grondin, et al., 2004). NeACT showed remarkable remediation of *S. aureus* infection from the mice mammary glands. Drug molecules from NeACT release slowly, which could potentially improve drug retention time in the mammary microenvironment, leading to better antibacterial efficacy. The mammary tissues were analyzed through histopathological examination using H&E and Masson's trichrome staining. The untreated non-infected tissues and those treated with NeACT showed no signs of pro-inflammation immune or toxic responses. There was only minimal PMN infiltration or lesions in the supportive connective tissue, which is ideal for the healing process. This indicates that exposure to NeACT at 78 μg/gland did not affect the cell and

tissue morphology. TA, CD, and CH have been reported earlier to modulate growth factors, activate the ERK1/2 pathway, promote the secretion of anti-inflammatory mediators (IL-1ra, IL-10), and reduce pro-inflammatory cytokines (IL-1α. TNF, and IL-6) (Chen et al., 2019; Jhundoo et al., 2020; Lucia Appleton et al., 2021). In contrast, untreated infected tissues showed evidence of pro-inflammation PMN infiltration in both the connective tissue and intraluminal space and necrotic areas.

6.2. Conclusion

BM, primarily caused by microbial infections, is a major concern for the dairy cattle industry worldwide. The economic impact of this disease is significant, resulting in billions of dollars in losses due to reduced milk production, milk loss, extra labor charges, and treatment. Despite efforts to maintain hygienic milking practices, use pre- and post-milking teat disinfectants, and antibiotic dry cow therapy, several studies have shown the persistence of mastitis pathogens. These pathogens are more likely to develop AMR due to exposure to high antibiotic concentrations as part of preventive or prophylactic treatment regimens in dairy farms. From a public health perspective, the spread of these pathogens to environmental sources is a concern, as some of them can be highly pathogenic to humans despite originating from cows. Consequently, it is essential to continuously monitor mastitis pathogens for virulence and AMR characteristics. Therefore, in the initial phase of this thesis, I examined a library of *E. coli* and *S. aureus* isolated from dairy cows for AMR, mechanisms of AMR, and virulence characteristics through phenotypic and genotypic profiling.

I concluded *E. coli* and *S. aureus* originating from mastitis dairy cows to possess multiple drug resistance and virulence characteristics. Apart from implications for public health, this study, was

crucial to custom design effective therapeutics. My studies suggested that antimicrobials with a single mode of action may be insufficient for eliminating pathogenic bacteria with multiple mechanisms of resistance and virulence characteristics. Although the *S. aureus* isolates did not contain genes that allow them to invade human immune systems, they could still invade human cells and cause intestinal infections in *C. elegans* (model organism). Interestingly, the antibiotics that were effective against the isolates in the disc diffusion test did not have the same success in eliminating intracellular and intestinal infections.

I concluded that resident *E. coli* and *S. aureus* in milk can harbor multiple drug resistance and virulence characteristics. Thus, this has significant implications for public health, particularly given the potential for AMR transmission to other pathogenic bacteria. It is crucial to uncover prevalent mechanisms of AMR in pathogenic bacteria from animal farms to design effective drugs and treatment strategies. Our study suggests that antimicrobials with a single mode of action may be insufficient for curbing AMR bacteria with multiple mechanisms of resistance and virulence factors, highlighting the need for combinatorial therapy in managing AMR infections in dairy farms and preventing potential transmission to the food supply chain. Our findings on the relationship between efflux property and biofilm-forming ability could also pave the way for the development of new combinatorial-therapeutic strategies, as biofilm formation and efflux activity are significant contributors to bacterial persistence and resistance to multiple antimicrobials in bovine udders. Although the *S. aureus* isolates did not contain genes that allow them to invade human immune systems, they could still invade human cells and cause intestinal infections in model organisms. This highlights the importance of ongoing monitoring for zoonosis. Interestingly, the antibiotics that were effective against the isolates in the disc diffusion test did not have the same success in treating their intracellular and intestinal infections. This suggests the need for models to test antibiotic

effectiveness against internalized bacteria and the urgent need to develop therapies to combat antibiotic-resistant bacteria and intracellular pathogens.

While new antimicrobial strategies have been identified since the 1930s, achieving an effective concentration of therapeutics at the site of infection remains a major challenge due to specific BM tissue environments. As a result, there is a need for alternate, cost-effective, and sustainable therapeutic strategies for the clinical management of bovine mastitis that align with the United Nations' "One Health" approach. Recent advancements in nanotechnology have shown significant potential in diagnosing and treating multifactorial infectious diseases. However, there is still an untapped area of research and application when it comes to effective nano-enabled strategies for BM treatment. Therefore, the final phase of the thesis focused on developing NeACT for effective treatment of BM.

I concluded that nanomaterials as carriers for antibacterial combination therapy can effectively combat recalcitrant infections in animal agriculture. Our unique nanocomposite, NeACT that contained CF as the primary antibiotic, CPZ and TA as effector molecules loaded into nanodelivery system consisting of CD and chitosan has proven highly effective in remediating BM infection *in vivo* with no toxic responses, exhibiting colloidal stability, biocompatibility, and a slow-release mechanism . By reducing the effective concentration of CF, CPZ, and TA through NeACT, this study raised the prospects of antimicrobials that were considered redundant due to poor efficiency. Overall, our research has demonstrated that when the potential of nanotechnology is harnessed strategically, it can improve the outcome of antibiotics in BM treatment.

Some limitations of this research work are as follows:

- While testing NeACT's efficiency against intracellular pathogens, I used intestinal epithelial cells instead of mammary epithelial cells. Although our primary objective was to assess NeACT's ability

to reduce internalized bacteria from epithelial cells, evaluating its performance in mammary cell lines like MAC-T cells could have shed light on its relationship to the BM microenvironment.

- During the *in vivo* study involving CD-1 lactating mice to evaluate the effectiveness of NeACT against MRSA, I opted not to utilize the non-encapsulated controls of CF, CPZ, and TA. While the *in vitro* assessments demonstrated the superior efficiency of the nano-enabled control groups (CPZ-CD-TA, CH CF Np, and NeACT), incorporating the non-encapsulated controls in the *in vivo* study could have provided insight into their effectiveness in the BM infection model.
- No studies were conducted to analyze the pro-inflammatory response in a CD-1 mouse model of BM infection. Although histopathological evidence has been leveraged to demonstrate the superior efficacy of NeACT in mitigating infections while avoiding inflammatory and toxic side effects, a deeper understanding of inflammatory responses may be obtained through cytokine profiling.

6.3. Future Perspectives

As I move forward, maintaining a continuous and thorough monitoring of BM pathogens is of utmost importance. This will allow us to comprehensively understand their antimicrobial resistance, virulence traits, and potential to cause zoonotic diseases. A collaborative research effort is necessary to achieve this goal, where data on AMR and virulence among mastitis pathogens from dairy farms worldwide can be shared and analyzed. Furthermore, it is imperative that I conduct studies to identify new bacterial targets, as this will be a fundamental prerequisite for the development of innovative drugs. By working together and focusing on these key areas, I can better protect both animal and human health in the face of this ongoing challenge. To optimize the potential

of NeACT as a site-specific drug delivery method, extensive research is necessary to understand its delivery mechanisms. This includes evaluating how NeACT interacts with the various components of the BM microenvironment, such as the mammary epithelium, the immune cells, and the extracellular matrix. In addition, it is essential to investigate the cellular uptake and intracellular distribution of NeACT, as well as the factors that impact its efficacy, such as the dose, frequency, and duration of treatment. Moreover, it is crucial to evaluate the fate of NeACT after it has achieved its therapeutic goals in the mammary gland. This involves assessing how NeACT is degraded and metabolized and whether it leaves behind any toxic residues that could harm the animal or the environment. While scaling up the production of nanocomposites cost-effectively has been challenging, it is essential to prioritize scaling up NeACT. This requires developing efficient and scalable methods for synthesizing, functionalizing, and characterizing the nanocomposites and optimizing their stability, shelf-life, and quality control. To demonstrate the sustainability of NeACT, a comprehensive LCA should be conducted in the future. This would involve assessing the environmental impact of the entire life cycle of NeACT, from the extraction of raw materials to the disposal of waste products and comparing it to other BM treatment options. Ultimately, clinical studies must be performed to assess the efficacy of NeACT in treating BM in cattle. This involves conducting randomized controlled trials that compare the therapeutic outcomes of NeACT to those of other treatments, such as antibiotics, probiotics, or vaccines. The clinical trials should also evaluate the safety and tolerability of NeACT in cattle, as well as any potential side effects or adverse reactions. Overall, the success of any nano-enabled antibacterial combination therapy for BM treatment depends on its performance, safety for animals and humans, financial feasibility, and social acceptance by consumers, suppliers, and regulatory agencies. These important factors are critical in ensuring that the therapy is widely adopted and able to make a positive impact on animal agriculture.

References

Abed, N., & Couvreur, P. (2014). Nanocarriers for antibiotics: a promising solution to treat intracellular bacterial infections. *International Journal of Antimicrobial Agents, 43*(6), 485-496. doi:10.1016/j.ijantimicag.2014.02.009

Aghamohammadi, M., Haine, D., Kelton, D. F., Barkema, H. W., Hogeveen, H., Keefe, G. P., & Dufour, S. (2018). Herd-level mastitis-associated costs on Canadian dairy farms. *Frontiers in Veterinary Science, 5*(100). doi:10.3389/fvets.2018.00100

Aibani, N., Rai, R., Patel, P., Cuddihy, G., & Wasan, E. K. (2021). Chitosan nanoparticles at the biological interface: implications for drug delivery. *Pharmaceutics, 13*(10). doi:10.3390/pharmaceutics13101686

Akers, R. M., & Nickerson, S. C. (2011). Mastitis and its impact on structure and function in the ruminant mammary gland. *Journal of Mammary Gland Biology and Neoplasia, 16*(4), 275-289. doi:10.1007/s10911-011-9231-3

Alav, I., Sutton, J. M., & Rahman, K. M. (2018). Role of bacterial efflux pumps in biofilm formation. *Journal of Antimicrobial Chemotherapy, 73*(8), 2003-2020. doi:10.1093/jac/dky042

Algharib, S. A., Dawood, A., & Xie, S. (2020). Nanoparticles for treatment of bovine Staphylococcus aureus mastitis. *Drug Delivery, 27*(1), 292-308. doi:10.1080/10717544.2020.1724209

Ali, T., ur Rahman, S., Zhang, L., Shahid, M., Zhang, S., Liu, G., . . . Han, B. (2016). ESBL-producing Escherichia coli from cows suffering mastitis in China contain clinical class 1 Integrons with CTX-M linked to ISCR1. *Frontiers in Microbiology, 7*. doi:10.3389/fmicb.2016.01931

Alkekhia, D., Hammond, P. T., & Shukla, A. (2020). Layer-by-layer biomaterials for drug delivery. *Annual Review of Biomedical Engineering, 22*(1), 1-24. doi:10.1146/annurev-bioeng-060418-052350

Allore, H. G., & Erb, H. N. (1998). Partial budget of the discounted annual benefit of mastitis control strategies. *Journal of Dairy Science, 81*(8), 2280-2292. doi:10.3168/jds.S0022-0302(98)75808-4

Almeida, R. A., Matthews, K. R., Cifrian, E., Guidry, A. J., & Oliver, S. P. (1996). Staphylococcus aureus invasion of bovine mammary epithelial cells. *Journal of Dairy Science, 79*(6), 1021-1026. doi: 10.3168/jds.S0022-0302(96)76454-8

Amanatidou, E., Matthews, A. C., Kuhlicke, U., Neu, T. R., McEvoy, J. P., & Raymond, B. (2019). Biofilms facilitate cheating and social exploitation of β-lactam resistance in Escherichia coli. *npj Biofilms and Microbiomes, 5*(1), 36. doi:10.1038/s41522-019-0109-2

Anatomy of the mammary gland. (2022). Retrieved from https://nydairyadmin.cce.cornell.edu/uploads/doc_113.pdf

Anderl, J. N., Franklin, M. J., & Stewart, P. S. (2000). Role of antibiotic penetration limitation in Klebsiella pneumoniae biofilm resistance to ampicillin and ciprofloxacin. *Antimicrobial Agents and Chemotherapy, 44*(7), 1818-1824. doi:10.1128/aac.44.7.1818-1824.2000

Andres, A.-C., & Djonov, V. (2010). The mammary gland vasculature revisited. *Journal of Mammary Gland Biology and Neoplasia, 15*(3), 319-328. doi:10.1007/s10911-010-9186-9

Arciola, C. R., Campoccia, D., Ravaioli, S., & Montanaro, L. (2015). Polysaccharide intercellular adhesin in biofilm: structural and regulatory aspects. *Frontiers in Cellular and Infection Microbiology, 5*. doi:10.3389/fcimb.2015.00007

Argudín, M. A., Hoefer, A., & Butaye, P. (2019). Heavy metal resistance in bacteria from animals. *Research in Veterinary Science, 122*, 132-147. doi:10.1016/j.rvsc.2018.11.007

Atalla, H., Gyles, C., Jacob, C. L., Moisan, H., Malouin, F., & Mallard, B. (2008). Characterization of a Staphylococcus aureus small colony variant (SCV) associated with persistent bovine mastitis. *Foodborne Pathogens and Disease, 5*(6), 785-799. doi: 10.1089/fpd.2008.0110

Atulya, M., Mathew, A. J., Rao, J. V., & Rao, C. M. (2014). Influence of milk components in establishing biofilm mediated bacterial mastitis infections in cattle: a fractional factorial approach. *Research in Veterinary Science, 96*(1), 25-27. doi:10.1016/j.rvsc.2013.12.001

Audarya, S. D., Chhabra, D., Sharda, R., Gangil, R., Sikrodia, R., Jogi, J., & Shrivastava, N. (2021). Epidemiology of bovine mastitis and its diagnosis, prevention, and control. In D. Oudessa Kerro (Ed.), *Mastitis in Dairy Cattle, Sheep and Goats* (Ch. 1). doi: 10.5772/intechopen.100582

Awosile, B., McClure, J., Sanchez, J., Rodriguez-Lecompte, J. C., Keefe, G., & Heider, L. C. (2018). Salmonella enterica and extended-spectrum cephalosporin-resistant Escherichia

coli recovered from Holstein dairy calves from 8 farms in New Brunswick, Canada. *Journal of Dairy Science, 101*(4), 3271-3284. doi:10.3168/jds.2017-13277

Awosile, B. B., McClure, J. T., Sanchez, J., VanLeeuwen, J., Rodriguez-Lecompte, J. C., Keefe, G., & Heider, L. C. (2017). Short communication: Extended-spectrum cephalosporin-resistant Escherichia coli in colostrum from New Brunswick, Canada, dairy cows harbor blaCMY-2 and blaTEM resistance genes. *Journal of Dairy Science, 100*(10), 7901-7905. doi:10.3168/jds.2017-12941

Azad, A. K., Rajaram, M. V., & Schlesinger, L. S. (2014). Exploitation of the macrophage mannose receptor (CD206) in infectious disease diagnostics and therapeutics. *Journal of Cytology & Molecular Biology, 1*(1). doi:10.13188/2325-4653.1000003

Azevedo, C., Macedo, M. H., & Sarmento, B. (2018). Strategies for the enhanced intracellular delivery of nanomaterials. *Drug Discovery Today, 23*(5), 944-959. doi:10.1016/j.drudis.2017.08.011

Azzopardi, E. A., Ferguson, E. L., & Thomas, D. W. (2012). The enhanced permeability retention effect: a new paradigm for drug targeting in infection. *Journal of Antimicrobial Chemotherapy, 68*(2), 257-274. doi:10.1093/jac/dks379

Balcázar, J. L., Subirats, J., & Borrego, C. M. (2015). The role of biofilms as environmental reservoirs of antibiotic resistance. *Frontiers in Microbiology, 6*. doi:10.3389/fmicb.2015.01216

Bank, U., & Ansorge, S. (2001). More than destructive: neutrophil-derived serine proteases in cytokine bioactivity control. *Journal of Leukocyte Biology, 69*(2), 197-206. doi:10.1189/jlb.69.2.197

Barbosa, T. M., & Levy, S. B. (2000). The impact of antibiotic use on resistance development and persistence. *Drug Resistance Updates, 3*(5), 303-311. doi: 10.1054/drup.2000.0167

Barkema, H., Schukken, Y., & Zadoks, R. (2006). The role of cow, pathogen, and treatment regimen in the therapeutic success of bovine Staphylococcus aureus mastitis. *Journal of Dairy Science, 89*(6), 1877-1895. doi: 10.3168/jds.S0022-0302(06)72256-1

Barnhart, M. M., & Chapman, M. R. (2006). Curli biogenesis and function. *Annual Review of Microbiology, 60*, 131-147. doi:10.1146/annurev.micro.60.080805.142106

Bashal, A. H., Riyadh, S. M., Alharbi, W., Alharbi, K. H., Farghaly, T. A., & Khalil, K. D. (2022). Bio-based (Chitosan-ZnO) nanocomposite: synthesis, characterization, and Its use as

recyclable, ecofriendly biocatalyst for synthesis of thiazoles tethered Azo groups. *Polymers, 14*(3), 386. doi:10.3390/polym14030386

Baugh, S., Phillips, C. R., Ekanayaka, A. S., Piddock, L. J. V., & Webber, M. A. (2013). Inhibition of multidrug efflux as a strategy to prevent biofilm formation. *Journal of Antimicrobial Chemotherapy, 69*(3), 673-681. doi:10.1093/jac/dkt420

Bay, D. C., Stremick, C. A., Slipski, C. J., & Turner, R. J. (2017). Secondary multidrug efflux pump mutants alter Escherichia coli biofilm growth in the presence of cationic antimicrobial compounds. *Research in Microbiology, 168*(3), 208-221. doi:10.1016/j.resmic.2016.11.003

Beaber, J. W., Hochhut, B., & Waldor, M. K. (2004). SOS response promotes horizontal dissemination of antibiotic resistance genes. *Nature, 427*(6969), 72-74. doi:10.1038/nature02241

Becerra-Castro, C., Machado, R. A., Vaz-Moreira, I., & Manaia, C. M. (2015). Assessment of copper and zinc salts as selectors of antibiotic resistance in Gram-negative bacteria. *Science of the Total Environment, 530*, 367-372. doi:10.1016/j.scitotenv.2015.05.102

Begun, J., Gaiani, J. M., Rohde, H., Mack, D., Calderwood, S. B., Ausubel, F. M., & Sifri, C. D. (2007). Staphylococcal biofilm exopolysaccharide protects against Caenorhabditis elegans immune defenses. *PLOS Pathogens, 3*(4), e57. doi:10.1371/journal.ppat.0030057

Behl, G., Iqbal, J., O'Reilly, N. J., McLoughlin, P., & Fitzhenry, L. (2016). Synthesis and characterization of Poly(2-hydroxyethylmethacrylate) contact lenses containing chitosan nanoparticles as an ocular delivery system for Dexamethasone sodium phosphate. *Pharmaceutical Research, 33*(7), 1638-1648. doi:10.1007/s11095-016-1903-7

Bennett, J. E., Dolin, R., & Blaser, M. J. (2020). *Mandell, Douglas, and Bennett's Principles and Practice of Infectious Diseases* [1 online resource (2 volumes (xxxviii, 3839, I-125 pages)) : illustrations (some color)](Ninth edition. ed.). Retrieved from http://www.r2library.com/Resource/Title/0323482554

Bennett, R. M., & Kokocinski, T. (1978). Lactoferrin content of peripheral blood cells. *British Journal of Haematology, 39*(4), 509-521. doi:10.1111/j.1365-2141.1978.tb03620.x

Bennett, S., Fliss, I., Ben Said, L., Malouin, F., & Lacasse, P. (2022). Efficacy of bacteriocin-based formula for reducing staphylococci, streptococci, and total bacterial counts on teat skin of dairy cows. *Journal of Dairy Science, 105*(5), 4498-4507. doi:10.3168/jds.2021-21381

Berlutti, F., Morea, C., Battistoni, A., Sarli, S., Cipriani, P., Superti, F., . . . Valenti, P. (2005). Iron availability influences aggregation, biofilm, adhesion and invasion of Pseudomonas aeruginosa and Burkholderia cenocepacia. *International Journal of Immunopathology and Pharmacology, 18*(4), 661-670. doi: 10.1177/039463200501800407

Bernardi, S., Anderson, A., Macchiarelli, G., Hellwig, E., Cieplik, F., Vach, K., & Al-Ahmad, A. (2021). Subinhibitory antibiotic concentrations enhance biofilm formation of clinical Enterococcus faecalis isolates. *Antibiotics, 10*(7). doi:10.3390/antibiotics10070874

Bernkop-Schnürch, A., Hornof, M., & Guggi, D. (2004). Thiolated chitosans. *European Journal of Pharmaceutics and Biopharmaceutics, 57*(1), 9-17. doi:10.1016/s0939-6411(03)00147-4

Blum, S. E., Goldstone, R. J., Connolly, J. P., Répérant-Ferter, M., Germon, P., Inglis, N. F., . . . Mclean, K. (2018). Postgenomics characterization of an essential genetic determinant of mammary pathogenic Escherichia coli. *mBio, 9*(2), e00423-00418. doi:10.1128/mBio.00423-18

Bohnert, J. A., Karamian, B., & Nikaido, H. (2010). Optimized Nile Red efflux assay of AcrAB-TolC multidrug efflux system shows competition between substrates. *Antimicrobial Agents and Chemotherapy, 54*(9), 3770-3775. doi:10.1128/aac.00620-10

Bongers, S., Hellebrekers, P., Leenen, L. P. H., Koenderman, L., & Hietbrink, F. (2019). Intracellular penetration and effects of antibiotics on Staphylococcus aureus inside human neutrophils: A comprehensive review. *Antibiotics, 8*(2), 54. doi:10.3390/antibiotics8020054

Boss, R., Cosandey, A., Luini, M., Artursson, K., Bardiau, M., Breitenwieser, F., . . . Graber, H. U. (2016). Bovine Staphylococcus aureus: subtyping, evolution, and zoonotic transfer. *Journal of Dairy Science, 99*(1), 515-528. doi:10.3168/jds.2015-9589

Bourzac, K. (2012). Nanotechnology: carrying drugs. *Nature, 491*(7425), S58-S60. doi:10.1038/491S58a

Bradley, A., & Green, M. (2001). Adaptation of Escherichia coli to the bovine mammary gland. *Journal of Clinical Microbiology, 39*(5), 1845-1849. doi:10.1128/JCM.39.5.1845-1849.2001

Bradley, A., & Green, M. (2009). Factors affecting cure when treating bovine clinical mastitis with cephalosporin-based intramammary preparations. *Journal of Dairy Science, 92*(5), 1941-1953. doi: 10.3168/jds.2008-1497

Bradley, A. J. (2002). Bovine mastitis: an evolving disease. *The Veterinary Journal, 164*(2), 116-128. doi: 10.1053/tvjl.2002.0724

Bradley, A. J., Breen, J., Payne, B., White, V., & Green, M. J. (2015). An investigation of the efficacy of a polyvalent mastitis vaccine using different vaccination regimens under field conditions in the United Kingdom. *Journal of Dairy Science, 98*(3), 1706-1720. doi: 10.3168/jds.2014-8332

Brar, A., Majumder, S., Navarro, M. Z., Benoit-Biancamano, M.-O., Ronholm, J., & George, S. (2022). Nanoparticle-enabled combination therapy showed superior activity against multi-drug resistant bacterial pathogens in comparison to free drugs. *Nanomaterials, 12*(13), 2179. doi:10.3390/nano12132179

Breyne, K., De Vliegher, S., De Visscher, A., Piepers, S., & Meyer, E. (2015). Technical note: a pilot study using a mouse mastitis model to study differences between bovine associated coagulase-negative staphylococci. *Journal of Dairy Science, 98*(2), 1090-1100. doi:10.3168/jds.2014-8699

Brouillette, E., Grondin, G., Lefebvre, C., Talbot, B. G., & Malouin, F. (2004). Mouse mastitis model of infection for antimicrobial compound efficacy studies against intracellular and extracellular forms of Staphylococcus aureus. *Veterinary Microbiology, 101*(4), 253-262. doi:10.1016/j.vetmic.2004.04.008

Brouillette, E., Grondin, G., Talbot, B. G., & Malouin, F. (2005). Inflammatory cell infiltration as an indicator of Staphylococcus aureus infection and therapeutic efficacy in experimental mouse mastitis. *Veterinary Immunology and Immunopathology, 104*(3), 163-169. doi:10.1016/j.vetimm.2004.11.006

Brouillette, E., & Malouin, F. (2005). The pathogenesis and control of Staphylococcus aureus-induced mastitis: study models in the mouse. *Microbes and Infection, 7*(3), 560-568. doi:10.1016/j.micinf.2004.11.008

Brouillette, E., Martinez, A., Boyll, B. J., Allen, N. E., & Malouin, F. (2004). Persistence of a Staphylococcus aureus small-colony variant under antibiotic pressure in vivo. *FEMS Immunology & Medical Microbiology, 41*(1), 35-41. doi: 10.1016/j.femsim.2003.12.007

Burvenich, C., Van Merris, V., Mehrzad, J., Diez-Fraile, A., & Duchateau, L. (2003). Severity of E. coli mastitis is mainly determined by cow factors. *Veterinary Research, 34*(5), 521-564. doi:10.1051/vetres:2003023

Bush, K., & Bradford, P. A. (2016). β-Lactams and β-Lactamase inhibitors: an overview. *Cold Spring Harbor Perspectives in Medicine, 6*(8). doi:10.1101/cshperspect.a025247

Butler, M. S., & Cooper, M. A. (2011). Antibiotics in the clinical pipeline in 2011. *The Journal of Antibiotics, 64*(6), 413-425. doi:10.1038/ja.2011.44

Buxton, R. (2005). Blood agar plates and hemolysis protocols. *American Society for Microbiology*. Retrieved from https://asm.org/getattachment/7ec0de2b-bb16-4f6e-ba07-2aea25a43e76/protocol-2885.pdf

Calvinho, L., & Oliver, S. (1998). Invasion and persistence of Streptococcus dysgalactiae within bovine mammary epithelial cells. *Journal of Dairy Science, 81*(3), 678-686. doi: 10.3168/jds.S0022-0302(98)75623-1

Campos, B., Pickering, A. C., Rocha, L. S., Aguilar, A. P., Fabres-Klein, M. H., de Oliveira Mendes, T. A., . . . de Oliveira Barros Ribon, A. (2022). Diversity and pathogenesis of Staphylococcus aureus from bovine mastitis: current understanding and future perspectives. *BMC Veterinary Research, 18*(1), 115. doi:10.1186/s12917-022-03197-5

Carlson, S. K., Erickson, D. L., & Wilson, E. (2020). Staphylococcus aureus metal acquisition in the mastitic mammary gland. *Microbial Pathogenesis, 144*, 104179. doi:10.1016/j.micpath.2020.104179

Catry, B., Laevens, H., Devriese, L. A., Opsomer, G., & De Kruif, A. (2003). Antimicrobial resistance in livestock. *Journal of Veterinary Pharmacology and Therapeutics, 26*(2), 81-93. doi:10.1046/j.1365-2885.2003.00463.x

Chen, Y., Tian, L., Yang, F., Tong, W., Jia, R., Zou, Y., . . . Yin, Z. (2019). Tannic acid accelerates cutaneous wound healing in rats via activation of the erk 1/2 signaling pathways. *Advanced Wound Care, 8*(7), 341-354. doi:10.1089/wound.2018.0853

Cheng, X., Pei, X., Xie, W., Chen, J., Li, Y., Wang, J., . . . Wan, Q. (2022). ph-triggered size-tunable silver nanoparticles: targeted aggregation for effective bacterial infection therapy. *Small, 18*(22), 2200915. doi:10.1002/smll.202200915

Performance standards for antimicrobial susceptibility testing; CLSI document M100–S27, Wayne, PA: Clinical Laboratory Standards Institute (CLSI). (2017).

Coates, A. R. M., Hu, Y., Holt, J., & Yeh, P. (2020). Antibiotic combination therapy against resistant bacterial infections: synergy, rejuvenation and resistance reduction. *Expert Review of Anti-infective Therapy, 18*(1), 5-15. doi:10.1080/14787210.2020.1705155

Cobirka, M., Tancin, V., & Slama, P. (2020). Epidemiology and classification of mastitis. *Animals, 10*(12). doi:10.3390/ani10122212

Cockeran, R., Mutepe, N. D., Theron, A. J., Tintinger, G. R., Steel, H. C., Stivaktas, P. I., . . . Anderson, R. (2012). Calcium-dependent potentiation of the pro-inflammatory functions of human neutrophils by tigecycline in vitro. *Journal of Antimicrobial Chemotherapy, 67*(1), 130-137. doi:10.1093/jac/dkr441

Collado, R., Montbrau, C., Sitjà, M., & Prenafeta, A. (2018). Study of the efficacy of a Streptococcus uberis mastitis vaccine against an experimental intramammary infection with a heterologous strain in dairy cows. *Journal of Dairy Science, 101*(11), 10290-10302. doi: 10.3168/jds.2018-14840

Collado, R., Prenafeta, A., González-González, L., Pérez-Pons, J. A., & Sitjà, M. (2016). Probing vaccine antigens against bovine mastitis caused by Streptococcus uberis. *Vaccine, 34*(33), 3848-3854. doi:10.1016/j.vaccine.2016.05.044

Cortinhas, C. S., Tomazi, T., Zoni, M. S. F., Moro, E., & Veiga dos Santos, M. (2016). Randomized clinical trial comparing ceftiofur hydrochloride with a positive control protocol for intramammary treatment of nonsevere clinical mastitis in dairy cows. *Journal of Dairy Science, 99*(7), 5619-5628. doi:10.3168/jds.2016-10891

Costa, J. C. M., de Freitas Espeschit, I., Pieri, F. A., dos Anjos Benjamin, L., & Moreira, M. A. S. (2012). Increased production of biofilms by Escherichia coli in the presence of enrofloxacin. *Veterinary Microbiology, 160*(3-4), 488-490. doi:10.1016/j.vetmic.2012.05.036

Côté-Gravel, J., Brouillette, E., & Malouin, F. (2019). Vaccination with a live-attenuated small-colony variant improves the humoral and cell-mediated responses against Staphylococcus aureus. *PLOS One, 14*(12), e0227109. doi:10.1371/journal.pone.0227109

Côté-Gravel, J., Brouillette, E., Obradović, N., Ster, C., Talbot, B. G., & Malouin, F. (2016). Characterization of a vrag mutant in a genetically stable Staphylococcus aureus small-colony variant and preliminary assessment for use as a live-attenuated vaccine against intrammamary infections. *PLOS One, 11*(11), e0166621. doi:10.1371/journal.pone.0166621

Cruz, C. D., Shah, S., & Tammela, P. (2018). Defining conditions for biofilm inhibition and eradication assays for Gram-positive clinical reference strains. *BMC Microbiology, 18*(1), 173. doi:10.1186/s12866-018-1321-6

D. Jung, Park S, Ruffini J, Dussault F, Dufour S, & Ronholm J. (2021). Comparative genomic analysis of *Escherichia coli* isolates from cases of bovine clinical mastitis identifies nine specific pathotype marker genes. *Microbial Genomics*. doi:10.1099/mgen.0.000597

Dai, X., Xiang, S., Li, J., Gao, Q., & Yang, K. (2012). Development of a colorimetric assay for rapid quantitative measurement of clavulanic acid in microbial samples. *Science China Life Sciences, 55*(2), 158-163. doi:10.1007/s11427-012-4287-x

Danhier, F. (2016). To exploit the tumor microenvironment: Since the EPR effect fails in the clinic, what is the future of nanomedicine? *Journal of Controlled Release, 244*, 108-121. doi:10.1016/j.jconrel.2016.11.015

Davis, M. A., Besser, T. E., Orfe, L. H., Baker, K. N. K., Lanier, A. S., Broschat, S. L., . . . Call, D. R. (2011). Genotypic-phenotypic discrepancies between antibiotic resistance characteristics of Escherichia coli isolates from calves in management settings with high and low antibiotic use. *Applied and Environmental Microbiology, 77*(10), 3293-3299. doi:10.1128/AEM.02588-10

De Kievit, T. R., Parkins, M. D., Gillis, R. J., Srikumar, R., Ceri, H., Poole, K., . . . Storey, D. G. (2001). Multidrug efflux pumps: expression patterns and contribution to antibiotic resistance in Pseudomonas aeruginosa biofilms. *Antimicrobial Agents and Chemotherapy, 45*(6), 1761-1770. doi:10.1128/aac.45.6.1761-1770.2001

Dego, O. (2020). Bovine Mastitis: Part I. In *Animal Reproduction in Veterinary Medicine*. doi:10.5772/intechopen.93483

Dego, O. K. (2020). Control and Prevention of Mastitis: Part Two. In R. P.-C. a. M. Q. Faruk Aral (Ed.), *Animal Reproduction in Veterinary Medicine*. doi:10.5772/intechopen.93484

Dego, O. K., Van Dijk, J., & Nederbragt, H. (2002). Factors involved in the early pathogenesis of bovine Staphylococcus aureus mastitis with emphasis on bacterial adhesion and invasion. A review. *Veterinary Quarterly, 24*(4), 181-198. doi:10.1080/01652176.2002.9695135

Diarra, M. S., Block, G., Rempel, H., Oomah, B. D., Harrison, J., McCallum, J., . . . Malouin, F. (2013). In vitro and in vivo antibacterial activities of cranberry press cake extracts alone or in combination with β-lactams against Staphylococcus aureus. *BMC Complementary and Alternative Medicine, 13*(1), 90. doi:10.1186/1472-6882-13-90

Ding, Y., Onodera, Y., Lee, J. C., & Hooper, D. C. (2008). NorB, an efflux pump in Staphylococcus aureus strain MW2, contributes to bacterial fitness in abscesses. *Journal of Bacteriology, 190*(21), 7123-7129. doi:10.1128/jb.00655-08

Dingwell, R. T., Leslie, K. E., Sabour, P., Lepp, D., & Pacan, J. (2006). Influence of the genotype of Staphylococcus aureus, determined by pulsed-field gel electrophoresis, on dry-period elimination of subclinical mastitis in Canadian dairy herds. *Canadian Journal of Veterinary Research, 70*(2), 115-120. PMCID: PMC1410724

Dong, G., Liu, H., Yu, X., Zhang, X., Lu, H., Zhou, T., & Cao, J. (2018). Antimicrobial and anti-biofilm activity of tannic acid against Staphylococcus aureus. *Natural Product Research, 32*(18), 2225-2228. doi:10.1080/14786419.2017.1366485

Dubin, G. (2002). Extracellular proteases of Staphylococcus spp. *Journal of Biological Chemistry, 383*(7-8), 1075-1086. doi:10.1515/bc.2002.116

Dufour, S., Labrie, J., & Jacques, M. (2019). The mastitis pathogens culture collection. *Microbiology Resource Announcements, 8*(15), e00133-00119. doi:10.1128/MRA.00133-19

Duval, V., & Lister, I. M. (2013). MarA, SoxS and Rob of Escherichia coli - Global regulators of multidrug resistance, virulence and stress response. *International Journal of Biotechnology for Wellness Industries, 2*(3), 101-124. doi:10.6000/1927-3037.2013.02.03.2

Dziewanowska, K., Patti, J. M., Deobald, C. F., Bayles, K. W., Trumble, W. R., & Bohach, G. A. (1999). Fibronectin binding protein and host cell tyrosine kinase are required for internalization of Staphylococcus aureus by epithelial cells. *Infection and Immunity, 67*(9), 4673-4678. doi: 10.1128/IAI.67.9.4673-4678.1999

Echániz-Aviles, G., Velazquez-Meza, M. E., Rodríguez-Arvizu, B., Carnalla-Barajas, M. N., & Noguerón, A. S. (2022). Detection of capsular genotypes of methicillin-resistant Staphylococcus aureus and clonal distribution of the cap5 and cap8 genes in clinical isolates. *Archives of Microbiology, 204*(3), 186. doi:10.1007/s00203-022-02793-1

Eckersall, P. D., Young, F. J., McComb, C., Hogarth, C. J., Safi, S., Weber, A., . . . Fitzpatrick, J. L. (2001). Acute phase proteins in serum and milk from dairy cows with clinical mastitis. *Veterinary Research, 148*(2), 35-41. doi:10.1136/vr.148.2.35

Efthymia, P., & Constantinos, P. (2018). Resistance of staphylococci to Macrolides-Lincosamides-Streptogramins B (MLSB): epidemiology and mechanisms of resistance. In H. Hassan, O. Hani, & A. Farhat (Eds.), *Staphylococcus Aureus* (Ch. 7). doi: 10.5772/intechopen.75192

El-Tahawy, A. S., & El-Far, A. H. (2010). Influences of somatic cell count on milk composition and dairy farm profitability. *International Journal of Dairy Technology, 63*(3), 463-469. doi:10.1111/j.1471-0307.2010.00597.x

Engering, A., Hogerwerf, L., & Slingenbergh, J. (2013). Pathogen-host-environment interplay and disease emergence. *Emerging Microbes & Infections, 2*(2), e5. doi:10.1038/emi.2013.5

Fairbrother, J.-H., Dufour, S., Fairbrother, J. M., Francoz, D., Nadeau, É., & Messier, S. (2015). Characterization of persistent and transient Escherichia coli isolates recovered from clinical mastitis episodes in dairy cows. *Veterinary Microbiology, 176*(1), 126-133. doi:10.1016/j.vetmic.2014.12.025

Fairbrother, J. H., Dufour, S., Fairbrother, J. M., Francoz, D., Nadeau, E., & Messier, S. (2015). Characterization of persistent and transient Escherichia coli isolates recovered from clinical mastitis episodes in dairy cows. *Veterinary Microbiology, 176*(1-2), 126-133. doi:10.1016/j.vetmic.2014.12.025

Farha, A. K., Yang, Q.-Q., Kim, G., Li, H.-B., Zhu, F., Liu, H.-Y., . . . Corke, H. (2020). Tannins as an alternative to antibiotics. *Food Bioscience, 38*, 100751. doi:10.1016/j.fbio.2020.100751

Federman, C., Ma, C., & Biswas, D. (2016). Major components of orange oil inhibit Staphylococcus aureus growth and biofilm formation, and alter its virulence factors. *Journal of Medical Microbiology, 65*(7), 688-695. doi:10.1099/jmm.0.000286

Feßler, A., Scott, C., Kadlec, K., Ehricht, R., Monecke, S., & Schwarz, S. (2010). Characterization of methicillin-resistant Staphylococcus aureus ST398 from cases of bovine mastitis. *Journal of Antimicrobial Chemotherapy, 65*(4), 619-625. doi:10.1093/jac/dkq021

Foroozandeh, P., & Aziz, A. A. (2018). Insight into cellular uptake and intracellular trafficking of nanoparticles. *Nanoscale Research Letters, 13*(1), 339. doi:10.1186/s11671-018-2728-6

Foster, T. J., Geoghegan, J. A., Ganesh, V. K., & Höök, M. (2014). Adhesion, invasion and evasion: the many functions of the surface proteins of Staphylococcus aureus. *Nature Reviews Microbiology, 12*(1), 49-62. doi: 10.1038/nrmicro3161

Fox, L., Zadoks, R., & Gaskins, C. (2005). Biofilm production by Staphylococcus aureus associated with intramammary infection. *Veterinary Microbiology, 107*(3-4), 295-299. doi:10.1016/j.vetmic.2005.02.005

Franke, S., Grass, G., Rensing, C., & Nies, D. H. (2003). Molecular analysis of the copper-transporting efflux system CusCFBA of Escherichia coli. *Journal of Bacteriology, 185*(13), 3804-3812. doi:10.1128/jb.185.13.3804-3812.2003

Freick, M., Frank, Y., Steinert, K., Hamedy, A., Passarge, O., & Sobiraj, A. (2016). Mastitis vaccination using a commercial polyvalent vaccine or a herd-specific Staphylococcus

aureus vaccine. *Tierärztliche Praxis Ausgabe G: Großtiere/Nutztiere, 44*(04), 219-229. doi: 10.15653/TPG-150912

Freu, G., Tomazi, T., Filho, A. F. S., Heinemann, M. B., & dos Santos, M. V. (2022). Antimicrobial Resistance and Molecular Characterization of Staphylococcus aureus Recovered from Cows with Clinical Mastitis in Dairy Herds from Southeastern Brazil. *Antibiotics, 11*(4). doi:10.3390/antibiotics11040424

Fu, Y., Gao, R., Cao, Y., Guo, M., Wei, Z., Zhou, E., . . . Zhang, N. (2014). Curcumin attenuates inflammatory responses by suppressing TLR4-mediated NF-κB signaling pathway in lipopolysaccharide-induced mastitis in mice. *International Immunopharmacology, 20*(1), 54-58. doi:10.1016/j.intimp.2014.01.024

Gadade, D. D., & Pekamwar, S. S. (2020). Cyclodextrin based nanoparticles for drug delivery and theranostics. *Advanced Pharmaceutical Bulletin, 10*(2), 166-183. doi:10.34172/apb.2020.022

Gao, F., Shao, T., Yu, Y., Xiong, Y., & Yang, L. (2021). Surface-bound reactive oxygen species generating nanozymes for selective antibacterial action. *Nature Communications, 12*(1), 745. doi:10.1038/s41467-021-20965-3

Gao, W., Thamphiwatana, S., Angsantikul, P., & Zhang, L. (2014). Nanoparticle approaches against bacterial infections. *Wiley Interdisciplinary Reviews Nanomedicine and Nanobiotechnology, 6*(6), 532-547. doi:10.1002/wnan.1282

Garnsworthy, P., Masson, L., Lock, A., & Mottram, T. (2006). Variation of milk citrate with stage of lactation and de novo fatty acid synthesis in dairy cows. *Journal of Dairy Science, 89*(5), 1604-1612. doi:10.3168/jds.S0022-0302(06)72227-5

Garzoni, C., & Kelley, W. L. (2009). Staphylococcus aureus: new evidence for intracellular persistence. *Trends in Microbiology, 17*(2), 59-65. doi: 10.1016/j.tim.2008.11.005

Gehring, R., & Smith, G. W. (2006). An overview of factors affecting the disposition of intramammary preparations used to treat bovine mastitis. *Journal of Veterinary Pharmacology and Therapeutics, 29*(4), 237-241. doi:10.1111/j.1365-2885.2006.00750.x

Geiser, M. (2010). Update on macrophage clearance of inhaled micro-and nanoparticles. *Journal of Aerosol Medicine and Pulmonary Drug Delivery, 23*(4), 207-217. doi:10.1089/jamp.2009.0797

George, Teo, L. L., Majumder, S., Chew, W. L., & Khoo, G. H. (2020). Low levels of silver in food packaging materials may have no functional advantage, instead enhance microbial

spoilage of food through hormetic effect. *Food Control*, 107768. doi:10.1016/j.foodcont.2020.107768

George, S. (2015). Nanomaterial properties: Implications for safe medical applications of nanotechnology. In A. Kishen (Ed.), *Nanotechnology in Endodontics: Current and Potential Clinical Applications* (45-69). doi: 10.1007/978-3-319-13575-5_4

George, S., Tay, I., Phue, W. H., Gardner, H., & Sukumaran, B. (2019). Enhancing the bioavailability of silver through nanotechnology approaches could overcome efflux pump mediated silver resistance in methicillin resistant staphylococcus aureus. *Journal of Biomedical Nanotechnology, 15*(11), 2216-2228. doi:10.1166/jbn.2019.2858

Gholipourmalekabadi, M., Mobaraki, M., Ghaffari, M., Zarebkohan, A., Omrani, V. F., Urbanska, A. M., & Seifalian, A. (2017). Targeted Drug Delivery Based on Gold Nanoparticle Derivatives. *Current Pharmaceutical Design, 23*(20), 2918-2929. doi:10.2174/1381612823666170419105413

Gillespie, B., & Oliver, S. (2005). Simultaneous detection of mastitis pathogens, Staphylococcus aureus, Streptococcus uberis, and Streptococcus agalactiae by multiplex real-time polymerase chain reaction. *Journal of Dairy Science, 88*(10), 3510-3518.

Giovaninni, G., Moore, C. J., Hall, A. J., Byrne, H. J., & Gubala, V. (2018). pH-dependent silica nanoparticle dissolution and cargo release. *Colloids and Surfaces B: Biointerfaces, 169*, 242-248. doi:10.1016/j.colsurfb.2018.04.064

Gogoi-Tiwari, J., Williams, V., Waryah, C. B., Eto, K. Y., Tau, M., Costantino, P., . . . Mukkur, T. (2015). Comparative studies of the immunogenicity and protective potential of biofilm vs planktonic Staphylococcus aureus vaccine against bovine mastitis using non-invasive mouse mastitis as a model system. *Biofouling, 31*(7), 543-554. doi:10.1080/08927014.2015.1074681

Gogoi-Tiwari, J., Williams, V., Waryah, C. B., Mathavan, S., Tiwari, H. K., Costantino, P., & Mukkur, T. (2016). Intramammary immunization of pregnant mice with staphylococcal protein a reduces the post-challenge mammary gland bacterial load but not pathology. *PLOS One, 11*(2), e0148383. doi:10.1371/journal.pone.0148383

Gonçalves, J. L., Kamphuis, C., Martins, C. M. M. R., Barreiro, J. R., Tomazi, T., Gameiro, A. H., . . . dos Santos, M. V. (2018). Bovine subclinical mastitis reduces milk yield and economic return. *Livestock Science, 210*, 25-32. doi:10.1016/j.livsci.2018.01.016

Gonzalez, C. D., Ledo, C., Giai, C., Garófalo, A., & Gómez, M. I. (2015). The sbi protein contributes to staphylococcus aureus inflammatory response during systemic infection. *PLOS One, 10*(6), e0131879-e0131879. doi:10.1371/journal.pone.0131879

Guinane, C. M., Sturdevant, D. E., Herron-Olson, L., Otto, M., Smyth, D. S., Villaruz, A. E., . . . Fitzgerald, J. R. (2008). Pathogenomic analysis of the common bovine Staphylococcus aureus clone (ET3): emergence of a virulent subtype with potential risk to public health. *The Journal of Infectious Diseases, 197*(2), 205-213. doi:10.1086/524689

Günther, J., Petzl, W., Bauer, I., Ponsuksili, S., Zerbe, H., Schuberth, H.-J., . . . Seyfert, H.-M. (2017a). Differentiating Staphylococcus aureus from Escherichia coli mastitis: S. aureus triggers unbalanced immune-dampening and host cell invasion immediately after udder infection. *Scientific Reports, 7*(1), 4811. doi:10.1038/s41598-017-05107-4

Günther, J., Petzl, W., Bauer, I., Ponsuksili, S., Zerbe, H., Schuberth, H.-J., . . . Seyfert, H.-M. (2017b). Differentiating Staphylococcus aureus from Escherichia coli mastitis: S. aureus triggers unbalanced immune-dampening and host cell invasion immediately after udder infection. *Scientific reports, 7*(1), 1-14. doi: 10.1038/s41598-017-05107-4

Gupta, P. V., Nirwane, A. M., Belubbi, T., & Nagarsenker, M. S. (2017). Pulmonary delivery of synergistic combination of fluoroquinolone antibiotic complemented with proteolytic enzyme: a novel antimicrobial and antibiofilm strategy. *Nanomedicine: Nanotechnology, Biology and Medicine, 13*(7), 2371-2384. doi:10.1016/j.nano.2017.06.011

Han, R., Li, S., Wang, J., Yu, Z., Wang, J., & Zheng, N. (2017). Elimination kinetics of ceftiofur hydrochloride in milk after an 8-day extended intramammary administration in healthy and infected cows. *PLOS One, 12*(11), e0187261. doi:10.1371/journal.pone.0187261

He, X., Wei, Z., Zhou, E., Chen, L., Kou, J., Wang, J., & Yang, Z. (2015). Baicalein attenuates inflammatory responses by suppressing TLR4 mediated NF-κB and MAPK signaling pathways in LPS-induced mastitis in mice. *International Immunopharmacology, 28*(1), 470-476. doi:10.1016/j.intimp.2015.07.012

Head, B., & Aballay, A. (2014). Recovery from an acute infection in C. elegans requires the GATA transcription factor ELT-2. *PLOS Genetics, 10*(10), e1004609-e1004609. doi:10.1371/journal.pgen.1004609

Herdiana, Y., Wathoni, N., Shamsuddin, S., & Muchtaridi, M. (2022). Drug release study of the chitosan-based nanoparticles. *Heliyon, 8*(1), e08674. doi:10.1016/j.heliyon.2021.e08674

Hogan, J., Weiss, W., Smith, K., Todhunter, D., Schoenberger, P., & Sordillo, L. (1995). Effects of an Escherichia coli J5 vaccine on mild clinical coliform mastitis. *Journal of Dairy Science, 78*(2), 285-290. doi: 10.3168/jds.S0022-0302(95)76636-X

Hong, Q., Huo, S., Tang, H., Qu, X., & Yue, B. (2021). Smart nanomaterials for treatment of biofilm in orthopedic implants. *Frontiers in Bioengineering and Biotechnology, 9*. doi:10.3389/fbioe.2021.694635

Hong, X., Qin, J., Li, T., Dai, Y., Wang, Y., Liu, Q., . . . Li, M. (2016). Staphylococcal protein a promotes colonization and immune evasion of the epidemic healthcare-associated mrsa st239. *Frontiers in Microbiology, 7*. doi:10.3389/fmicb.2016.00951

Hoque, M. N., Istiaq, A., Clement, R. A., Gibson, K. M., Saha, O., Islam, O. K., . . . Hossain, M. A. (2020). Insights into the resistome of bovine clinical mastitis microbiome, a key factor in disease complication. *Frontiers in Microbiology, 11*(860). doi:10.3389/fmicb.2020.00860

How much does mastitis cost dairy producers annually? (2020). Retrieved from https://www.thecattlesite.com/focus/thermo-fisher-scientific/2335/bovine-diagnostics-how-much-does-mastitis-cost-dairy-producers-annually

Hubbell, J. A., & Chilkoti, A. (2012). Chemistry. nanomaterials for drug delivery. *Science, 337*(6092), 303-305. doi:10.1126/science.1219657

Huey, S., Kavanagh, M., Regan, A., Dean, M., McKernan, C., McCoy, F., . . . McAloon, C. I. (2021). Engaging with selective dry cow therapy: understanding the barriers and facilitators perceived by Irish farmers. *Irish Veterinary Journal, 74*(1), 28. doi:10.1186/s13620-021-00207-0

Hussain, W., Kushwaha, P., Rahman, M., & Akhtar, J. (2017). Development and evaluation of fast dissolving film for oro-buccal drug delivery of chlorpromazine. *Indian Journal of Pharmaceutical Education and Research, 51*, s539-s547. doi:10.5530/ijper.51.4s.81

Irazoqui, J. E., Troemel, E. R., Feinbaum, R. L., Luhachack, L. G., Cezairliyan, B. O., & Ausubel, F. M. (2010). Distinct pathogenesis and host responses during infection of C. elegans by P. aeruginosa and S. aureus. *PLOS Pathogens, 6*(7), e1000982. doi:10.1371/journal.ppat.1000982

Ismail, Z. B. (2017). Mastitis vaccines in dairy cows: Recent developments and recommendations of application. *Veterinary World, 10*(9), 1057. doi: 10.14202/vetworld.2017.1057-1062

Iyer, R., Ferrari, A., Rijnbrand, R., & Erwin, A. L. (2015). A fluorescent microplate assay quantifies bacterial efflux and demonstrates two distinct compound binding sites in acrb. *Antimicrobial Agents and Chemotherapy, 59*(4), 2388. doi:10.1128/AAC.05112-14

Jacobs, R. F., & Wilson, C. B. (1983). Intracellular penetration and antimicrobial activity of antibiotics. *Journal of Antimicrobial Chemotherapy, 12*(suppl_C), 13-20. doi:10.1093/jac/12.suppl_c.13

Jayarao, B., & Henning, D. (2001). Prevalence of foodborne pathogens in bulk tank milk. *Journal of Dairy Science, 84*(10), 2157-2162. doi: 10.3168/jds.S0022-0302(01)74661-9

Jensen, K., Günther, J., Talbot, R., Petzl, W., Zerbe, H., Schuberth, H.-J., . . . Glass, E. J. (2013). Escherichia coli-and Staphylococcus aureus-induced mastitis differentially modulate transcriptional responses in neighbouring uninfected bovine mammary gland quarters. *BMC Genomics, 14*(1), 1-19. doi:10.1186/1471-2164-14-36

Jhundoo, H. D., Siefen, T., Liang, A., Schmidt, C., Lokhnauth, J., Béduneau, A., . . . Lamprecht, A. (2020). Anti-inflammatory activity of chitosan and 5-amino salicylic acid combinations in experimental colitis. *Pharmaceutics, 12*(11). doi:10.3390/pharmaceutics12111038

Ji, C., Juárez-Hernández, R. E., & Miller, M. J. (2012). Exploiting bacterial iron acquisition: siderophore conjugates. *Future Medicinal Chemistry, 4*(3), 297-313. doi:10.4155/fmc.11.191

Jiang, H., & Wang, D. (2018). The microbial zoo in the C. Elegans intestine: bacteria, fungi and viruses. *Viruses, 10*(2), 85. doi:10.3390/v10020085

Jiang, L. Q., Wang, T. Y., Webster, T. J., Duan, H. J., Qiu, J. Y., Zhao, Z. M., . . . Zheng, C. L. (2017). Intracellular disposition of chitosan nanoparticles in macrophages: intracellular uptake, exocytosis, and intercellular transport. *International Journal of Nanomedicine, 12*, 6383-6398. doi:10.2147/ijn.S142060

Jiang, W., Kim, B., Rutka, J. T., & Chan, W. C. (2008). Nanoparticle-mediated cellular response is size-dependent. *Nature Nanotechnology, 3*(3), 145-150. doi:10.1038/nnano.2008.30

Jing, W., Xiaolan, C., Yu, C., Feng, Q., & Haifeng, Y. (2022). Pharmacological effects and mechanisms of tannic acid. *Biomedicine & Pharmacotherapy, 154*, 113561. doi:10.1016/j.biopha.2022.113561

Jolley, K. A., & Maiden, M. C. J. (2010). BIGSdb: Scalable analysis of bacterial genome variation at the population level. *BMC Bioinformatics, 11*(1), 595. doi:10.1186/1471-2105-11-595

Josse, J., Laurent, F., & Diot, A. (2017). Staphylococcal adhesion and host cell invasion: fibronectin-binding and other mechanisms. *Frontiers in Microbiology, 8*, 2433. doi: 10.3389/fmicb.2017.02433

Joyce, P., Ulmefors, H., Maghrebi, S., Subramaniam, S., Wignall, A., Jõemetsa, S., . . . Prestidge, C. A. (2020). Enhancing the cellular uptake and antibacterial activity of rifampicin through encapsulation in mesoporous silica nanoparticles. *Nanomaterials, 10*(4). doi:10.3390/nano10040815

Jung, D., Park, S., Ruffini, J., Dufour, S., & Ronholm, J. (2021). Draft genome sequences of 113 Escherichia coli strains isolated from intramammary infections in dairy cattle. *Microbiology Resource Announcements, 10*(7), e01464-01420. doi:10.1128/mra.01464-20

Kaatz, G. W., McAleese, F., & Seo, S. M. (2005). Multidrug resistance in Staphylococcus aureus due to overexpression of a novel multidrug and toxin extrusion (MATE) transport protein. *Antimicrobial Agents and Chemotherapy, 49*(5), 1857-1864. doi:10.1128/AAC.49.5.1857-1864.2005

Kaim, A. H., Wischer, T., O'Reilly, T., Jundt, G., Fröhlich, J., von Schulthess, G. K., & Allegrini, P. R. (2002). MR imaging with ultrasmall superparamagnetic iron oxide particles in experimental soft-tissue infections in rats. *Radiology, 225*(3), 808-814. doi:10.1148/radiol.2253011485

Kang, J.-j., Liu, Y.-m., Zhao, L.-l., Xu, F., Chen, X.-j., Yan, X., & Li, X.-b. (2018). Elimination of ceftiofur hydrochloride residue in postpartum cows' milk after intramammary infusing at dry-off. *Journal of Integrative Agriculture, 17*(6), 1234-1240. doi:10.1016/S2095-3119(17)61703-9

Katas, H., Hussain, Z., & Ling, T. C. (2012). Chitosan nanoparticles as a percutaneous drug delivery system for hydrocortisone. *Journal of Nanomaterials, 2012*, 45-45. doi:10.1155/2012/372725

Kato, N., Morohoshi, T., Nozawa, T., Matsumoto, H., & Ikeda, T. (2006). Control of gram-negative bacterial quorum sensing with cyclodextrin immobilized cellulose ether gel. *Journal of Inclusion Phenomena and Macrocyclic Chemistry, 56*(1-2), 55-59. doi: 10.1007/s10847-006-9060-y

Kayano, M., Itoh, M., Kusaba, N., Hayashiguchi, O., Kida, K., Tanaka, Y., . . . Gröhn, Y. T. (2018). Associations of the first occurrence of pathogen-specific clinical mastitis with milk yield

and milk composition in dairy cows. *Journal of Dairy Research, 85*(3), 309-316. doi:10.1017/S0022029918000456

Khan, M., Weary, D., & Von Keyserlingk, M. (2011). Invited review: effects of milk ration on solid feed intake, weaning, and performance in dairy heifers. *Journal of Dairy Science, 94*(3), 1071-1081. doi:10.3168/jds.2010-3733

Khan, M. Z., Khan, A., Xiao, J., Ma, J., Ma, Y., Chen, T., . . . Cao, Z. (2020). Overview of research development on the role of NF-κB signaling in mastitis. *Animals, 10*(9). doi:10.3390/ani10091625

Khosravi, A. D., Jenabi, A., & Montazeri, E. A. (2017). Distribution of genes encoding resistance to aminoglycoside modifying enzymes in methicillin-resistant Staphylococcus aureus (MRSA) strains. *The Kaohsiung Journal of Medical Sciences, 33*(12), 587-593. doi:10.1016/j.kjms.2017.08.001

Kong, R., Kang, O.-H., Seo, Y.-S., Mun, S.-H., Zhou, T., Shin, D.-W., & Kwon, D.-Y. (2016). The inhibition effect of chlorpromazine against the β-lactam resistance of MRSA. *Asian Pacific Journal of Tropical Medicine, 9*(6), 542-546. doi:10.1016/j.apjtm.2016.04.008

Kulshrestha, S., Qayyum, S., & Khan, A. U. (2017). Antibiofilm efficacy of green synthesized graphene oxide-silver nanocomposite using Lagerstroemia speciosa floral extract: a comparative study on inhibition of gram-positive and gram-negative biofilms. *Microbial Pathogenesis, 103*, 167-177. doi:10.1016/j.micpath.2016.12.022

Kumar, L., Brenner, N., Brice, J., Klein-Seetharaman, J., & Sarkar, S. K. (2021). Cephalosporins interfere with quorum sensing and improve the ability of Caenorhabditis elegans to survive Pseudomonas aeruginosa infection. *Frontiers in Microbiology, 12*, 598498-598498. doi:10.3389/fmicb.2021.598498

Kumar, S., & Varela, M. F. (2012). Biochemistry of bacterial multidrug efflux pumps. *International Journal of Molecular Sciences, 13*(4), 4484-4495. doi:10.3390/ijms13044484

Kvist, M., Hancock, V., & Klemm, P. (2008). Inactivation of efflux pumps abolishes bacterial biofilm formation. *Applied and Environmental Microbiology, 74*(23), 7376-7382. doi:10.1128/aem.01310-08

Kwak, Y.-K., Vikström, E., Magnusson, K.-E., Vécsey-Semjén, B., Colque-Navarro, P., & Möllby, R. (2012). The Staphylococcus aureus alpha-toxin perturbs the barrier function in

Caco-2 epithelial cell monolayers by altering junctional integrity. *Infection and Immunity, 80*(5), 1670-1680. doi:10.1128/IAI.00001-12

Kyaw, B. M., Arora, S., & Lim, C. S. (2012). Bactericidal antibiotic-phytochemical combinations against methicillin resistant Staphylococcus aureus. *Brazilian Journal of Microbiology, 43*(3), 938-945. doi:10.1590/s1517-838220120003000013

Lakin, S. M., Dean, C., Noyes, N. R., Dettenwanger, A., Ross, A. S., Doster, E., . . . Boucher, C. (2017). MEGARes: an antimicrobial resistance database for high throughput sequencing. *Nucleic Acids Research, 45*(D1), D574-D580. doi:10.1093/nar/gkw1009

Lam, S. J., O'Brien-Simpson, N. M., Pantarat, N., Sulistio, A., Wong, E. H., Chen, Y.-Y., . . . Reynolds, E. C. (2016). Combating multidrug-resistant Gram-negative bacteria with structurally nanoengineered antimicrobial peptide polymers. *Nature Microbiology, 1*(11), 1-11. doi:10.1038/nmicrobiol.2016.162

Lammers, A., Nuijten, P. J., & Smith, H. E. (1999). The fibronectin binding proteins of Staphylococcus aureus are required for adhesion to and invasion of bovine mammary gland cells. *FEMS Microbiology Letters, 180*(1), 103-109. doi: 10.1111/j.1574-6968.1999.tb08783.x

Landin, H., Mörk, M. J., Larsson, M., & Waller, K. P. (2015). Vaccination against Staphylococcus aureus mastitis in two Swedish dairy herds. *Acta Veterinaria Scandinavica, 57*(1), 1-6. doi: 10.1186/s13028-015-0171-6

Larsen, J., Raisen, C. L., Ba, X., Sadgrove, N. J., Padilla-González, G. F., Simmonds, M. S. J., . . . Larsen, A. R. (2022). Emergence of methicillin resistance predates the clinical use of antibiotics. *Nature, 602*(7895), 135-141. doi:10.1038/s41586-021-04265-w

Latasa, C., Roux, A., Toledo-Arana, A., Ghigo, J. M., Gamazo, C., Penadés, J. R., & Lasa, I. (2005). BapA, a large secreted protein required for biofilm formation and host colonization of Salmonella enterica serovar Enteritidis. *Molecular Microbiology, 58*(5), 1322-1339. doi: 10.1111/j.1365-2958.2005.04907.x

Le, K. Y., & Otto, M. (2015). Quorum-sensing regulation in staphylococci-an overview. *Frontiers of Microbiology, 6*, 1174. doi:10.3389/fmicb.2015.01174

Lewis, K. J. N. R. M. (2007). Persister cells, dormancy and infectious disease. *Nature Reviews Microbioliology,* **5**, 48–56. doi: 10.1038/nrmicro1557

Li, W., Xue, M., Yu, L., Qi, K., Ni, J., Chen, X., . . . Xue, T. (2020). QseBC is involved in the biofilm formation and antibiotic resistance in Escherichia coli isolated from bovine mastitis. *PeerJ, 8*, e8833-e8833. doi:10.7717/peerj.8833

Liang, D., Li, F., Fu, Y., Cao, Y., Song, X., Wang, T., . . . Zhang, N. (2014). Thymol inhibits LPS-stimulated inflammatory response via down-regulation of NF-κB and MAPK signaling pathways in mouse mammary epithelial cells. *Inflammation, 37*(1), 214-222. doi:10.1007/s10753-013-9732-x

Linde, A., Ross, C. R., Davis, E. G., Dib, L., Blecha, F., & Melgarejo, T. (2008). Innate immunity and host defense peptides in veterinary medicine. *Journal of Veterinary Internal Medicine, 22*(2), 247-265. doi:10.1111/j.1939-1676.2007.0038.x

Lucia Appleton, S., Navarro-Orcajada, S., Martínez-Navarro, F. J., Caldera, F., López-Nicolás, J. M., Trotta, F., & Matencio, A. (2021). Cyclodextrins as anti-inflammatory agents: Basis, drugs and perspectives. *Biomolecules, 11*(9). doi:10.3390/biom11091384

Lustriane, C., Dwivany, F. M., Suendo, V., & Reza, M. (2018). Effect of chitosan and chitosan-nanoparticles on post harvest quality of banana fruits. *Journal of Plant Biotechnology, 45*(1), 36-44. doi:10.5010/JPB.2018.45.1.036

Mah, T. F. (2012). Biofilm-specific antibiotic resistance. *Future Microbiology, 7*(9), 1061-1072. doi:10.2217/fmb.12.76

Maity, S., & Ambatipudi, K. (2021). Mammary microbial dysbiosis leads to the zoonosis of bovine mastitis: a One-Health perspective. *FEMS Microbiology Ecology, 97*(1), fiaa241. doi:10.1093/femsec/fiaa241

Majumder, S., Eckersall, P. D., & George, S. (2023). Bovine mastitis: examining factors contributing to treatment failure and prospects of nano-enabled antibacterial combination therapy. *ACS Agricultural Science & Technology, 3*(7), 562-582. doi:10.1021/acsagscitech.3c00066

Majumder, S., & George, S. (2023). Multi-functional properties of halloysite nano-clays in food safety and security. In *Materials Science and Engineering in Food Product Development* (261-277). doi: 10.1002/9781119860594.ch13

Majumder, S., Huang, S., Zhou, J., Wang, Y., & George, S. (2023). Tannic acid-loaded halloysite clay grafted with silver nanoparticles enhanced the mechanical and antimicrobial properties of soy protein isolate films for food-packaging applications. *Food Packaging and Shelf Life, 39*, 101142. doi:10.1016/j.fpsl.2023.101142

Majumder, S., Jung, D., Ronholm, J., & George, S. (2021). Prevalence and mechanisms of antibiotic resistance in Escherichia coli isolated from mastitic dairy cattle in Canada. *BMC Microbiology, 21*(1), 222. doi:10.1186/s12866-021-02280-5

Majumder, S., Sackey, T., Viau, C., Park, S., Xia, J., Ronholm, J., & George, S. (2023). Genomic and phenotypic profiling of Staphylococcus aureus isolates from bovine mastitis for antibiotic resistance and intestinal infectivity. *BMC Microbiology, 23*(1), 43. doi:10.1186/s12866-023-02785-1

Majumder, S., Viau, C., Brar, A., Xia, J., & George, S. (2022). Silver nanoparticles grafted onto tannic acid-modified halloysite clay eliminated multidrug-resistant Salmonella Typhimurium in a Caenorhabditis elegans model of intestinal infection. *Applied Clay Science*, 106569. doi:10.1016/j.clay.2022.106569

Makovec, J. A., & Ruegg, D. P. L. (2003). Antimicrobial resistance of bacteria isolated from dairy cow milk samples submitted for bacterial culture: 8,905 samples (1994–2001). *Journal of the American Veterinary Medical Association, 222*(11), 1582-1589. doi:10.2460/javma.2003.222.1582

Manyi-Loh, C. E., Mamphweli, S. N., Meyer, E. L., Makaka, G., Simon, M., & Okoh, A. I. (2016). An overview of the control of bacterial pathogens in cattle manure. *Journal of Veterinary Internal Medicine, 13*(9). doi:10.3390/ijerph13090843

Mattmiller, S., Corl, C., Gandy, J., Loor, J., & Sordillo, L. (2011). Glucose transporter and hypoxia-associated gene expression in the mammary gland of transition dairy cattle. *Journal of Dairy Science, 94*(6), 2912-2922. doi:10.3168/jds.2010-3936

Maya, S., Indulekha, S., Sukhithasri, V., Smitha, K., Nair, S. V., Jayakumar, R., & Biswas, R. (2012). Efficacy of tetracycline encapsulated O-carboxymethyl chitosan nanoparticles against intracellular infections of Staphylococcus aureus. *International Journal of Biological Macromolecules, 51*(4), 392-399. doi:10.1016/j.ijbiomac.2012.06.009

Mazmanian, S. K., Skaar, E. P., Gaspar, A. H., Humayun, M., Gornicki, P., Jelenska, J., . . . Schneewind, O. (2003). Passage of heme-iron across the envelope of Staphylococcus aureus. *Science, 299*(5608), 906-909. doi:10.1126/science.1081147

McDougall, S. (2003). Intramammary treatment of clinical mastitis of dairy cows with a combination of lincomycin and neomycin, or penicillin and dihydrostreptomycin. *New Zealand Veterinary Journal, 51*(3), 111-116. doi:10.1080/00480169.2003.36349

McDougall, S., Agnew, K. E., Cursons, R., Hou, X. X., & Compton, C. R. W. (2007). Parenteral treatment of clinical mastitis with tylosin base or penethamate hydriodide in dairy cattle. *Journal of Dairy Science, 90*(2), 779-789. doi:10.3168/jds.S0022-0302(07)71562-X

McDougall, S., Clausen, L., Hintukainen, J., & Hunnam, J. (2019). Randomized, controlled, superiority study of extended duration of therapy with an intramammary antibiotic for treatment of clinical mastitis. *Journal of Dairy Science, 102*(5), 4376-4386. doi:10.3168/jds.2018-15141

McDougall, S., Clausen, L. M., Hussein, H. M., & Compton, C. W. R. (2022). Therapy of subclinical mastitis during lactation. *Antibiotics, 11*(2), 209. doi:10.3390/antibiotics11020209

McKenney, D., Hübner, J., Muller, E., Wang, Y., Goldmann, D. A., & Pier, G. B. (1998). The ica locus of Staphylococcus epidermidis encodes production of the capsular polysaccharide/adhesin. *Infection and Immunity, 66*(10), 4711-4720. doi: 10.1128/iai.66.10.4711-4720.1998

McLeod, T. F., Manyan, D. R., & Yunis, A. A. (1977). The cellular transport of chloramphenicol and thiamphenicol. *Journal of Laboratory and Clinical Medicine, 90*(2), 347-353. PMID: 267694

Medina-Estrada, I., López-Meza, J. E., & Ochoa-Zarzosa, A. (2016). Anti-inflammatory and antimicrobial effects of estradiol in bovine mammary epithelial cells during Staphylococcus aureus internalization. *Mediators of Inflammation, 2016*. doi: 10.1155/2016/6120509

Mehrzad, J., Desrosiers, C., Lauzon, K., Robitaille, G., Zhao, X., & Lacasse, P. (2005). Proteases involved in mammary tissue damage during endotoxin-induced mastitis in dairy cows. *Journal of Dairy Science, 88*(1), 211-222. doi:10.3168/jds.S0022-0302(05)72679-5

Meng, Y., Li, W., Pan, X., & Gadd, G. M. (2020). Applications of nanozymes in the environment. *Environmental Science: Nano, 7*(5), 1305-1318. doi:10.1039/C9EN01089K

Merrill, C., Ensermu, D., Abdi, R., Gillespie, B., Vaughn, J., Headrick, S., . . . Dego, O. K. (2019). Immunological responses and evaluation of the protection in dairy cows vaccinated with staphylococcal surface proteins. *Veterinary Immunology and Immunopathology, 214*, 109890. doi: 10.1016/j.vetimm.2019.109890

Middleton, J. R., Ma, J., Rinehart, C. L., Taylor, V. N., Luby, C. D., & Steevens, B. J. (2006). Efficacy of different Lysigin (TM) formulations in the prevention of Staphylococcus

aureus intramammary infection in dairy heifers. *The Journal of Dairy Research, 73*(1), 10. doi: 10.1017/S0022029905001354

Middleton, J. R., Saeman, A., Fox, L. K., Lombard, J., Hogan, J. S., & Smith, K. L. (2014). The National Mastitis Council: a global organization for mastitis control and milk quality, 50 years and beyond. *Journal of Mammary Gland Biology and Neoplasia, 19*(3-4), 241-251. doi: 10.1007/s10911-014-9328-6

Miller, M. J., Zhu, H., Xu, Y., Wu, C., Walz, A. J., Vergne, A., . . . McKee-Dolence, J. (2009). Utilization of microbial iron assimilation processes for the development of new antibiotics and inspiration for the design of new anticancer agents. *Biometals, 22*(1), 61. doi: 10.1007/s10534-008-9185-0

Mndlovu, H., du Toit, L. C., Kumar, P., & Choonara, Y. E. (2023). Tannic acid-loaded chitosan-RGD-alginate scaffolds for wound healing and skin regeneration. *Biomedical Materials, 18*(4), 045009. doi:10.1088/1748-605X/acce88

Möllmann, U., Heinisch, L., Bauernfeind, A., Köhler, T., & Ankel-Fuchs, D. (2009). Siderophores as drug delivery agents: application of the "Trojan Horse" strategy. *Biometals, 22*(4), 615-624. doi: 10.1007/s10534-009-9219-2

Naess, A., Andreeva, H., & Sørnes, S. (2011). Tigecycline attenuates polymorphonuclear leukocyte (PMN) receptors but not functions. *Acta Pharmaceutica, 61*(3), 297-302. doi:10.2478/v10007-011-0024-4

Narui, K., Noguchi, N., Wakasugi, K., & Sasatsu, M. (2002). Cloning and characterization of a novel chromosomal drug efflux gene in Staphylococcus aureus. *Biological and Pharmaceutical Bulletin, 25*(12), 1533-1536. doi:10.1248/bpb.25.1533

Nasti, A., Zaki, N. M., De Leonardis, P., Ungphaiboon, S., Sansongsak, P., Rimoli, M. G., & Tirelli, N. (2009). Chitosan/TPP and chitosan/TPP-hyaluronic acid nanoparticles: systematic optimisation of the preparative process and preliminary biological evaluation. *Pharmaceutical Research, 26*, 1918-1930. doi:10.1007/s11095-009-9908-0

Neave, F., Dodd, F., Kingwill, R., & Westgarth, D. (1969). Control of mastitis in the dairy herd by hygiene and management. *Journal of Dairy Science, 52*(5), 696-707. doi: 10.3168/jds.S0022-0302(69)86632-4

Neyfakh, A. A., Borsch, C., & Kaatz, G. (1993). Fluoroquinolone resistance protein NorA of Staphylococcus aureus is a multidrug efflux transporter. *Antimicrobial Agents and Chemotherapy, 37*(1), 128-129. doi:10.1128/AAC.37.1.128

Nichols, S. (2022). Chapter 23.2 - Chronic udder abscess. In J. A. Orsini, N. S. Grenager, & A. de Lahunta (Eds.), *Comparative Veterinary Anatomy* (1236-1241): Academic Press. doi: 10.1016/B978-0-323-91015-6.00113-8

Nishino, K., Yamada, J., Hirakawa, H., Hirata, T., & Yamaguchi, A. (2003). Roles of TolC-dependent multidrug transporters of Escherichia coli in resistance to beta-lactams. *Antimicrobial Agents of Chemotherapy, 47*(9), 3030-3033. doi:10.1128/aac.47.9.3030-3033.2003

Nistorescu, S., Gradisteanu Pircalabioru, G., Udrea, A.-M., Simon, Á., Pascu, M. L., & Chifiriuc, M.-C. (2020). Laser-irradiated Chlorpromazine as a potent anti-biofilm agent for coating of biomedical devices. *Coatings, 10*(12), 1230. doi:10.3390/coatings10121230

Normanno, G., La Salandra, G., Dambrosio, A., Quaglia, N., Corrente, M., Parisi, A., . . . Celano, G. (2007). Occurrence, characterization and antimicrobial resistance of enterotoxigenic Staphylococcus aureus isolated from meat and dairy products. *International Journal of Food Microbiology, 115*(3), 290-296. doi: 10.1016/j.ijfoodmicro.2006.10.049

Notebaert, S., & Meyer, E. (2006). Mouse models to study the pathogenesis and control of bovine mastitis. A review. *Veterinary Quarterly, 28*(1), 2-13. doi:10.1080/01652176.2006.9695201

O'Reilly, L. P., Luke, C. J., Perlmutter, D. H., Silverman, G. A., & Pak, S. C. (2014). C. elegans in high-throughput drug discovery. *Advanced Drug Delivery Reviews, 69-70*, 247-253. doi:10.1016/j.addr.2013.12.001

Oh, N., & Park, J. H. (2014). Endocytosis and exocytosis of nanoparticles in mammalian cells. *International journal of nanomedicine, 9 Suppl 1*(Suppl 1), 51-63. doi:10.2147/ijn.S26592

Ojkic, N., Serbanescu, D., & Banerjee, S. (2022). Antibiotic Resistance via Bacterial Cell Shape-Shifting. *mBio, 13*(3), e0065922. doi:10.1128/mbio.00659-22

Olaitan, A. O., Morand, S., & Rolain, J.-M. (2014). Mechanisms of polymyxin resistance: acquired and intrinsic resistance in bacteria. *Frontiers in Microbiology, 5*(643). doi:10.3389/fmicb.2014.00643

Oliver, S., & Mitchell, B. (1984). Prevalence of mastitis pathogens in herds participating in a mastitis control program. *Journal of Dairy Science, 67*(10), 2436-2440. doi: 10.3168/jds.S0022-0302(84)81592-1

Olson, M. A., Siebach, T. W., Griffitts, J. S., Wilson, E., & Erickson, D. L. (2018). Genome-wide identification of fitness factors in mastitis-associated Escherichia coli. *Applied and Environmental Microbiology, 84*(2), e02190-02117. doi:10.1128/AEM.02190-17

Ortíz-Castro, R., Martínez-Trujillo, M., & López-Bucio, J. (2008). N-acyl-L-homoserine lactones: a class of bacterial quorum-sensing signals alter post-embryonic root development in Arabidopsis thaliana. *Plant Cell Environment, 31*(10), 1497-1509. doi:10.1111/j.1365-3040.2008.01863.x

Oye, V. (1999). A multilocation clinical trial in lactating dairy cows affected with clinical mastitis to compare the efficacy of treatment with intramammary infusions of a lincomycin/neomycin combination with an ampicillin/cloxacillin combination. *Journal of Veterinary Pharmacology and Therapeutics, 22*(4), 274-282. doi:10.1046/j.1365-2885.1999.00205.x

Paharik, A. E., & Horswill, A. R. (2016). The Staphylococcal Biofilm: Adhesins, Regulation, and Host Response. *Microbiology Spectrum, 4*(2), 10.1128/microbiolspec.VMBF-0022-2015. doi:10.1128/microbiolspec.VMBF-0022-2015

Pal, C., Bengtsson-Palme, J., Kristiansson, E., & Larsson, D. J. (2015). Co-occurrence of resistance genes to antibiotics, biocides and metals reveals novel insights into their co-selection potential. *BMC Genomics, 16*(1), 964. doi:10.1186/s12864-015-2153-5

Park, K. H., Kurokawa, K., Zheng, L., Jung, D. J., Tateishi, K., Jin, J. O., . . . Lee, B. L. (2010). Human serum mannose-binding lectin senses wall teichoic acid Glycopolymer of Staphylococcus aureus, which is restricted in infancy. *Journal of Biological Chemistry, 285*(35), 27167-27175. doi:10.1074/jbc.M110.141309

Park, S., Classen, A., Gohou, H. M., Maldonado, R., Kretschmann, E., Duvernay, C., . . . Ronholm, J. (2021). A new, reliable, and high-throughput strategy to screen bacteria for antagonistic activity against Staphylococcus aureus. *BMC Microbiology, 21*(1), 189. doi:10.1186/s12866-021-02265-4

Park, S., Jung, D., Dufour, S., & Ronholm, J. (2020). Draft genome sequences of 27 Staphylococcus aureus strains and 3 Staphylococcus species strains isolated from bovine intramammary infections. *Microbiology Resource Announcements, 9*(19), e00300-00320. doi:10.1128/MRA.00300-20

Park, S., Jung, D., O'Brien, B., Ruffini, J., Dussault, F., Dube-Duquette, A., . . . Ronholm, J. (2022). Comparative genomic analysis of Staphylococcus aureus isolates associated with

either bovine intramammary infections or human infections demonstrates the importance of restriction-modification systems in host adaptation. *Microbial Genomics, 8*(2). doi:10.1099/mgen.0.000779

Park, S., & Ronholm, J. (2021). Staphylococcus aureus in agriculture: Lessons in evolution from a multispecies pathogen. *Clinical Microbiology Reviews, 34*(2). doi:10.1128/cmr.00182-20

Petrovski, K., Buneski, G., & Trajcev, M. (2006). A review of the factors affecting the costs of bovine mastitis. *Journal of the South African Veterinary Association, 77*(2), 52-60. doi: 10.4102/jsava.v77i2.344

Piddock, L. J. (1996). Does the use of antimicrobial agents in veterinary medicine and animal husbandry select antibiotic-resistant bacteria that infect man and compromise antimicrobial chemotherapy? *Journal of Antimicrobial Chemotherapy, 38*(1), 1-3. doi:10.1093/jac/38.1.1

Pissuwan, D., Niidome, T., & Cortie, M. B. (2011). The forthcoming applications of gold nanoparticles in drug and gene delivery systems. *Journal of Controlled Release, 149*(1), 65-71. doi:10.1016/j.jconrel.2009.12.006

Poole, K. (2000). Efflux-mediated resistance to fluoroquinolones in gram-positive bacteria and the mycobacteria. *Antimicrobial Agents and Chemotherapy, 44*(10), 2595-2599. doi:10.1128/aac.44.10.2595-2599.2000

Prabhakaran, P., Ashraf, M. A., & Aqma, W. S. (2016). Microbial stress response to heavy metals in the environment. *RSC Advances, 6*(111), 109862-109877. doi:10.1039/C6RA10966G

Pragman, A. A., Yarwood, J. M., Tripp, T. J., & Schlievert, P. M. (2004). Characterization of virulence factor regulation by SrrAB, a two-component system in Staphylococcus aureus. *Journal of Bacteriology, 186*(8), 2430-2438. doi: 10.1128/JB.186.8.2430-2438.2004

Prenafeta, A., March, R., Foix, A., Casals, I., & Costa, L. (2010). Study of the humoral immunological response after vaccination with a Staphylococcus aureus biofilm-embedded bacterin in dairy cows: Possible role of the exopolysaccharide specific antibody production in the protection from Staphylococcus aureus induced mastitis. *Veterinary Immunology and Immunopathology, 134*(3), 208-217. doi:10.1016/j.vetimm.2009.09.020

Proctor, R. A., Kahl, B., von Eiff, C., Vaudaux, P. E., Lew, D. P., & Peters, G. (1998). Staphylococcal small colony variants have novel mechanisms for antibiotic resistance. *Clinical Infectious Diseases, 27*(Supplement_1), S68-S74. doi: 10.1086/514906

Prosser, C., Davis, S., Farr, V., & Lacasse, P. (1996). Regulation of blood flow in the mammary microvasculature. *Journal of Dairy Science, 79*(7), 1184-1197. doi:10.3168/jds.S0022-0302(96)76472-X

Pyörälä, S., & Pyörälä, E. O. (1998). Efficacy of parenteral administration of three antimicrobial agents in treatment of clinical mastitis in lactating cows: 487 cases (1989-1995). *Journal of the American Veterinary Medical Association, 212*(3), 407-412. doi: 10.2460/javma.1998.212.03.407

Radziwill-Bienkowska, J. M., Talbot, P., Kamphuis, J. B. J., Robert, V., Cartier, C., Fourquaux, I., . . . Mercier-Bonin, M. (2018). Toxicity of food-grade TiO2 to commensal intestinal and transient food-borne bacteria: New insights using nano-sims and synchrotron uv fluorescence imaging. *Frontiers in Microbiology, 9*. doi:10.3389/fmicb.2018.00794

Reinders, A., Hee, C.-S., Ozaki, S., Mazur, A., Boehm, A., Schirmer, T., & Jenal, U. (2016). Expression and genetic activation of cyclic Di-GMP-specific phosphodiesterases in Escherichia coli. *Journal of Bacteriology, 198*(3), 448-462. doi:10.1128/jb.00604-15

Renna, M. S., Silvestrini, P., Beccaria, C., Velázquez, N. S., Baravalle, C., Engler, C., . . . Dallard, B. E. (2019). Effects of chronic Staphylococcus aureus infection on immunological parameters and functionality of macrophages isolated from bovine mammary secretions. *Microbial Pathogenesis, 137*, 103743. doi: 10.1016/j.micpath.2019.103743

Rensing, C., Mitra, B., & Rosen, B. P. (1997). The zntA gene of Escherichia coli encodes a Zn (II)-translocating P-type ATPase. *Proceedings of the National Academy of Sciences, 94*(26), 14326-14331. doi:10.1073/pnas.94.26.14326

Reygaert, W. C. (2018). An overview of the antimicrobial resistance mechanisms of bacteria. *AIMS Microbiology, 4*(3), 482-501. doi:10.3934/microbiol.2018.3.482

Reyher, K. K., Dufour, S., Barkema, H. W., Des Côteaux, L., DeVries, T. J., Dohoo, I. R., . . . Scholl, D. T. (2011). The national cohort of dairy farms—a data collection platform for mastitis research in Canada. *Journal of Dairy Science, 94*(3), 1616-1626. doi:10.3168/jds.2010-3180

Ribeiro, M., & Simões, M. (2019). Advances in the antimicrobial and therapeutic potential of siderophores. *Environmental Chemistry Letters, 17*(4), 1485-1494. doi:10.1007/s10311-019-00887-9

Rice, K., Peralta, R., Bast, D., de Azavedo, J., & McGavin, M. J. (2001). Description of staphylococcus serine protease (ssp) operon in Staphylococcus aureus and nonpolar

inactivation of sspA-encoded serine protease. *Infection and Immunity, 69*(1), 159-169. doi:10.1128/IAI.69.1.159-169.2001

Richter, K., Thomas, N., Zhang, G., Prestidge, C. A., Coenye, T., Wormald, P.-J., & Vreugde, S. (2017). Deferiprone and gallium-protoporphyrin have the capacity to potentiate the activity of antibiotics in Staphylococcus aureus small colony variants. *Frontiers in Cellular and Infection Microbiology, 7*, 280. doi:10.3389/fcimb.2017.00280

Ridley, R. A., Douglas, I., & Whawell, S. A. (2012). Differential adhesion and invasion by Staphylococcus aureus of epithelial cells derived from different anatomical sites. *Journal of Medical Microbiology, 61*(12), 1654-1661.

Rivolta, I., Panariti, A., Lettiero, B., Sesana, S., Gasco, P., Gasco, M., . . . Miserocchi, G. (2011). Cellular uptake of coumarin-6 as a model drug loaded in solid lipid nanoparticles. *Journal of Physiology and Pharmacology, 62*(1), 45.

Roberson, J., Warnick, L., & Moore, G. (2004). Mild to moderate clinical mastitis: Efficacy of intramammary amoxicillin, frequent milk-out, a combined intramammary amoxicillin, and frequent milk-out treatment versus no treatment. *Journal of Dairy Science, 87*(3), 583-592. doi:10.3168/jds.S0022-0302(04)73200-2

Roy, J. P., DesCôteaux, L., DuTremblay, D., Beaudry, F., & Elsener, J. (2009). Efficacy of a 5-day extended therapy program during lactation with cephapirin sodium in dairy cows chronically infected with Staphylococcus aureus. *Canadian Veterinary Journal, 50*(12), 1257-1262. PMCID: PMC2777288

Ruegg, P. L. (2017). A 100-year review: mastitis detection, management, and prevention. *Journal of Dairy Science, 100*(12), 10381-10397. doi:10.3168/jds.2017-13023

Rusznyák, Á., Malanga, M., Fenyvesi, É., Szente, L., Váradi, J., Bácskay, I., . . . Fenyvesi, F. (2021). Investigation of the cellular effects of beta- cyclodextrin derivatives on Caco-2 intestinal epithelial cells. *Pharmaceutics, 13*(2). doi:10.3390/pharmaceutics13020157

Ryman, V. E., Packiriswamy, N., & Sordillo, L. M. (2015). Role of endothelial cells in bovine mammary gland health and disease. *Animal Health Research Reviews, 16*(2), 135-149. doi:10.1017/S1466252315000158

Sağlam, A. G., Şahin, M., Çelik, E., Çelebi, Ö., Akça, D., & Otlu, S. (2017). The role of staphylococci in subclinical mastitis of cows and lytic phage isolation against to Staphylococcus aureus. *Veterinary World, 10*(12), 1481-1485. doi:10.14202/vetworld.2017.1481-1485

Sahay, G., Alakhova, D. Y., & Kabanov, A. V. (2010). Endocytosis of nanomedicines. *Journal of Controlled Release, 145*(3), 182-195. doi:10.1016/j.jconrel.2010.01.036

Saini, V., McClure, J. T., Léger, D., Dufour, S., Sheldon, A. G., Scholl, D. T., & Barkema, H. W. (2012). Antimicrobial use on Canadian dairy farms. *Journal of Dairy Science, 95*(3), 1209-1221. doi:10.3168/jds.2011-4527

Saini, V., McClure, J. T., Léger, D., Keefe, G. P., Scholl, D. T., Morck, D. W., & Barkema, H. W. (2012). Antimicrobial resistance profiles of common mastitis pathogens on Canadian dairy farms. *Journal of Dairy Science, 95*(8), 4319-4332. doi:10.3168/jds.2012-5373

Sana, S., Datta, S., Biswas, D., & Sengupta, D. (2018). Assessment of synergistic antibacterial activity of combined biosurfactants revealed by bacterial cell envelop damage. *Biochimica et Biophysica Acta (BBA) - Biomembranes, 1860*(2), 579-585. doi:10.1016/j.bbamem.2017.09.027

Sandvig, K., Pust, S., Skotland, T., & van Deurs, B. (2011). Clathrin-independent endocytosis: mechanisms and function. *Current Opinion in Cell Biology, 23*(4), 413-420. doi:10.1016/j.ceb.2011.03.007

Schalk, I. J. (2018). Siderophore-antibiotic conjugates: exploiting iron uptake to deliver drugs into bacteria. *Clinical Microbiology and Infection, 24*(8), 801-802. doi:10.1016/j.cmi.2018.03.037

Schmidt, T., Kock, M. M., & Ehlers, M. M. (2017). Molecular characterization of Staphylococcus aureus isolated from bovine mastitis and close human contacts in south african dairy herds: genetic diversity and inter-species host transmission. *Frontiers in Microbiology, 8*. doi:10.3389/fmicb.2017.00511

Schukken, Y., Bronzo, V., Locatelli, C., Pollera, C., Rota, N., Casula, A., . . . Zalduendo, D. (2014). Efficacy of vaccination on Staphylococcus aureus and coagulase-negative staphylococci intramammary infection dynamics in 2 dairy herds. *Journal of Dairy Science, 97*(8), 5250-5264. doi: 10.3168/jds.2014-8008

Schwaiger, K., Harms, K. S., Bischoff, M., Preikschat, P., Mölle, G., Bauer-Unkauf, I., . . . Hölzel, C. S. (2014). Insusceptibility to disinfectants in bacteria from animals, food and humans-is there a link to antimicrobial resistance? *Frontiers in Microbiology, 5*, 88. doi:10.3389/fmicb.2014.00088

Seemann, T. (2014). Prokka: rapid prokaryotic genome annotation. *Bioinformatics, 30*(14), 2068-2069. doi:10.1093/bioinformatics/btu153

Sérieys, F., Raguet, Y., Goby, L., Schmidt, H., & Friton, G. (2005). Comparative efficacy of local and systemic antibiotic treatment in lactating cows with clinical mastitis. *Journal of Dairy Science, 88*(1), 93-99. doi:10.3168/jds.S0022-0302(05)72666-7

Seukep, A. J., Kuete, V., Nahar, L., Sarker, S. D., & Guo, M. (2020). Plant-derived secondary metabolites as the main source of efflux pump inhibitors and methods for identification. *Journal of Pharmaceutical Analysis, 10*(4), 277-290. doi:10.1016/j.jpha.2019.11.002

Shaheen, M., Tantary, H., & Nabi, S. (2016). A treatise on bovine mastitis: disease and disease economics, etiological basis, risk factors, impact on human health, therapeutic management, prevention and control strategy. *Advances in Dairy Research*, 1-10. doi:10.4172/2329-888X.1000150

Shao, L., Majumder, S., Liu, Z., Xu, K., Dai, R., & George, S. (2022). Light activation of gold nanorods but not gold nanospheres enhance antibacterial effect through photodynamic and photothermal mechanisms. *Journal of Photochemistry and Photobiology B: Biology, 231*, 112450. doi:10.1016/j.jphotobiol.2022.112450

Sharma, N., Singh, N., Singh, O., Pandey, V., & Verma, P. (2011). Oxidative stress and antioxidant status during transition period in dairy cows. *Asian-Australasian Journal of Animal Sciences, 24*(4), 479-484. doi:10.5713/ajas.2011.10220

Sharma, S., Ramnani, P., & Virdi, J. S. (2004). Detection and assay of β-lactamases in clinical and non-clinical strains of Yersinia enterocolitica biovar 1A. *Journal of Antimicrobial Chemotherapy, 54*(2), 401-405. doi:10.1093/jac/dkh365

Sharp, J. A., Lefevre, C., Brennan, A. J., & Nicholas, K. R. (2007). The fur seal—a model lactation phenotype to explore molecular factors involved in the initiation of apoptosis at involution. *Journal of Mammary Gland Biology and Neoplasia, 12*(1), 47-58. doi:10.1007/s10911-007-9037-5

Shephard, R., Burman, S., & Marcun, P. (2004). A comparative field trial of cephalonium and cloxacillin for dry cow therapy for mastitis in Australian dairy cows. *Australian Veterinary Journal, 82*(10), 624-629. doi:10.1111/j.1751-0813.2004.tb12610.x

Shi, S. F., Jia, J. F., Guo, X. K., Zhao, Y. P., Chen, D. S., Guo, Y. Y., & Zhang, X. L. (2016). Reduced Staphylococcus aureus biofilm formation in the presence of chitosan-coated iron oxide nanoparticles. *International Journal of Nanomedicine, 11*, 6499-6506. doi:10.2147/ijn.S41371

Sifri, C. D., Begun, J., Ausubel, F. M., & Calderwood, S. B. (2003). Caenorhabditis elegans as a model host for Staphylococcus aureus pathogenesis. *Infection and Immunity, 71*(4), 2208-2217. doi:10.1128/IAI.71.4.2208-2217.2003

Singh, B. N., Prateeksha, Upreti, D. K., Singh, B. R., Defoirdt, T., Gupta, V. K., . . . Vahabi, K. (2017). Bactericidal, quorum quenching and anti-biofilm nanofactories: a new niche for nanotechnologists. *Critical Reviews in Biotechnology, 37*(4), 525-540. doi:10.1080/07388551.2016.1199010

Singh, R., Ray, P., Das, A., & Sharma, M. (2009). Role of persisters and small-colony variants in antibiotic resistance of planktonic and biofilm-associated Staphylococcus aureus: an in vitro study. *Journal of Medical Microbiology, 58*(8), 1067-1073. doi: 10.1099/jmm.0.009720-0

Sinha, B., Francois, P., Que, Y. A., Hussain, M., Heilmann, C., Moreillon, P., . . . Herrmann, M. (2000). Heterologously expressed Staphylococcus aureus fibronectin-binding proteins are sufficient for invasion of host cells. *Infection and Immunity, 68*(12), 6871-6878. doi:10.1128/IAI.68.12.6871-6878.2000

Sinha, B., & Fraunholz, M. (2010). Staphylococcus aureus host cell invasion and post-invasion events. *International Journal of Medical Microbiology, 300*(2-3), 170-175. doi: 10.1016/j.ijmm.2009.08.019

Smith, E. J., Visai, L., Kerrigan, S. W., Speziale, P., & Foster, T. J. (2011). The Sbi protein is a multifunctional immune evasion factor of Staphylococcus aureus. *Infection and Immunity, 79*(9), 3801-3809. doi:10.1128/IAI.05075-11

Solarte, A. L., Astorga, R. J., Aguiar, F., Galán-Relaño, Á., Maldonado, A., & Huerta, B. (2017). Combination of antimicrobials and essential oils as an alternative for the control of Salmonella enterica multiresistant strains related to foodborne disease. *Foodborne Pathogens and Disease, 14*(10), 558-563. doi:10.1089/fpd.2017.2295

Soliman, N. M., Shakeel, F., Haq, N., Alanazi, F. K., Alshehri, S., Bayomi, M., . . . Alsarra, I. A. (2022). Development and optimization of ciprofloxacin HCl-loaded chitosan nanoparticles using box-behnken experimental design. *Molecules, 27*(14). doi:10.3390/molecules27144468

Sordillo, L. M., & Streicher, K. L. (2002). Mammary gland immunity and mastitis susceptibility. *Journal of Mammary Gland Biology and Neoplasia, 7*(2), 135-146. doi: 10.1023/a:1020347818725

Steele, M. L., McNAB, W. B., Poppe, C., Griffiths, M. W., Chen, S., DeGrandis, S. A., . . . Odumeru, J. A. (1997). Survey of Ontario bulk tank raw milk for food-borne pathogens. *Journal of Food Protection, 60*(11), 1341-1346. doi: 10.4315/0362-028X-60.11.1341

Stein, C., Makarewicz, O., Bohnert, J. A., Pfeifer, Y., Kesselmeier, M., Hagel, S., & Pletz, M. W. (2015). Three dimensional checkerboard synergy analysis of colistin, meropenem, tigecycline against multidrug-resistant clinical Klebsiella pneumonia isolates. *PLOS One, 10*(6), e0126479. doi:10.1371/journal.pone.0126479

Stella, V. J., Rao, V. M., Zannou, E. A., & Zia, V. (1999). Mechanisms of drug release from cyclodextrin complexes. *Advanced Drug Delivery Reviews, 36*(1), 3-16. doi:10.1016/s0169-409x(98)00052-0

Stelwagen, K., Carpenter, E., Haigh, B., Hodgkinson, A., & Wheeler, T. (2009). Immune components of bovine colostrum and milk. *Journal of Animal Science, 87*(suppl_13), 3-9. doi:10.2527/jas.2008-1377

Stelzner, K., Boyny, A., Hertlein, T., Sroka, A., Moldovan, A., Paprotka, K., . . . Rudel, T. (2021). Intracellular Staphylococcus aureus employs the cysteine protease staphopain A to induce host cell death in epithelial cells. *PLOS Pathogens, 17*(9), e1009874. doi:10.1371/journal.ppat.1009874

Ster, C., Allard, M., Côté-Gravel, J., Boulanger, S., Lacasse, P., & Malouin, F. (2021). Immune and experimental infection responses of dairy cows vaccinated with the combination of six Staphylococcus aureus proteins that are expressed during bovine intramammary infection and a triple adjuvant. *Veterinary Immunology and Immunopathology, 238*, 110290. doi:10.1016/j.vetimm.2021.110290

Sugiyama, M., Watanabe, M., Sonobe, T., Kibe, R., Koyama, S., & Kataoka, Y. (2022). Efficacy of antimicrobial therapy for bovine acute Klebsiella pneumoniae mastitis. *Journal of Veterinary Medical Science, 84*(7), 1023-1028. doi:10.1292/jvms.21-0617

Summary report on antimicrobials sold or distributed for use in food-producing animals. (2022). www.fda.gov: FDA Retrieved from https://www.fda.gov/media/163739/download

Taponen, S., Jantunen, A., Pyörälä, E., & Pyörälä, S. (2003). Efficacy of targeted 5-day combined parenteral and intramammary treatment of clinical mastitis caused by penicillin-susceptible or penicillin-resistant Staphylococcus aureus. *Acta Veterinaria Scandinavica, 44*(1), 53. doi:10.1186/1751-0147-44-53

Taylor, S. L., Wahl-Jensen, V., Copeland, A. M., Jahrling, P. B., & Schmaljohn, C. S. (2013). Endothelial cell permeability during hantavirus infection involves factor XII-dependent increased activation of the kallikrein-kinin system. *PLOS Pathogens, 9*(7), e1003470. doi:10.1371/journal.ppat.1003470

Thammavongsa, V., Kern, J. W., Missiakas, D. M., & Schneewind, O. (2009). Staphylococcus aureus synthesizes adenosine to escape host immune responses. *The Journal of Experimental Medicine, 206*(11), 2417-2427. doi:10.1084/jem.20090097

Thorberg, B. M., Danielsson-Tham, M. L., Emanuelson, U., & Persson Waller, K. (2009). Bovine subclinical mastitis caused by different types of coagulase-negative staphylococci. *Journal of Dairy Science, 92*(10), 4962-4970. doi:10.3168/jds.2009-2184

Tian, X., Wang, P., Li, T., Huang, X., Guo, W., Yang, Y., . . . Jia, X. (2020). Self-assembled natural phytochemicals for synergistically antibacterial application from the enlightenment of traditional Chinese medicine combination. *Acta Pharmaceutica Sinica B, 10*(9), 1784-1795. doi:10.1016/j.apsb.2019.12.014

Tiwari, G., Tiwari, R., & Rai, A. K. (2010). Cyclodextrins in delivery systems: Applications. *Journal of Pharmacy and Bioallied Sciences, 2*(2), 72-79. doi:10.4103/0975-7406.67003

Tong, S. Y., Davis, J. S., Eichenberger, E., Holland, T. L., & Fowler, V. G., Jr. (2015). Staphylococcus aureus infections: epidemiology, pathophysiology, clinical manifestations, and management. *Clinical Microbiology Reviews, 28*(3), 603-661. doi:10.1128/cmr.00134-14

Tong, Z., He, W., Fan, X., & Guo, A. (2022). Biological function of plant tannin and its application in animal health. *Frontiers in Veterinary Science, 8*. doi:10.3389/fvets.2021.803657

Truchetti, G., Bouchard, E., Descôteaux, L., Scholl, D., & Roy, J. P. (2014). Efficacy of extended intramammary ceftiofur therapy against mild to moderate clinical mastitis in Holstein dairy cows: a randomized clinical trial. *Canadian Journal of Veterinary Research, 78*(1), 31-37. doi:10.3168/jds.S0022-0302(04)73361-5

Truong-Bolduc, Q., Dunman, P., Strahilevitz, J., Projan, S., & Hooper, D. (2005). MgrA is a multiple regulator of two new efflux pumps in Staphylococcus aureus. *Journal of Bacteriology, 187*(7), 2395-2405. doi:10.1128/JB.187.7.2395-2405.2005

Tuchscherr, L., Bischoff, M., Lattar, S. M., Llana, M. N., Pförtner, H., Niemann, S., . . . Cheung, A. L. (2015). Sigma factor SigB is crucial to mediate Staphylococcus aureus adaptation during chronic infections. *PLOS Pathogen, 11*(4), e1004870.

Úbeda, C., Maiques, E., Knecht, E., Lasa, Í., Novick, R. P., & Penadés, J. R. (2005). Antibiotic-induced SOS response promotes horizontal dissemination of pathogenicity island-encoded virulence factors in staphylococci. *Molecular Microbiology, 56*(3), 836-844. doi:10.1111/j.1365-2958.2005.04584.x

USDA APHIS. Antibiotic use on U.S. dairy operations, 2002 and 2007. Infosheet, 5p, October, 2008 Retrieved from https://www.aphis.usda.gov/animal_health/nahms/dairy/downloads/dairy07/Dairy07_is_AntibioticUse_1.pdf

Uses of antimicrobials in food animals in Canada: impact on resistance and human health. (2002). Retrieved from https://www.canada.ca/content/dam/hc-sc/migration/hc-sc/dhp-mps/alt_formats/hpfb-dgpsa/pdf/pubs/amr-ram_final_report-rapport_06-27-eng.pdf

Uskoković, V., & Desai, T. A. (2014). Simultaneous bactericidal and osteogenic effect of nanoparticulate calcium phosphate powders loaded with clindamycin on osteoblasts infected with Staphylococcus aureus. *Materials Science and Engineering: C, 37*, 210-222. doi:10.1016/j.msec.2014.01.008

Uthaisangsook, S., Day, N. K., Bahna, S. L., Good, R. A., & Haraguchi, S. (2002). Innate immunity and its role against infections. *Annals of Allergy, Asthma & Immunology, 88*(3), 253-265. doi:10.1016/S1081-1206(10)62005-4

Veh, K. A., Klein, R. C., Ster, C., Keefe, G., Lacasse, P., Scholl, D., . . . Malouin, F. (2015). Genotypic and phenotypic characterization of Staphylococcus aureus causing persistent and nonpersistent subclinical bovine intramammary infections during lactation or the dry period. *Journal of Dairy Science, 98*(1), 155-168. doi:https://doi.org/10.3168/jds.2014-8044

Veterinary new drug list. (2000). www.canada.ca: Governement of Canada Retrieved from https://www.canada.ca/en/health-canada/services/drugs-health-products/veterinary-drugs/legislation-guidelines/guidance-documents/veterinary-new-drug-list.html

Villanueva, X., Zhen, L., Ares, J. N., Vackier, T., Lange, H., Crestini, C., & Steenackers, H. P. (2023). Effect of chemical modifications of tannins on their antimicrobial and antibiofilm effect against Gram-negative and Gram-positive bacteria. *Frontiers in Microbiology, 13*. doi:10.3389/fmicb.2022.987164

Viveros, M., Lopez-Ordaz, R., Gutiérrez, L., Miranda-Calderón, J., & Sumano, H. (2018). Efficacy assessment of an intramammary treatment with a new recrystallized enrofloxacin vs

ceftiofur and parenteral enrofloxacin in dairy cows with nonsevere clinical mastitis. *Journal of Veterinary Pharmacology and Therapeutics, 41*(1), e1-e9. doi:10.1111/jvp.12441

Waller, D. G., & Sampson, A. P. (2018). 51 - Chemotherapy of infections. In D. G. Waller & A. P. Sampson (Eds.), *Medical Pharmacology and Therapeutics (Fifth Edition)* (581-629): Elsevier. doi: 10.1016/B978-0-7020-7167-6.00051-8

Walters, M. C., Roe, F., Bugnicourt, A., Franklin, M. J., Stewart, P. S. J. (2003). Contributions of antibiotic penetration, oxygen limitation, and low metabolic activity to tolerance of Pseudomonas aeruginosa biofilms to ciprofloxacin and tobramycin. *Antimicrobial Agents and Chemotherapy*, *47*(1), 317-323. doi: 10.1128/AAC.47.1.317-323.2003

Wang, L., He, H., Yu, Y., Sun, L., Liu, S., Zhang, C., & He, L. (2014). Morphology-dependent bactericidal activities of Ag/CeO2 catalysts against Escherichia coli. *Journal of Inorganic Biochemistry, 135*, 45-53. doi:10.1016/j.jinorgbio.2014.02.016

Wang, W., Song, Y., Petrovski, K., Eats, P., Trott, D. J., Wong, H. S., . . . Garg, S. (2015). Development of intramammary delivery systems containing lasalocid for the treatment of bovine mastitis: impact of solubility improvement on safety, efficacy, and milk distribution in dairy cattle. *Drug Design, Development, and Therapy, 9*, 631-642. doi:10.2147/dddt.S74731

Wang, X., Wu, J., Li, P., Wang, L., Zhou, J., Zhang, G., . . . Xing, X. (2018). Microenvironment-responsive magnetic nanocomposites based on silver nanoparticles/gentamicin for enhanced biofilm disruption by magnetic field. *ACS Applied Materials & Interfaces, 10*(41), 34905-34915. doi:10.1021/acsami.8b10972

Wittek, T., Mader, C., Ribitsch, V., & Burgstaller, J. (2019). Measurement of oxygen concentration for detection of subclinical mastitis. *Schweiz Arch Tierheilkd, 161*, 659-665. doi:10.17236/sat00228

Worthington, R. J., & Melander, C. (2013). Combination approaches to combat multidrug-resistant bacteria. *Trends in Biotechnology, 31*(3), 177-184. doi:10.1016/j.tibtech.2012.12.006

Wraight, M. (2003). A comparative efficacy trial between cefuroxime and cloxacillin as intramammary treatments for clinical mastitis in lactating cows on commercial dairy farms. *New Zealand Veterinary Journal, 51*(1), 26-32. doi:10.1080/00480169.2003.36326.

Wyres, K. L., Hawkey, J., Hetland, M. A., Fostervold, A., Wick, R. R., Judd, L. M., . . . Holt, K. E. (2019). Emergence and rapid global dissemination of CTX-M-15-associated Klebsiella

pneumoniae strain ST307. *Journal of Antimicrobial Chemotherapy, 74*(3), 577-581. doi: 10.1093/jac/dky492

Wyres, K. L., & Holt, K. E. (2018). Klebsiella pneumoniae as a key trafficker of drug resistance genes from environmental to clinically important bacteria. *Current Opinion in Microbiology, 45*, 131-139. doi: 10.1016/j.mib.2018.04.004

Xie, S., Tao, Y., Pan, Y., Qu, W., Cheng, G., Huang, L., . . . Yuan, Z. (2014). Biodegradable nanoparticles for intracellular delivery of antimicrobial agents. *Journal of Controlled Release, 187*, 101-117. doi:10.1016/j.jconrel.2014.05.034

Xie, S., Yang, F., Tao, Y., Chen, D., Qu, W., Huang, L., . . . Yuan, Z. (2017). Enhanced intracellular delivery and antibacterial efficacy of enrofloxacin-loaded docosanoic acid solid lipid nanoparticles against intracellular Salmonella. *Scientific Reports, 7*(1), 41104. doi:10.1038/srep41104

Xiong, M. H., Li, Y. J., Bao, Y., Yang, X. Z., Hu, B., & Wang, J. (2012). Bacteria-responsive multifunctional nanogel for targeted antibiotic delivery. *Advanced Materials, 24*(46), 6175-6180. doi:10.1002/adma.201202847

Xu, K., Basu, N., & George, S. (2021). Dietary nanoparticles compromise epithelial integrity and enhance translocation and antigenicity of milk proteins: An in vitro investigation. *NanoImpact, 24*, 100369. doi:10.1016/j.impact.2021.100369

Yadav, P., Yadav, A. B., Gaur, P., Mishra, V., Huma, Z. I., Sharma, N., & Son, Y. O. (2022). Bioengineered ciprofloxacin-loaded chitosan nanoparticles for the treatment of bovine mastitis. *Biomedicines, 10*(12). doi:10.3390/biomedicines10123282

Yang, Y., & Alvarez, P. J. J. (2015). Sublethal concentrations of silver nanoparticles stimulate biofilm development. *Environmental Science & Technology Letters, 2*(8), 221-226. doi:10.1021/acs.estlett.5b00159

Yap, P. S., Lim, S. H., Hu, C. P., & Yiap, B. C. (2013). Combination of essential oils and antibiotics reduce antibiotic resistance in plasmid-conferred multidrug resistant bacteria. *Phytomedicine, 20*(8-9), 710-713. doi:10.1016/j.phymed.2013.02.013

Yuan, C., Liu, B., & Liu, H. (2015). Characterization of hydroxypropyl-β-cyclodextrins with different substitution patterns via FTIR, GC–MS, and TG–DTA. *Carbohydrate Polymers, 118*, 36-40. doi:10.1016/j.carbpol.2014.10.070

Zaatout, N., Ayachi, A., & Kecha, M. (2019). Interaction of primary mammary bovine epithelial cells with biofilm-forming staphylococci associated with subclinical bovine mastitis. *Iranian Journal of Veterinary research, 20*(1), 27. doi:10.22099/ijvr.2019.5139

Zaki, N. M., & Hafez, M. M. (2012). Enhanced antibacterial effect of ceftriaxone sodium-loaded chitosan nanoparticles against intracellular Salmonella typhimurium. *AAPS PharmSciTech, 13*(2), 411-421. doi:10.1208/s12249-012-9758-7

Zaki, N. M., Nasti, A., & Tirelli, N. (2011). Nanocarriers for cytoplasmic delivery: cellular uptake and intracellular fate of chitosan and hyaluronic acid-coated chitosan nanoparticles in a phagocytic cell model. *Macromolecular Bioscience, 11*(12), 1747-1760. doi:10.1002/mabi.201100156

Zeinhom, M. M., Abdel Aziz, R. L., Mohammed, A. N., & Bernabucci, U. (2016). Impact of seasonal conditions on quality and pathogens content of milk in friesian cows. *Asian-Australasian Journal of Animal Sciences, 29*(8), 1207-1213. doi:10.5713/ajas.16.0143

Zeng, X., & Lin, J. (2013). Beta-lactamase induction and cell wall metabolism in Gram-negative bacteria. *Frontiers in Microbiology, 4*, 128. doi:10.3389/fmicb.2013.00128

Zhang, L., Gao, J., Barkema, H. W., Ali, T., Liu, G., Deng, Y., . . . Han, B. (2018). Virulence gene profiles: alpha-hemolysin and clonal diversity in Staphylococcus aureus isolates from bovine clinical mastitis in China. *BMC Veterinary Research, 14*(1), 63-63. doi:10.1186/s12917-018-1374-7

Zhang, Y. N., Poon, W., Tavares, A. J., McGilvray, I. D., & Chan, W. C. W. (2016). Nanoparticle-liver interactions: cellular uptake and hepatobiliary elimination. *Journal of Controlled Release, 240*, 332-348. doi:10.1016/j.jconrel.2016.01.020

Zhao, Q. Y., Yuan, F. W., Liang, T., Liang, X. C., Luo, Y. R., Jiang, M., . . . Zhang, W. M. (2018). Baicalin inhibits Escherichia coli isolates in bovine mastitic milk and reduces antimicrobial resistance. *Journal of Dairy Science, 101*(3), 2415-2422. doi:10.3168/jds.2017-13349

Zhou, K., Li, C., Chen, D., Pan, Y., Tao, Y., Qu, W., . . . Xie, S. (2018). A review on nanosystems as an effective approach against infections of Staphylococcus aureus. *International Journal of Nanomedicine, 13*, 7333-7347. doi:10.2147/ijn.S169935

Ziv, G., & Storper, M. (1985). Intramuscular treatment of subclinical staphylococcal mastitis in lactating cows with penicillin G, methicillin and their esters. *Journal of Veterinary Pharmacology and Therapeutics, 8*(3), 276-283. doi:10.1111/j.1365-2885.1985.tb00957.x

Zwierzchowski, G., & Ametaj, B. N. (2019). Mineral elements in the raw milk of several dairy farms in the province of alberta. *Foods, 8*(8). doi:10.3390/foods8080345